Springer Tracts in Mechanical Engineering

Vladimir Stojanović
Predrag Kozić

Vibrations and Stability of Complex Beam Systems

Springer

Springer Tracts in Mechanical Engineering

About this Series

Springer Tracts in Mechanical Engineering (STME) publishes the latest developments in Mechanical Engineering - quickly, informally and with high quality. The intent is to cover all the main branches of mechanical engineering, both theoretical and applied, including:

- Engineering Design
- Machinery and Machine Elements
- Mechanical structures and stress analysis
- Automotive Engineering
- Engine Technology
- Aerospace Technology and Astronautics
- Nanotechnology and Microengineering
- Control, Robotics, Mechatronics
- MEMS
- Theoretical and Applied Mechanics
- Dynamical Systems, Control
- Fluids mechanics
- Engineering Thermodynamics, Heat and Mass Transfer
- Manufacturing
- Precision engineering, Instrumentation, Measurement
- Materials Engineering
- Tribology and surface technology

Within the scopes of the series are monographs, professional books or graduate textbooks, edited volumes as well as outstanding PhD theses and books purposely devoted to support education in mechanical engineering at graduate and post-graduate levels.

More information about this series at http://www.springer.com/series/11693

Vladimir Stojanović · Predrag Kozić

Vibrations and Stability of Complex Beam Systems

First author: *To My Family*

Springer

Dr. Sc. Vladimir Stojanović
Faculty of Mechanical Engineering
University of Niš
Niš
Serbia

Dr. Sc. Predrag Kozić
Faculty of Mechanical Engineering
University of Niš
Niš
Serbia

ISSN 2195-9862 ISSN 2195-9870 (electronic)
Springer Tracts in Mechanical Engineering
ISBN 978-3-319-13766-7 ISBN 978-3-319-13767-4 (eBook)
DOI 10.1007/978-3-319-13767-4

Library of Congress Control Number: 2014956102

Springer Cham Heidelberg New York Dordrecht London

Printed on acid-free paper

Springer International Publishing AG Switzerland is part of Springer Science+Business Media (www.springer.com)

Preface

The progress in vibration analysis in the previous period has been made as a consequence of the global advances in technology. The development of powerful and fast computers which can be used for computational techniques has brought about a numerical revolution in validation of complex mathematical models and analytically obtained results. A significant progress has been made in linear large-order systems. Indeed, one of the most significant advances in recent years has been the finite element method, a method developed originally for the analysis of complex structures. Proper knowledge of these two areas (the knowledge of analytical theory of vibrations and the knowledge of numerical techniques with FEM implementation) prepares researches for investigating new phenomena in vibrations, some of which are presented here.

This book contains the obtained results within the author's research during the preparation of the doctoral dissertation, and as such it is primarily intended for postgraduate students in the field of theory of vibrations. Detailed theoretical investigations have yielded original results in linear vibrations of elastically connected beams and geometrically nonlinear vibrations of damaged beams, which together may represent a group of complex beam systems.

The co-author of the book (the first author's supervisor) Dr. Predrag Kozić, full professor of the Faculty of Mechanical Engineering, University of Niš, provided meaningful assistance in the research within the field of linear vibrations. During the author's specialization at the Faculty of Mechanical Engineering, University of Engenharia in Porto, the author conducted research in the field of geometrically nonlinear vibrations with Dr. Pedro Ribeiro, and as a result the chapter which describes the vibrations of damaged beams is presented here.

The authors would like to express their sincere acknowledgements to Dr. Ratko Pavlović, Dr. Goran Janevski, Dr. Zoran Golubović, Dr. Stanislav Stoykov and Dr. Marko D. Petković for cooperation during the theoretical investigation. This research was supported by the research grant of the Serbian Ministry of Science and Environmental Protection under the number ON 174011.

The presented work consists of seven parts which are separately formed by chapters. The first chapter relates to the introductory discussion and review of previous research in the theory of elastic and related damaged structures. It is one of the ways to perform partial differential equations of motion of mechanical systems and provides a basic overview of the methods used. Chapters 2-6 are devoted to the analysis of linear elastic oscillations. The seventh chapter is

devoted to geometric nonlinear oscillations of damaged beams using the new finite element method.

Free oscillations and static stability of two elastically connected beams are considered in Chapter 2. Through various examples analytically obtained results are shown and impacts of some mechanical parameters of the system on the natural frequency and amplitudes are presented. The verification of the obtained analytical results is shown by comparison with the results of the existing classical models. A new scientific contribution in this chapter is the formulation of the new double-beam model described with new derived equations of motion with rotational inertia effects and with inertia of rotation with transverse shear (Timoshenko's model, Reddy-Bickford's model). The static stability conditions of two elastically connected beams of different types are formulated with analytical expressions for the values of critical forces. Numerical experiments confirmed the validity of the analytical results obtained by comparing the results of the models existing in the literature. From chapter 2 it can be concluded that the effects of rotational inertia and transverse shear must be taken into account in the model of thick beams because errors that occur by ignoring them increase with the mode of vibration.

Chapter 3 presents the solution for forced vibrations of two elastically connected beams of Rayleigh, Timoshenko and Reddy-Bickford type under the influence of axial forces. The scientific contribution lies in the presented analytical solutions for the forms of three types of forced vibration: harmonic arbitrarily continuous excitation, continuous uniform harmonic excitation, and harmonic concentrated excitation. Analytical solutions were obtained by using the modal analysis method. The chapter also presents the analytical solutions of forced vibration for the case when harmonic excitation effects are concentrated on one of the beams under the effect of compressive axial forces. Based on the results derived in this chapter, it can be concluded that the differences in the approximations of the solutions depending on the used model provided good solutions only in the case of Timoshenko and Reddy-Bickford theory for thick beams in higher modes. Classical theories did not yield good results.

Chapter 4 considers the static and stochastic stability of two and three elastically connected beams and a single beam on elastic foundation. A new set of partial differential equations is derived for static analysis of deflections and critical buckling force of the complex mechanical systems. The critical buckling force is analytically determined for each system individually. It is concluded that the system is most stable in the case of one beam on elastic foundation.

Chapters 5 and 6 analyze free vibrations of more elastically connected beams of Timoshenko and Reddy-Bickford type on elastic foundation under the influence of axial forces. Analytical solutions for the natural frequencies and the critical force are determined by the trigonometric method and verified numerically.

Chapter 7 presents geometrically nonlinear forced vibrations of damaged Timoshenko beams. The study develops a new p-version of the finite element method for damaged beams. The advantage of the new method is compared with the traditional method, showing that it provides better approximations of solutions with a small number of degrees of freedom used in numerical analysis. The

scientific contribution can be found in two topics-computational mechanics and non-linear vibrations of beams. It is concluded that the traditional method cannot provide good approximations of solutions in the case of a very small width of damage. This benefit is also shown in the comparison with the obtained results in the commercial software Ansys. A new p-version finite element is suggested to deal with geometrically non-linear vibrations of damaged Timoshenko beams. The novelty of the p-element comes from the use of new displacement shape functions, which are the functions of the damage location, therefore, providing more efficient models, where accuracy is improved at lower computational cost. In numerical tests in the linear regime, coupling between cross-sectional rotation and longitudinal vibrations is discovered, with longitudinal displacements suddenly changing direction at the damage location and with a peculiar change in the cross-section rotation at the same place. Geometrically nonlinear, forced vibrations are then investigated in the time domain using Newmark's method and further couplings between displacement components are found.

Dr. Vladimir Stojanović

Contents

Chapter 1
Introductory Remarks

1.1 Introduction

A great number of mechanical systems are complex structures composed of two or more basic mechanical systems whose dynamic behavior is conditioned by their interaction. The systems connected by an elastic layer constitute one group of such mechanical structures which are commonly encountered in mechanical, construction and aeronautical industry. Mechanical systems formed by elastic connection of their members, due to the nature of the dynamic interaction conditioned by elastic connections are characterized by complex vibration and a higher number of natural frequencies. Since the number of natural frequencies depends on the number of basic elements joint together, such mechanical systems are exposed to an increased likelihood of creating resonance conditions which can cause breakage and damage. With the view to putting theoretical research into engineering practice, a great number of linear dynamic models describing the motion of a system were created. Such models are important as they give the initial approximation of the solution and a general insight into a dynamic behavior of the system at slight motion. If technical practice requires further investigation of system behavior, these dynamic models provide solid ground for the continuation of research with non-linearity effects.

The parts of mechanical structures performing a great number of cyclical operations exposed to loads often sustain damage. As soon as the damage occurs, the dynamic behavior of the system changes requiring good knowledge thereof in order to prevent resonance conditions and the resulting consequences. In already damaged structures, the displacement of deformable elements is greater; hence the effect of geometric non-linearity is more common. Such dynamic behaviors are different in non-damaged structures, and it is essential to determine the conditions leading to resonance as the consequence of interaction between vibration modes.

The effects of rotary inertia and transverse shear have been taken into consideration in creating mathematical models for both elastically connected beams and damaged beams. Vibrations and the stability of such systems have been the subject of scientific, academic and practical research by many authors for decades. Increased interest by the scientific public in the problem of vibrations

V. Stojanović and P. Kozić, *Vibrations and Stability of Complex Beam Systems,*
Springer Tracts in Mechanical Engineering, DOI: 10.1007/978-3-319-13767-4_1

and the stability of such systems is motivated by breakage prevention and the prevention of permanent damage to real mechanical, construction and other systems. This led to the development of analytical and numerical methods used for analyzing the vibrations of both linear and non-linear mechanical systems.

The problem concerning the vibrations of beams joint by a Winkler elastic layer has attracted the interest of a large group of scientists. The problem of two elastically connected beams joint by the Winkler elastic layer emerged in order to determine the conditions for the behavior of the system acting as a dynamic absorber in technical practice. A mathematical model was developed by Seelig and Hoppman [1]. They investigated the problem of an impulse load effect on a beam and produced a system of partial differential equations describing its vibration. The obtained theoretical and experimental results confirmed a sound approximation of an analytical solution obtained for slender beams at small transverse motions using the Euler-Bernoulli theory.

Oniszczuk [2, 3] analyzed the problem of free and forced vibration of two elastically connected Euler-Bernoulli beams. He determined analytical solutions for eigenfrequencies, amplitudinous functions and vibration modes. He discussed the effect of stiffness which the elastic interlayer had on the frequencies and amplitudes of the system. He determined the conditions for the occurrence of resonance and the behavior of the system as a dynamic absorber.

The analysis of the system composed of two connected beams was carried on by Zhang et al. [4, 5] in their investigation of free and forced vibrations by two elastically connected Euler-Bernoulli beams affected by axial compression forces. They presented analytical solutions for natural frequencies of the system in the function of axial compression force impact and their effect on the vibration amplitude. They determined the co-dependency between the system's critical force and the Euler critical load in the function of an axial force of the other beam.

Vu et al. [6] studied the problem of forced and damped vibrations of the system composed of two elastically connected Euler-Bernoulli beams. They provided analytical solutions to partial differential equations with a damping factor. They determined the influence of system damping on vibration and amplitudes under harmonic forcing. Their analytical results showed close correspondence to experimental results obtained by Seelig and Hoppmann [1] for dynamic absorbers.

Li and Hua [7], using the spectral finite element method arrived at numerical solutions for natural frequencies of the two elastically connected Timoshenko beams with different supports. They determined vibration modes and amplitude-frequency dependence for forced vibration of the system.

The investigation of system vibration in complex structures which are encountered in technical practice as physical models of reinforcement, coupled support structures in mechanical engineering and multistory buildings in civil engineering, has made its way into the study fields of many researchers. These

structures made up of three or more elastically connected elementary member beams were the subject of recent investigations. The development of computer resources and the application of numerical mathematics on such models led to the increased interest in the matter by a group of scientists in the 20th century.

Li et al. [8] addressed the problem of three elastically connected Timoshenko beams in their paper. They numerically determined natural frequencies for different types of support, mode shapes and the effect the stiffness of elastic inter-layers had on vibration of the system. Kelly and Srinivas [9] discussed the problem of multiple elastically connected Euler beams. They determined natural frequencies and mode shapes for the beams with identical characteristics using the Rayleigh-Ritz numerical method. Ariaei et al. [10] studied the problem of a movable body according to the system of multiple elastically connected Timoshenko beams on an elastic foundation using the Transfer-matrix method. They concluded that the maximum deflection of the beam system decreases in case of a body moving on the beams closer to the surface. Mao [11] determined mode shapes for the first ten system modes of multiple elastically connected Euler beams on an elastic foundation using the Adomian decomposition method.

Stojanović et al. [12] analyzed free vibration and static stability of two elastically connected beams taking into account the effects of rotary inertia and transverse shear which leads to the rotation of the cross-section. They used an example to show the analytical solutions for natural frequencies and determined the critical force for the coupled beam system.

Stojanović and Kozić [13] discussed the case of forced vibration of two elastically connected beams and the effect of axial compression force on amplitude ratio of system vibration for three types of external forcing - arbitrarily continuous harmonic excitation, uniformly continuous harmonic excitation and concentrated harmonic excitation. They determined general conditions of resonance and dynamic vibration absorption. In the paper [14], Stojanović et al. discussed the analytic analysis of static stability of a system consisting of three elastically connected Timoshenko beams on an elastic foundation. They provided expressions for critical force of the system under the influence of elastic Winkler layers. Stojanović et al. [15] using the example of multiple elastically connected Timoshenko and Reddy-Bickford beams, determined the analytical forms of natural frequencies, their change under the effect of axial compression forces and the conditions for static stability for a different number of connected beams.

The issues of the vibration in damaged beams have a significant place in theoretical and experimental research into the behavior of dynamic systems. The occurrence of various types of damage in constructions leads to their permanent modification and increased risk of breakage. Considerable engineering practice in the field prompted a great number of researchers to examine the vibration of damaged dynamic system. Christides and Barr [16] experimentally determined the

impact factor on natural frequencies of a simply supported beam with closed damage. The obtained results showed that the occurrence of damage decreases the natural frequencies of the system. Several studies in the field of damaged beam analysis have been carried out on a beam model with altered stiffness as a consequence of damage occurrence and its impact on natural frequencies, vibration modes and the damping factor in linear mode. Thus Sinha et al. [17] developed a model of the apparent change in the beam geometry at the place of damage. Using the experimentally determined impact factor on natural frequencies of damaged beams published by Christides and Barr [16] for a closed crack, they determined the required change in the beam geometry at the place of damage using the triangle model type of an open crack. They examined the vibration of a thus formulated mathematical model using the finite element method and confirmed the results by experimental verification thereof. Pandey et al. [18] investigated the effect of damage on natural mode shapes in their paper. A group of researchers focused dynamic analysis on damage detection and localization. They used the occurrence of greatest deviation from the mode shapes as a method of detecting the damage on the beam. Panteliou et al. [19] used the change in the damping factor to localize the damage. A great number of papers in non-linear vibration of damaged beams confirmed the interest of scholars in the field. Thus Bikri et al. [20] considered geometrically non-linear vibration of a doubly-clamped beam with a crack and showed the difference in mode shapes between the linear and non-linear model. Andreaus et al. [21] investigated geometrically non-linear vibration of a bracket under the influence of harmonic excitation. They formed the model as a bilinear oscillator which implied the opening and closing of the damage at vibration. Based on earlier research on non-linear vibration of damaged beams, Stojanović et al. [22, 23, 50] developed a new *p*-version of a finite element method for geometrically non-linear vibration of damaged Timoshenko beams. Unlike its previous versions, they formed the damage model so as to take into account the change in the weight of the system in addition to the change in the stiffness thereof. The advantage of the new method is the ability to determine natural frequencies of the system using a smaller number of functions of motion, i.e. lower vibration freedom degree. The paper shows the occurrence of longitudinal vibration of the doubly clamped beam which occurs solely as the consequence of damage.

Numerical experiments were performed on the Timoshenko beam model taking into account the effects of rotary inertia and transverse shear as in the case of elastically connected beams. It was shown that the coupling between transverse vibration and component vibration of cross-sections caused asymmetry in a non-linear vibration time mode. For the non-linear vibration region the Newmark method of direct integration was used to solve non-linear partial differential equations for forced vibration of the damaged Timoshenko beam. Continuation

method was applied to the free non-linear vibration model to determine bifurcation points, Stojanović and Ribeiro [23]. The new *p*-version of the finite element method was developed within the mathematical model of Timoshenko beams, determining the effects of the cross-section rotation (rotary inertia and transverse shear) on geometrically non-linear vibration of beams with different thickness.

1.2 Vibrations of Euler, Rayleigh, Timoshenko and Reddy-Bickford Beams

This part of the chapter relates to the basic review of the beam theories. It is shown the different aspect and perform of partial differential equations of motion which are used in further theoretical investigation of the complex beam systems. The Euler–Bernoulli theory for a beam originated in the 18th century. The effect of rotary inertia was introduced by Rayleigh in 1894. In 1921, Timoshenko proposed his theory where shear is also taken into account. Since shear and rotary inertia are ignored in the Euler–Bernoulli theory is reasonable to assume that the Timoshenko theory is an improvement. Reddy-Bickford theory ensures a more exact stress-deformation mathematical interpretation in the analysis and provide a approximations which are more accurate and important in vibrations of thick beams.

Euler-Bernoulli theory on homogeneous elastic slender prismatic beams (Figure 1.2.1a,b) implies that the vibration takes place so that the beams' cross-sections are always normal to the neutral axis at deformation ignoring the effects of rotary inertia and transverse shear, [2, 3]. The theory gives a good approximation of solutions at small transverse motions for slender beams.

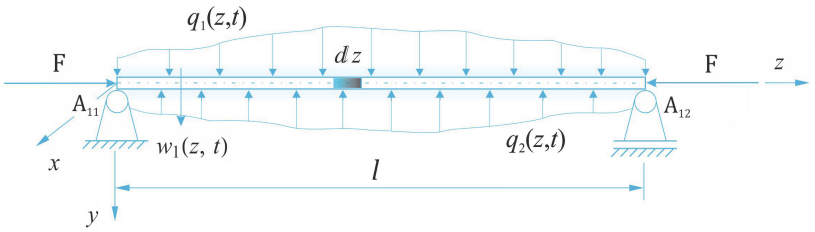

(a)

Fig. 1.2.1 (a) A simply supported beam under the influence of axial compression forces F and continuous loads $q_1(z,t)$ and $q_2(z,t)$ (b) Deformation in various beam theories

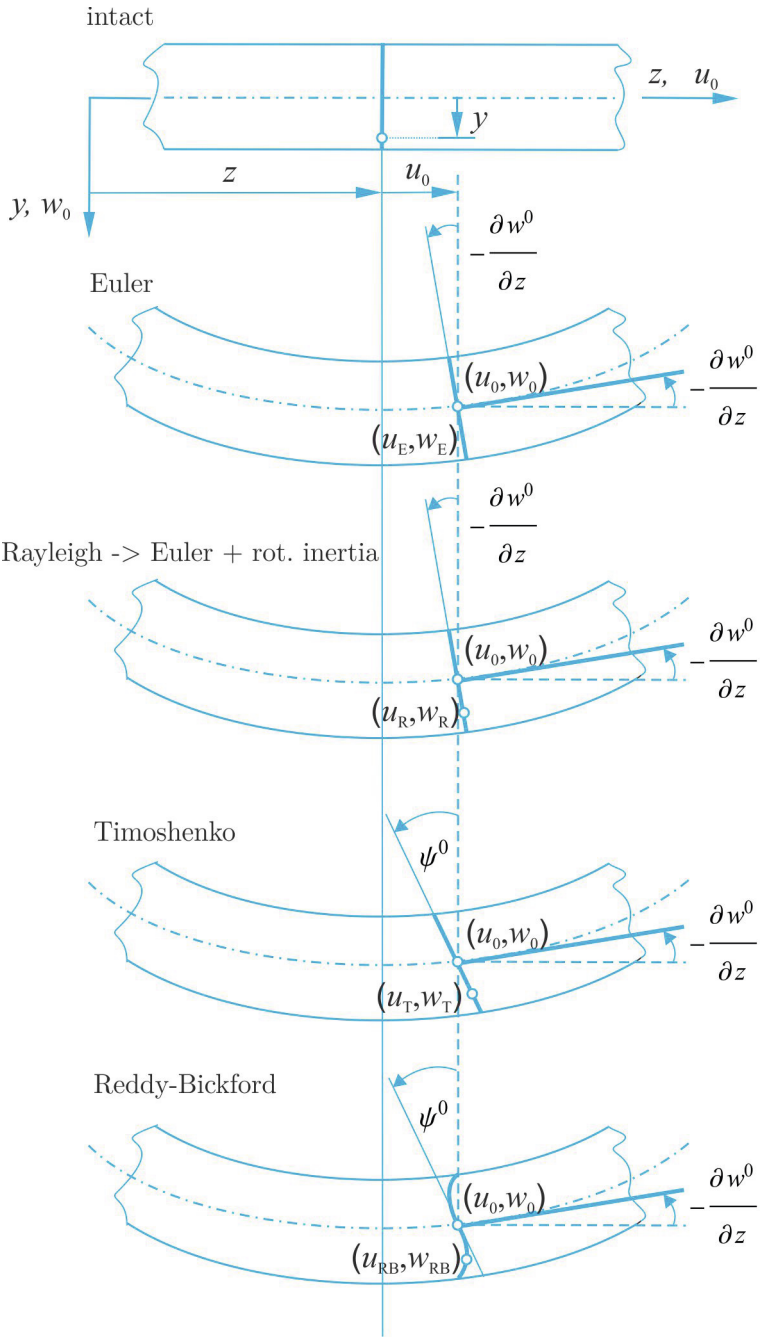

(b)

Fig. 1.2.1 (*continued*)

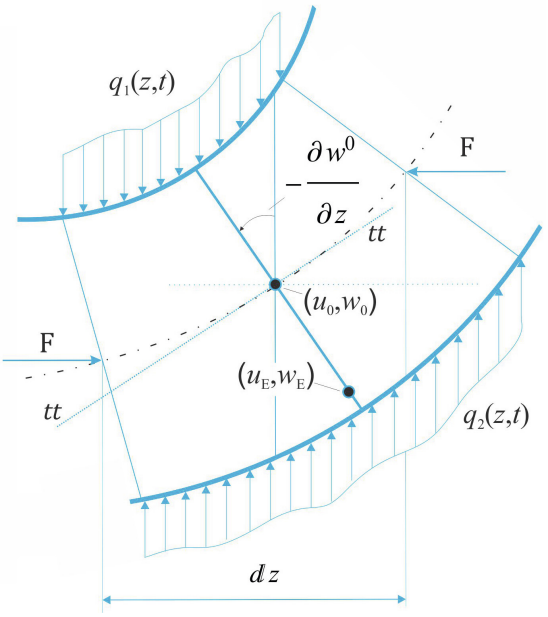

Fig. 1.2.2 An elementary part of a Euler beam

If we label the functions of longitudinal and transverse motions as $u(y,z,t)$ and$w(y,z,t)$, then the following relations apply to the angles shown in Figure 1.2.2 of the elementary beam part shown in Figure 1.2.1a

$$u_E(y,z,t) = u_E^0(z,t) - y\frac{\partial w_E^0(z,t)}{\partial z}, \quad w_E(y,z,t) = w_E^0(z,t), \tag{1.2.1}$$

where $u^0(z,t)$ and $w(y,z,t)$ represent longitudinal and transverse motions of the beam's point $(0,z,t)$ belonging to the z-axis. The deformation taking place in the z direction in the function of motion and the stress-deformation ratio according to the Hooke's law are given by

$$\varepsilon_z(y,z,t) = \frac{\partial u_E(y,z,t)}{\partial z} = \frac{\partial u_E^0(z,t)}{\partial z} - y\frac{\partial^2 w_E^0(z,t)}{\partial z^2}, \tag{1.2.2}$$

$$\sigma_z(y,z,t) = E\varepsilon_z(y,z,t), \tag{1.2.3}$$

where E is Young's modulus. The equations are derived based on the principle of virtual work to which the following applies

$$\delta W_{in} + \delta W_V + \delta W_{ex} = 0, \tag{1.2.4}$$

where $\delta W_{in}, \delta W_V$ and δW_{ex} represent virtual work of inertial, internal and external forces respectively. Virtual work of inertial forces is

$$\delta W_{in} = -\rho b \int_0^l \int_{-\frac{h}{2}}^{\frac{h}{2}} \left[\frac{\partial^2 w_E(y,z,t)}{\partial t^2} \delta w_E(y,z,t) + \frac{\partial^2 u_E(y,z,t)}{\partial t^2} \delta u_E(y,z,t) \right] dydz. \quad (1.2.5)$$

Having regard to the relation of longitudinal motion, $u_E(y,z,t) = u_E^0(z,t) - y\frac{\partial w_E^0(z,t)}{\partial z}$, a member in an integrand $\frac{\partial^2 u_E(y,z,t)}{\partial t^2}\delta u_E(y,z,t)$ represents the effect of rotary inertia. Mathematical model of Euler beam does not take the effect of rotary inertia into account, therefore it can be disregarded in deriving the wave equation of the Euler beam. Virtual work of internal forces is expressed as

$$\delta W_V = -b \int_0^l \int_{-\frac{h}{2}}^{\frac{h}{2}} \sigma_z(z,t)\delta\varepsilon_z(z,t) dydz. \quad (1.2.6)$$

Virtual work of external forces acting transversally is given by

$$\delta W_{ex} = \int_0^l \left[q(z,t)\delta w_E^0(z,t) + F\frac{\partial w_E^0(z,t)}{\partial z}\frac{\partial \delta w_E^0(z,t)}{\partial z} \right] dz,$$

$$q(z,t) = q_1(z,t) - q_2(z,t), \quad (1.2.7)$$

where δ stands for variation operator. By substituting the equations (1.2.5-1.2.7) into the equation (1.2.4), we get

$$-b\int_0^l \int_{-\frac{h}{2}}^{\frac{h}{2}} \sigma_z(z,t)\delta\varepsilon_z(z,t) dydz - \rho b \int_0^l \int_{-\frac{h}{2}}^{\frac{h}{2}} \frac{\partial^2 w_E(y,z,t)}{\partial t^2}\delta w_E(y,z,t) dydz$$
$$+ \int_0^l \left[q(z,t)\delta w_E^0(z,t) + F\frac{\partial w_E^0(z,t)}{\partial z}\frac{\partial \delta w_E^0(z,t)}{\partial z} \right] dz = 0. \quad (1.2.8)$$

By successive application of Green's theorem on the equation (1.2.8), the partial equation for transverse vibration of the Euler beam is obtained

$$\rho A\frac{\partial^2 w_E^0(z,t)}{\partial t^2} + \frac{\partial^2}{\partial z^2}\left(EI_x \frac{\partial^2 w_E^0(z,t)}{\partial z^2} \right) + F\frac{\partial^2 w_E^0(z,t)}{\partial z^2} = q(z,t). \quad (1.2.9)$$

Rayleigh theory of homogeneous elastic slender prismatic beams implies the motion of beam points takes place so that the beams' cross-sections, as in the case of the Euler mathematical model, are always normal to its neutral axis at deformation having the effect of rotary inertia in regard. Constitutive relations are identical to those in the case of a Euler beam although the dynamic equation changes and takes the member $\frac{\partial^2 u_E(y,z,t)}{\partial t^2}\delta u_E(y,z,t)$ into account in the expression for virtual work of inertial forces. If we label the functions of longitudinal and transverse motions as $u_R(y,z,t)$ and $w_R(y,z,t)$, then the following relations of longitudinal and transverse motions of the Euler beam apply based on the position of the beam's point $u_R(y,z,t)$

$$u_R(y,z,t) = u_R^0(z,t) - y\frac{\partial w_R^0(z,t)}{\partial z}, \quad w_R(y,z,t) = w_R^0(z,t), \tag{1.2.10}$$

where $u_R^0(z,t)$ and $w_R^0(z,t)$ denote longitudinal and transverse motion of the beam point $(0,z,t)$ belonging to z–axis. The deformation taking place in z direction in the function of motion and the relation between stress and deformation according to the Hooke's law have the following form

$$\varepsilon_z(y,z,t) = \frac{\partial u_R^0(z,t)}{\partial z} - y\frac{\partial^2 w_R^0(z,t)}{\partial z^2}, \tag{1.2.11}$$

$$\sigma_z(y,z,t) = E\varepsilon_z(y,z,t). \tag{1.2.12}$$

Hence, virtual work of inertial forces is given by

$$\delta W_{in} = -\rho b\int_0^l\int_{-\frac{h}{2}}^{\frac{h}{2}}\left[\frac{\partial^2 w_R(y,z,t)}{\partial t^2}\delta w_R(y,z,t) + \frac{\partial^2 u_R(y,z,t)}{\partial t^2}\delta u_R(y,z,t)\right]dydz. \tag{1.2.13}$$

Virtual work of internal forces is

$$\delta W_V = -b\int_0^l\int_{-\frac{h}{2}}^{\frac{h}{2}}\sigma_z(z,t)\delta\varepsilon_z(z,t)dydz. \tag{1.2.14}$$

Virtual work of external forces is expressed as

$$\delta W_{ex} = \int_0^l\left[q(z,t)\delta w_R^0(z,t) + F\frac{\partial w_R^0(z,t)}{\partial z}\frac{\partial\delta w_R^0(z,t)}{\partial z}\right]dz,$$
$$q(z,t) = q_1(z,t) - q_2(z,t), \tag{1.2.15}$$

Substituting the equations (1.2.13-1.2.15) into the equation (1.2.4), yields

$$-b\int_0^l\int_{-\frac{h}{2}}^{\frac{h}{2}}\sigma_z(z,t)\delta\varepsilon_z(z,t)dydz$$
$$-\rho b\int_0^l\int_{-\frac{h}{2}}^{\frac{h}{2}}\left[\frac{\partial^2 w_R(y,z,t)}{\partial t^2}\delta w_R(y,z,t) + \frac{\partial^2 u_R(y,z,t)}{\partial t^2}\delta u_R(y,z,t)\right]dydz$$
$$+\int_0^l\left[q(z,t)\delta w_R^0(z,t) + F\frac{\partial w_R^0(z,t)}{\partial z}\frac{\partial\delta w_R^0(z,t)}{\partial z}\right]dz = 0. \tag{1.2.16}$$

By applying Green's theorem to the equation (1.2.16), we get the equation of transverse vibration of the Rayleigh beam in the following form

$$\rho A\frac{\partial^2 w_R^0(z,t)}{\partial t^2} - \rho I_x\frac{\partial^4 w_R^0(z,t)}{\partial z^2\,\partial t^2} + \frac{\partial^2}{\partial z^2}\left(EI_x\frac{\partial^2 w_R^0(z,t)}{\partial z^2}\right) + F\frac{\partial^2 w_R^0(z,t)}{\partial z^2} = q(z,t), \tag{1.2.17}$$

where ρ denotes mass density, A the area of the cross-section, E Young's modulus, I_x moment of inertia of the cross-section area for x –axis and F the axial compression force.

The theory of homogeneous elastic prismatic Timoshenko beams constitutes a mathematical model which, in addition to the effects of rotary inertia, implies taking into account the shear forces causing the rotation of the beams' cross-sections. Based on this assumption, the function of the cross-section rotation is introduced. Based on the elementary deformed beam part shown in Figure 1.2.3., the following functions of motion are given

$$u_T(y,z,t) = u_T^0(z,t) + y\psi_T^0(z,t), \qquad w_T(y,z,t) = w_T^0(z,t), \tag{1.2.18}$$

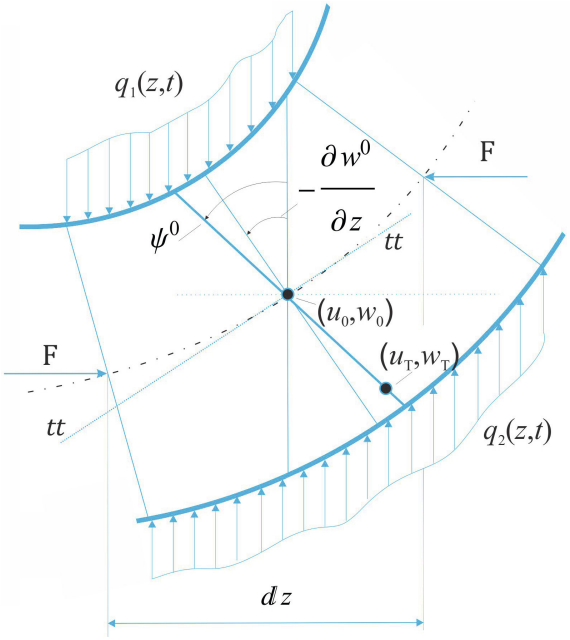

Fig. 1.2.3 An elementary part of a Timoshenko beam

where $u_T^0(z,t)$,$w_T^0(z,t)$and $\psi_T^0(z,t)$ denote longitudinal and transverse motion of the beam point $(0,z,t)$ on the z–axis and the angle between the cross-section of the deformed beam and y–axis, Figure 1.2.3. The deformations taking place in z direction and ε_z tangentially due to shear forces γ_{zy} have the following form

$$\varepsilon_z(y,z,t) = \frac{\partial u_T^0(z,t)}{\partial z} + y\frac{\partial \psi_T^0(z,t)}{\partial z}, \tag{1.2.19}$$

$$\gamma_{zy}(y,z,t) = \frac{\partial w_T^0(z,t)}{\partial z} + \psi_T^0(z,t). \tag{1.2.20}$$

Assuming the material is isotropic and elastic, the Hooke's law on the relation between stress and deformation applies

$$\begin{Bmatrix}\sigma_z\\ \tau_{zy}\end{Bmatrix}=\begin{bmatrix}E & 0\\ 0 & kG\end{bmatrix}\begin{Bmatrix}\varepsilon_z\\ \gamma_{zy}\end{Bmatrix}, \tag{1.2.21}$$

where G is the shear modulus and k is the shear factor. The equations of motion are derived based on the principle of virtual work for which the following applies

$$\delta W_{in}+\delta W_V+\delta W_{ex}=0, \tag{1.2.22}$$

where $\delta W_{in}, \delta W_V$ and δW_{ex} represent virtual work of inertial, internal and external forces respectively. Virtual work of inertial forces is given by

$$\delta W_{in}=-\rho b\int_0^l\int_{-\frac{h}{2}}^{\frac{h}{2}}\left[\frac{\partial^2 w_T(y,z,t)}{\partial t^2}\delta w_T(y,z,t)+\frac{\partial^2 u_T(y,z,t)}{\partial t^2}\delta u_T(y,z,t)\right]dydz. \tag{1.2.23}$$

Virtual work of internal forces is

$$\delta W_V=-b\int_0^l\int_{-\frac{h}{2}}^{\frac{h}{2}}\left[\sigma_z(z,t)\delta\varepsilon_z(z,t)+\tau_{zy}(z,t)\delta\gamma_{zy}(z,t)\right]dydz. \tag{1.2.24}$$

Virtual work of external forces is expressed as

$$\delta W_{ex}=\int_0^l\left[q(z,t)\delta w_T^0(z,t)+F\frac{\partial w_T^0(z,t)}{\partial z}\frac{\partial\delta w_T^0(z,t)}{\partial z}\right]dz,$$
$$q(z,t)=\ q_1(z,t)-q_2(z,t). \tag{1.2.25}$$

Substituting the equations (1.2.23-1.2.25) into an equation (1.2.22) yields

$$-b\int_0^l\int_{-\frac{h}{2}}^{\frac{h}{2}}\left[\sigma_z(z,t)\delta\varepsilon_z(z,t)+\tau_{zy}(z,t)\delta\gamma_{zy}(z,t)\right]dydz$$
$$-\rho b\int_0^l\int_{-\frac{h}{2}}^{\frac{h}{2}}\left[\frac{\partial^2 w_T(y,z,t)}{\partial t^2}\delta w_T(y,z,t)+\frac{\partial^2 u_T(y,z,t)}{\partial t^2}\delta u_T(y,z,t)\right]dydz$$
$$+\int_0^l\left[q(z,t)\delta w_T^0(z,t)+F\frac{\partial w_T^0(z,t)}{\partial z}\frac{\partial\delta w_T^0(z,t)}{\partial z}\right]dz=0. \tag{1.2.26}$$

By applying Green's theorem on the equation (1.2.26), we get the equations of vibration for Timoshenko beam in the following form

$$\rho A\frac{\partial^2 w_T^0(z,t)}{\partial t^2} - GAk\left(\frac{\partial^2 w_T^0(z,t)}{\partial z^2} + \frac{\partial \psi_T^0(z,t)}{\partial x}\right) + F\frac{\partial^2 w_T^0(z,t)}{\partial z^2} = q(z,t), \quad (1.2.27)$$

$$\rho I_x\frac{\partial^2 \psi_T^0(z,t)}{\partial t^2} - EI_x\frac{\partial^2 \psi_T^0(z,t)}{\partial z^2} + kGA\left(\frac{\partial w_T^0(z,t)}{\partial z} + \psi_T^0(z,t)\right) = 0. \quad (1.2.28)$$

Through the application of Timoshenko theory [27], the equations of transverse vibration of beams were derived taking into account the rotation of cross-sections caused by shear forces.

Based on the knowledge of shear stress distribution, Timoshenko theory does not take into account the fact that the stress at the cross-sections' end points equals zero, instead the shear factor k is applied. The application of Reddy-Bickford beam mathematical model shown in references to Reddy [29, 30] and Wang et al. [31] implies approximating the deformation of the beam's cross-section in yz plane along the line of shear stress value points. This ensures a more exact stress-deformation mathematical interpretation in the analysis of beam point motion without the necessity to apply the shear factor k. The functions of stress and deformation, according to reference [31] have the following form

$$u_{RB}(y,z,t) = u_{RB}^0(z,t) + y\psi_{RB}^0(z,t) - \alpha y^3\left(\psi_{RB}^0(z,t) + \frac{\partial w_{RB}^0(z,t)}{\partial z}\right),$$

$$w_{RB}(y,z,t) = w_{RB}^0(z,t), \quad (1.2.29)$$

$$\varepsilon_z(z,t) = \frac{\partial u_{RB}^0(z,t)}{\partial z} + y\frac{\partial \psi_{RB}^0(z,t)}{\partial z} - \alpha y^3\left(\frac{\partial \psi_{RB}^0(z,t)}{\partial z} + \frac{\partial^2 w_{RB}^0(z,t)}{\partial z^2}\right), \quad (1.2.30)$$

$$\gamma_{zy}(z,t) = \psi_{RB}^0(z,t) + \frac{\partial w_{RB}^0(z,t)}{\partial z} - \beta y^2\left(\psi_{RB}^0(z,t) + \frac{\partial w_{RB}^0(z,t)}{\partial z}\right), \quad (1.2.31)$$

where $\alpha = 4/3h^2$,$\beta = 3\alpha$,$u_{RB}^0(z,t)$ denote longitudinal movement of the beam point $(0,z,t)$ belonging to z–axis, $w_{RB}^0(z,t)$ transversal movement of the beam point $(0,z,t)$ belonging to z–axis, and $\psi_{RB}^0(z,t)$ the angle of the beam's cross-section at the place of its intersection with the neutral line in relation to y–axis as shown in Figure 1.2.4. Assuming the material is isotropic and elastic, Hooke's law applies

$$\begin{Bmatrix}\sigma_z\\ \tau_{zy}\end{Bmatrix} = \begin{bmatrix}E & 0\\ 0 & G\end{bmatrix}\begin{Bmatrix}\varepsilon_z\\ \gamma_{zy}\end{Bmatrix}, \quad (1.2.32)$$

where G stands for shear modulus. The equations of motion are derived based on virtual work principle like in the previous examples for which the following applies

$$\delta W_{in} + \delta W_V + \delta W_{ex} = 0, \tag{1.2.33}$$

where $\delta W_{in}, \delta W_V$ and δW_{ex} represent virtual work of inertial, internal and external forces respectively. Virtual work of inertial forces is given by

$$\delta W_{in} = -\rho b \int_0^l \int_{-\frac{h}{2}}^{\frac{h}{2}} \left[\frac{\partial^2 w_{RB}(y,z,t)}{\partial t^2} \delta w_{RB}(y,z,t) + \frac{\partial^2 u_{RB}(y,z,t)}{\partial t^2} \delta u_{RB}(y,z,t) \right] dydz. \tag{1.2.34}$$

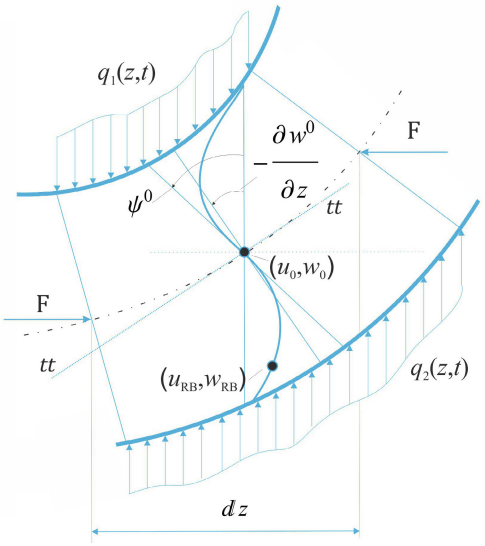

Fig. 1.2.4 An elementary part of a Reddy-Bickford beam

Virtual work of internal forces is expressed as

$$\delta W_V = -b \int_0^l \int_{-\frac{h}{2}}^{\frac{h}{2}} \left[\sigma_z(z,t) \delta \varepsilon_z(z,t) + \tau_{zy}(z,t) \delta \gamma_{zy}(z,t) \right] dydz. \tag{1.2.35}$$

Virtual work of external forces is

$$\delta W_{ex} = \int_0^l \left[q(z,t) \delta w_{RB}^0(z,t) + F \frac{\partial w_{RB}^0(z,t)}{\partial z} \frac{\partial \delta w_{RB}^0(z,t)}{\partial z} \right] dz,$$

$$q(z,t) = q_1(z,t) - q_2(z,t). \tag{1.2.36}$$

where δ stands for variation operator. By substituting the equations (1.2.34-1.2.36) into the equation (1.2.33), we have

$$-b\int_0^l\int_{-\frac{h}{2}}^{\frac{h}{2}}\left[\sigma_z(z,t)\delta\varepsilon_z(z,t)+\tau_{zy}(z,t)\delta\gamma_{zy}(z,t)\right]dydz$$

$$-\rho b\int_0^l\int_{-\frac{h}{2}}^{\frac{h}{2}}\left[\frac{\partial^2 w_{RB}(y,z,t)}{\partial t^2}\delta w_{RB}(y,z,t)+\frac{\partial^2 u_{RB}(y,z,t)}{\partial t^2}\delta u_{RB}(y,z,t)\right]dydz$$

$$+\int_0^l\left[q(z,t)\delta w_{RB}^0(z,t)+F\frac{\partial w_{RB}^0(z,t)}{\partial z}\frac{\partial\delta w_{RB}^0(z,t)}{\partial z}\right]dz=0. \qquad (1.2.37)$$

By applying the Green's theorem on the equation (1.2.37), we get the equation of vibration for Reddy-Bickford beam in the following form

$$C_w^{4,0}\frac{\partial^4 w_{RB}^0(z,t)}{\partial z^4}+C_w^{2,2}\frac{\partial^4 w_{RB}^0(z,t)}{\partial z^2\,\partial t^2}+C_w^{2,0}\frac{\partial^2 w_{RB}^0(z,t)}{\partial z^2}+C_w^{0,2}\frac{\partial^2 w_{RB}^0(z,t)}{\partial t^2}+C_\psi^{1,2}\frac{\partial^3\psi_{RB}^0(z,t)}{\partial z\,\partial t^2}$$

$$+C_\psi^{1,0}\frac{\partial\psi_{RB}^0(z,t)}{\partial z}+C_\psi^{3,0}\frac{\partial^3\psi_{RB}^0(z,t)}{\partial z^3}=q(z,t), \qquad (1.2.38)$$

$$C_w^{3,0}\frac{\partial^3 w_{RB}^0(z,t)}{\partial z^3}+C_w^{1,2}\frac{\partial^3 w_{RB}^0(z,t)}{\partial z\,\partial t^2}+C_w^{1,0}\frac{\partial w_{RB}^0(z,t)}{\partial z}+C_\psi^{2,0}\frac{\partial^2\psi_{RB}^0(z,t)}{\partial z^2}$$

$$+C_\psi^{0,2}\frac{\partial^2\psi_{RB}^0(z,t)}{\partial t^2}+C_\psi^{0,0}\psi_{RB}^0(z,t)=0, \qquad (1.2.39)$$

where

$$C_w^{4,0}=\frac{1}{448}bh^7\alpha^2E,\ \ C_w^{2,2}=-\frac{1}{448}bh^7\alpha^2\rho, C_w^{2,0}=-\frac{1}{80}bG\beta^2h^5+\frac{1}{6}bG\beta h^3-bGh+F,$$

$$C_w^{0,2}=bh\rho, C_\psi^{1,2}=\frac{1}{80}bh^5\alpha\rho-\frac{1}{448}bh^7\alpha^2\rho, C_\psi^{1,0}=-\frac{1}{80}bG\beta^2h^5+\frac{1}{6}bG\beta h^3-bGh,$$

$$C_\psi^{3,0}=\frac{1}{448}bh^7\alpha^2E-\frac{1}{80}bh^5\alpha E, C_w^{3,0}=\frac{1}{80}bh^5\alpha E-\frac{1}{448}bh^7\alpha^2E, C_w^{1,2}=\frac{1}{448}bh^7\alpha^2\rho-\frac{1}{80}bh^5\alpha\rho,$$

$$C_w^{1,0}=\frac{1}{80}bG\beta^2h^5-\frac{1}{6}bG\beta h^3+bGh, C_\psi^{2,0}=-\frac{1}{448}b\alpha^2Eh^7+\frac{1}{40}b\alpha Eh^5-\frac{1}{12}bEh^3,$$

$$C_\psi^{0,2}=\frac{1}{448}b\alpha^2\rho h^7-\frac{1}{40}b\alpha\rho h^5+\frac{1}{12}b\rho h^3.\ \ C_\psi^{0,0}=\frac{1}{80}b\beta^2Gh^5-\frac{1}{6}b\beta Gh^3+bGh. \qquad (1.2.40)$$

The application of the theory taking into account the effects of rotary inertia and transverse shear (Timoshenko and Reddy-Bickford model) gives a better approximation of solutions which is convenient in the analysis of thick beams in which the rotation of cross-sections takes place.

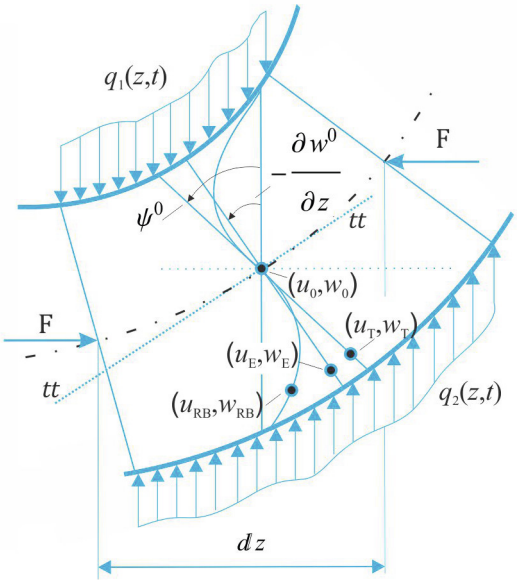

Fig. 1.2.5 An elementary part of a cross-sectioned Euler, Rayleigh, Timoshenko and Reddy-Bickford beam

The mathematical model for Euler and Rayleigh beams are based on the assumption that the beams' cross section are always perpendicular to the neutral axis, which is not the case with thick beams. In addition to rotary inertia, the Timoshenko and Reddy-Bickford models take into account the effects of shear forces affecting the rotation of the beams' cross-sections. Unlike the Timoshenko model, the Reddy-Bickford model meets the criteria of shear stress in boundary regions. Figure 1.2.5 shows the deformation of fibers in the beams' cross-section according to the type of theory applied.

Chapter 2

Free Vibrations and Stability of an Elastically Connected Double-Beam System

Free oscillations and static stability of two elastically connected beams are considered in Chapter 2. At various examples it is shown analytically obtained results and impacts of some mechanical parameters of the system on the natural frequencies and amplitudes. Verification of obtained results is shown by comparison with results of the existed classical models. New scientific contribution in this chapter is formulation of the new double-beam model described with new derived equations of motion with rotational inertia effects and with inertia of rotation with transverse shear (Rayleigh's model, Timoshenko's model, Reddy - Bickford's model). It is formulized the static stability condition of the two elastically connected beams of different types with analytical expressions for the various values of critical forces. Numerical experiments confirmed the validity of the analytical results obtained by comparing the results of the models existing in the literature. From chapter 2 it can be concluded that the effects of rotational inertia and transverse shear must be taken into account in the model of thick beams because errors that occur by ignoring them are increasing with the increasing the mode of vibration.

2.1 Free Vibration of Two Elastically Connected Rayleigh Beams

Let us analyze the influence of rotary inertia on free transverse vibration of an elastically connected double-beam system joined by a Winkler layer, Stojanović et al. [12]. Let the two beams be of the same length l, and connected by an elastic layer with the stiffness modulus K. At its ends, the beams are exposed to axial compression forces F_1 and F_2 as illustrated in Figure 2.1.1.

V. Stojanović and P. Kozić, *Vibrations and Stability of Complex Beam Systems,*
Springer Tracts in Mechanical Engineering, DOI: 10.1007/978-3-319-13767-4_2

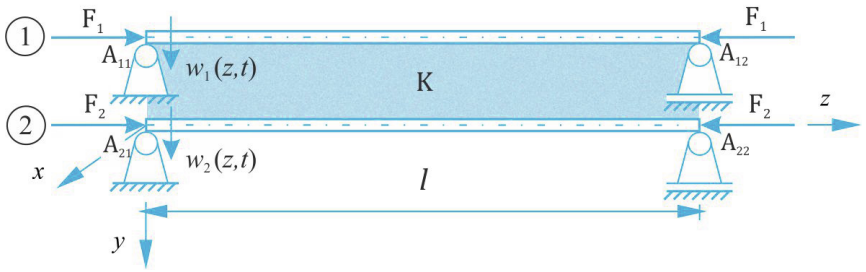

Fig. 2.1.1 An elastically connected double-beam system

Let the functions of longitudinal and transverse motion of the Rayleigh-beam system be as follows$u_{R1}(y,z,t)$, $w_{R1}(y,z,t)$, $u_{R2}(y,z,t)$ and$w_{R2}(y,z,t)$. Analogous to the relation (1.2.10), the following applies to the double-beam system

$$u_{R1}(y,z,t) = u_{R1}^0(z,t) - y\frac{\partial w_{R1}^0(z,t)}{\partial z}, \quad w_{R1}(y,z,t) = w_{R1}^0(z,t), \tag{2.1.1}$$

$$u_{R2}(y,z,t) = u_{R2}^0(z,t) - y\frac{\partial w_{R2}^0(z,t)}{\partial z}, \quad w_{R2}(y,z,t) = w_{R2}^0(z,t). \tag{2.1.2}$$

Deformation in the z- direction in the function of motion and the stress-deformation relation according to the Hooke's law are as follows

$$\varepsilon_{z1}(y,z,t) = \frac{\partial u_{R1}^0(z,t)}{\partial z} - y\frac{\partial^2 w_{R1}^0(z,t)}{\partial z^2}, \quad \varepsilon_{z2}(y,z,t) = \frac{\partial u_{R2}^0(z,t)}{\partial z} - y\frac{\partial^2 w_{R2}^0(z,t)}{\partial z^2}, \tag{2.1.3}$$

$$\sigma_{z1}(y,z,t) = E\varepsilon_{z1}(y,z,t), \qquad \sigma_{z2}(y,z,t) = E\varepsilon_{z2}(y,z,t). \tag{2.1.4}$$

Virtual work of inertial forces is expressed as

$$\delta W_{in1} = -\rho b_1 \int_0^l \int_{-\frac{h_1}{2}}^{\frac{h_1}{2}} \left[\frac{\partial^2 w_{R1}(y,z,t)}{\partial t^2}\delta w_{R1}(y,z,t) + \frac{\partial^2 u_{R1}(y,z,t)}{\partial t^2}\delta u_{R1}(y,z,t)\right] dydz, \tag{2.1.5}$$

$$\delta W_{in2} = -\rho b_2 \int_0^l \int_{-\frac{h_2}{2}}^{\frac{h_2}{2}} \left[\frac{\partial^2 w_{R2}(y,z,t)}{\partial t^2}\delta w_{R2}(y,z,t) + \frac{\partial^2 u_{R2}(y,z,t)}{\partial t^2}\delta u_{R2}(y,z,t)\right] dydz. \tag{2.1.6}$$

Virtual work of internal forces is

$$\delta W_{V1} = -b_1 \int_0^l \int_{-\frac{h_1}{2}}^{\frac{h_1}{2}} \sigma_{z1}(z,t)\delta\varepsilon_{z1}(z,t)dydz, \quad \delta W_{V2} = -b_2 \int_0^l \int_{-\frac{h_2}{2}}^{\frac{h_2}{2}} \sigma_{z2}(z,t)\delta\varepsilon_{z2}(z,t)dydz. \tag{2.1.7}$$

Virtual work of external forces is given by

$$\delta W_{ex1} = \int_0^l \left[\delta w_{R1}^0(z,t)K\left(w_{R2}^0(z,t) - w_{R1}^0(z,t)\right) + F_1\frac{\partial w_{R1}^0(z,t)}{\partial z}\frac{\partial \delta w_{R1}^0(z,t)}{\partial z}\right] dz, \tag{2.1.8}$$

$$\delta W_{ex2} = \int_0^l \left[\delta w_{R2}^0(z,t) K\left(w_{R1}^0(z,t) - w_{R2}^0(z,t)\right) + F_2 \frac{\partial w_{R2}^0(z,t)}{\partial z} \frac{\partial \delta w_{R2}^0(z,t)}{\partial z} \right] dz, \tag{2.1.9}$$

Based on the principle of virtual work $\delta W_{ini} + \delta W_{Vi} + \delta W_{exi} = 0,\ i = 1,2$ and the equations (2.1.5-2.1.9), we have

$$-b_1 \int_0^l \int_{-\frac{h_1}{2}}^{\frac{h_1}{2}} \sigma_{z1}(z,t) \delta \varepsilon_{z1}(z,t) dy dz -$$

$$-\rho b_1 \int_0^l \int_{-\frac{h_1}{2}}^{\frac{h_1}{2}} \left[\frac{\partial^2 w_{R1}(y,z,t)}{\partial t^2} \delta w_{R1}(y,z,t) + \frac{\partial^2 u_{R1}(y,z,t)}{\partial t^2} \delta u_{R1}(y,z,t) \right] dy dz$$

$$+ \int_0^l \left[\delta w_{R1}^0(z,t) K\left(w_{R2}^0(z,t) - w_{R1}^0(z,t)\right) + F_1 \frac{\partial w_{R1}^0(z,t)}{\partial z} \frac{\partial \delta w_{R1}^0(z,t)}{\partial z} \right] dz = 0, \tag{2.1.10}$$

$$-b_2 \int_0^l \int_{-\frac{h_2}{2}}^{\frac{h_2}{2}} \sigma_{z2}(z,t) \delta \varepsilon_{z2}(z,t) dy dz -$$

$$-\rho b_2 \int_0^l \int_{-\frac{h_2}{2}}^{\frac{h_2}{2}} \left[\frac{\partial^2 w_{R2}(y,z,t)}{\partial t^2} \delta w_{R2}(y,z,t) + \frac{\partial^2 u_{R2}(y,z,t)}{\partial t^2} \delta u_{R2}(y,z,t) \right] dy dz$$

$$+ \int_0^l \left[\delta w_{R2}^0(z,t) K\left(w_{R1}^0(z,t) - w_{R2}^0(z,t)\right) + F_2 \frac{\partial w_{R2}^0(z,t)}{\partial z} \frac{\partial \delta w_{R2}^0(z,t)}{\partial z} \right] dz = 0. \tag{2.1.11}$$

By successive application of Green's theorem on the expressions (2.1.10-2.1.11), we obtain the equations of transverse vibration for elastically connected Rayleigh-beam system in the following form

$$\rho A_1 \frac{\partial^2 w_{R1}^0(z,t)}{\partial t^2} - \rho I_{x1} \frac{\partial^4 w_{R1}^0(z,t)}{\partial z^2 \partial t^2} + E I_{x1} \frac{\partial^4 w_{R1}^0(z,t)}{\partial z^4} + F_1 \frac{\partial^2 w_{R1}^0(z,t)}{\partial z^2}$$
$$+ K\left(w_{R1}^0(z,t) - w_{R2}^0(z,t)\right) = 0, \tag{2.1.12}$$

$$\rho A_2 \frac{\partial^2 w_{R2}^0(z,t)}{\partial t^2} - \rho I_{x2} \frac{\partial^4 w_{R2}^0(z,t)}{\partial z^2 \partial t^2} + E I_{x2} \frac{\partial^4 w_{R2}^0(z,t)}{\partial z^4} + F_2 \frac{\partial^2 w_{R2}^0(z,t)}{\partial z^2}$$
$$+ K\left(w_{R2}^0(z,t) - w_{R1}^0(z,t)\right) = 0, \tag{2.1.13}$$

where ρ is mass density, A the area of a cross-section, E Young's modulus, I_x the second moment of inertia for the cross-sectional area of the beam for the x-axis. The initial and boundary conditions for the elastically connected double-beam system composed of simply supported Rayleigh beams are

$$w_{Ri}^0(z,0) = w_{i0}(z), \quad \frac{dw_{R1}^0(z,0)}{dt} = v_{i0}(z), \tag{2.1.14}$$

$$w_{Ri}^0(0,t) = \frac{d^2 w_{R1}^0(0,t)}{dz^2} = \frac{d^2 w_{R1}^0(l,t)}{dz^2} = w_{Ri}^0(l,t) = 0, \quad i = 1,2. \quad (2.1.15)$$

Considering the harmonic motion of beams' points, we assume the solutions to the equations (2.1.12) and (2.1.13) as the product of functions

$$w_{Ri}^0(z,t) = \sum_{n=1}^{\infty} Z_n(z) T_{in}(t), \qquad i = 1,2, \quad (2.1.16)$$

where $T_{in}(t)$ is the unknown time function and $Z_n(z)$ is the mode shape function

$$Z_n(z) = \sin(k_n z), \qquad k_n = n\pi/l, \qquad n = 1,2,3, \ldots \quad (2.1.17)$$

By substituting the assumed solutions (2.1.16) into the equations for transverse vibration of the elastically connected Rayleigh double-beam system (2.1.12) and (2.1.13), we get the set of two differential equations in the form

$$\sum_{n=1}^{\infty} \left\{ J_1 \frac{d^2 T_{1n}}{dt^2} + (N_1 - F_1\eta_1) T_{1n} - H_1 T_{2n} \right\} Z_n = 0, \quad (2.1.18)$$

$$\sum_{n=1}^{\infty} \left\{ J_2 \frac{d^2 T_{2n}}{dt^2} + (N_2 - F_2\eta_2) T_{2n} - H_2 T_{1n} \right\} Z_n = 0, \quad (2.1.19)$$

where the following substitutions $i = 1,2$ have been introduced

$$J_i = 1 + C_{ri}^2 k_n^2, \; N_i = C_{bi}^2 k_n^4 + H_i, H_i = \frac{K}{\rho A_i}, \; \eta_i = \frac{k_n^2}{\rho A_i}, \; C_{ri} = \sqrt{\frac{I_i}{A_i}}, C_{bi} = \sqrt{\frac{EI_i}{\rho A_i}}.$$

The solutions to differential equations (2.1.18) and (2.1.19) can be assumed in the following form

$$T_{1n} = C_n e^{j\omega_n t}, \qquad T_{2n} = D_n e^{j\omega_n t}, \qquad j = \sqrt{-1}, \quad (2.1.20)$$

where ω_n denotes the natural frequency of the system. If we substitute the expression (2.1.20) into equations (2.1.18) and (2.1.19), we get the set of homogeneous algebraic equations

$$(N_1 - F_1\eta_1 - J_1\omega_n^2) C_n - H_1 D_n = 0, \quad (2.1.21)$$

$$(N_2 - F_2\eta_2 - J_2\omega_n^2) D_n - H_2 C_n = 0. \quad (2.1.22)$$

The system of algebraic equations (2.1.21) and (2.1.22) has non-trivial solutions when the matrix determinant equals zero. From this condition, the characteristic system equation in the form of a fourth-degree polynomial is obtained

$$J_1J_2\omega_n^4 - (N_1J_2 + N_2J_1 - F_1\eta_1J_2 - F_2\eta_2J_1)\omega_n^2 + (N_1 - F_1\eta_1)(N_2 - F_2\eta_2) - H_1H_2 = 0. \quad (2.1.23)$$

The characteristic equation (2.1.23) has two different positive real roots

$$\omega_{n1}^2 = \frac{J_2(N_1 - F_1\eta_1) + J_1(N_2 - F_2\eta_2)}{2J_1J_2} - \frac{1}{2J_1J_2}\sqrt{[J_2(N_1 - F_1\eta_1) - J_1(N_2 - F_2\eta_2)]^2 + 4J_1J_2H_1H_2}, \quad (2.1.24)$$

$$\omega_{n2}^2 = \frac{J_2(N_1 - F_1\eta_1) + J_1(N_2 - F_2\eta_2)}{2J_1J_2} + \frac{1}{2J_1J_2}\sqrt{[J_2(N_1 - F_1\eta_1) - J_1(N_2 - F_2\eta_2)]^2 + 4J_1J_2H_1H_2}\,. \quad (2.1.25)$$

The amplitude ratio of vibration mode for each frequency ω_{n1}, ω_{n2} is given by

$$\alpha_{ni} = \frac{C_n}{D_n} = \frac{H_1}{N_1 - F_1\eta_1 - J_1\omega_{ni}^2} = \frac{N_2 - F_2\eta_2 - J_2\omega_{ni}^2}{H_2}, \ \ i = 1,2. \quad (2.1.26)$$

The general solution to the system of differential equations (2.1.18) and (2.1.19) is in the form of

$$T_{1n}(t) = C_{1n}e^{j\omega_{n1}t} + C_{2n}e^{-j\omega_{n1}t} + C_{3n}e^{j\omega_{n2}t} + C_{4n}e^{-j\omega_{n2}t}, \quad (2.1.27)$$

$$T_{2n}(t) = D_{1n}e^{j\omega_{n1}t} + D_{2n}e^{-j\omega_{n1}t} + D_{3n}e^{j\omega_{n2}t} + D_{4n}e^{-j\omega_{n2}t}, \quad (2.1.28)$$

i.e.

$$T_{1n}(t) = \sum_{i=1}^{2}[A_{ni}\sin(\omega_{ni}t) + B_{ni}\cos(\omega_{ni}t)], \quad (2.1.29)$$

$$T_{2n}(t) = \sum_{i=1}^{2}\alpha_{ni}[A_{ni}\sin(\omega_{ni}t) + B_{ni}\cos(\omega_{ni}t)], \quad (2.1.30)$$

where A_{ni} and B_{ni} (i = 1, 2) denote unknown constants. The solutions to the system of partial differential equations (2.1.12) and (2.1.13) of free transverse vibration of the system made up of two elastically connected simply supported beams subjected to rotary inertia are in the following form

$$w_{R1}^0(z,t) = \sum_{n=1}^{\infty} Z_n(z)T_{1n}(t) = \sum_{n=1}^{\infty} \sin(k_n z) \sum_{i=1}^{2} [A_{ni}\sin(\omega_{ni}t) + B_{ni}\cos(\omega_{ni}t)], \quad (2.1.31)$$

$$w_{R2}^0(z,t) = \sum_{n=1}^{\infty} Z_n(z)T_{2n}(t) = \sum_{n=1}^{\infty} \sin(k_n z) \sum_{i=1}^{2} \alpha_{ni}[A_{ni}\sin(\omega_{ni}t) + B_{ni}\cos(\omega_{ni}t)]. \quad (2.1.32)$$

Unknown constants A_{ni} and B_{ni} (i = 1, 2) are determined from initial conditions (2.1.14) by using the orthogonality condition of functions expressed by

$$\int_0^l Z_n Z_m dx = \int_0^l \sin(k_n z)\sin(k_m z)\mathrm{d}z = c\delta_{nm}, \quad (2.1.33)$$

$$c = \int_0^l Z_n^2 dx = \int_0^l [\sin(k_n z)]^2 \mathrm{d}z = \frac{l}{2},$$

where δ_{nm} is the Kronecker delta function. If we enter the initial conditions (2.1.14) into expressions (2.1.31) and (2.1.32), we obtain

$$w_{R1}^0(z,0) = w_{10}(z) = \sum_{n=1}^{\infty} \sin(k_n z) \sum_{i=I}^{2} B_{ni},$$

$$w_{R2}^0(z,0) = w_{20}(z) = \sum_{n=1}^{\infty} \sin(k_n z) \sum_{i=I}^{2} \alpha_{ni} B_{ni}, \quad (2.1.34)$$

$$\frac{dw_{R1}^0(z,0)}{dt} = v_{10}(z) = \sum_{n=1}^{\infty} \sin(k_n z) \sum_{i=I}^{2} \omega_{ni} A_{ni},$$

$$\frac{dw_{R2}^0(z,0)}{dt} = v_{20}(z) = \sum_{n=1}^{\infty} \sin(k_n z) \sum_{i=I}^{2} \alpha_{ni}\omega_{ni} A_{ni}. \quad (2.1.35)$$

By multiplying the expressions (2.1.34) and (2.1.35) by the eigenfunction Z_n, then integrating them with respect to z from 0 to l and using the orthogonality condition (2.1.33), we have

$$\frac{2}{l}\int_0^l w_{10}\sin(k_n z)\,dz = \sum_{i=I}^{2} B_{ni}, \qquad \frac{2}{l}\int_0^l w_{20}\sin(k_n z)\,dz = \sum_{i=I}^{2} \alpha_{ni} B_{ni}, \quad (2.1.36)$$

$$\frac{2}{l}\int_0^l v_{10}\sin(k_n z)\,dz = \sum_{i=I}^{2} \omega_{ni} A_{ni}, \qquad \frac{2}{l}\int_0^l v_{20}\sin(k_n z)\,dz = \sum_{i=I}^{2} \alpha_{ni}\omega_{ni} A_{ni}. \quad (2.1.37)$$

After solving the system of equations (2.1.36) and (2.1.37), we determine the unknown constants in the following form

$$A_{n1} = \frac{2}{\omega_{n1}(\alpha_{n2} - \alpha_{n1})l} \int_0^l (v_{10}\alpha_{n2} - v_{20}) \sin(k_n z)\, \mathrm{d}z, \tag{2.1.38}$$

$$A_{n2} = \frac{2}{\omega_{n2}(\alpha_{n1} - \alpha_{n2})l} \int_0^l (v_{20}\alpha_{n1} - v_{10}) \sin(k_n z)\, \mathrm{d}z, \tag{2.1.39}$$

$$B_{n1} = \frac{2}{(\alpha_{n2} - \alpha_{n1})l} \int_0^l (w_{10}\alpha_{n2} - w_{20}) \sin(k_n z)\, \mathrm{d}z, \tag{2.1.40}$$

$$B_{n2} = \frac{2}{(\alpha_{n1} - \alpha_{n2})l} \int_0^l (w_{10}\alpha_{n1} - w_{20}) \sin(k_n z)\, \mathrm{d}z. \tag{2.1.41}$$

2.2 Free Vibrations of Two Elastically Connected Timoshenko Beams

Let us consider the influences of rotary inertia and transverse shear on free transverse vibration of the double-beam system elastically connected by a Winkler layer, Stojanović et al. [12]. Let, as in the case of the Rayleigh model, the beams be of the same length l and connected by an elastic layer of the stiffness modulus K. At its ends, the beams are exposed to the action of axial compression forces F_1 and F_2, Figure 2.1.1. Let the functions of longitudinal and transversal motion as well as the angle of the cross-section rotation be $u_{T1}(y,z,t)$, $w_{T1}(y,z,t), \psi^0_{T1}(z,t), u_{T2}(y,z,t), w_{T2}(y,z,t)$ and $\psi^0_{T2}(z,t)$ respectively. Analogous to the relation (1.2.18), the following equations of motion now apply to the double-beam system

$$u_{T1}(y,z,t) = u^0_{T1}(z,t) + y\psi^0_{T1}(z,t), \qquad w_{T1}(y,z,t) = w^0_{T1}(z,t), \tag{2.2.1}$$

$$u_{T2}(y,z,t) = u^0_{T2}(z,t) + y\psi^0_{T2}(z,t), \qquad w_{T2}(y,z,t) = w^0_{T2}(z,t). \tag{2.2.2}$$

Deformation in the function of motion and the stress-strain ratio according to the Hooke's law are

$$\varepsilon_{z1}(z,t) = \frac{\partial u^0_{T1}(z,t)}{\partial z} + y\frac{\partial \psi^0_{T1}(z,t)}{\partial z}, \quad \gamma_{zy1}(z,t) = \frac{\partial w^0_{T1}(z,t)}{\partial z} + \psi^0_{T1}(z,t), \tag{2.2.3}$$

$$\varepsilon_{z2}(z,t) = \frac{\partial u^0_{T2}(z,t)}{\partial z} + y\frac{\partial \psi^0_{T2}(z,t)}{\partial z}, \quad \gamma_{zy2}(z,t) = \frac{\partial w^0_{T2}(z,t)}{\partial z} + \psi^0_{T2}(z,t), \tag{2.2.4}$$

$$\begin{Bmatrix} \sigma_{z1} \\ \tau_{zy1} \end{Bmatrix} = \begin{bmatrix} E & 0 \\ 0 & kG \end{bmatrix} \begin{Bmatrix} \varepsilon_{z1} \\ \gamma_{zy1} \end{Bmatrix}, \qquad \begin{Bmatrix} \sigma_{z2} \\ \tau_{zy2} \end{Bmatrix} = \begin{bmatrix} E & 0 \\ 0 & kG \end{bmatrix} \begin{Bmatrix} \varepsilon_{z2} \\ \gamma_{zy2} \end{Bmatrix}. \tag{2.2.5}$$

Virtual work of inertial forces is

$$\delta W_{in1} = -\rho b_1 \int_0^l \int_{-\frac{h_1}{2}}^{\frac{h_1}{2}} \left[\frac{\partial^2 w_{T1}(y,z,t)}{\partial t^2} \delta w_{T1}(y,z,t) + \frac{\partial^2 u_{T1}(y,z,t)}{\partial t^2} \delta u_{T1}(y,z,t) \right] dydz, \quad (2.2.6)$$

$$\delta W_{in2} = -\rho b_2 \int_0^l \int_{-\frac{h_2}{2}}^{\frac{h_2}{2}} \left[\frac{\partial^2 w_{T2}(y,z,t)}{\partial t^2} \delta w_{T2}(y,z,t) + \frac{\partial^2 u_{T2}(y,z,t)}{\partial t^2} \delta u_{T2}(y,z,t) \right] dydz. \quad (2.2.7)$$

Virtual work of internal forces is

$$\delta W_{V1} = -b_1 \int_0^l \int_{-\frac{h_1}{2}}^{\frac{h_1}{2}} \left[\sigma_{z1}(z,t) \delta \varepsilon_{z1}(z,t) + \tau_{zy1}(z,t) \delta \gamma_{zy1}(z,t) \right] dydz, \quad (2.2.8)$$

$$\delta W_{V2} = -b_2 \int_0^l \int_{-\frac{h_2}{2}}^{\frac{h_2}{2}} \left[\sigma_{z2}(z,t) \delta \varepsilon_{z2}(z,t) + \tau_{zy2}(z,t) \delta \gamma_{zy2}(z,t) \right] dydz. \quad (2.2.9)$$

Virtual work of external forces is given by

$$\delta W_{ex1} = \int_0^l \left[\delta w_{T1}^0(z,t) K \left(w_{T2}^0(z,t) - w_{T1}^0(z,t) \right) + F_1 \frac{\partial w_{T1}^0(z,t)}{\partial z} \frac{\partial \delta w_{T1}^0(z,t)}{\partial z} \right] dz, \quad (2.2.10)$$

$$\delta W_{ex2} = \int_0^l \left[\delta w_{T2}^0(z,t) K \left(w_{T1}^0(z,t) - w_{T2}^0(z,t) \right) + F_2 \frac{\partial w_{T2}^0(z,t)}{\partial z} \frac{\partial \delta w_{T2}^0(z,t)}{\partial z} \right] dz, \quad (2.2.11)$$

Substituting the equations (2.2.6-2.2.11) into a general equation of virtual work principle $\delta W_{ini} + \delta W_{Vi} + \delta W_{exi} = 0,\ i = 1,2$, yields

$$\begin{aligned} &-b_1 \int_0^l \int_{-\frac{h_1}{2}}^{\frac{h_1}{2}} \left[\sigma_{z1}(z,t) \delta \varepsilon_{z1}(z,t) + \tau_{zy1}(z,t) \delta \gamma_{zy1}(z,t) \right] dydz - \\ &-\rho b_1 \int_0^l \int_{-\frac{h_1}{2}}^{\frac{h_1}{2}} \left[\frac{\partial^2 w_{T1}(y,z,t)}{\partial t^2} \delta w_{T1}(y,z,t) + \frac{\partial^2 u_{T1}(y,z,t)}{\partial t^2} \delta u_{T1}(y,z,t) \right] dydz + \\ &+ \int_0^l \left[\delta w_{T1}^0(z,t) K \left(w_{T2}^0(z,t) - w_{T1}^0(z,t) \right) + F_1 \frac{\partial w_{T1}^0(z,t)}{\partial z} \frac{\partial \delta w_{T1}^0(z,t)}{\partial z} \right] dz = 0, \end{aligned} \quad (2.2.12)$$

$$\begin{aligned} &-b_2 \int_0^l \int_{-\frac{h_2}{2}}^{\frac{h_2}{2}} \left[\sigma_{z2}(z,t) \delta \varepsilon_{z1}(z,t) + \tau_{zy2}(z,t) \delta \gamma_{zy2}(z,t) \right] dydz - \\ &-\rho b_2 \int_0^l \int_{-\frac{h_2}{2}}^{\frac{h_2}{2}} \left[\frac{\partial^2 w_{T2}(y,z,t)}{\partial t^2} \delta w_{T2}(y,z,t) + \frac{\partial^2 u_{T2}(y,z,t)}{\partial t^2} \delta u_{T2}(y,z,t) \right] dydz + \\ &+ \int_0^l \left[\delta w_{T2}^0(z,t) K \left(w_{T1}^0(z,t) - w_{T2}^0(z,t) \right) + F_2 \frac{\partial w_{T2}^0(z,t)}{\partial z} \frac{\partial \delta w_{T2}^0(z,t)}{\partial z} \right] dz = 0. \end{aligned} \quad (2.2.13)$$

By successive application of Green's theorem on the expressions (2.2.12-2.2.13), we get the equations of the vibration for the system consisting of two elastically connected Timoshenko beams in the following form

$$\rho A_1 \frac{\partial^2 w_{T1}^0(z,t)}{\partial t^2} - GA_1 k\left(\frac{\partial^2 w_{T1}^0(z,t)}{\partial z^2} + \frac{\partial \psi_{T1}^0(z,t)}{\partial x}\right) + F_1 \frac{\partial^2 w_{T1}^0(z,t)}{\partial z^2} + K\left(w_{T1}^0(z,t) - w_{T2}^0(z,t)\right) = 0, \quad (2.2.14)$$

$$\rho I_{x1} \frac{\partial^2 \psi_{T1}^0(z,t)}{\partial t^2} - EI_{x1} \frac{\partial^2 \psi_{T1}^0(z,t)}{\partial z^2} + GA_1 k\left(\frac{\partial w_{T1}^0(z,t)}{\partial z} + \psi_{T1}^0(z,t)\right) = 0, \quad (2.2.15)$$

$$\rho A_2 \frac{\partial^2 w_{T1}^0(z,t)}{\partial t^2} - GA_2 k\left(\frac{\partial^2 w_{T2}^0(z,t)}{\partial z^2} + \frac{\partial \psi_{T2}^0(z,t)}{\partial x}\right) + F_2 \frac{\partial^2 w_{T2}^0(z,t)}{\partial z^2} + K\left(w_{T2}^0(z,t) - w_{T1}^0(z,t)\right) = 0, \quad (2.2.16)$$

$$\rho I_{x2} \frac{\partial^2 \psi_{T2}^0(z,t)}{\partial t^2} - EI_{x2} \frac{\partial^2 \psi_{T2}^0(z,t)}{\partial z^2} + GA_2 k\left(\frac{\partial w_{T2}^0(z,t)}{\partial z} + \psi_{T2}^0(z,t)\right) = 0, \quad (2.2.17)$$

where ρ is mass density, A the area of a cross-section, E Young's modulus, G shear modulus, k shear factor, I_x the moment of inertia for the cross-sectional area of the beam for the x-axis. The initial and boundary conditions for the two elastically connected simply supported Timoshenko beams are

$$w_{Ti}^0(z,0) = \widetilde{w}_{i0}(z), \quad \frac{dw_{Ti}^0(z,0)}{dt} = \widetilde{v}_{i0}(z), \quad \psi_{Ti}^0(z,0) = \widetilde{\psi}_{i0}(z), \quad \frac{d\psi_{Ti}^0(z,0)}{dt} = \widetilde{\Theta}_{i0}(z), \quad (2.2.18)$$

$$w_{Ti}^0(0,t) = \frac{d^2 w_{Ti}^0(0,t)}{dz^2} = \frac{d^2 w_{Ti}^0(l,t)}{dz^2} = w_{Ti}^0(l,t) = 0, \quad i = 1,2, \quad (2.2.19)$$

$$\frac{d\psi_{Ti}^0(0,t)}{dz} = \frac{d\psi_{Ti}^0(l,t)}{dz} = 0, \quad i = 1,2. \quad (2.2.20)$$

Considering the harmonic motion of beams' points, we assume the solutions to the equations (2.2.14-2.2.17) as the product of functions

$$w_{Ti}^0(z,t) = \sum_{n=1}^{\infty} Z_n(z)\tilde{T}_{in}(t), \quad \psi_{Ti}^0(z,t) = \sum_{n=1}^{\infty} \Psi_n(z)\tilde{T}_{in(r)}(t), \quad i = 1,2, \quad (2.2.21)$$

where $\tilde{T}_{in}(t)$ and $\tilde{T}_{in(r)}(t)$ are the unknown time functions, while $Z_n(z)$ and $\Psi_n(z)$ are the mode shapes functions

$$Z_n(z) = \sin(k_n z), \quad \Psi_n(z) = \cos(k_n z), k_n = n\pi/l, \qquad n = 1,2,3,\ldots \quad (2.2.22)$$

By substituting the assumed solutions (2.2.21) into the equations of transverse vibration of the system composed of two elastically connected Timoshenko beams (2.2.14-2.2.17), we get a system of four differential equations of the second degree in the form

$$\begin{bmatrix} A_1\rho & 0 & 0 & 0 \\ 0 & A_2\rho & 0 & 0 \\ 0 & 0 & I_1\rho & 0 \\ 0 & 0 & 0 & I_2\rho \end{bmatrix} \begin{Bmatrix} \ddot{\tilde{T}}_{1n}(t) \\ \ddot{\tilde{T}}_{2n}(t) \\ \ddot{\tilde{T}}_{1n(r)}(t) \\ \ddot{\tilde{T}}_{2n(r)}(t) \end{Bmatrix} +$$

$$+ \begin{bmatrix} A_1Gkk_n{}^2 - F_1k_n{}^2 + K & -K & A_1Gkk_n & 0 \\ -K & A_2Gkk_n{}^2 - F_2k_n{}^2 + K & 0 & A_2Gkk_n \\ A_1Gkk_n & 0 & A_1Gk + EI_1k_n{}^2 & 0 \\ 0 & A_2Gkk_n & 0 & A_2Gk + EI_2k_n{}^2 \end{bmatrix} \begin{Bmatrix} \tilde{T}_{1n}(t) \\ \tilde{T}_{2n}(t) \\ \tilde{T}_{1n(r)}(t) \\ \tilde{T}_{2n(r)}(t) \end{Bmatrix} = \begin{Bmatrix} 0 \\ 0 \\ 0 \\ 0 \end{Bmatrix}. \quad (2.2.23)$$

We assume the solutions of the equation system (2.2.23) in the following form

$$\tilde{T}_{1n} = \tilde{C}_n e^{j\tilde{\omega}_n t}, \ \tilde{T}_{2n} = \tilde{D}_n e^{j\tilde{\omega}_n t}, \ \tilde{T}_{1n(r)}(t) = \tilde{C}_{n(r)} e^{j\tilde{\omega}_n t},$$
$$\tilde{T}_{2n(r)}(t) = \tilde{D}_{n(r)} e^{j\tilde{\omega}_n t}, j = \sqrt{-1}. \quad (2.2.24)$$

If we substitute the assumed solutions (2.2.24) into the system of equations (2.2.23), we get a homogeneous set of algebraic equations which has non-trivial solutions when the system determinant equals zero

$$\begin{bmatrix} A_1Gkk_n{}^2 - A_1\rho\tilde{\omega}_n{}^2 - F_1k_n{}^2 + K & -K & A_1Gkk_n & 0 \\ -K & A_2Gkk_n{}^2 - A_2\rho\tilde{\omega}_n{}^2 - F_2k_n{}^2 + K & 0 & A_2Gkk_n \\ A_1Gkk_n & 0 & A_1Gk + EI_1k_n{}^2 - I_1\rho\tilde{\omega}_n{}^2 & 0 \\ 0 & A_2Gkk_n & 0 & A_2Gk + EI_2k_n{}^2 - I_2\rho\tilde{\omega}_n{}^2 \end{bmatrix} \begin{Bmatrix} \tilde{C}_n \\ \tilde{D}_n \\ \tilde{C}_{n(r)} \\ \tilde{D}_{n(r)} \end{Bmatrix} = \begin{Bmatrix} 0 \\ 0 \\ 0 \\ 0 \end{Bmatrix}. \quad (2.2.25)$$

Characteristic system equation (2.2.25) is obtained from the conditions for the existence of non-trivial solutions in the form of an eighth-degree polynomial. If we introduce a substitution $\tilde{\lambda} = \tilde{\omega}_n^2$, the frequency equation is

$$\tilde{\lambda}^4 + \tilde{c}_1\tilde{\lambda}^3 + \tilde{c}_2\tilde{\lambda}^2 + \tilde{c}_3\tilde{\lambda} + \tilde{c}_4 = 0. \quad (2.2.26)$$

Constants $\tilde{c}_1, \tilde{c}_2, \tilde{c}_3$ and $\tilde{c}_4$ are given in the Appendix 2.2.1. The polynomial of the fourth degree may be factored in the following form

$$\left(\tilde{\lambda}^2+\tilde{p}_1\tilde{\lambda}+\tilde{q}_1\right)\left(\lambda^2+\tilde{p}_2\tilde{\lambda}+\tilde{q}_2\right)=0, \tag{2.2.27}$$

where

$$\begin{Bmatrix}\tilde{p}_1\\ \tilde{p}_2\end{Bmatrix}=\frac{1}{2}\left[\tilde{c}_1\pm\sqrt{\tilde{c}_1^2-4\tilde{c}_2+4\tilde{\chi}_1}\right],$$

$$\begin{Bmatrix}\tilde{q}_1\\ \tilde{q}_2\end{Bmatrix}=\frac{1}{2}\left[\tilde{\chi}_1\pm\frac{\tilde{c}_1\tilde{\chi}_1-2\tilde{c}_3}{\sqrt{\tilde{c}_1^2-4\tilde{c}_2+4\tilde{\chi}_1}}\right].$$

In the expressions $\tilde{\chi}_1$ presents one of the roots of the third-degree equation

$$\tilde{\chi}^3-\tilde{c}_2\tilde{\chi}^2+(\tilde{c}_1\tilde{c}_3-4\tilde{c}_4)\tilde{\chi}+(4\tilde{c}_2\tilde{c}_4-\tilde{c}_3^2-\tilde{c}_1^2\tilde{c}_4)=0. \tag{2.2.28}$$

After factoring the equation (2.2.26), the solutions may be written as a square of natural frequencies

$$\tilde{\omega}_{n1}^2=\tilde{\lambda}_1=-\frac{\tilde{p}_1}{2}-\sqrt{\frac{\tilde{p}_1^2}{4}-\tilde{q}_1},\tilde{\omega}_{n2}^2=\tilde{\lambda}_2=-\frac{\tilde{p}_2}{2}-\sqrt{\frac{\tilde{p}_2^2}{4}-\tilde{q}_2},$$

$$\tilde{\omega}_{n3}^2=\tilde{\lambda}_3=-\frac{\tilde{p}_2}{2}+\sqrt{\frac{\tilde{p}_2^2}{4}-\tilde{q}_2},\qquad \tilde{\omega}_{n4}^2=\tilde{\lambda}_4=-\frac{\tilde{p}_1}{2}+\sqrt{\frac{\tilde{p}_1^2}{4}-\tilde{q}_1}. \tag{2.2.29}$$

The three roots of the equation (2.2.28) are

$$\tilde{\chi}_1=\tilde{c}_2/3+2\sqrt{-\tilde{Q}}\cos(\tilde{\theta}/3),$$

$$\tilde{\chi}_2=\tilde{c}_2/3+2\sqrt{-\tilde{Q}}\cos[(\tilde{\theta}+2\pi)/3], \tag{2.2.30}$$

$$\tilde{\chi}_3=\tilde{c}_2/3+2\sqrt{-\tilde{Q}}\cos[(\tilde{\theta}+4\pi)/3],$$

where

$$\tilde{\theta}=cos^{-1}\left(\tilde{S}/\sqrt{-\tilde{Q}^3}\right),\quad \tilde{Q}=-\frac{1}{9}(\tilde{c}_2^2-3\tilde{c}_1\tilde{c}_3+12\tilde{c}_4),$$

$$\tilde{S}=\frac{1}{54}(2\tilde{c}_2^3-9\tilde{c}_1\tilde{c}_2\tilde{c}_3+27\tilde{c}_3^2+27\tilde{c}_1^2\tilde{c}_4-72\tilde{c}_2\tilde{c}_4).$$

By choosing one of the three roots in the expression (2.2.30), we get unique solutions to the equation (2.2.26) where four natural frequencies of a system are real positive roots $\tilde{\omega}_{n1}=\sqrt{\tilde{\lambda}_1}$, $\tilde{\omega}_{n2}=\sqrt{\tilde{\lambda}_2}$, $\tilde{\omega}_{n3}=\sqrt{\tilde{\lambda}_3}$, $\tilde{\omega}_{n4}=\sqrt{\tilde{\lambda}_4}$. The amplitude ratio is determined from the equation (2.2.25) for each frequency,

Appendix 2.2.2. General solution to the system of differential equations (2.2.23) is of the following form

$$\tilde{T}_{1n}(t) = \tilde{C}_{1n}e^{j\tilde{\omega}_{n1}t} + \tilde{C}_{2n}e^{-j\tilde{\omega}_{n1}t} + \tilde{C}_{3n}e^{j\tilde{\omega}_{n2}t} + \tilde{C}_{4n}e^{-j\tilde{\omega}_{n2}t}, \quad (2.2.31)$$

$$\tilde{T}_{2n}(t) = \widetilde{D}_{1n}e^{j\tilde{\omega}_{n1}t} + \widetilde{D}_{2n}e^{-j\tilde{\omega}_{n1}t} + \widetilde{D}_{3n}e^{j\tilde{\omega}_{n2}t} + \widetilde{D}_{4n}e^{-j\tilde{\omega}_{n2}t}, \quad (2.2.32)$$

$$\tilde{T}_{1n(r)}(t) = \tilde{C}_{1n(r)}e^{j\tilde{\omega}_{n3}t} + \tilde{C}_{2n(r)}e^{-j\tilde{\omega}_{n3}t} + \tilde{C}_{3n(r)}e^{j\tilde{\omega}_{n4}t} + \tilde{C}_{4n(r)}e^{-j\tilde{\omega}_{n4}t}, \quad (2.2.33)$$

$$\tilde{T}_{2n(r)}(t) = \widetilde{D}_{1n(r)}e^{j\tilde{\omega}_{n3}t} + \widetilde{D}_{2n(r)}e^{-j\tilde{\omega}_{n3}t} + \widetilde{D}_{3n(r)}e^{j\tilde{\omega}_{n4}t} + \widetilde{D}_{4n(r)}e^{-j\tilde{\omega}_{n4}t}, \quad (2.2.34)$$

i.e.

$$\tilde{T}_{1n}(t) = \sum_{i=\mathrm{I}}^{2}\left[\tilde{A}_{ni}\sin(\tilde{\omega}_{ni}t) + \tilde{B}_{ni}\cos(\tilde{\omega}_{ni}t)\right], \quad (2.2.35)$$

$$\tilde{T}_{2n}(t) = \sum_{i=\mathrm{I}}^{2}\tilde{\alpha}_{ni}\left[\tilde{A}_{ni}\sin(\tilde{\omega}_{ni}t) + \tilde{B}_{ni}\cos(\tilde{\omega}_{ni}t)\right], \quad (2.2.36)$$

$$\tilde{T}_{1n(r)}(t) = \sum_{g=3}^{4}\left[\tilde{A}_{ng}\sin\left(\tilde{\omega}_{ng}t\right) + \tilde{B}_{ng}\cos\left(\tilde{\omega}_{ng}t\right)\right], \quad (2.2.37)$$

$$\tilde{T}_{2n(r)}(t) = \sum_{g=3}^{4}\tilde{\alpha}_{ng}\left[\tilde{A}_{ng}\sin\left(\tilde{\omega}_{ng}t\right) + \tilde{B}_{ng}\cos\left(\tilde{\omega}_{ng}t\right)\right], \quad (2.2.38)$$

where $\tilde{A}_{ni}$,$\tilde{B}_{ni}$,$\tilde{A}_{ng}$ and $\tilde{B}_{ng}$ (i = 1, 2; g=3, 4;) are unknown constants. The solutions to the set of partial differential equations of free transverse vibrations for the system composed of two elastically connected simply supported beams considering the effects of rotary inertia and transverse shear are

$$w_{T1}^{0}(z,t) = \sum_{n=1}^{\infty}Z_n(z)\tilde{T}_{1n}(t) = \sum_{n=1}^{\infty}\sin(k_n z)\sum_{i=1}^{2}\left[\tilde{A}_{ni}\sin(\tilde{\omega}_{ni}t) + \tilde{B}_{ni}\cos(\tilde{\omega}_{ni}t)\right], \quad (2.2.39)$$

$$w_{T2}^{0}(z,t) = \sum_{n=1}^{\infty}Z_n(z)\tilde{T}_{2n}(t) = \sum_{n=1}^{\infty}\sin(k_n z)\sum_{i=1}^{2}\tilde{\alpha}_{ni}\left[\tilde{A}_{ni}\sin(\tilde{\omega}_{ni}t) + \tilde{B}_{ni}\cos(\tilde{\omega}_{ni}t)\right]. \quad (2.2.40)$$

$$\psi_{T1}^{0}(z,t) = \sum_{n=1}^{\infty}\Psi_n(z)\tilde{T}_{1n(r)}(t) = \sum_{n=1}^{\infty}\cos(k_n z)\sum_{g=3}^{4}\left[\tilde{A}_{ng}\sin\left(\tilde{\omega}_{ng}t\right) + \tilde{B}_{ng}\cos\left(\tilde{\omega}_{ng}t\right)\right], \quad (2.2.41)$$

$$\psi_{T2}^{0}(z,t) = \sum_{n=1}^{\infty}\Psi_n(z)\tilde{T}_{2n(r)}(t) = \sum_{n=1}^{\infty}\cos(k_n z)\sum_{g=3}^{4}\tilde{\alpha}_{ng}\left[\tilde{A}_{ng}\sin\left(\tilde{\omega}_{ng}t\right) + \tilde{B}_{ng}\cos\left(\tilde{\omega}_{ng}t\right)\right]. \quad (2.2.42)$$

The unknown constants $\tilde{A}_{ni}$,$\tilde{B}_{ni}$,$\tilde{A}_{ng}$ and $\tilde{B}_{ng}$ (i = 1, 2; g=3, 4) are determined based on initial conditions (2.2.18) using the orthogonality condition for trigonometric functions

$$\int_0^l Z_n Z_m dx = \int_0^l \sin(k_n z)\sin(k_m z)\mathrm{d}z = c\delta_{nm},$$

$$c = \int_0^l Z_n^2 dx = \int_0^l [\sin(k_n z)]^2 \mathrm{d}z = \frac{l}{2}, \qquad c = \int_0^l \Psi_n^2 dz = \int_0^l [\cos(k_n z)]^2 \mathrm{d}z = \frac{l}{2}. \tag{2.2.43}$$

where δ_{nm} is the Knocker delta function. If we substitute the initial conditions (2.2.18) into the expressions $(2.2.39 - 2.2.42)$, we obtain

$$w_{T1}^0(z,0) = \widetilde{w}_{10}(z) = \sum_{n=1}^{\infty}\sin(k_n z)\sum_{i=1}^{2}\widetilde{B}_{ni}, w_{T2}^0(z,0) = \widetilde{w}_{20}(z) = \sum_{n=1}^{\infty}\sin(k_n z)\sum_{i=1}^{2}\tilde{\alpha}_{ni}\widetilde{B}_{ni},$$

$$\dot{w}_{T1}^0(z,0) = \tilde{v}_{10}(z) = \sum_{n=1}^{\infty}\sin(k_n z)\sum_{i=1}^{2}\widetilde{\omega}_{ni}\tilde{A}_{ni}, \dot{w}_{T2}^0(z,0) = \tilde{v}_{20}(z) = \sum_{n=1}^{\infty}\sin(k_n z)\sum_{i=1}^{2}\tilde{\alpha}_{ni}\widetilde{\omega}_{ni}\tilde{A}_{ni},$$

$$\psi_{T1}^0(z,0) = \tilde{\psi}_{10}(z) = \sum_{n=1}^{\infty}\cos(k_n z)\sum_{g=3}^{4}\tilde{B}_{ng}, \psi_{T2}^0(z,0) = \tilde{\psi}_{20}(z) = \sum_{n=1}^{\infty}\cos(k_n z)\sum_{g=3}^{4}\tilde{\alpha}_{ng}\tilde{B}_{ng},$$

$$\dot{\psi}_{T1}^0(z,0) = \widetilde{\Theta}_{10}(z) = \sum_{n=1}^{\infty}\cos(k_n z)\sum_{g=3}^{4}\widetilde{\omega}_{ng}\tilde{A}_{ng}, \dot{\psi}_{T2}^0(z,0) = \widetilde{\Theta}_{20}(z) = \sum_{n=1}^{\infty}\cos(k_n z)\sum_{g=3}^{4}\tilde{\alpha}_{ng}\widetilde{\omega}_{ng}\tilde{A}_{ng}. \tag{2.2.44}$$

By multiplying the expression (2.2.44) by appropriate eigenfunctions Z_n, i.e. Ψ_n then integrating it with respect to z from 0 to l and using the orthogonality condition (2.2.43), we have

$$\frac{2}{l}\int_0^l \widetilde{w}_{10}\sin(k_n z)\,dz = \sum_{i=1}^{2}\tilde{B}_{ni}, \qquad \frac{2}{l}\int_0^l \widetilde{w}_{20}\sin(k_n z)\,dz = \sum_{i=1}^{2}\tilde{\alpha}_{ni}\tilde{B}_{ni}, \tag{2.2.45}$$

$$\frac{2}{l}\int_0^l \tilde{v}_{10}\sin(k_n z)\,dz = \sum_{i=1}^{2}\widetilde{\omega}_{ni}\tilde{A}_{ni}, \qquad \frac{2}{l}\int_0^l \tilde{v}_{20}\sin(k_n z)\,dz = \sum_{i=1}^{2}\tilde{\alpha}_{ni}\widetilde{\omega}_{ni}\tilde{A}_{ni}, \tag{2.2.46}$$

$$\frac{2}{l}\int_0^l \tilde{\psi}_{10}\cos(k_n z)\,dz = \sum_{g=3}^{4}\tilde{B}_{ng}, \qquad \frac{2}{l}\int_0^l \tilde{\psi}_{20}\cos(k_n z)\,dz = \sum_{g=3}^{4}\tilde{\alpha}_{ng}\tilde{B}_{ng}, \tag{2.2.47}$$

$$\frac{2}{l}\int_0^l \widetilde{\Theta}_{10}\cos(k_n z)\,dz = \sum_{g=3}^{4}\widetilde{\omega}_{ng}\tilde{A}_{ng}, \qquad \frac{2}{l}\int_0^l \widetilde{\Theta}_{20}\cos(k_n z)\,dz = \sum_{g=3}^{4}\tilde{\alpha}_{ng}\widetilde{\omega}_{ng}\tilde{A}_{ng}. \tag{2.2.48}$$

After solving the system of equations (2.2.45-2.2.48), the unknown constants are obtained in the following form

$$\tilde{A}_{n1} = \frac{2}{\tilde{\omega}_{n1}(\tilde{\alpha}_{n2} - \tilde{\alpha}_{n1})l}\int_0^l (\tilde{v}_{10}\tilde{\alpha}_{n2} - \tilde{v}_{20})\sin(k_n z)\,\mathrm{d}z,$$

$$\tilde{A}_{n2} = \frac{2}{\tilde{\omega}_{n2}(\tilde{\alpha}_{n1} - \tilde{\alpha}_{n2})l}\int_0^l (\tilde{v}_{20}\tilde{\alpha}_{n1} - \tilde{v}_{10})\sin(k_n z)\,\mathrm{d}z,$$

$$\tilde{B}_{n1} = \frac{2}{(\tilde{\alpha}_{n2} - \tilde{\alpha}_{n1})l}\int_0^l (\tilde{w}_{10}\tilde{\alpha}_{n2} - \tilde{w}_{20})\sin(k_n z)\,\mathrm{d}z,$$

$$\tilde{B}_{n2} = \frac{2}{(\tilde{\alpha}_{n1} - \tilde{\alpha}_{n2})l}\int_0^l (\tilde{w}_{10}\tilde{\alpha}_{n1} - \tilde{w}_{20})\sin(k_n z)\,\mathrm{d}z,$$

$$\tilde{A}_{n3} = \frac{2}{\tilde{\omega}_{n3}(\tilde{\alpha}_{n4} - \tilde{\alpha}_{n3})l}\int_0^l \left(\tilde{\Theta}_{10}\tilde{\alpha}_{n4} - \tilde{\Theta}_{20}\right)\cos(k_n z)\,\mathrm{d}z,$$

$$\tilde{A}_{n4} = \frac{2}{\tilde{\omega}_{n4}(\tilde{\alpha}_{n3} - \tilde{\alpha}_{n4})l}\int_0^l \left(\tilde{\Theta}_{20}\tilde{\alpha}_{n3} - \tilde{\Theta}_{10}\right)\cos(k_n z)\,\mathrm{d}z,$$

$$\tilde{B}_{n3} = \frac{2}{(\tilde{\alpha}_{n4} - \tilde{\alpha}_{n3})l}\int_0^l \left(\tilde{\Theta}_{10}\tilde{\alpha}_{n4} - \tilde{\Theta}_{20}\right)\cos(k_n z)\,\mathrm{d}z,$$

$$\tilde{B}_{n4} = \frac{2}{(\tilde{\alpha}_{n3} - \tilde{\alpha}_{n4})l}\int_0^l \left(\tilde{\Theta}_{10}\tilde{\alpha}_{n3} - \tilde{\Theta}_{20}\right)\cos(k_n z)\,\mathrm{d}z. \qquad (2.2.49)$$

2.3 Free Vibrations of Two Elastically Connected Reddy-Bickford Beams

Let, as in the case of the Timoshenko model, the beams be of the same length l and connected by an elastic layer with the stiffness modulus K. At its ends, the beams are exposed to the action of axial compression forces F_1 and F_2, Figure 2.1.1. Let us label the functions of longitudinal and transverse motion as well as the rotation angle of the beam's cross-section on a neutral line as $u_{RB1}(y,z,t)$, $w_{RB1}(y,z,t)$, $\psi^0_{RB1}(z,t)$, $u_{RB2}(y,z,t)$, $w_{RB2}(y,z,t)$ and $\psi^0_{RB2}(z,t)$ respectively. Analogous to the relation(1.2.29), the following equations of motion apply to the double-beam system

$$u_{RB1}(y,z,t) = u^0_{RB1}(z,t) + y\psi^0_{RB1}(z,t) - \alpha y^3\left(\psi^0_{RB1}(z,t) + \frac{\partial w^0_{RB1}(z,t)}{\partial z}\right),$$
$$w_{RB1}(y,z,t) = w^0_{RB1}(z,t), \qquad (2.3.1)$$

$$u_{RB2}(y,z,t) = u^0_{RB2}(z,t) + y\psi^0_{RB2}(z,t) - \alpha y^3\left(\psi^0_{RB2}(z,t) + \frac{\partial w^0_{RB2}(z,t)}{\partial z}\right),$$
$$w_{RB2}(y,z,t) = w^0_{RB2}(z,t). \qquad (2.3.2)$$

Deformation in the function of motion and the stress-strain ratio according to the Hooke's law are

$$\varepsilon_{z1}(z,t) = \frac{\partial u^0_{RB1}(z,t)}{\partial z} + y\frac{\partial \psi^0_{RB1}(z,t)}{\partial z} - \alpha y^3\left(\frac{\partial \psi^0_{RB1}(z,t)}{\partial z} + \frac{\partial^2 w^0_{RB1}(z,t)}{\partial z^2}\right), \tag{2.3.3}$$

$$\gamma_{zy1}(z,t) = \psi^0_{RB1}(z,t) + \frac{\partial w^0_{RB1}(z,t)}{\partial z} - \beta y^2\left(\psi^0_{RB1}(z,t) + \frac{\partial w^0_{RB1}(z,t)}{\partial z}\right), \tag{2.3.4}$$

$$\varepsilon_{z2}(z,t) = \frac{\partial u^0_{RB2}(z,t)}{\partial z} + y\frac{\partial \psi^0_{RB2}(z,t)}{\partial z} - \alpha y^3\left(\frac{\partial \psi^0_{RB2}(z,t)}{\partial z} + \frac{\partial^2 w^0_{RB2}(z,t)}{\partial z^2}\right), \tag{2.3.5}$$

$$\gamma_{zy2}(z,t) = \psi^0_{RB2}(z,t) + \frac{\partial w^0_{RB2}(z,t)}{\partial z} - \beta y^2\left(\psi^0_{RB2}(z,t) + \frac{\partial w^0_{RB2}(z,t)}{\partial z}\right), \tag{2.3.6}$$

$$\begin{Bmatrix}\sigma_{z1}\\ \tau_{zy1}\end{Bmatrix} = \begin{bmatrix}E & 0\\ 0 & G\end{bmatrix}\begin{Bmatrix}\varepsilon_{z1}\\ \gamma_{zy1}\end{Bmatrix}, \qquad \begin{Bmatrix}\sigma_{z2}\\ \tau_{zy2}\end{Bmatrix} = \begin{bmatrix}E & 0\\ 0 & G\end{bmatrix}\begin{Bmatrix}\varepsilon_{z2}\\ \gamma_{zy2}\end{Bmatrix}. \tag{2.3.7}$$

Virtual work of inertial forces is given by

$$\delta W_{in1} = -\rho b_1 \int_0^l \int_{-\frac{h_1}{2}}^{\frac{h_1}{2}} \left[\frac{\partial^2 w_{RB1}(y,z,t)}{\partial t^2}\delta w_{T1}(y,z,t) + \frac{\partial^2 u_{RB1}(y,z,t)}{\partial t^2}\delta u_{T1}(y,z,t)\right] dydz, \tag{2.3.8}$$

$$\delta W_{in2} = -\rho b_2 \int_0^l \int_{-\frac{h_2}{2}}^{\frac{h_2}{2}} \left[\frac{\partial^2 w_{RB2}(y,z,t)}{\partial t^2}\delta w_{T2}(y,z,t) + \frac{\partial^2 u_{RB2}(y,z,t)}{\partial t^2}\delta u_{T2}(y,z,t)\right] dydz. \tag{2.3.9}$$

Virtual work of internal forces is

$$\delta W_{V1} = -b_1 \int_0^l \int_{-\frac{h_1}{2}}^{\frac{h_1}{2}} \left[\sigma_{z1}(z,t)\delta\varepsilon_{z1}(z,t) + \tau_{zy1}(z,t)\delta\gamma_{zy1}(z,t)\right] dydz, \tag{2.3.10}$$

$$\delta W_{V2} = -b_2 \int_0^l \int_{-\frac{h_2}{2}}^{\frac{h_2}{2}} \left[\sigma_{z2}(z,t)\delta\varepsilon_{z2}(z,t) + \tau_{zy2}(z,t)\delta\gamma_{zy2}(z,t)\right] dydz. \tag{2.3.11}$$

irtual work of external forces is expressed as

$$\delta W_{ex1} = \int_0^l \left[\delta w^0_{RB1}(z,t)K\left(w^0_{T2}(z,t) - w^0_{T1}(z,t)\right) + F_1\frac{\partial w^0_{RB1}(z,t)}{\partial z}\frac{\partial \delta w^0_{RB1}(z,t)}{\partial z}\right] dz, \tag{2.3.12}$$

$$\delta W_{ex2} = \int_0^l \left[\delta w^0_{RB2}(z,t)K\left(w^0_{RB1}(z,t) - w^0_{RB2}(z,t)\right) + F_2\frac{\partial w^0_{RB2}(z,t)}{\partial z}\frac{\partial \delta w^0_{RB2}(z,t)}{\partial z}\right] dz, \tag{2.3.13}$$

By substituting the equations (2.3.8-2.3.11) into a general equation based on the virtual work principle $\delta W_{ini} + \delta W_{Vi} + \delta W_{exi} = 0,\ i = 1{,}2$, we get

$$-b_1 \int_0^l \int_{-\frac{h_1}{2}}^{\frac{h_1}{2}} \left[\sigma_{z1}(z,t)\delta\varepsilon_{z1}(z,t) + \tau_{zy1}(z,t)\delta\gamma_{zy1}(z,t)\right] dydz -$$

$$-\rho b_1 \int_0^l \int_{-\frac{h_1}{2}}^{\frac{h_1}{2}} \left[\frac{\partial^2 w_{RB1}(y,z,t)}{\partial t^2}\delta w_{RB1}(y,z,t) + \frac{\partial^2 u_{RB1}(y,z,t)}{\partial t^2}\delta u_{RB1}(y,z,t)\right] dydz +$$

$$+ \int_0^l \left[\delta w^0_{RB1}(z,t)K\left(w^0_{RB2}(z,t) - w^0_{RB1}(z,t)\right) + F_1\frac{\partial w^0_{RB1}(z,t)}{\partial z}\frac{\partial \delta w^0_{RB1}(z,t)}{\partial z}\right] dz = 0, \tag{2.3.14}$$

$$-b_2\int_0^l\int_{-\frac{h_2}{2}}^{\frac{h_2}{2}}\left[\sigma_{z2}(z,t)\delta\varepsilon_{z1}(z,t)+\tau_{zy2}(z,t)\delta\gamma_{zy2}(z,t)\right]dydz-$$

$$-\rho b_2\int_0^l\int_{-\frac{h_2}{2}}^{\frac{h_2}{2}}\left[\frac{\partial^2 w_{RB2}(y,z,t)}{\partial t^2}\delta w_{RB2}(y,z,t)+\frac{\partial^2 u_{RB2}(y,z,t)}{\partial t^2}\delta u_{RB2}(y,z,t)\right]dydz+$$

$$+\int_0^l\left[\delta w^0_{RB2}(z,t)K\left(w^0_{RB1}(z,t)-w^0_{RB2}(z,t)\right)+F_2\frac{\partial w^0_{RB2}(z,t)}{\partial z}\frac{\partial\delta w^0_{RB2}(z,t)}{\partial z}\right]dz=0. \tag{2.3.15}$$

By successive application of Green's theorem on the expressions (2.3.14-2.3.15), we get the equations of vibration for the system composed of elastically connected Reddy-Bickford beams in the following form

$$C_w^{4,0}\frac{\partial^4 w^0_{RB1}(z,t)}{\partial z^4}+C_w^{2,2}\frac{\partial^4 w^0_{RB1}(z,t)}{\partial z^2\,\partial t^2}+C_w^{2,0}\frac{\partial^2 w^0_{RB}(z,t)}{\partial z^2}+C_w^{0,2}\frac{\partial^2 w^0_{RB1}(z,t)}{\partial t^2}+C_\psi^{1,2}\frac{\partial^3\psi^0_{RB1}(z,t)}{\partial z\,\partial t^2}$$
$$+C_\psi^{1,0}\frac{\partial\psi^0_{RB1}(z,t)}{\partial z}+C_\psi^{3,0}\frac{\partial^3\psi^0_{RB1}(z,t)}{\partial z^3}+K\left(w^0_{RB1}(z,t)-w^0_{RB2}(z,t)\right)=0, \tag{2.3.16}$$

$$C_w^{3,0}\frac{\partial^3 w^0_{RB1}(z,t)}{\partial z^3}+C_w^{1,2}\frac{\partial^3 w^0_{RB1}(z,t)}{\partial z\,\partial t^2}+C_w^{1,0}\frac{\partial w^0_{RB1}(z,t)}{\partial z}+C_\psi^{2,0}\frac{\partial^2\psi^0_{RB1}(z,t)}{\partial z^2}$$
$$+C_\psi^{0,2}\frac{\partial^2\psi^0_{RB1}(z,t)}{\partial t^2}+C_\psi^{0,0}\psi^0_{RB1}(z,t)=0, \tag{2.3.17}$$

$$D_w^{4,0}\frac{\partial^4 w^0_{RB2}(z,t)}{\partial z^4}+D_w^{2,2}\frac{\partial^4 w^0_{RB2}(z,t)}{\partial z^2\,\partial t^2}+D_w^{2,0}\frac{\partial^2 w^0_{RB2}(z,t)}{\partial z^2}+D_w^{0,2}\frac{\partial^2 w^0_{RB2}(z,t)}{\partial t^2}+D_\psi^{1,2}\frac{\partial^3\psi^0_{RB2}(z,t)}{\partial z\,\partial t^2}$$
$$+D_\psi^{1,0}\frac{\partial\psi^0_{RB2}(z,t)}{\partial z}+D_\psi^{3,0}\frac{\partial^3\psi^0_{RB2}(z,t)}{\partial z^3}+K\left(w^0_{RB2}(z,t)-w^0_{RB1}(z,t)\right)=0, \tag{2.3.18}$$

$$D_w^{3,0}\frac{\partial^3 w^0_{RB2}(z,t)}{\partial z^3}+D_w^{1,2}\frac{\partial^3 w^0_{RB2}(z,t)}{\partial z\,\partial t^2}+D_w^{1,0}\frac{\partial w^0_{RB2}(z,t)}{\partial z}+D_\psi^{2,0}\frac{\partial^2\psi^0_{RB2}(z,t)}{\partial z^2}$$
$$+D_\psi^{0,2}\frac{\partial^2\psi^0_{RB2}(z,t)}{\partial t^2}+D_\psi^{0,0}\psi^0_{RB2}(z,t)=0, \tag{2.3.19}$$

where

$$C_w^{4,0}=\frac{1}{448}b_1{h_1}^7\alpha^2E,\ \ C_w^{2,2}=-\frac{1}{448}b_1{h_1}^7\alpha^2\rho,\ C_w^{2,0}=-\frac{1}{80}b_1G\beta^2{h_1}^5+\frac{1}{6}bG\beta{h_1}^3-b_1Gh_1+F_1,$$
$$C_w^{0,2}=b_1h_1\rho, C_\psi^{1,2}=\frac{1}{80}b_1{h_1}^5\alpha\rho-\frac{1}{448}b_1{h_1}^7\alpha^2\rho, C_\psi^{1,0}=-\frac{1}{80}b_1G\beta^2{h_1}^5+\frac{1}{6}b_1G\beta{h_1}^3-b_1Gh_1,$$
$$C_\psi^{3,0}=\frac{1}{448}b_1{h_1}^7\alpha^2E-\frac{1}{80}b_1{h_1}^5\alpha E, C_w^{3,0}=\frac{1}{80}b_1{h_1}^5\alpha E-\frac{1}{448}b_1{h_1}^7\alpha^2E,$$
$$C_w^{1,2}=\frac{1}{448}b_1{h_1}^7\alpha^2\rho-\frac{1}{80}b_1{h_1}^5\alpha\rho, C_w^{1,0}=\frac{1}{80}b_1G\beta^2{h_1}^5-\frac{1}{6}b_1G\beta{h_1}^3+b_1Gh_1,$$
$$C_\psi^{2,0}=-\frac{1}{448}b_1\alpha^2E{h_1}^7+\frac{1}{40}b_1\alpha E{h_1}^5-\frac{1}{12}b_1E{h_1}^3,$$
$$C_\psi^{0,2}=\frac{1}{448}b_1\alpha^2\rho{h_1}^7-\frac{1}{40}b_1\alpha\rho{h_1}^5+\frac{1}{12}b_1\rho{h_1}^3,$$
$$C_\psi^{0,0}=\frac{1}{80}b_1\beta^2G{h_1}^5-\frac{1}{6}b_1\beta G{h_1}^3+b_1Gh_1, \tag{2.3.20}$$

$$D_w^{4,0}=\frac{1}{448}b_2{h_2}^7\alpha^2E,\ D_w^{2,2}=-\frac{1}{448}b_2{h_2}^7\alpha^2\rho,\ D_w^{2,0}=-\frac{1}{80}b_2G\beta^2{h_2}^5+\frac{1}{6}bG\beta{h_2}^3-b_2Gh_2+F_2,$$

$$D_w^{0,2}=b_2h_2\rho, D_\psi^{1,2}=\frac{1}{80}b_2{h_2}^5\alpha\rho-\frac{1}{448}b_2{h_2}^7\alpha^2\rho, D_\psi^{1,0}=-\frac{1}{80}b_2G\beta^2{h_2}^5+\frac{1}{6}b_2G\beta{h_2}^3-b_2Gh_2,$$

$$D_\psi^{3,0}=\frac{1}{448}b_2{h_2}^7\alpha^2E-\frac{1}{80}b_2{h_2}^5\alpha E, D_w^{3,0}=\frac{1}{80}b_2{h_2}^5\alpha E-\frac{1}{448}b_2{h_2}^7\alpha^2E,$$

$$D_w^{1,2}=\frac{1}{448}b_2{h_2}^7\alpha^2\rho-\frac{1}{80}b_2{h_2}^5\alpha\rho, D_w^{1,0}=\frac{1}{80}b_2G\beta^2{h_2}^5-\frac{1}{6}b_2G\beta{h_2}^3+b_2Gh_2,$$

$$D_\psi^{2,0}=-\frac{1}{448}b_2\alpha^2E{h_2}^7+\frac{1}{40}b_2\alpha E{h_2}^5-\frac{1}{12}b_2E{h_2}^3,$$

$$D_\psi^{0,2}=\frac{1}{448}b_2\alpha^2\rho{h_2}^7-\frac{1}{40}b_2\alpha\rho{h_2}^5+\frac{1}{12}b_2\rho{h_2}^3,$$

$$D_\psi^{0,0}=\frac{1}{80}b_2\beta^2G{h_2}^5-\frac{1}{6}b_2\beta G{h_2}^3+b_2Gh_2, \tag{2.3.21}$$

In the expressions (2.3.20-2.3.21), ρ denotes mass density, A the area of the cross-section, E Young's modulus, and G is the shear modulus.

Unlike the Euler and the Timoshenko beam theory, which belong to the theories of the fourth order, Reddy-Bickford's is a theory of the sixth order and it takes 6 boundary conditions (three for each end of the beam). If we apply the variation to constitutive relations (2.3.10-2.3.11) with the virtual work of internal forces, we get

$$-\frac{dM_{zi}}{dz}+(Q_{zi}-\beta R_{zi})=0,$$

$$-\alpha\frac{d^2P_{zi}}{dz^2}-\frac{d}{dz}(Q_{zi}-\beta R_{zi})=0,\quad i=1,2. \tag{2.3.22}$$

where

$$M_{zi}=\int_{A_i}y\sigma_{zi}dA-\alpha P_{zi},\qquad Q_{zi}=\int_{A_i}\tau_{zyi}dA,\qquad P_{zi}=\int_{A_i}y^3\sigma_{zi}dA,\qquad R_{zi}=\int_{A_i}y^2\tau_{zyi}dA, \tag{2.3.23}$$

are the bending moment, shear force, resulting stress in normal direction and the resulting tangent stress respectively. By substituting the relations (2.3.3-2.3.7) into (2.3.23), we get

$$M_{zi}=-\frac{1}{80}\alpha b_iE{h_i}^5\frac{\partial^2w_{RBi}}{\partial z^2}-\frac{1}{240}b_iE{h_i}^3\left(3\alpha{h_i}^2-20\right)\frac{\partial\psi_{RBi}}{\partial z}-\alpha P_{zi},$$

$$Q_{zi}=-\frac{1}{12}b_iGh_i\left(\beta h^2-12\right)\left(\frac{\partial w_{RBi}}{\partial z}+\psi_{RBi}\right),$$

$$P_{zi}=-\frac{1}{448}\alpha b_iE{h_i}^7\frac{\partial^2w_{RBi}}{\partial z^2}-\frac{b_iE{h_i}^5\left(5\alpha{h_i}^2-28\right)}{2240}\frac{\partial\psi_{RBi}}{\partial z},$$

$$R_{zi}=-\frac{1}{240}b_iG{h_i}^3\left(3\beta{h_i}^2-20\right)\left(\frac{\partial w_{RBi}}{\partial z}+\psi_{RBi}\right). \tag{2.3.24}$$

In case of simply supported beams, the moment and the deflection at beam ends must equal zero, hence based on the relations (2.3.24) the three conditions follow for each beam end: $w_{RBi} = 0,\ M_{zi} = 0,$ (in order for the moment M_{zi} to equal zero, the third condition must be fulfilled given as $P_{zi} = 0$). Based on the relations (2.3.24), boundary conditions are reduced to the same conditions as applied in the case of Timoshenko beam and have the following form

$$w^0_{RBi}(0,t) = \frac{d^2 w^0_{RBi}(0,t)}{dz^2} = \frac{d^2 w^0_{RBi}(l,t)}{dz^2} = w^0_{RBi}(l,t) = 0, \quad i = 1,2, \quad (2.3.25)$$

$$\frac{d\psi^0_{RBi}(0,t)}{dz} = \frac{d\psi^0_{RBi}(l,t)}{dz} = 0, \qquad i = 1,2. \quad (2.3.26)$$

We define initial conditions as

$$w^0_{RBi}(z,0) = \tilde{\bar{w}}_{i0}(z),\ \frac{dw^0_{RBi}(z,0)}{dt} = \tilde{\bar{v}}_{i0}(z),\ \psi^0_{RBi}(z,0) = \tilde{\bar{\psi}}_{i0}(z),\ \frac{d\psi^0_{RBi}(z,0)}{dt} = \tilde{\bar{\Theta}}_{i0}(z), \quad (2.3.27)$$

Considering the harmonic motion of the beams' points, we assume the solutions to the equations (2.3.16-2.3.19) as the product of functions

$$w^0_{RBi}(z,t) = \sum_{n=1}^{\infty} Z_n(z)\tilde{\bar{T}}_{in}(t), \quad \psi^0_{RBi}(z,t) = \sum_{n=1}^{\infty} \Psi_n(z)\tilde{\bar{T}}_{in(r)}(t), \quad i = 1,2, \quad (2.3.28)$$

where $\tilde{\bar{T}}_{in}(t)$ and $\tilde{\bar{T}}_{in(r)}$ are unknown time functions whereas $Z_n(z)$ and $\Psi_n(z)$ are mode shape functions

$$Z_n(z) = \sin(k_n z), \quad \Psi_n(z) = \cos(k_n z), k_n = n\pi/l, \qquad n = 1,2,3,\ldots \quad (2.3.29)$$

By substituting the assumed solutions (2.3.28) into equations (2.3.16-2.3.19), we get a system of four differential equations of the second degree as follows

$$\begin{bmatrix} u_{11} & 0 & u_{13} & 0 \\ 0 & u_{22} & 0 & u_{24} \\ u_{31} & 0 & u_{33} & 0 \\ 0 & u_{42} & 0 & u_{44} \end{bmatrix} \begin{Bmatrix} \ddot{\tilde{\bar{T}}}_{1n}(t) \\ \ddot{\tilde{\bar{T}}}_{2n}(t) \\ \ddot{\tilde{\bar{T}}}_{1n(r)}(t) \\ \ddot{\tilde{\bar{T}}}_{2n(r)}(t) \end{Bmatrix} + \begin{bmatrix} v_{11} & -K & v_{13} & 0 \\ -K & v_{22} & 0 & v_{24} \\ v_{31} & 0 & v_{33} & 0 \\ 0 & v_{42} & 0 & v_{44} \end{bmatrix} \begin{Bmatrix} \tilde{\bar{T}}_{1n}(t) \\ \tilde{\bar{T}}_{2n}(t) \\ \tilde{\bar{T}}_{1n(r)}(t) \\ \tilde{\bar{T}}_{2n(r)}(t) \end{Bmatrix} = \begin{Bmatrix} 0 \\ 0 \\ 0 \\ 0 \end{Bmatrix}, \quad (2.3.30)$$

where

$$u_{11} = \frac{1}{448}\rho b_1 h_1 \left(\alpha^2 {h_1}^6 {k_n}^2 + 448\right), u_{13} = u_{31} = \frac{\alpha\rho b_1 {h_1}^5 k_n (5\alpha {h_1}^2 - 28)}{2240},$$

$$u_{33} = \frac{\rho b_1 {h_1}^3 [3\alpha {h_1}^2 (5\alpha {h_1}^2 - 56) + 560]}{6720}, u_{22} = \frac{1}{448}\rho b_2 h_2 \left(\alpha^2 {h_2}^6 {k_n}^2 + 448\right),$$

$$u_{24} = u_{42} = \frac{\alpha\rho b_2 {h_2}^5 k_n \left(5\alpha {h_2}^2 - 28\right)}{2240}, u_{44} = \frac{\rho b_2 {h_2}^3 (3\alpha {h_2}^2 (5\alpha {h_2}^2 - 56) + 560)}{6720},$$

$$v_{11} = \frac{b_1 h_1 {k_n}^2 \{15\alpha^2 E {h_1}^6 {k_n}^2 + 28G[\beta {h_1}^2 (3\beta {h_1}^2 - 40) + 240]\}}{6720} - F_1 {k_n}^2 + K,$$

$$v_{31} = v_{13} = \frac{b_1 h_1 k_n \{3\alpha E {h_1}^4 {k_n}^2 (5\alpha {h_1}^2 - 28) + 28G[\beta {h_1}^2 (3\beta {h_1}^2 - 40) + 240]\}}{6720},$$

$$v_{22} = \frac{b_2 h_2 {k_n}^2 \{15\alpha^2 E {h_2}^6 {k_n}^2 + 28G[\beta {h_2}^2 (3\beta {h_2}^2 - 40) + 240]\}}{6720} - F_2 {k_n}^2 + K,$$

$$v_{42} = v_{24} = \frac{b_2 h_2 k_n \{3\alpha E {h_2}^4 {k_n}^2 (5\alpha {h_2}^2 - 28) + 28G[\beta {h_2}^2 (3\beta {h_2}^2 - 40) + 240]\}}{6720},$$

$$v_{44} = \frac{b_2 h_2 \{E {h_2}^2 {k_n}^2 [3\alpha {h_2}^2 (5\alpha {h_2}^2 - 56) + 560] + 28G[\beta {h_2}^2 (3\beta {h_2}^2 - 40) + 240]\}}{6720}.$$

We assume the solutions to the system of equations (2.3.30) in the following form

$$\tilde{\tilde{T}}_{1n} = \tilde{\tilde{C}}_n e^{j\tilde{\tilde{\omega}}_n t},\ \tilde{\tilde{T}}_{2n} = \tilde{\tilde{D}}_n e^{j\tilde{\tilde{\omega}}_n t},\ \tilde{\tilde{T}}_{1n(r)}(t) = \tilde{\tilde{C}}_{n(r)} e^{j\tilde{\tilde{\omega}}_n t},\quad \tilde{\tilde{T}}_{2n(r)}(t) = \tilde{\tilde{D}}_{n(r)} e^{j\tilde{\tilde{\omega}}_n t}, j = \sqrt{-1}. \quad (2.3.31)$$

If we substitute the assumed solutions (2.3.28) into the system of equations (2.3.16 − 2.3.19), we get a homogeneous system of algebraic equations which has non-trivial solutions when system determinant equals zero

$$[\boldsymbol{P_p}]\{\boldsymbol{C_c}\} = \{\mathbf{0}\} <=> \begin{bmatrix} p_{11} & -K & p_{13} & 0 \\ -K & p_{22} & 0 & p_{24} \\ p_{31} & 0 & p_{33} & 0 \\ 0 & p_{42} & 0 & p_{44} \end{bmatrix} \begin{Bmatrix} \tilde{\tilde{C}}_n \\ \tilde{\tilde{D}}_n \\ \tilde{\tilde{C}}_{n(r)} \\ \tilde{\tilde{D}}_{n(r)} \end{Bmatrix} = \begin{Bmatrix} 0 \\ 0 \\ 0 \\ 0 \end{Bmatrix}, \quad (2.3.32)$$

where

$$p_{11} = \frac{b_1 h_1 \{{k_n}^2 [15\alpha^2 {h_1}^6 (E{k_n}^2 - \rho\tilde{\tilde{\omega}}_n^{\,2}) + 28G[\beta {h_1}^2 (3\beta {h_1}^2 - 40) + 240)] - 6720\rho\omega_n{}^2\}}{6720}$$

$$-F_1 {k_n}^2 + K,$$

$$p_{31} = p_{13} = \frac{b_1 h_1 k_n \{3\alpha {h_1}^4 (5\alpha {h_1}^2 - 28)(E{k_n}^2 - \rho\tilde{\tilde{\omega}}_n^{\,2}) + 28G[\beta {h_1}^2 (3\beta {h_1}^2 - 40) + 240]\}}{6720},$$

$$p_{22} = \frac{b_2 h_2 \{{k_n}^2 [15\alpha^2 {h_2}^6 (E{k_n}^2 - \rho\tilde{\tilde{\omega}}_n^{\,2}) + 28G[\beta {h_2}^2 (3\beta {h_2}^2 - 40) + 240)] - 6720\rho\tilde{\tilde{\omega}}_n^{\,2}\}}{6720}$$

$$-F_2 {k_n}^2 + K,$$

$$p_{42} = p_{24} = \frac{b_2 h_2 k_n \{3\alpha {h_2}^4 (5\alpha {h_2}^2 - 28)(E{k_n}^2 - \rho\tilde{\tilde{\omega}}_n^{\,2}) + 28G[\beta {h_2}^2 (3\beta {h_2}^2 - 40) + 240]\}}{6720},$$

$$p_{44} = \frac{b_2 h_2 \{{h_2}^2 [3\alpha {h_2}^2 (5\alpha {h_2}^2 - 56) + 560](E{k_n}^2 - \rho\tilde{\tilde{\omega}}_n^{\,2}) + 28G[\beta {h_2}^2 (3\beta {h_2}^2 - 40) + 240]\}}{6720}.$$

Frequency system equation (2.3.32) is obtained from the condition for the existence of non-trivial solutions $\mathrm{Det}[\boldsymbol{P_p}] = 0$, in the form of an eighth degree polynomial. If we introduce a substitution $\tilde{\tilde{\lambda}} = \tilde{\tilde{\omega}}_n^2$, the polynomial may be reduced to the following form

$$\tilde{\tilde{\lambda}}^4 + \tilde{\tilde{c}}_1\tilde{\tilde{\lambda}}^3 + \tilde{\tilde{c}}_2\tilde{\tilde{\lambda}}^2 + \tilde{\tilde{c}}_3\tilde{\tilde{\lambda}} + \tilde{\tilde{c}}_4 = 0. \tag{2.3.33}$$

Constants $\tilde{\tilde{c}}_1, \tilde{\tilde{c}}_2, \tilde{\tilde{c}}_3$ and $\tilde{\tilde{c}}_4$ are given in the Appendix 2.3.1. The fourth degree polynomial can be factored as

$$\left(\tilde{\tilde{\lambda}}^2 + \tilde{\tilde{p}}_1\tilde{\tilde{\lambda}} + \tilde{\tilde{q}}_1\right)\left(\tilde{\tilde{\lambda}}^2 + \tilde{\tilde{p}}_2\tilde{\tilde{\lambda}} + \tilde{\tilde{q}}_2\right) = 0, \tag{2.3.34}$$

where

$$\begin{Bmatrix}\tilde{\tilde{p}}_1\\ \tilde{\tilde{p}}_2\end{Bmatrix} = \frac{1}{2}\left[\tilde{\tilde{c}}_1 \pm \sqrt{\tilde{\tilde{c}}_1^2 - 4\tilde{\tilde{c}}_2 + 4\tilde{\tilde{\chi}}_1}\right],$$

$$\begin{Bmatrix}\tilde{\tilde{q}}_1\\ \tilde{\tilde{q}}_2\end{Bmatrix} = \frac{1}{2}\left[\tilde{\tilde{\chi}}_1 \pm \frac{\tilde{\tilde{c}}_1\chi_1 - 2\tilde{\tilde{c}}_3}{\sqrt{\tilde{\tilde{c}}_1^2 - 4\tilde{\tilde{c}}_2 + 4\tilde{\tilde{\chi}}_1}}\right].$$

In the expressions $\tilde{\tilde{\chi}}_1$ presents one of the roots of a third degree equation

$$\tilde{\tilde{\chi}}^3 - c_2\tilde{\tilde{\chi}}^2 + (\tilde{\tilde{c}}_1\tilde{\tilde{c}}_3 - 4\tilde{\tilde{c}}_4)\tilde{\tilde{\chi}} + (4\tilde{\tilde{c}}_2\tilde{\tilde{c}}_4 - \tilde{\tilde{c}}_3^2 - \tilde{\tilde{c}}_1^2\tilde{\tilde{c}}_4) = 0. \tag{2.3.35}$$

After factoring the equation (2.3.33), the solutions may be written as the square of natural frequencies

$$\tilde{\tilde{\omega}}_{n1}^2 = \tilde{\tilde{\lambda}}_1 = -\frac{\tilde{\tilde{p}}_1}{2} - \sqrt{\frac{\tilde{\tilde{p}}_1^2}{4} - \tilde{\tilde{q}}_1}, \tilde{\tilde{\omega}}_{n2}^2 = \tilde{\tilde{\lambda}}_2 = -\frac{\tilde{\tilde{p}}_2}{2} - \sqrt{\frac{\tilde{\tilde{p}}_2^2}{4} - \tilde{\tilde{q}}_2},$$

$$\tilde{\tilde{\omega}}_{n3}^2 = \tilde{\tilde{\lambda}}_3 = -\frac{\tilde{\tilde{p}}_2}{2} + \sqrt{\frac{\tilde{\tilde{p}}_2^2}{4} - \tilde{\tilde{q}}_2}, \qquad \tilde{\tilde{\omega}}_{n4}^2 = \tilde{\tilde{\lambda}}_4 = -\frac{\tilde{\tilde{p}}_1}{2} + \sqrt{\frac{\tilde{\tilde{p}}_1^2}{4} - \tilde{\tilde{q}}_1}. \tag{2.3.36}$$

The three roots of the equation (2.3.35) are

$$\begin{aligned}\tilde{\tilde{\chi}}_1 &= \tilde{\tilde{c}}_2/3 + 2\sqrt{-\tilde{\tilde{Q}}}\cos\left(\tilde{\tilde{\theta}}/3\right),\\ \tilde{\tilde{\chi}}_2 &= \tilde{\tilde{c}}_2/3 + 2\sqrt{-\tilde{\tilde{Q}}}\cos\left[\left(\tilde{\tilde{\theta}} + 2\pi\right)/3\right],\\ \tilde{\tilde{\chi}}_3 &= \tilde{\tilde{c}}_2/3 + 2\sqrt{-\tilde{\tilde{Q}}}\cos\left[\left(\tilde{\tilde{\theta}} + 4\pi\right)/3\right],\end{aligned} \tag{2.3.37}$$

where

$$\tilde{\tilde{\theta}} = cos^{-1}\left(\tilde{\tilde{S}}/\sqrt{-\tilde{\tilde{Q}}^3}\right), \quad Q = -\tfrac{1}{9}(\tilde{\tilde{c}}_2^2 - 3\tilde{\tilde{c}}_1\tilde{\tilde{c}}_3 + 12\tilde{\tilde{c}}_4),$$

$$S = \tfrac{1}{54}(2\tilde{\tilde{c}}_2^3 - 9\tilde{\tilde{c}}_1\tilde{\tilde{c}}_2\tilde{\tilde{c}}_3 + 27\tilde{\tilde{c}}_3^2 + 27\tilde{\tilde{c}}_1^2\tilde{\tilde{c}}_4 - 72\tilde{\tilde{c}}_2\tilde{\tilde{c}}_4).$$

By choosing one of the three roots in the expression (2.3.37), we get unique solutions to the equation (2.3.33) where four natural frequencies of the system are real positive roots $\widetilde{\widetilde{\omega}}_{n1} = \sqrt{\tilde{\tilde{\lambda}}_1}$, $\widetilde{\widetilde{\omega}}_{n2} = \sqrt{\tilde{\tilde{\lambda}}_2}$, $\widetilde{\widetilde{\omega}}_{n3} = \sqrt{\tilde{\tilde{\lambda}}_3}$, $\widetilde{\widetilde{\omega}}_{n4} = \sqrt{\tilde{\tilde{\lambda}}_4}$. Amplitude ratios are determined from the equation (2.3.31) for each frequency, Appendix 2.3.2. The general solution to differential equations (2.3.30) is given as

$$\tilde{\tilde{T}}_{1n}(t) = \tilde{\tilde{C}}_{1n}e^{j\widetilde{\widetilde{\omega}}_{n1}t} + \tilde{\tilde{C}}_{2n}e^{-j\widetilde{\widetilde{\omega}}_{n1}t} + \tilde{\tilde{C}}_{3n}e^{j\widetilde{\widetilde{\omega}}_{n2}t} + \tilde{\tilde{C}}_{4n}e^{-j\widetilde{\widetilde{\omega}}_{n2}t}, \tag{2.3.38}$$

$$\tilde{\tilde{T}}_{2n}(t) = \widetilde{\widetilde{D}}_{1n}e^{j\widetilde{\widetilde{\omega}}_{n1}t} + \widetilde{\widetilde{D}}_{2n}e^{-j\widetilde{\widetilde{\omega}}_{n1}t} + \widetilde{\widetilde{D}}_{3n}e^{j\widetilde{\widetilde{\omega}}_{n2}t} + \widetilde{\widetilde{D}}_{4n}e^{-j\widetilde{\widetilde{\omega}}_{n2}t}, \tag{2.3.39}$$

$$\tilde{\tilde{T}}_{1n(r)}(t) = \tilde{\tilde{C}}_{1n(r)}e^{j\widetilde{\widetilde{\omega}}_{n3}t} + \tilde{\tilde{C}}_{2n(r)}e^{-j\widetilde{\widetilde{\omega}}_{n3}t} + \tilde{\tilde{C}}_{3n(r)}e^{j\widetilde{\widetilde{\omega}}_{n4}t} + \tilde{\tilde{C}}_{4n(r)}e^{-j\widetilde{\widetilde{\omega}}_{n4}t}, \tag{2.3.40}$$

$$\tilde{\tilde{T}}_{2n(r)}(t) = \widetilde{\widetilde{D}}_{1n(r)}e^{j\widetilde{\widetilde{\omega}}_{n3}t} + \widetilde{\widetilde{D}}_{2n(r)}e^{-j\widetilde{\widetilde{\omega}}_{n3}t} + \widetilde{\widetilde{D}}_{3n(r)}e^{j\widetilde{\widetilde{\omega}}_{n4}t} + \widetilde{\widetilde{D}}_{4n(r)}e^{-j\widetilde{\widetilde{\omega}}_{n4}t}, \tag{2.3.41}$$

i.e.

$$\tilde{\tilde{T}}_{1n}(t) = \sum_{i=1}^{2}\left[\tilde{\tilde{A}}_{ni}\sin\left(\widetilde{\widetilde{\omega}}_{ni}t\right) + \tilde{\tilde{B}}_{ni}\cos\left(\widetilde{\widetilde{\omega}}_{ni}t\right)\right], \tag{2.3.42}$$

$$\tilde{\tilde{T}}_{2n}(t) = \sum_{i=1}^{2}\tilde{\tilde{\alpha}}_{ni}\left[\tilde{\tilde{A}}_{ni}\sin\left(\widetilde{\widetilde{\omega}}_{ni}t\right) + \tilde{\tilde{B}}_{ni}\cos\left(\widetilde{\widetilde{\omega}}_{ni}t\right)\right], \tag{2.3.43}$$

$$\tilde{\tilde{T}}_{1n(r)}(t) = \sum_{g=3}^{4}\left[\tilde{\tilde{A}}_{ng}\sin\left(\widetilde{\widetilde{\omega}}_{ng}t\right) + \tilde{\tilde{B}}_{ng}\cos\left(\widetilde{\widetilde{\omega}}_{ng}t\right)\right], \tag{2.3.44}$$

$$\tilde{\tilde{T}}_{2n(r)}(t) = \sum_{g=3}^{4}\tilde{\tilde{\alpha}}_{ng}\left[\tilde{\tilde{A}}_{ng}\sin\left(\widetilde{\widetilde{\omega}}_{ng}t\right) + \tilde{\tilde{B}}_{ng}\cos\left(\widetilde{\widetilde{\omega}}_{ng}t\right)\right], \tag{2.3.45}$$

where $\tilde{\tilde{A}}_{ni}$,$\tilde{\tilde{B}}_{ni}$,$\tilde{\tilde{A}}_{ng}$ and $\tilde{\tilde{B}}_{ng}$ (i = 1, 2; g=3, 4;) are unknown constants. The solutions to the partial differential equations for free transverse vibration for the system of two elastically connected simply supported beams considering the influences of rotary inertia and transverse shear are given as

$$w_{RB1}^{0}(z,t)=\sum_{n=1}^{\infty}Z_n(z)\tilde{\tilde{T}}_{1n}(t)=\sum_{n=1}^{\infty}\sin(k_nz)\sum_{i=1}^{2}\left[\tilde{\tilde{A}}_{ni}\sin(\tilde{\tilde{\omega}}_{ni}t)+\tilde{\tilde{B}}_{ni}\cos(\tilde{\tilde{\omega}}_{ni}t)\right], \tag{2.3.46}$$

$$w_{RB2}^{0}(z,t)=\sum_{n=1}^{\infty}Z_n(z)\tilde{\tilde{T}}_{2n}(t)=\sum_{n=1}^{\infty}\sin(k_nz)\sum_{i=1}^{2}\tilde{\tilde{\alpha}}_{ni}\left[\tilde{\tilde{A}}_{ni}\sin(\tilde{\tilde{\omega}}_{ni}t)+\tilde{\tilde{B}}_{ni}\cos(\tilde{\tilde{\omega}}_{ni}t)\right]. \tag{2.3.47}$$

$$\psi_{RB1}^{0}(z,t)=\sum_{n=1}^{\infty}\Psi_n(z)\tilde{\tilde{T}}_{1n(r)}(t)=\sum_{n=1}^{\infty}\cos(k_nz)\sum_{g=3}^{4}\left[\tilde{\tilde{A}}_{ng}\sin(\tilde{\tilde{\omega}}_{ng}t)+\tilde{\tilde{B}}_{ng}\cos(\tilde{\tilde{\omega}}_{ng}t)\right], \tag{2.3.48}$$

$$\psi_{RB2}^{0}(z,t)=\sum_{n=1}^{\infty}\Psi_n(z)\tilde{\tilde{T}}_{2n(r)}(t)=\sum_{n=1}^{\infty}\cos(k_nz)\sum_{g=3}^{4}\tilde{\tilde{\alpha}}_{ng}\left[\tilde{\tilde{A}}_{ng}\sin(\tilde{\tilde{\omega}}_{ng}t)+\tilde{\tilde{B}}_{ng}\cos(\tilde{\tilde{\omega}}_{ng}t)\right]. \tag{2.3.49}$$

Unknown constants $\tilde{\tilde{A}}_{ni}$,$\tilde{\tilde{B}}_{ni}$,$\tilde{\tilde{A}}_{ng}$ and $\tilde{\tilde{B}}_{ng}$ (i = 1, 2; g=3,4) are determined based on initial conditions (2.3.27) using the orthogonality condition for trigonometric functions

$$\int_0^l Z_nZ_m\,dx=\int_0^l\sin(k_nz)\sin(k_mz)\mathrm{d}z=c\delta_{nm}\,,$$

$$c=\int_0^l Z_n^2dx=\int_0^l[\sin(k_nz)]^2\mathrm{d}z=\frac{l}{2},\qquad c=\int_0^l\Psi_n^2dz=\int_0^l[\cos(k_nz)]^2\mathrm{d}z=\frac{l}{2}. \tag{2.3.50}$$

where δ_{nm} is the Kronecker delta function. If we substitute initial conditions (2.3.27) and include them in the expressions $(2.3.46-2.3.49)$, we get

$$\begin{aligned}
&w_{RB1}^{0}(z,0)=\tilde{\tilde{w}}_{10}(z)=\sum_{n=1}^{\infty}\sin(k_nz)\sum_{i=1}^{2}\tilde{\tilde{B}}_{ni}\,,w_{RB2}^{0}(z,0)=\tilde{\tilde{w}}_{20}(z)=\sum_{n=1}^{\infty}\sin(k_nz)\sum_{i=1}^{2}\tilde{\tilde{\alpha}}_{ni}\tilde{\tilde{B}}_{ni}\,,\\
&\dot{w}_{RB1}^{0}(z,0)=\tilde{\tilde{v}}_{10}(z)=\sum_{n=1}^{\infty}\sin(k_nz)\sum_{i=1}^{2}\tilde{\tilde{\omega}}_{ni}\tilde{\tilde{A}}_{ni}\,,\dot{w}_{RB2}^{0}(z,0)=\tilde{\tilde{v}}_{20}(z)=\sum_{n=1}^{\infty}\sin(k_nz)\sum_{i=1}^{2}\tilde{\tilde{\alpha}}_{ni}\tilde{\tilde{\omega}}_{ni}\tilde{\tilde{A}}_{ni},\\
&\psi_{RB1}^{0}(z,0)=\tilde{\tilde{\psi}}_{10}(z)=\sum_{n=1}^{\infty}\cos(k_nz)\sum_{g=3}^{4}\tilde{\tilde{B}}_{ng}\,,\psi_{T2}^{0}(z,0)=\tilde{\tilde{\psi}}_{20}(z)=\sum_{n=1}^{\infty}\cos(k_nz)\sum_{g=3}^{4}\tilde{\tilde{\alpha}}_{ng}\tilde{\tilde{B}}_{ng},\\
&\dot{\psi}_{RB1}^{0}(z,0)=\tilde{\tilde{\Theta}}_{10}(z)=\sum_{n=1}^{\infty}\cos(k_nz)\sum_{g=3}^{4}\tilde{\tilde{\omega}}_{ng}\tilde{\tilde{A}}_{ng}\,,\dot{\psi}_{RB1}^{0}(z,0)=\tilde{\tilde{\Theta}}_{20}(z)=\sum_{n=1}^{\infty}\cos(k_nz)\sum_{g=3}^{4}\tilde{\tilde{\alpha}}_{ng}\tilde{\tilde{\omega}}_{ng}\tilde{\tilde{A}}_{ng}\,.
\end{aligned} \tag{2.3.51}$$

By multiplying the expression (2.3.51) by appropriate eigenfunctions Z_n, i.e. Ψ_n then integrating it with respect to z from 0 to l and using the orthogonality condition (2.3.50), we have

$$\frac{2}{l}\int_0^l \tilde{\bar{w}}_{10}\sin(k_n z)\,dz = \sum_{i=I}^{2}\tilde{\bar{B}}_{ni}, \qquad \frac{2}{l}\int_0^l \tilde{\bar{w}}_{20}\sin(k_n z)\,dz = \sum_{i=\mathrm{I}}^{2}\tilde{\bar{\alpha}}_{ni}\tilde{\bar{B}}_{ni}, \tag{2.3.52}$$

$$\frac{2}{l}\int_0^l \tilde{\bar{v}}_{10}\sin(k_n z)\,dz = \sum_{i=\mathrm{I}}^{2}\tilde{\bar{\omega}}_{ni}\tilde{\bar{A}}_{ni}, \qquad \frac{2}{l}\int_0^l \tilde{\bar{v}}_{20}\sin(k_n z)\,dz = \sum_{i=\mathrm{I}}^{2}\tilde{\bar{\alpha}}_{ni}\tilde{\bar{\omega}}_{ni}\tilde{\bar{A}}_{ni}, \tag{2.3.53}$$

$$\frac{2}{l}\int_0^l \tilde{\bar{\psi}}_{10}\cos(k_n z)\,dz = \sum_{g=\mathrm{III}}^{4}\tilde{\bar{B}}_{ng}, \qquad \frac{2}{l}\int_0^l \tilde{\bar{\psi}}_{20}\cos(k_n z)\,dz = \sum_{g=\mathrm{III}}^{4}\tilde{\bar{\alpha}}_{ng}\tilde{\bar{B}}_{ng}, \tag{2.3.54}$$

$$\frac{2}{l}\int_0^l \tilde{\bar{\Theta}}_{10}\cos(k_n z)\,dz = \sum_{g=\mathrm{III}}^{4}\tilde{\bar{\omega}}_{ng}\tilde{\bar{A}}_{ng}, \qquad \frac{2}{l}\int_0^l \tilde{\bar{\Theta}}_{20}\cos(k_n z)\,dz = \sum_{g=\mathrm{III}}^{4}\tilde{\bar{\alpha}}_{ng}\tilde{\bar{\omega}}_{ng}\tilde{\bar{A}}_{ng}. \tag{2.3.55}$$

After solving the system of equations (2.3.52-2.3.55), we get the unknown constants in the following form

$$\tilde{\bar{A}}_{n1} = \frac{2}{\tilde{\bar{\omega}}_{n1}\left(\tilde{\bar{\alpha}}_{n2}-\tilde{\bar{\alpha}}_{n1}\right)l}\int_0^l \left(\tilde{\bar{v}}_{10}\tilde{\bar{\alpha}}_{n2}-\tilde{\bar{v}}_{20}\right)\sin(k_n z)\,\mathrm{d}z,$$

$$\tilde{\bar{A}}_{n2} = \frac{2}{\tilde{\bar{\omega}}_{n2}\left(\tilde{\bar{\alpha}}_{n1}-\tilde{\bar{\alpha}}_{n2}\right)l}\int_0^l \left(\tilde{\bar{v}}_{20}\tilde{\bar{\alpha}}_{n1}-\tilde{\bar{v}}_{10}\right)\sin(k_n z)\,\mathrm{d}z,$$

$$\tilde{\bar{B}}_{n1} = \frac{2}{\left(\tilde{\bar{\alpha}}_{n2}-\tilde{\bar{\alpha}}_{n1}\right)l}\int_0^l \left(\tilde{\bar{w}}_{10}\tilde{\bar{\alpha}}_{n2}-\tilde{\bar{w}}_{20}\right)\sin(k_n z)\,\mathrm{d}z,$$

$$\tilde{\bar{B}}_{n2} = \frac{2}{\left(\tilde{\bar{\alpha}}_{n1}-\tilde{\bar{\alpha}}_{n2}\right)l}\int_0^l \left(\tilde{\bar{w}}_{10}\tilde{\bar{\alpha}}_{n1}-\tilde{\bar{w}}_{20}\right)\sin(k_n z)\,\mathrm{d}z,$$

$$\tilde{\bar{A}}_{n3} = \frac{2}{\tilde{\bar{\omega}}_{n3}\left(\tilde{\bar{\alpha}}_{n4}-\tilde{\bar{\alpha}}_{n3}\right)l}\int_0^l \left(\tilde{\bar{\Theta}}_{10}\tilde{\bar{\alpha}}_{n4}-\tilde{\bar{\Theta}}_{20}\right)\cos(k_n z)\,\mathrm{d}z,$$

$$\tilde{\bar{A}}_{n4} = \frac{2}{\tilde{\bar{\omega}}_{n4}\left(\tilde{\bar{\alpha}}_{n3}-\tilde{\bar{\alpha}}_{n4}\right)l}\int_0^l \left(\tilde{\bar{\Theta}}_{20}\tilde{\bar{\alpha}}_{n3}-\tilde{\bar{\Theta}}_{10}\right)\cos(k_n z)\,\mathrm{d}z,$$

$$\tilde{\bar{B}}_{n3} = \frac{2}{\left(\tilde{\bar{\alpha}}_{n4}-\tilde{\bar{\alpha}}_{n3}\right)l}\int_0^l \left(\tilde{\bar{\Theta}}_{10}\tilde{\bar{\alpha}}_{n4}-\tilde{\bar{\Theta}}_{20}\right)\cos(k_n z)\,\mathrm{d}z,$$

$$\tilde{\bar{B}}_{n4} = \frac{2}{\left(\tilde{\bar{\alpha}}_{n3}-\tilde{\bar{\alpha}}_{n4}\right)l}\int_0^l \left(\tilde{\bar{\Theta}}_{10}\tilde{\bar{\alpha}}_{n3}-\tilde{\bar{\Theta}}_{20}\right)\cos(k_n z)\,\mathrm{d}z.$$

2.4 Critical Buckling Force of the Two Elastically Connected Beams with Numerical Analysis

The conditions for static stability of the system composed of two elastically connected beams (of Timoshenko's or Reddy-Bickford's type) shall be

determined for the case in which the beams' material properties and transverse shear are identical.

$$A_1 = A_2 = A, \quad I_1 = I_2 = I, \; h_1 = h_2 = h, \; b_1 = b_2 = b. \tag{2.4.1}$$

As the compression forces rise, the natural frequency of vibration declines. When compression forces equal critical value, the vibration frequency equals zero and the beam system is in the state of indifferent equilibrium. If we introduce a new label ζ as the ratio of axial compression force on the second beam and the compression force on the first beam ($F_2 = \zeta F_{1,} \; 0 \le \zeta \le 1.$), by solving the frequency equations (2.2.26) and (2.3.33) under conditions $\widetilde{\omega}_n = 0, \widetilde{\widetilde{\omega}}_n = 0$, we get two solutions, the lower of which represents the critical buckling force of the system, ref. [12].

$$[F_b^{kr}]_T = \frac{(1+\zeta)(C_b^2 k_n^4 + HR) - \sqrt{(1+\zeta)^2 (C_b^2 k_n^4 + HR)^2 - 4\zeta C_b^2 k_n^4 (C_b^2 k_n^4 + 2HR)}}{2\zeta\eta R}. \tag{2.4.2}$$

Critical buckling force of the system composed of two elastically connected Reddy-Bickford beams is given in Appendix 2.4.1. Let us analyze the effects of rotary inertia and transverse shear for system parameters in references [2- 5].

$$E = 1 \times 10^{10}\mathrm{Nm}^{-2}, \qquad \nu = 0.34, \qquad K_0 = 2 \times 10^5 \mathrm{Nm}^{-2},$$
$$\rho = 2 \times 10^3 \mathrm{kgm}^{-3}, \; A = 5 \times 10^{-2}\mathrm{m}^2, \qquad I = 4 \times 10^{-4}\mathrm{m}^4,$$
$$l = 10 \text{ m}, b = \frac{1}{8}\sqrt{\frac{5}{3}}\text{m}, h_1 = \frac{2}{5}\sqrt{\frac{3}{5}}\text{m}, \tag{2.4.3}$$

The values of natural frequencies taking into account the effects of rotary inertia and transverse shear of the system composed of two elastically connected beams are shown in Tables 2.4.1-2.4.3. In the numerical experiment two set of values were used for shear modulus and shear factor, ref. Kaneko [24] in the form $G = \frac{E}{2(1+\nu)}, \; k = \frac{5+5\nu}{6+5\nu}$, which best corresponds to experimental results, and based on the beams' material properties for the example used in reference [12]$G = 0.417 * 10^{10}\mathrm{Nm}^{-2}, \; k = \frac{5}{6}$. Differences in approximate solutions are shown by model in Tables 2.4.1-2.4.3 and in set of Figures 2.4.1-2.4.7 where the values for shear factor, shear modulus and the stiffness modulus of the Winkler's layer were taken from the Table 2.4.1.

Table 2.4.1 The effects of rotary inertia and transverse shear on natural frequencies ω_{ni} $[s^{-1}]$ of the system composed of two elastically connected beams

$G = \frac{E}{2(1+\nu)}$, $k = \frac{5+5\nu}{6+5\nu}$, $K = K_0$, $h = h_1$						
ω_{n1}	$n=1$	$n=2$	$n=3$	$n=4$	$n=5$	$n=6$
Euler Ref. [2]	19.7392088	78.95683521	177.6528792	315.8273408	493.48022	710.6115169
Rayleigh	19.73142068	78.83244614	177.0250126	313.8511075	488.6807037	700.7224681
Timoshenko	19.70750988	78.45416481	175.1450850	308.0582167	474.9781982	673.3499488
Reddy – Bickford	19.70645683	78.43763349	175.0639586	307.8124549	474.4089419	672.2401494
ω_{n2}						
Euler	66.25433091	101.1641331	188.5750394	322.0976703	497.5165601	713.4204426
Rayleigh	66.22819023	101.0047585	187.9085713	320.0822015	492.6777869	703.4923041
Timoshenko	66.22118522	100.7109845	186.1417643	314.4098382	479.0983084	676.2439654
Reddy – Bickford	66.22087688	100.6981586	186.0655667	314.1692786	478.5342958	675.1393769
$G = 0.417 * 10^{10}\mathrm{Nm}^{-2}$, $k = \frac{5}{6}$, $K = K_0$, $h = h_1$						
ω_{n1}	1	2	3	4	5	6
Euler Ref. [2]	19.7392088	78.95683521	177.6528792	315.8273408	493.48022	710.6115169
Rayleigh Ref. [12]	19.73142068	78.83244614	177.0250126	313.8511075	488.6807037	700.7224681
Timoshenko Ref. [12]	19.70907774	78.47884506	175.2667468	308.4290616	475.8439077	675.0535094
Reddy – Bickford	19.70907834	78.47888294	175.2671655	308.4313202	475.8520989	675.076565
ω_{n2}						
Euler Ref. [2]	66.25433091	101.1641331	188.5750394	322.0976703	497.5165601	713.4204426
Rayleigh Ref. [12]	66.22819023	101.0047585	187.9085713	320.0822015	492.6777869	703.4923041
Timoshenko Ref. [12]	66.22164431	100.7301345	186.2560413	314.7728451	479.9560596	677.9395464
Reddy – Bickford	66.22164449	100.7301639	186.2564343	314.7750549	479.964173	677.9624891

Table 2.4.2 Differences in approximate solutions for the system of beams with the thickness of h=5h_1 on natural frequencies of the system $\omega_{ni}[s^{-1}]$

$G = \frac{E}{2(1+\nu)}$, $k = \frac{5+5\nu}{6+5\nu}$, $K = K_0$, $h = 5h_1$						
ω_{n1}	1	2	3	4	5	6
Euler	98.69604401	394.784176	888.2643961	1579.136704	2467.4011	3553.057584
Rayleigh	97.73614075	380.0648459	818.5281234	1376.639653	2019.017189	2716.605342
Timoshenko	94.99563965	345.2596898	688.0823255	1078.122727	1490.714755	1913.386112
Reddy – Bickford	94.88178838	344.0089987	684.15508	1070.713232	1480.196228	1901.278312
ω_{nII}	1	2	3	4	5	6
Euler	102.6689295	395.796091	888.7145984	1579.389986	2467.563209	3553.170161
Rayleigh	101.6703866	381.0390321	818.942981	1376.860456	2019.149839	2716.691416
Timoshenko	99.04721409	346.3588862	688.6203052	1078.461698	1490.959154	1913.57705
Reddy – Bickford	98.9383564	345.1129821	684.6970415	1071.055235	1480.442691	1901.47038

In Table 2.4.1 a small difference can be seen in the approximations of solutions for natural frequencies for different values of shear factor in Timoshenko and Reddy-Bickford models. A more significant difference is noticeable in thicker beams (Table 2.4.2) where the Euler and Rayleigh model fail to give satisfactory approximations.

Table 2.4.3 Differences in approximate solutions of the second natural frequency of the system ω_{n2} $[s^{-1}]$ for the beam system joined by a Winkler layer with different stiffness modulus K

$G = \frac{E}{2(1+\nu)}, \quad k = \frac{5+5\nu}{6+5\nu}, \quad K = 2K_0, \quad h = h_1$						
ω_{n2}	1	2	3	4	5	6
Euler	91.59495818	119.3070904	198.8983295	328.2482433	501.5204159	716.2183521
Rayleigh	91.55881934	119.1191333	198.1953765	326.1942884	496.6427018	706.2512772
Timoshenko	91.55383484	118.8711418	196.5240723	320.6356594	483.183285	679.1256472
Reddy – Bickford	91.55361544	118.8603191	196.4520286	320.4000033	482.6243859	678.0262049
$G = \frac{E}{2(1+\nu)}, \quad k = \frac{5+5\nu}{6+5\nu}, \quad K = 3K_0, \quad h = h_1$						
ω_{n2}	1	2	3	4	5	6
Euler	111.3087434	135.0340024	208.7116324	334.2856701	505.4925594	719.0053741
Rayleigh	111.2648265	134.8212691	207.9739969	332.193937	500.5762128	708.9995142
Timoshenko	111.2607921	134.6030973	206.3847488	326.7428715	487.2340118	681.9951506
Reddy – Bickford	111.2606144	134.5935781	206.3162691	326.5118478	486.6801011	680.9007912
$G = \frac{E}{2(1+\nu)}, \quad k = \frac{5+5\nu}{6+5\nu}, \quad K = 4K_0, \quad h = h_1$						
ω_{n2}	1	2	3	4	5	6
Euler	128.0220151	149.1113068	218.0838038	340.2159743	509.4337323	721.7816345
Rayleigh	127.9715040	148.8763959	217.3130449	338.0871335	504.4790544	711.7371396
Timoshenko	127.9680542	148.6796516	215.7953129	332.7380057	491.251336	684.8526286
Reddy – Bickford	127.9679024	148.6710684	215.7299358	332.5113677	490.7022939	683.7632902
$G = \frac{E}{2(1+\nu)}, \quad k = \frac{5+5\nu}{6+5\nu}, \quad K = 5K_0, \quad h = h_1$						
ω_{n2}	1	2	3	4	5	6
Euler	142.7922839	161.9696941	227.0694728	346.0446636	513.3446479	724.5472572
Rayleigh	142.7359452	161.7145261	226.2669564	343.8793508	508.3519331	714.4642751
Timoshenko	142.7329038	161.5341552	224.8122963	338.6270146	495.2360704	687.6982311
Reddy – Bickford	142.7327699	161.526287	224.7496527	338.4045372	494.691782	686.6138531
$G = \frac{E}{2(1+\nu)}, \quad k = \frac{5+5\nu}{6+5\nu}, \quad K = 6K_0, \quad h = h_1$						
ω_{n2}	1	2	3	4	5	6
Euler	156.1718168	173.8797913	235.7128454	351.7767889	517.2259927	727.3023635
Rayleigh	156.1101991	173.60586	234.8797813	349.5756083	512.1955285	717.1810407
Timoshenko	156.1074651	173.4385405	233.4813034	344.4153421	499.1889956	690.532105
Reddy – Bickford	156.1073447	173.431242	233.4210928	344.1968189	498.6493502	689.4526279

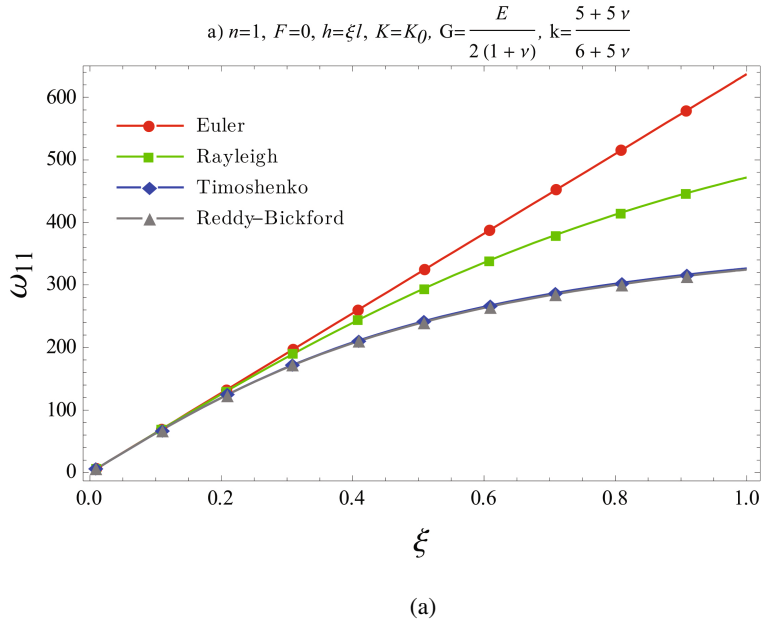

(a)

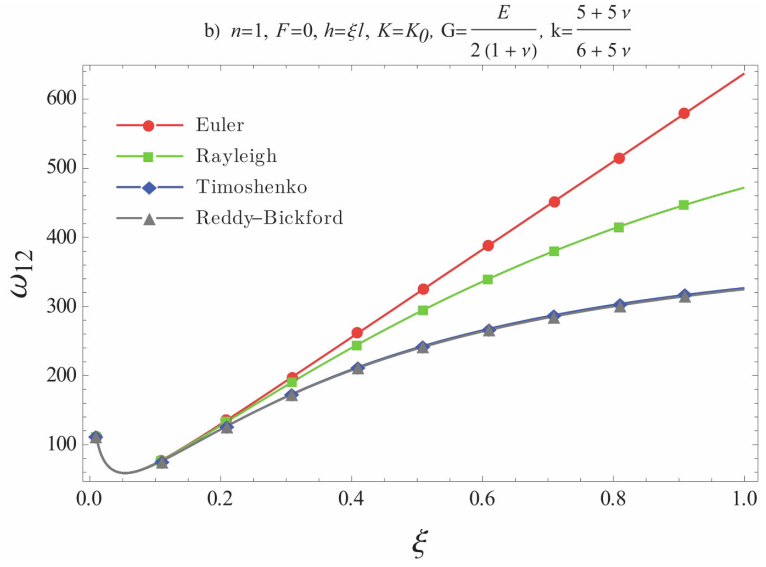

(b)

Fig. 2.4.1 a) The influence of beam thickness ξ on natural frequencies of the system ω_{ni} $[s^{-1}]$ for the first mode b) The influence of beam thickness ξ on natural frequencies of the system ω_{ni} $[s^{-1}]$ for the first mode

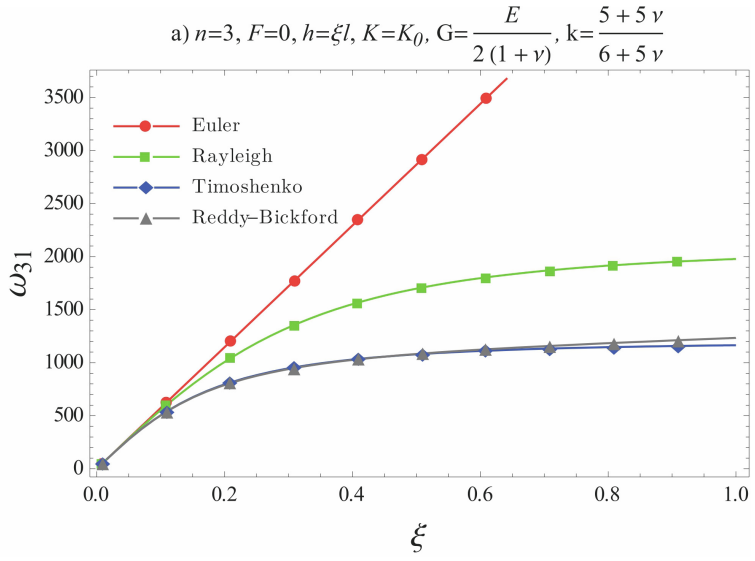

Fig. 2.4.2 a) The influence of beam's thickness factor ξ on natural frequencies ω_{ni} $[s^{-1}]$ of the system for the third mode b) The influence of beam's thickness factor ξ on natural frequencies ω_{ni} $[s^{-1}]$ of the system for the third mode

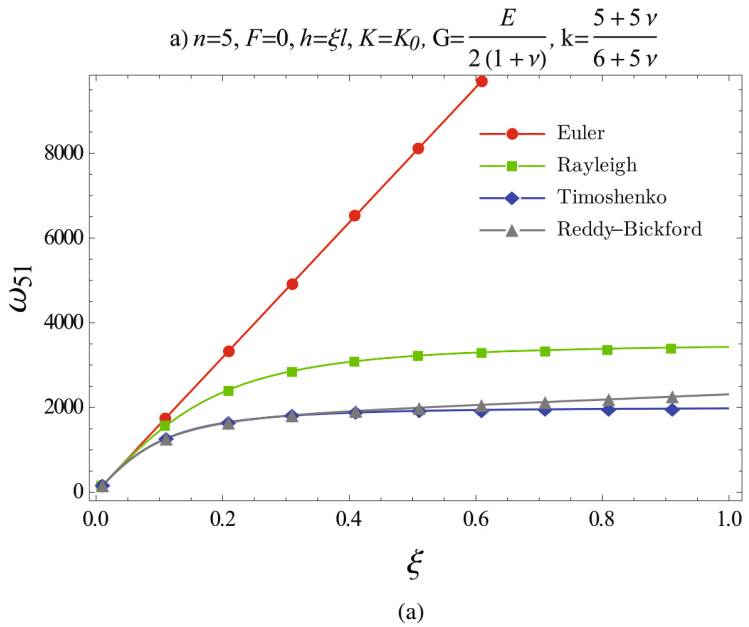

(a)

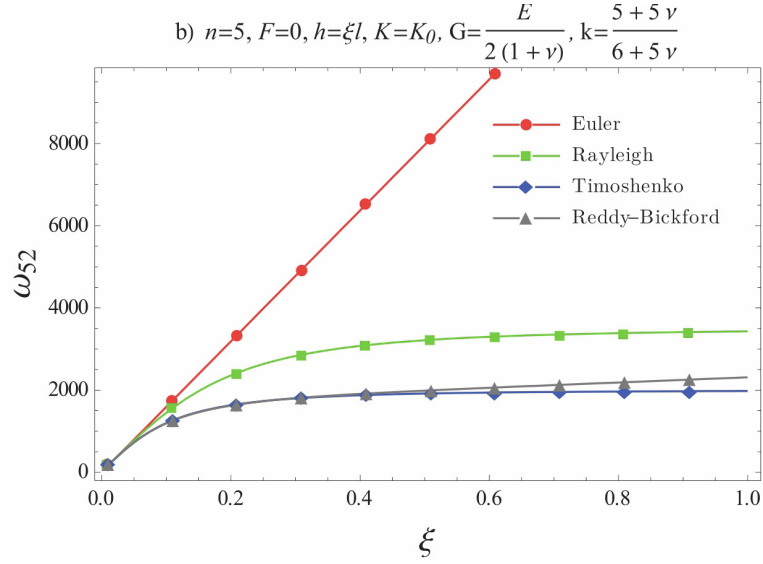

(b)

Fig. 2.4.3 a) The influence of beam thickness ξ on natural frequencies ω_{ni} $[s^{-1}]$ of the system for the fifth mode b) The influence of beam thickness ξ on natural frequencies ω_{ni} $[s^{-1}]$ of the system for the fifth mode

The considered models offer almost the same approximate solutions in lower modes, although the difference significantly increases in thicker beams. In a set of figures 2.4.1-2.4.3 the changes in natural frequencies were shown depending on beam thickness factor $\xi = h/l$ in different modes. It can be concluded that with the ξ values higher than 0.2, a significant difference occurs between the results obtained for Euler and Rayleigh model on the one hand, and quite better approximations obtained for Timoshenko and Reddy-Bickford model on the other.

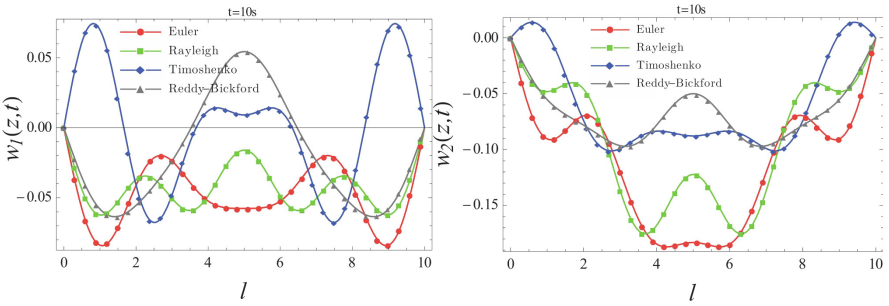

Fig. 2.4.4 Transverse motion of beam's centre lines for the sum of the first seven members of the order with the given initial conditions $t = 10s, w_{10} = 0.1m, w_{20} = 0.2m,\ v_{10} = 1\,m/s\,, v_{20} = 2\,m/s.$

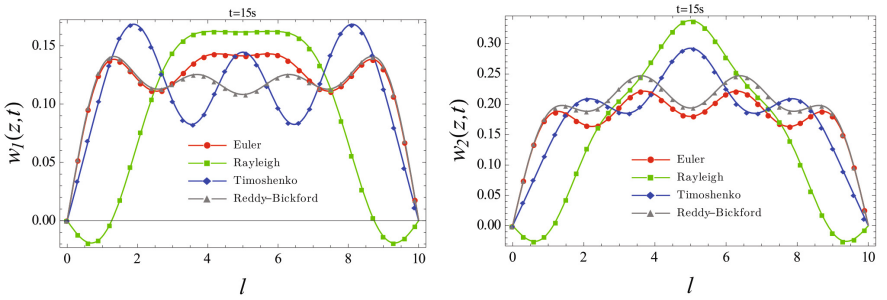

Fig. 2.4.5 Transverse motion of beam's centre lines for the sum of the first seven members of the order with the given initial conditions $t = 15s, w_{10} = 0.1m, w_{20} = 0.2m,\ v_{10} = 1\,m/s\,, v_{20} = 2\,m/s.$

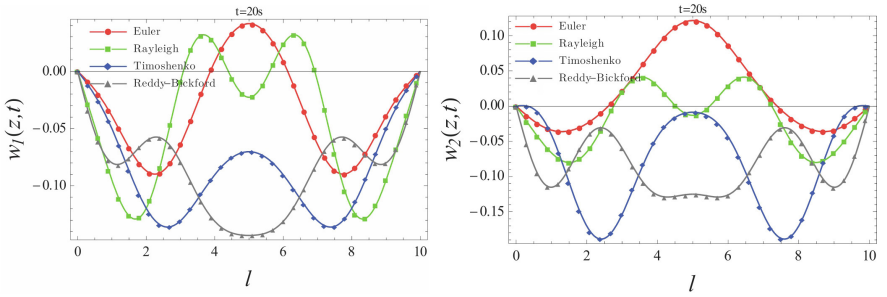

Fig. 2.4.6 Transverse motion of beam's centre lines for the sum of the first seven members of the order with the given initial conditions $t = 20s, w_{10} = 0.1m, w_{20} = 0.2m,\ v_{10} = 1\,m/s\,, v_{20} = 2\,m/s.$

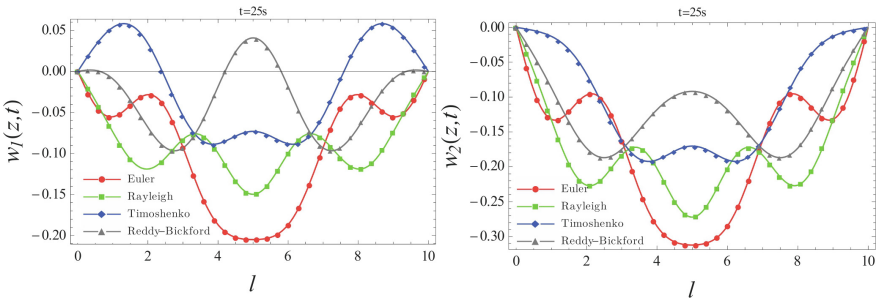

Fig. 2.4.7 Transverse motion of beam's centre lines for the sum of the first seven members of the order with the given initial conditions $t = 25s, w_{10} = 0.1m, w_{20} = 0.2m$, $v_{10} = 1\,m/s\,, v_{20} = 2\,m/s$.

The set of Figures 2.4.1-2.4.3 show changes in the frequency up to the value $\xi = 1$ as in such cases it is possible to analyze the frequencies of elastic bodies whose all three spatial dimensions are close. This dimension ratio can be seen in multi-span beams [27] when the distances between the supports are small compared to beam thickness or at the vibration of hulls on small wave-lengths. Figures 2.4.4-2.4.6 show transverse motion of the beams' centre lines for different models at different times determined for the first 7 members of the order in the sum under set initial conditions. It can be concluded that with different model types there is a difference between transverse motions of the beam's centre lines which increases if the greater number of members are taken in the sum.

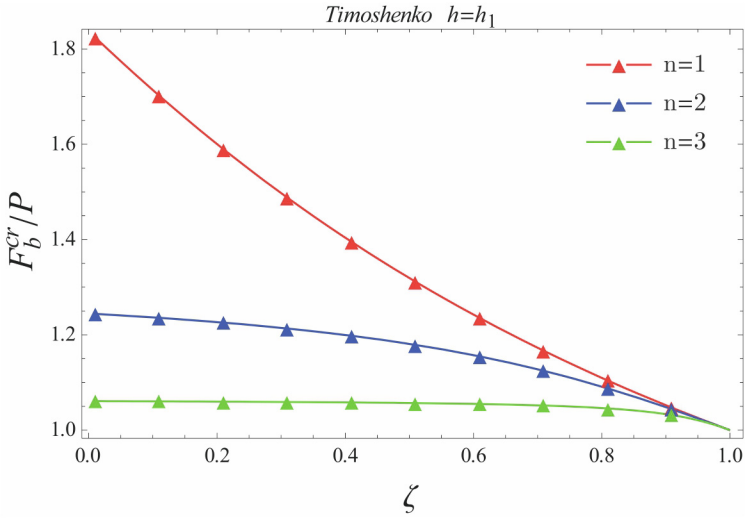

Fig. 2.4.8 The influence of axial compression forces ζ on the critical force ratio F_b^{cr}/P_n in modes 1, 2 and 3 ($h = h_1$, Timoshenko model)

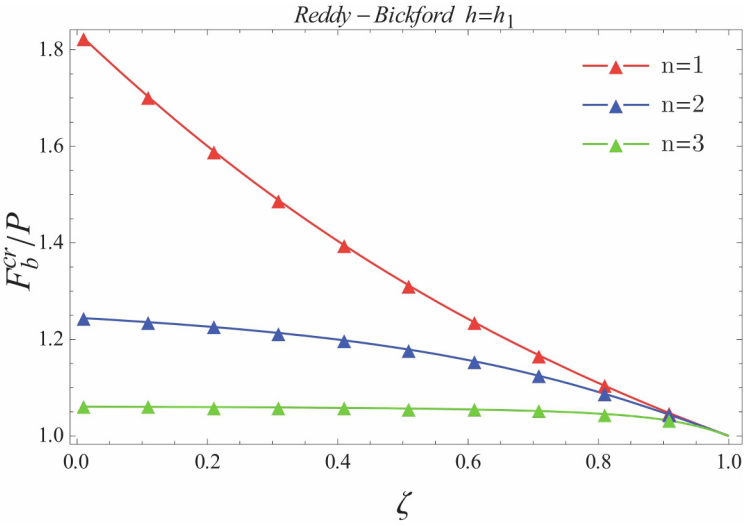

Fig. 2.4.9 The influence of axial compression forces ζ on the critical force ratio F_b^{kr}/P_n in modes 1, 2 and 3 ($h = h_1$, Reddy-Bickford model)

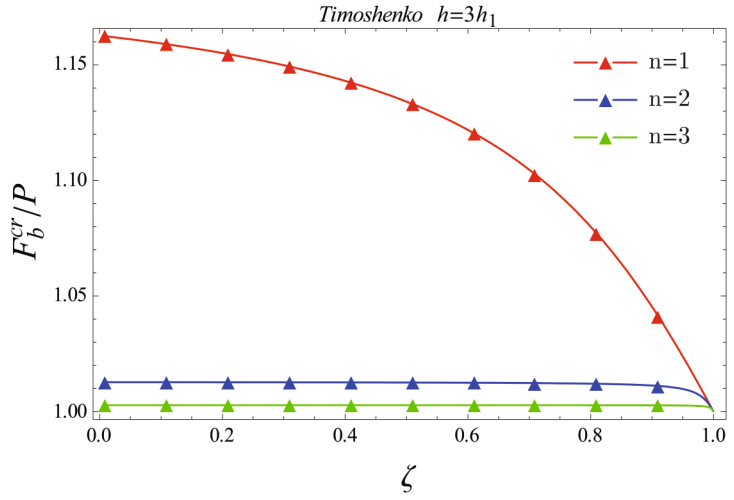

Fig. 2.4.10 The influence of axial compression forces ζ on the critical force ratio F_b^{kr}/P_n in modes 1, 2 and 3 ($h = 3h_1$,Timoshenko model)

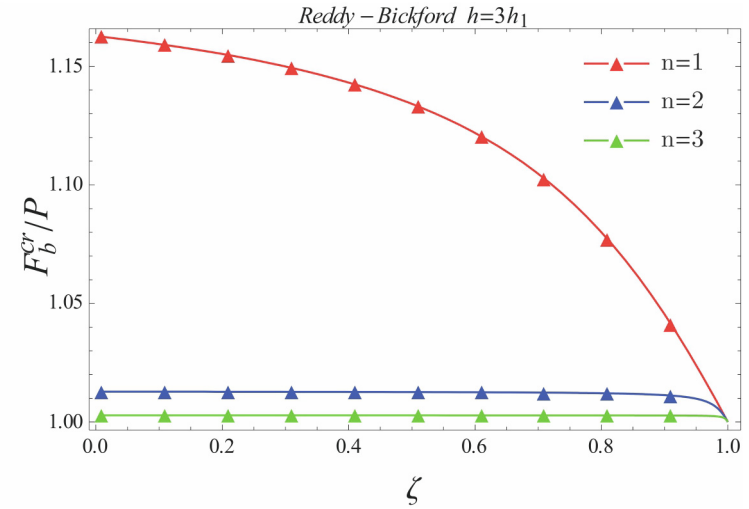

Fig. 2.4.11 The influence of axial compression forces ζ on the critical force ratio F_b^{kr}/P_n in modes 1, 2 and 3 ($h = 3h_1$, Reddy-Bickford model)

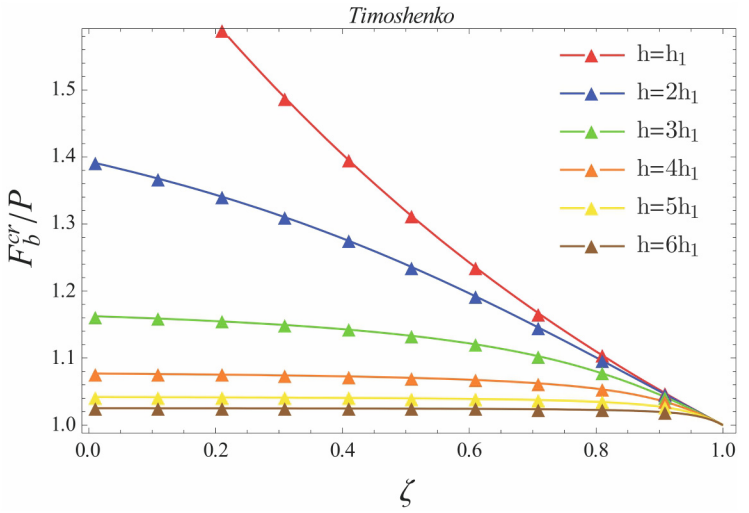

Fig. 2.4.12 The influence of axial compression forces ζ on the critical force ratio F_b^{kr}/P_n for different beam thickness (Timoshenko model)

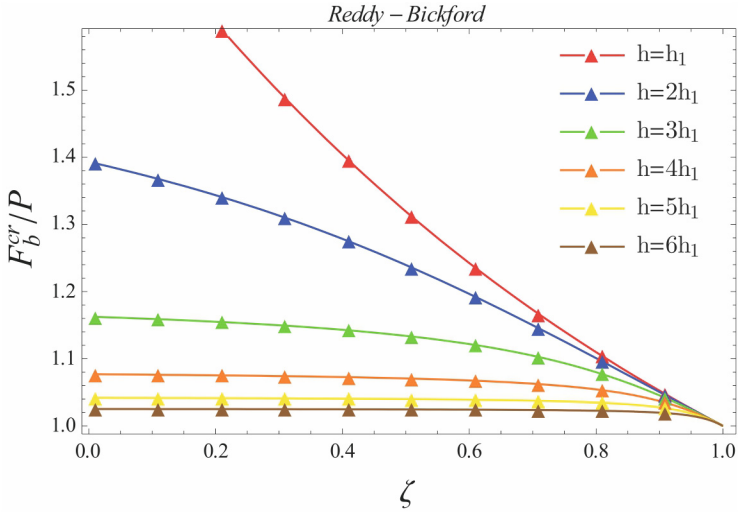

Fig. 2.4.13 The influence of axial compression forces ζ on the critical force ratio F_b^{kr}/P_n for different beam thickness (Reddy-Bickford model)

Set of Figures 2.4.8-2.4.13 show the critical force ratio depending on the axial compression force on the second beam ζ. It can be concluded that in the critical force ratio there is a minor difference between the Timoshenko and Reddy-Bickford model, and that regardless of beam thickness and the mode in which the critical force is considered, both theories can be applied with equal success. The general conclusion based on the shown results may be that only the Timoshenko and the Reddy-Bickford theory can apply to thicker beams. The advantage of the latter is in determining the shear stress for which we do not need the shear factor. With the increase of the vibration mode, the best approximate solutions are provided by the Reddy-Bickford beam theory. Based on certain differences in approximate solutions between the applied theories, the presented results can be used in deciding which mathematical model to apply for dynamic consideration of the two elastically connected beams.

Chapter 3

Effects of Axial Compression Forces, Rotary Inertia and Shear on Forced Vibrations of the System of Two Elastically Connected Beams

This chapter covers the solution for forced vibrations of two elastically connected beams of Rayleigh's, Timoshenko's and Reddy–Bickford's type under the influence of axial forces. Scientific contribution is presented through the analytical solutions in forms of three cases of forced vibrations - Harmonic arbitrarily continuous excitation, the continuous uniform harmonic excitation and harmonic concentrated excitation. Analytical solutions were obtained by using the modal analysis method. Based on the results derived in this chapter, it can be made a conclusion that the differences in the approximations of the solutions depending of the used model gave a good solutions just in cases of Timoshenko's and Reddy-Bickford's theory for thick beams in higher modes also in forced vibrations regime and must be taken into account.

3.1 Forced Vibrations of Two Elastically Connected Rayleigh Beams

Let us analyze the effects of axial compression forces and rotary inertia on forced transverse vibration of the system composed of two elastically connected Rayleigh beams, Stojanović and Kozić [13]. Let the beams be of the same length l and connected by an elastic layer with stiffness modulus K. The beams are exposed to forced loads $f_1(z,t)$ and $f_2(z,t)$ and axial compression forces at their ends as shown in Figure 3.1.1.

Let the functions of longitudinal and transverse motion of the system composed of Rayleigh beams $u_{R1}(y,z,t)$, $w_{R1}(y,z,t)$, $u_{R2}(y,z,t)$ and $w_{R2}(y,z,t)$ be

$$u_{R1}(y,z,t) = u_{R1}^0(z,t) - y\frac{\partial w_{R1}^0(z,t)}{\partial z}, \quad w_{R1}(y,z,t) = w_{R1}^0(z,t), \qquad (3.1.1)$$

$$u_{R2}(y,z,t) = u_{R2}^0(z,t) - y\frac{\partial w_{R2}^0(z,t)}{\partial z}, \quad w_{R2}(y,z,t) = w_{R2}^0(z,t). \qquad (3.1.2)$$

V. Stojanović and P. Kozić, *Vibrations and Stability of Complex Beam Systems*,
Springer Tracts in Mechanical Engineering, DOI: 10.1007/978-3-319-13767-4_3

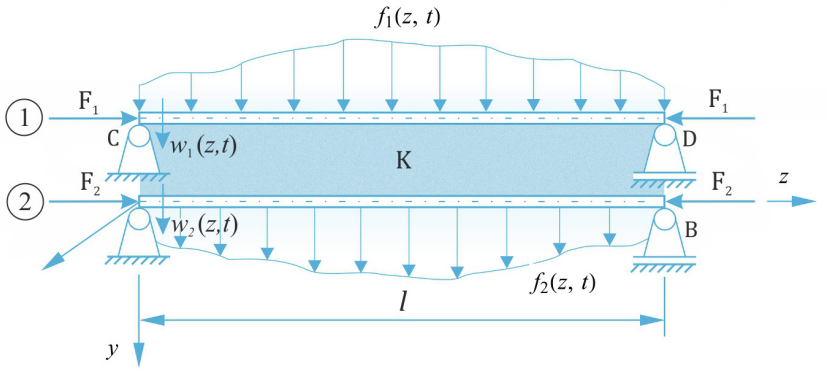

Fig. 3.1.1 The system of two elastically connected beams under the influence of forced loads

Deformation in z direction in the function of motion and the relation between stress and deformation according to Hooke's law are

$$\varepsilon_{z1}(y,z,t)=\frac{\partial u_{R1}^0(z,t)}{\partial z}-y\frac{\partial^2 w_{R1}^0(z,t)}{\partial z^2},\quad \varepsilon_{z2}(y,z,t)=\frac{\partial u_{R2}^0(z,t)}{\partial z}-y\frac{\partial^2 w_{R2}^0(z,t)}{\partial z^2}. \tag{3.1.3}$$

$$\sigma_{z1}(y,z,t)=E\varepsilon_{z1}(y,z,t),\qquad \sigma_{z2}(y,z,t)=E\varepsilon_{z2}(y,z,t), \tag{3.1.4}$$

Virtual work of inertial forces is given by

$$\delta W_{in1}=-\rho b_1\int_0^l\int_{-\frac{h_1}{2}}^{\frac{h_1}{2}}\left[\frac{\partial^2 w_{R1}(y,z,t)}{\partial t^2}\delta w_{R1}(y,z,t)+\frac{\partial^2 u_{R1}(y,z,t)}{\partial t^2}\delta u_{R1}(y,z,t)\right]dydz, \tag{3.1.5}$$

$$\delta W_{in2}=-\rho b_2\int_0^l\int_{-\frac{h_2}{2}}^{\frac{h_2}{2}}\left[\frac{\partial^2 w_{R2}(y,z,t)}{\partial t^2}\delta w_{R2}(y,z,t)+\frac{\partial^2 u_{R2}(y,z,t)}{\partial t^2}\delta u_{R2}(y,z,t)\right]dydz. \tag{3.1.6}$$

Virtual work of internal forces is expressed as

$$\delta W_{V1}=-b_1\int_0^l\int_{-\frac{h_1}{2}}^{\frac{h_1}{2}}\sigma_{z1}(z,t)\delta\varepsilon_{z1}(z,t)dydz,\ \ \delta W_{V2}=-b_2\int_0^l\int_{-\frac{h_2}{2}}^{\frac{h_2}{2}}\sigma_{z2}(z,t)\delta\varepsilon_{z2}(z,t)dydz. \tag{3.1.7}$$

Virtual work of external forces is

$$\delta W_{ex1}=\int_0^l\Big[f_1(z,t)\delta w_{R1}^0(z,t)+\delta w_{R1}^0(z,t)K\Big(w_{R2}^0(z,t)-w_{R1}^0(z,t)\Big)+F_1\frac{\partial w_{R1}^0(z,t)}{\partial z}\frac{\partial\delta w_{R1}^0(z,t)}{\partial z}\Big]dz, \tag{3.1.8}$$

$$\delta W_{ex2} = \int_0^l \Big[f_2(z,t)\delta w_{R2}^0(z,t) + \delta w_{R2}^0(z,t) K\Big(w_{R1}^0(z,t) - w_{R2}^0(z,t)\Big) + F_2 \frac{\partial w_{R2}^0(z,t)}{\partial z} \frac{\partial \delta w_{R2}^0(z,t)}{\partial z} \Big] dz, \tag{3.1.9}$$

Based on the principle of virtual work $\delta W_{ini} + \delta W_{Vi} + \delta W_{exi} = 0,\ i = 1,2$ and the equations (3.1.5-3.1.9), we have

$$\begin{aligned} &-b_1 \int_0^l \int_{-\frac{h_1}{2}}^{\frac{h_1}{2}} \sigma_{z1}(z,t)\delta\varepsilon_{z1}(z,t) dy dz \\ &- \rho b_1 \int_0^l \int_{-\frac{h_1}{2}}^{\frac{h_1}{2}} \Big[\frac{\partial^2 w_{R1}(y,z,t)}{\partial t^2} \delta w_{R1}(y,z,t) + \frac{\partial^2 u_{R1}(y,z,t)}{\partial t^2} \delta u_{R1}(y,z,t) \Big] dy dz \\ &+ \int_0^l \Big[f_1(z,t)\delta w_{R1}^0(z,t) + \delta w_{R1}^0(z,t) K\big(w_{R2}^0(z,t) - w_{R1}^0(z,t)\big) + F_1 \frac{\partial w_{R1}^0(z,t)}{\partial z} \frac{\partial \delta w_{R1}^0(z,t)}{\partial z} \Big] dz = 0, \end{aligned} \tag{3.1.10}$$

$$\begin{aligned} &-b_2 \int_0^l \int_{-\frac{h_2}{2}}^{\frac{h_2}{2}} \sigma_{z2}(z,t)\delta\varepsilon_{z2}(z,t) dy dz \\ &- \rho b_2 \int_0^l \int_{-\frac{h_2}{2}}^{\frac{h_2}{2}} \Big[\frac{\partial^2 w_{R2}(y,z,t)}{\partial t^2} \delta w_{R2}(y,z,t) + \frac{\partial^2 u_{R2}(y,z,t)}{\partial t^2} \delta u_{R2}(y,z,t) \Big] dy dz \\ &+ \int_0^l \Big[f_2(z,t)\delta w_{R2}^0(z,t) + \delta w_{R2}^0(z,t) K\big(w_{R1}^0(z,t) - w_{R2}^0(z,t)\big) + F_2 \frac{\partial w_{R2}^0(z,t)}{\partial z} \frac{\partial \delta w_{R2}^0(z,t)}{\partial z} \Big] dz = 0, \end{aligned} \tag{3.1.11}$$

By successive application of Green's theorem on expressions (3.1.10-3.1.11) we get the equations of transverse vibration for the system of elastically connected Rayleigh beams in the form

$$\rho A_1 \frac{\partial^2 w_{R1}^0(z,t)}{\partial t^2} - \rho I_{x1} \frac{\partial^4 w_{R1}^0(z,t)}{\partial z^2 \partial t^2} + E I_{x1} \frac{\partial^4 w_{R1}^0(z,t)}{\partial z^4} + F_1 \frac{\partial^2 w_{R1}^0(z,t)}{\partial z^2} + K\Big(w_{R1}^0(z,t) - w_{R2}^0(z,t)\Big) = f_1(z,t), \tag{3.1.12}$$

$$\rho A_2 \frac{\partial^2 w_{R2}^0(z,t)}{\partial t^2} - \rho I_{x2} \frac{\partial^4 w_{R2}^0(z,t)}{\partial z^2 \partial t^2} + E I_{x2} \frac{\partial^4 w_{R2}^0(z,t)}{\partial z^4} + F_2 \frac{\partial^2 w_{R2}^0(z,t)}{\partial z^2} + K\Big(w_{R2}^0(z,t) - w_{R1}^0(z,t)\Big) = f_2(z,t), \tag{3.1.13}$$

where ρ represents mass density, A the area of the cross-section, E Young's modulus, I_x moment of inertia of the beam's cross-section area for x-axis. The initial and boundary conditions for the system of two elastically connected simply supported Rayleigh beams are given by

$$w_{Ri}^0(z,0) = 0, \qquad \frac{dw_{R1}^0(z,0)}{dt} = 0, \tag{3.1.14}$$

$$w_{Ri}^0(0,t) = \frac{d^2w_{R1}^0(0,t)}{dz^2} = \frac{d^2w_{R1}^0(l,t)}{dz^2} = w_{Ri}^0(l,t) = 0, \quad i = 1,2. \tag{3.1.15}$$

Considering the harmonic motion of beams' points, the solutions to the equations (3.1.12) and (3.1.13) are assumed in the following form

$$w_{R1}^0(z,t) = \sum_{n=1}^{\infty} Z_n(z) \sum_{i=I}^{2} S_{in}(t)\,, \tag{3.1.16}$$

$$w_{R2}^0(z,t) = \sum_{n=1}^{\infty} Z_n(z) \sum_{i=I}^{2} \alpha_{ni} S_{in}(t)\,, \tag{3.1.17}$$

where $S_{in}(t)$ $(i = 1,2)$ are the unknown time functions with corresponding frequencies ω_{ni} of the Rayleigh model. If we substitute the assumed solutions (3.1.16) and (3.1.17) into the non-homogeneous system of partially differential equations (3.1.12) and (3.1.13), we get

$$\sum_{n=1}^{\infty} Z_n(z) \sum_{i=I}^{2} \left[J_1 \ddot{S}_{in} + (N_1 - F_1\eta_1 - H_1\alpha_{ni}) S_{in}\right] = m_1 f_1(z,t), \tag{3.1.18}$$

$$\sum_{n=1}^{\infty} Z_n(z) \sum_{i=I}^{2} \left[J_2 \ddot{S}_{in} + (N_2 - F_2\eta_2 - H_2\alpha_{ni}^{-1}) S_{in}\right] \alpha_{ni} = m_2 f_2(z,t), \tag{3.1.19}$$

where

$$m_1 = \frac{1}{\rho A_1}, \qquad m_2 = \frac{1}{\rho A_2}, \qquad H_1 = \frac{K}{\rho A_1}, \qquad H_2 = \frac{K}{\rho A_2}\,,$$

$$J_1 = 1 + C_{r1}^2 k_n^2, \qquad J_2 = 1 + C_{r2}^2 k_n^2, \qquad N_1 = C_{b1}^2 k_n^4 + H_1, N_2 = C_{b2}^2 k_n^4 + H_2.$$

$$C_{bi} = \sqrt{\frac{EI_i}{\rho A_i}}, \qquad C_{ri} = \sqrt{\frac{I_i}{A_i}}, \qquad i = 1,2.$$

Multiplying the equations (3.1.18) and (3.1.19) by eigenfunction Z_n, then integrating them with respect to z from 0 to l and using the orthogonality condition, we have

$$\sum_{i=1}^{2} \left[J_1 \ddot{S}_{in} + (N_1 - F_1\eta_1 - H_1\alpha_{ni}) S_{in}\right] = 2\frac{m_1}{l} \int_0^l Z_n\, f_1(z,t) dz. \tag{3.1.20}$$

$$\sum_{i=1}^{2}\left[J_2\ddot{S}_{in}+(N_2-F_2\eta_2-H_2\alpha_{ni}^{-1})S_{in}\right]\alpha_{ni}=2\frac{m_2}{l}\int_0^l Z_n f_2(z,t)dz. \quad (3.1.21)$$

Using the amplitude ratios determined in the previous chapter (2.1.26) and the equations (3.1.20) and (3.1.21), we get

$$\sum_{i=1}^{2}\left[\ddot{S}_{in}+\omega_{ni}^2 S_{in}\right]=2\frac{m_1}{J_1 l}\int_0^l Z_n f_1(z,t)\,dz, \quad (3.1.22)$$

$$\sum_{i=1}^{2}\left[\ddot{S}_{in}+\omega_{ni}^2 S_{in}\right]\alpha_{ni}=2\frac{m_2}{J_2 l}\int_0^l Z_n f_2(z,t)\,dz. \quad (3.1.23)$$

i.e.

$$\ddot{S}_{in}+\omega_{ni}^2 S_{in}=Y_{in}(t),\quad i=1,2, \quad (3.1.24)$$

where

$$Y_{n1}(t)=\frac{2}{\alpha_{n2}-\alpha_{n1}}\int_0^l[M_1\alpha_{n2}f_1(z,t)-M_2 f_2(z,t)]\sin(k_n z)\,dz, \quad (3.1.25)$$

$$Y_{n2}(t)=\frac{2}{\alpha_{n1}-\alpha_{n2}}\int_0^l[M_1\alpha_{n1}f_1(z,t)-M_2 f_2(z,t)]\sin(k_n z)\,dz, \quad (3.1.26)$$

$$M_1=\frac{m_1}{J_1 l},\qquad M_2=\frac{m_2}{J_2 l}.$$

From the equations (3.1.16), (3.1.17), (3.1.25) and (3.1.26) and the solution to the equation (3.1.24), ref. [5], the analytical forms of forced vibration of two elastically connected Rayleigh beams follow

$$w_{R1}^0(z,t)=\sum_{n=1}^{\infty}\sin(k_n z)\sum_{i=1}^{2}\frac{1}{\omega_{ni}}\int_0^t Y_{ni}(s)\sin[\omega_{ni}(t-s)]ds, \quad (3.1.27)$$

$$w_{R2}^0(z,t)=\sum_{n=1}^{\infty}\sin(k_n z)\sum_{i=1}^{2}\frac{\alpha_{ni}}{\omega_{ni}}\int_0^t Y_{ni}(s)\sin[\omega_{ni}(t-s)]ds. \quad (3.1.28)$$

General solutions for forced vibration (3.1.27) and (3.1.28) may be applied in analyzing the system under the influence of different types of forced loads.

3.2 Forced Vibrations of Two Elastically Connected Timoshenko Beams

Let us analyze the effects of axial compression forces, rotary inertia and transverse shear on forced transverse vibration of the system of two elastically connected

Timoshenko beams, Stojanović and Kozić [13]. Let us introduce the functions of longitudinal and transverse motion of the beam's points as well as the angle of rotation for Timoshenko beam's cross-section $u_{T1}(y,z,t)$, $w_{T1}(y,z,t), \psi^0_{T1}(z,t)$, $u_{T2}(y,z,t)$, $w_{T2}(y,z,t)$ and $\psi^0_{T2}(z,t)$. Equations of motion are given by

$$u_{T1}(y,z,t) = u^0_{T1}(z,t) + y\psi^0_{T1}(z,t), \qquad w_{T1}(y,z,t) = w^0_{T1}(z,t), \tag{3.2.1}$$

$$u_{T2}(y,z,t) = u^0_{T2}(z,t) + y\psi^0_{T2}(z,t), \qquad w_{T2}(y,z,t) = w^0_{T2}(z,t), \tag{3.2.2}$$

Deformation in the function of motion and the relation between stress and deformation according to the Hooke's law are

$$\varepsilon_{z1}(z,t) = \frac{\partial u^0_{T1}(z,t)}{\partial z} + y\frac{\partial \psi^0_{T1}(z,t)}{\partial z}, \quad \gamma_{zy1}(z,t) = \frac{\partial w^0_{T1}(z,t)}{\partial z} + \psi^0_{T1}(z,t), \tag{3.2.3}$$

$$\varepsilon_{z2}(z,t) = \frac{\partial u^0_{T2}(z,t)}{\partial z} + y\frac{\partial \psi^0_{T2}(z,t)}{\partial z}, \quad \gamma_{zy2}(z,t) = \frac{\partial w^0_{T2}(z,t)}{\partial z} + \psi^0_{T2}(z,t), \tag{3.2.4}$$

$$\begin{Bmatrix}\sigma_{z1}\\ \tau_{zy1}\end{Bmatrix} = \begin{bmatrix}E & 0\\ 0 & kG\end{bmatrix}\begin{Bmatrix}\varepsilon_{z1}\\ \gamma_{zy1}\end{Bmatrix}, \qquad \begin{Bmatrix}\sigma_{z2}\\ \tau_{zy2}\end{Bmatrix} = \begin{bmatrix}E & 0\\ 0 & kG\end{bmatrix}\begin{Bmatrix}\varepsilon_{z2}\\ \gamma_{zy2}\end{Bmatrix}. \tag{3.2.5}$$

Virtual work of inertial forces is given by

$$\delta W_{in1} = -\rho b_1 \int_0^l \int_{-\frac{h_1}{2}}^{\frac{h_1}{2}} \left[\frac{\partial^2 w_{T1}(y,z,t)}{\partial t^2}\delta w_{T1}(y,z,t) + \frac{\partial^2 u_{T1}(y,z,t)}{\partial t^2}\delta u_{T1}(y,z,t)\right] dydz, \tag{3.2.6}$$

$$\delta W_{in2} = -\rho b_2 \int_0^l \int_{-\frac{h_2}{2}}^{\frac{h_2}{2}} \left[\frac{\partial^2 w_{T2}(y,z,t)}{\partial t^2}\delta w_{T2}(y,z,t) + \frac{\partial^2 u_{T2}(y,z,t)}{\partial t^2}\delta u_{T2}(y,z,t)\right] dydz. \tag{3.2.7}$$

Virtual work of internal forces is expressed as

$$\delta W_{V1} = -b_1 \int_0^l \int_{-\frac{h_1}{2}}^{\frac{h_1}{2}} \left[\sigma_{z1}(z,t)\delta\varepsilon_{z1}(z,t) + \tau_{zy1}(z,t)\delta\gamma_{zy1}(z,t)\right] dydz, \tag{3.2.8}$$

$$\delta W_{V2} = -b_2 \int_0^l \int_{-\frac{h_2}{2}}^{\frac{h_2}{2}} \left[\sigma_{z2}(z,t)\delta\varepsilon_{z2}(z,t) + \tau_{zy2}(z,t)\delta\gamma_{zy2}(z,t)\right] dydz. \tag{3.2.9}$$

Virtual work of external forces is

$$\delta W_{ex1} = \int_0^l \Big[f_1(z,t)\delta w^0_{T1}(z,t) + \delta w^0_{T1}(z,t)K\big(w^0_{T2}(z,t) - w^0_{T1}(z,t)\big) + F_1\frac{\partial w^0_{T1}(z,t)}{\partial z}\frac{\partial \delta w^0_{T1}(z,t)}{\partial z}\Big] dz, \tag{3.2.10}$$

$$\delta W_{ex2} = \int_0^l \Big[f_2(z,t)\delta w_{T2}^0(z,t) + \delta w_{T2}^0(z,t)K\big(w_{T1}^0(z,t) - w_{T2}^0(z,t)\big) + F_2 \frac{\partial w_{T2}^0(z,t)}{\partial z}\frac{\partial \delta w_{T2}^0(z,t)}{\partial z}\Big] dz, \tag{3.2.11}$$

where δ represents variation operator. Substituting the equations (3.2.6-3.2.11) into a general equation of the virtual work principle $\delta W_{ini} + \delta W_{Vi} + \delta W_{exi} = 0$, $i = 1,2$, yields

$$-b_1 \int_0^l \int_{-\frac{h_1}{2}}^{\frac{h_1}{2}} \big[\sigma_{z1}(z,t)\delta\varepsilon_{z1}(z,t) + \tau_{zy1}(z,t)\delta\gamma_{zy1}(z,t)\big] dydz -$$

$$-\rho b_1 \int_0^l \int_{-\frac{h_1}{2}}^{\frac{h_1}{2}} \left[\frac{\partial^2 w_{T1}(y,z,t)}{\partial t^2}\delta w_{T1}(y,z,t) + \frac{\partial^2 u_{T1}(y,z,t)}{\partial t^2}\delta u_{T1}(y,z,t)\right] dydz +$$

$$+ \int_0^l \left[f_1(z,t)\delta w_{T1}^0(z,t) + \delta w_{T1}^0(z,t)K\big(w_{T2}^0(z,t) - w_{T1}^0(z,t)\big) + F_1 \frac{\partial w_{T1}^0(z,t)}{\partial z}\frac{\partial \delta w_{T1}^0(z,t)}{\partial z}\right] dz = 0, \tag{3.2.12}$$

$$-b_2 \int_0^l \int_{-\frac{h_2}{2}}^{\frac{h_2}{2}} \big[\sigma_{z2}(z,t)\delta\varepsilon_{z1}(z,t) + \tau_{zy2}(z,t)\delta\gamma_{zy2}(z,t)\big] dydz -$$

$$-\rho b_2 \int_0^l \int_{-\frac{h_2}{2}}^{\frac{h_2}{2}} \left[\frac{\partial^2 w_{T2}(y,z,t)}{\partial t^2}\delta w_{T2}(y,z,t) + \frac{\partial^2 u_{T2}(y,z,t)}{\partial t^2}\delta u_{T2}(y,z,t)\right] dydz +$$

$$+ \int_0^l \left[f_2(z,t)\delta w_{T2}^0(z,t) + \delta w_{T2}^0(z,t)K\big(w_{T1}^0(z,t) - w_{T2}^0(z,t)\big) + F_2 \frac{\partial w_{T2}^0(z,t)}{\partial z}\frac{\partial \delta w_{T2}^0(z,t)}{\partial z}\right] dz = 0. \tag{3.2.13}$$

By successive application of Green's theorem on the expressions (3.2.12-3.2.13), we get the equations of forced vibration for the system of elastically connected Timoshenko beams as

$$\rho A_1 \frac{\partial^2 w_{T1}^0(z,t)}{\partial t^2} - GA_1 k\left(\frac{\partial^2 w_{T1}^0(z,t)}{\partial z^2} + \frac{\partial \psi_{T1}^0(z,t)}{\partial x}\right) + F_1 \frac{\partial^2 w_{T1}^0(z,t)}{\partial z^2} + K\Big(w_{T1}^0(z,t) - w_{T2}^0(z,t)\Big) = f_1(z,t), \tag{3.2.14}$$

$$\rho I_{x1} \frac{\partial^2 \psi_{T1}^0(z,t)}{\partial t^2} - EI_{x1} \frac{\partial^2 \psi_{T1}^0(z,t)}{\partial z^2} + GA_1 k\left(\frac{\partial w_{T1}^0(z,t)}{\partial z} + \psi_{T1}^0(z,t)\right) = 0, \tag{3.2.15}$$

$$\rho A_2 \frac{\partial^2 w_{T1}^0(z,t)}{\partial t^2} - GA_2 k\left(\frac{\partial^2 w_{T2}^0(z,t)}{\partial z^2} + \frac{\partial \psi_{T2}^0(z,t)}{\partial x}\right) + F_2 \frac{\partial^2 w_{T2}^0(z,t)}{\partial z^2} + K\big(w_{T2}^0(z,t) - w_{T1}^0(z,t)\big) = f_2(z,t), \tag{3.2.16}$$

$$\rho I_{x2}\frac{\partial^2\psi_{T2}^0(z,t)}{\partial t^2}-EI_{x2}\frac{\partial^2\psi_{T2}^0(z,t)}{\partial z^2}+GA_2k\left(\frac{\partial w_{T2}^0(z,t)}{\partial z}+\psi_{T2}^0(z,t)\right)=0. \quad (3.2.17)$$

where material and geometrical properties of the beams have the same labels as in the previous chapter. Initial conditions for the system of two elastically connected beams are given by main coordinates hereinafter, while the boundary conditions for the system are as follows

$$w_{Ti}^0(0,t)=w_{Ti}^0(l,t)=0, \qquad i=1,2, \quad (3.2.18)$$

$$\frac{d^2w_{Ti}^0(0,t)}{dz^2}=\frac{d^2w_{Ti}^0(l,t)}{dz^2}=0, \quad i=1,2, \quad (3.2.19)$$

$$\frac{d\psi_{T1}^0(0,t)}{dz}=\frac{d\psi_{T1}^0(l,t)}{dz}=0, \quad i=1,2. \quad (3.2.20)$$

Considering the harmonic motion of beam's points, the solutions to the equations (3.2.14-3.2.17) are assumed as the product of the following functions

$$w_{Ti}^0(z,t)=\sum_{n=1}^{\infty}Z_n(z)\tilde{S}_{in}(t), \quad \psi_{Ti}^0(z,t)=\sum_{n=1}^{\infty}\Psi_n(z)\tilde{S}_{in(r)}(t), \quad i=1,2, \quad (3.2.21)$$

where $\tilde{S}_{in}(t)$ and $\tilde{S}_{in(r)}(t)$ are unknown time functions, while $Z_n(z)$ and $\Psi_n(z)$ are mode shape functions

$$Z_n(z)=\sin(k_nz), \quad \Psi_n(z)=\cos(k_nz), k_n=n\pi/l, \qquad n=1,2,3,\ldots \quad (3.2.22)$$

By substituting the assumed solutions (3.2.21) into the equations of system's transverse vibration (3.2.14-3.2.17), multiplying them by eigenfunctions, then integrating them from 0 to l along the beam and using the orthogonality condition, we have

$$\begin{bmatrix}A_1\rho & 0 & 0 & 0\\ 0 & A_2\rho & 0 & 0\\ 0 & 0 & I_1\rho & 0\\ 0 & 0 & 0 & I_2\rho\end{bmatrix}\begin{Bmatrix}\ddot{\tilde{S}}_{1n}(t)\\ \ddot{\tilde{S}}_{2n}(t)\\ \ddot{\tilde{S}}_{1n(r)}(t)\\ \ddot{\tilde{S}}_{2n(r)}(t)\end{Bmatrix}+$$

$$+\begin{bmatrix}GkA_1{k_n}^2-F_1{k_n}^2+K & -K & GkA_1k_n & 0\\ -K & GkA_2{k_n}^2-F_2{k_n}^2+K & 0 & GkA_2k_n\\ -GkA_1k_n & 0 & -EI_1{k_n}^2-GkA_1 & 0\\ 0 & -GkA_2k_n & 0 & -EI_2{k_n}^2-GkA_2\end{bmatrix}\begin{Bmatrix}\tilde{S}_{1n}(t)\\ \tilde{S}_{2n}(t)\\ \tilde{S}_{1n(r)}(t)\\ \tilde{S}_{2n(r)}(t)\end{Bmatrix}$$

$$=\begin{Bmatrix}\frac{2}{l}\int_0^l Z_n f_1(z,t)dz\\ \frac{2}{l}\int_0^l Z_n f_2(z,t)dz\\ 0\\ 0\end{Bmatrix}. \quad (3.2.23)$$

The solutions to the non-homogeneous system of differential equations are determined by way of modal analysis described in reference to Kelly [25]. The system of equations (3.2.23) may be written in matrix form

$$\left[\widetilde{\mathbf{M}}\right]\left\{\ddot{\tilde{\mathbf{S}}}\right\} + \left[\widetilde{\mathbf{K}}_{\mathbf{s}}\right]\{\tilde{\mathbf{S}}\} = \{\mathbf{F}\}, \tag{3.2.24}$$

where

$$\left\{\ddot{\tilde{\mathbf{S}}}\right\} = \begin{Bmatrix} \ddot{\tilde{S}}_{1n}(t) \\ \ddot{\tilde{S}}_{2n}(t) \\ \ddot{\tilde{S}}_{1n(r)}(t) \\ \ddot{\tilde{S}}_{2n(r)}(t) \end{Bmatrix}, \{\tilde{\mathbf{S}}\} = \begin{Bmatrix} \tilde{S}_{1n}(t) \\ \tilde{S}_{2n}(t) \\ \tilde{S}_{1n(r)}(t) \\ \tilde{S}_{2n(r)}(t) \end{Bmatrix}, \{\mathbf{F}\} = \begin{Bmatrix} \frac{2}{l}\int_0^l Z_n f_1(z,t)dz \\ \frac{2}{l}\int_0^l Z_n f_2(z,t)dz \\ 0 \\ 0 \end{Bmatrix}, \left[\widetilde{\mathbf{M}}\right] = \begin{bmatrix} A_1\rho & 0 & 0 & 0 \\ 0 & A_2\rho & 0 & 0 \\ 0 & 0 & I_1\rho & 0 \\ 0 & 0 & 0 & I_2\rho \end{bmatrix},$$

$$\left[\widetilde{\mathbf{K}}_{\mathbf{s}}\right] = \begin{bmatrix} GkA_1{k_n}^2 - F_1{k_n}^2 + K & -K & GkA_1k_n & 0 \\ -K & GkA_2{k_n}^2 - F_2{k_n}^2 + K & 0 & GkA_2k_n \\ -GkA_1k_n & 0 & -EI_1{k_n}^2 - GkA_1 & 0 \\ 0 & -GkA_2k_n & 0 & -EI_2{k_n}^2 - GkA_2 \end{bmatrix}.$$

The squares of the system's natural frequencies $\widetilde{\omega}_{1n}$,$\widetilde{\omega}_{2n}$, $\widetilde{\omega}_{3n}$ and $\widetilde{\omega}_{4n}$ represent eigenvalues in the matrix $\left[\widetilde{\mathbf{M}}\right]^{-1}\left[\widetilde{\mathbf{K}}_{\mathbf{s}}\right]$. Non-homogeneous system of differential equations with corresponding generalized coordinates $\left\{\tilde{\mathbf{S}}\right\}$ may be translated into the system of main coordinates $\tilde{p}_{jn}(t)$, $j = 1,2,3,4$, by introducing modal matrixes of the system $\left[\widetilde{\mathbf{P}}\right] = \left[\widetilde{\mathbf{X}}_1\widetilde{\mathbf{X}}_2\widetilde{\mathbf{X}}_3\widetilde{\mathbf{X}}_4\right]$ the columns of which represent normalized mode shapes.

$$\left\{\tilde{\mathbf{S}}(t)\right\} = \sum_{j=1}^{4} \tilde{p}_{jn}(t)\left\{\widetilde{\mathbf{X}}_j\right\}. \tag{3.2.25}$$

Transformation (3.2.25) is equivalent to linear transformation between generalized and main coordinates of the system

$$\left\{\tilde{\mathbf{S}}(t)\right\} = \left[\widetilde{\mathbf{P}}\right]\{\tilde{\mathbf{p}}(t)\}. \tag{3.2.26}$$

By substituting the equation (3.2.26) into the system (3.2.24), we get

$$\sum_{j=1}^{4} \ddot{\tilde{p}}_{jn}(t)\left[\widetilde{\mathbf{M}}\right]\left\{\widetilde{\mathbf{X}}_j\right\} + \sum_{j=1}^{4} \tilde{p}_{jn}(t)\left[\widetilde{\mathbf{K}}_S\right]\left\{\widetilde{\mathbf{X}}_j\right\} = \{\mathbf{F}\}. \tag{3.2.27}$$

If we multiply both sides of the expression by a scalar $\{\mathbf{X}_r\}$for arbitrary r=1,2,3,4, we get:

$$\sum_{j=1}^{4} \ddot{\tilde{p}}_{jn}(t)\left(\left\{\widetilde{\mathbf{X}}_r\right\}, \left[\widetilde{\mathbf{M}}\right]\left\{\widetilde{\mathbf{X}}_j\right\}\right) + \sum_{j=1}^{4} \tilde{p}_{jn}(t)\left(\left\{\widetilde{\mathbf{X}}_r\right\}, \left[\widetilde{\mathbf{K}}_S\right]\left\{\widetilde{\mathbf{X}}_j\right\}\right) = \left(\left\{\widetilde{\mathbf{X}}_r\right\}, \{\mathbf{F}\}\right). \tag{3.2.28}$$

By applying mode-shape orthogonality condition, we get a single member in each of the sums which is different from zero, namely for *r=j*. As mode shapes are normalized, the equation (3.2.28) has the following form

$$\ddot{\tilde{p}}_{rn}(t) + \tilde{\omega}_{nr}^2 \tilde{p}_{rn}(t) = \tilde{g}_{rn}(t), \qquad r = 1,2,3,4., \tag{3.2.29}$$

where $\tilde{g}_{rn}(t) = \left(\{\tilde{\mathbf{X}}_r\}, \{\mathbf{F}\}\right)$. If the initial conditions are defined by main coordinates $\tilde{p}_{rn}(0) = 0, \dot{\tilde{p}}_{rn}(0) = 0$, the solutions may be written in the form of convolution integral

$$\tilde{p}_{rn}(t) = \frac{1}{\tilde{\omega}_{nr}} \int_0^t \tilde{g}_{rn}(s) \sin[\tilde{\omega}_{nr}(t-s)] ds, \qquad r = 1,2,3,4, \tag{3.2.30}$$

By substituting the obtained solutions (3.2.30) into the equation of coordinate transformation (3.2.25), we get

$$\{\tilde{\mathbf{S}}\} = \begin{Bmatrix} \tilde{S}_{1n}(t) \\ \tilde{S}_{2n}(t) \\ \tilde{S}_{1n(r)}(t) \\ \tilde{S}_{2n(r)}(t) \end{Bmatrix} = \begin{Bmatrix} \tilde{X}_{11}(\tilde{\omega}_{n1})\tilde{p}_{1n}(t) + \tilde{X}_{12}(\tilde{\omega}_{n2})\tilde{p}_{2n}(t) + \tilde{X}_{13}(\tilde{\omega}_{n3})\tilde{p}_{3n}(t) + \tilde{X}_{14}(\tilde{\omega}_{n4})\tilde{p}_{4n}(t) \\ \tilde{X}_{21}(\tilde{\omega}_{n1})\tilde{p}_{1n}(t) + \tilde{X}_{22}(\tilde{\omega}_{n2})\tilde{p}_{2n}(t) + \tilde{X}_{23}(\tilde{\omega}_{n3})\tilde{p}_{3n}(t) + \tilde{X}_{24}(\tilde{\omega}_{n4})\tilde{p}_{4n}(t) \\ \tilde{X}_{31}(\tilde{\omega}_{n1})\tilde{p}_{1n}(t) + \tilde{X}_{32}(\tilde{\omega}_{n2})\tilde{p}_{2n}(t) + \tilde{X}_{33}(\tilde{\omega}_{n3})\tilde{p}_{3n}(t) + \tilde{X}_{34}(\tilde{\omega}_{n4})\tilde{p}_{4n}(t) \\ \tilde{X}_{41}(\tilde{\omega}_{n1})\tilde{p}_{1n}(t) + \tilde{X}_{42}(\tilde{\omega}_{n2})\tilde{p}_{2n}(t) + \tilde{X}_{43}(\tilde{\omega}_{n3})\tilde{p}_{3n}(t) + \tilde{X}_{44}(\tilde{\omega}_{n4})\tilde{p}_{4n}(t) \end{Bmatrix}. \tag{3.2.31}$$

The time functions thus obtained may now be substituted into assumed solutions (3.2.21) from where general solutions for forced transverse vibration of two elastically connected Timoshenko beams follow

$$w_{T1}^0(z,t) = \sum_{n=1}^{\infty} \sin(k_n z) \left[\tilde{X}_{11}(\tilde{\omega}_{n1})\tilde{p}_{1n}(t) + \tilde{X}_{12}(\tilde{\omega}_{n2})\tilde{p}_{2n}(t) + \tilde{X}_{13}(\tilde{\omega}_{n3})\tilde{p}_{3n}(t) + \tilde{X}_{14}(\tilde{\omega}_{n4})\tilde{p}_{4n}(t)\right] \tag{3.2.32}$$

$$w_{T2}^0(z,t) = \sum_{n=1}^{\infty} \sin(k_n z) \left[\tilde{X}_{21}(\tilde{\omega}_{n1})\tilde{p}_{1n}(t) + \tilde{X}_{22}(\tilde{\omega}_{n2})\tilde{p}_{2n}(t) + \tilde{X}_{23}(\tilde{\omega}_{n3})\tilde{p}_{3n}(t) + \tilde{X}_{24}(\tilde{\omega}_{n4})\tilde{p}_{4n}(t)\right], \tag{3.2.33}$$

$$\psi_{T1}^0(z,t) = \sum_{n=1}^{\infty} \cos(k_n z) \left[\tilde{X}_{31}(\tilde{\omega}_{n1})\tilde{p}_{1n}(t) + \tilde{X}_{32}(\tilde{\omega}_{n2})\tilde{p}_{2n}(t) + \tilde{X}_{33}(\tilde{\omega}_{n3})\tilde{p}_{3n}(t) + \tilde{X}_{34}(\tilde{\omega}_{n4})\tilde{p}_{4n}(t)\right], \tag{3.2.34}$$

$$\psi_{T2}^0(z,t) = \sum_{n=1}^{\infty} \cos(k_n z) \left[\tilde{X}_{41}(\tilde{\omega}_{n1})\tilde{p}_{1n}(t) + \tilde{X}_{42}(\tilde{\omega}_{n2})\tilde{p}_{2n}(t) + \tilde{X}_{43}(\tilde{\omega}_{n3})\tilde{p}_{3n}(t) + \tilde{X}_{44}(\tilde{\omega}_{n4})\tilde{p}_{4n}(t)\right]. \tag{3.2.35}$$

General solutions of forced vibration are necessary for determining the conditions of resonance dynamic vibration absorption, examining the amplitudes of the system under the influence of axial compression forces with different types of forcing. Modal matrix of the system $\left[\widetilde{\mathbf{P}}\right]$ is given in Appendix 3.2.1.

3.3 Forced Vibrations of Two Elastically Connected Reddy-Bickford Beams

Let, as in the case of Timoshenko model, the beams be of the same length *l,* and connected by the same elastic layer with the stiffness modulus *K*. The beams are exposed to the action of axial forces F_1 and F_2 at their ends and to forced variable continuous loads $f_1(z,t)$ and $f_2(z,t)$. Let us mark the functions of longitudinal and transverse motions as well as the angle of tangent of the deformed beam's cross-section on a neutral line as $u_{RB1}(y,z,t)$, $w_{RB1}(y,z,t)$, $\psi^0_{RB1}(z,t)$, $u_{RB2}(y,z,t)$, $w_{RB2}(y,z,t)$ and $\psi^0_{RB2}(z,t)$ respectively. The following functions of motion hold for the double-beam system

$$u_{RB1}(y,z,t) = u^0_{RB1}(z,t) + y\psi^0_{RB1}(z,t) - \alpha y^3\left(\psi^0_{RB1}(z,t) + \frac{\partial w^0_{RB1}(z,t)}{\partial z}\right),$$
$$w_{RB1}(y,z,t) = w^0_{RB1}(z,t), \tag{3.3.1}$$

$$u_{RB2}(y,z,t) = u^0_{RB2}(z,t) + y\psi^0_{RB2}(z,t) - \alpha y^3\left(\psi^0_{RB2}(z,t) + \frac{\partial w^0_{RB2}(z,t)}{\partial z}\right),$$
$$w_{RB2}(y,z,t) = w^0_{RB2}(z,t), \tag{3.3.2}$$

Deformation in the motion function and the relations between stress and deformation according to the Hooke's law are

$$\varepsilon_{z1}(y,z,t) = \frac{\partial u^0_{RB1}(z,t)}{\partial z} + y\frac{\partial \psi^0_{RB1}(z,t)}{\partial z} - \alpha y^3\left(\frac{\partial \psi^0_{RB1}(z,t)}{\partial z} + \frac{\partial^2 w^0_{RB1}(z,t)}{\partial z^2}\right), \tag{3.3.3}$$

$$\gamma_{zy1}(y,z,t) = \psi^0_{RB1}(z,t) + \frac{\partial w^0_{RB1}(z,t)}{\partial z} - \beta y^2\left(\psi^0_{RB1}(z,t) + \frac{\partial w^0_{RB1}(z,t)}{\partial z}\right), \tag{3.3.4}$$

$$\varepsilon_{z2}(y,z,t) = \frac{\partial u^0_{RB2}(z,t)}{\partial z} + y\frac{\partial \psi^0_{RB2}(z,t)}{\partial z} - \alpha y^3\left(\frac{\partial \psi^0_{RB2}(z,t)}{\partial z} + \frac{\partial^2 w^0_{RB2}(z,t)}{\partial z^2}\right), \tag{3.3.5}$$

$$\gamma_{zy2}(y,z,t) = \psi^0_{RB2}(z,t) + \frac{\partial w^0_{RB2}(z,t)}{\partial z} - \beta y^2\left(\psi^0_{RB2}(z,t) + \frac{\partial w^0_{RB2}(z,t)}{\partial z}\right). \tag{3.3.6}$$

$$\begin{Bmatrix}\sigma_{z1}\\ \tau_{zy1}\end{Bmatrix} = \begin{bmatrix}E & 0\\ 0 & G\end{bmatrix}\begin{Bmatrix}\varepsilon_{z1}\\ \gamma_{zy1}\end{Bmatrix}, \quad \begin{Bmatrix}\sigma_{z2}\\ \tau_{zy2}\end{Bmatrix} = \begin{bmatrix}E & 0\\ 0 & G\end{bmatrix}\begin{Bmatrix}\varepsilon_{z2}\\ \gamma_{zy2}\end{Bmatrix}. \tag{3.3.7}$$

Virtual work of inertial forces is given by

$$\delta W_{in1} = -\rho b_1 \int_0^l \int_{-\frac{h_1}{2}}^{\frac{h_1}{2}} \left[\frac{\partial^2 w_{RB1}(y,z,t)}{\partial t^2} \delta w_{T1}(y,z,t) + \frac{\partial^2 u_{RB1}(y,z,t)}{\partial t^2} \delta u_{T1}(y,z,t) \right] dydz, \tag{3.3.8}$$

$$\delta W_{in2} = -\rho b_2 \int_0^l \int_{-\frac{h_2}{2}}^{\frac{h_2}{2}} \left[\frac{\partial^2 w_{RB2}(y,z,t)}{\partial t^2} \delta w_{T2}(y,z,t) + \frac{\partial^2 u_{RB2}(y,z,t)}{\partial t^2} \delta u_{T2}(y,z,t) \right] dydz. \tag{3.3.9}$$

Virtual work of internal forces is expressed as

$$\delta W_{V1} = -b_1 \int_0^l \int_{-\frac{h_1}{2}}^{\frac{h_1}{2}} \left[\sigma_{z1}(z,t) \delta \varepsilon_{z1}(z,t) + \tau_{zy1} \delta \gamma_{zy1} \right] dydz, \tag{3.3.10}$$

$$\delta W_{V2} = -b_2 \int_0^l \int_{-\frac{h_2}{2}}^{\frac{h_2}{2}} \left[\sigma_{z2}(z,t) \delta \varepsilon_{z2}(z,t) + \tau_{zy2} \delta \gamma_{zy2} \right] dydz. \tag{3.3.11}$$

Virtual work of external forces is

$$\delta W_{ex1} = \int_0^l \Big[f_1(z,t) \delta w^0_{RB1}(z,t) + \delta w^0_{RB1}(z,t) K\left(w^0_{T2}(z,t) - w^0_{T1}(z,t) \right) + F_1 \frac{\partial w^0_{RB1}(z,t)}{\partial z} \frac{\partial \delta w^0_{RB1}(z,t)}{\partial z} \Big] dz, \tag{3.3.12}$$

$$\delta W_{ex2} = \int_0^l \Big[f_2(z,t) \delta w^0_{RB2}(z,t) + \delta w^0_{RB2}(z,t) K\left(w^0_{RB1}(z,t) - w^0_{RB2}(z,t) \right) + F_2 \frac{\partial w^0_{RB2}(z,t)}{\partial z} \frac{\partial \delta w^0_{RB2}(z,t)}{\partial z} \Big] dz, \tag{3.3.13}$$

where δ is the variation operator. By substituting the equations (3.3.10-3.3.13) into a general equation of virtual work principle $\delta W_{ini} + \delta W_{Vi} + \delta W_{exi} = 0,\ i = 1,2$, we get

$$-b_1 \int_0^l \int_{-\frac{h_1}{2}}^{\frac{h_1}{2}} \left[\sigma_{z1}(z,t) \delta \varepsilon_{z1}(z,t) + \tau_{zy1}(z,t) \delta \gamma_{zy1}(z,t) \right] dydz -$$

$$-\rho b_1 \int_0^l \int_{-\frac{h_1}{2}}^{\frac{h_1}{2}} \left[\frac{\partial^2 w_{RB1}(y,z,t)}{\partial t^2} \delta w_{RB1}(y,z,t) + \frac{\partial^2 u_{RB1}(y,z,t)}{\partial t^2} \delta u_{RB1}(y,z,t) \right] dydz +$$

$$+ \int_0^l \left[f_1(z,t) \delta w^0_{RB1}(z,t)' + \delta w^0_{RB1}(z,t) K\left(w^0_{RB2}(z,t) - w^0_{RB1}(z,t) \right) + F_1 \frac{\partial w^0_{RB1}(z,t)}{\partial z} \frac{\partial \delta w^0_{RB1}(z,t)}{\partial z} \right] dz = 0, \tag{3.3.14}$$

$$-b_2\int_0^l\int_{-\frac{h_2}{2}}^{\frac{h_2}{2}}\left[\sigma_{z2}(z,t)\delta\varepsilon_{z1}(z,t)+\tau_{zy2}(z,t)\delta\gamma_{zy2}(z,t)\right]dydz-$$

$$-\rho b_2\int_0^l\int_{-\frac{h_2}{2}}^{\frac{h_2}{2}}\left[\frac{\partial^2 w_{RB2}(y,z,t)}{\partial t^2}\delta w_{RB2}(y,z,t)+\frac{\partial^2 u_{RB2}(y,z,t)}{\partial t^2}\delta u_{RB2}(y,z,t)\right]dydz+$$

$$+\int_0^l\left[f_2(z,t)\delta w^0_{RB2}(z,t)+\delta w^0_{RB2}(z,t)K\left(w^0_{RB1}(z,t)-w^0_{RB2}(z,t)\right)+F_2\frac{\partial w^0_{RB2}(z,t)}{\partial z}\frac{\partial\delta w^0_{RB2}(z,t)}{\partial z}\right]dz=0. \tag{3.3.15}$$

By successive application of Green's theorem to the expressions (3.2.14-3.2.15), we get the equations of vibration for the system of two elastically connected Reddy-Bickford beams in the following form

$$C_w^{4,0}\frac{\partial^4 w^0_{RB1}(z,t)}{\partial z^4}+C_w^{2,2}\frac{\partial^4 w^0_{RB1}(z,t)}{\partial z^2\,\partial t^2}+C_w^{2,0}\frac{\partial^2 w^0_{RB1}(z,t)}{\partial z^2}+C_w^{0,2}\frac{\partial^2 w^0_{RB1}(z,t)}{\partial t^2}+C_\psi^{1,2}\frac{\partial^3\psi^0_{RB1}(z,t)}{\partial z\,\partial t^2}$$

$$+C_\psi^{1,0}\frac{\partial\psi^0_{RB1}(z,t)}{\partial z}+C_\psi^{3,0}\frac{\partial^3\psi^0_{RB1}(z,t)}{\partial z^3}+K\left(w^0_{RB1}(z,t)-w^0_{RB2}(z,t)\right)=f_1(z,t), \tag{3.3.16}$$

$$C_w^{3,0}\frac{\partial^3 w^0_{RB1}(z,t)}{\partial z^3}+C_w^{1,2}\frac{\partial^3 w^0_{RB1}(z,t)}{\partial z\,\partial t^2}+C_w^{1,0}\frac{\partial w^0_{RB1}(z,t)}{\partial z}+C_\psi^{2,0}\frac{\partial^2\psi^0_{RB1}(z,t)}{\partial z^2}$$

$$+C_\psi^{0,2}\frac{\partial^2\psi^0_{RB1}(z,t)}{\partial t^2}+C_\psi^{0,0}\psi^0_{RB1}(z,t)=0, \tag{3.3.17}$$

$$D_w^{4,0}\frac{\partial^4 w^0_{RB2}(z,t)}{\partial z^4}+D_w^{2,2}\frac{\partial^4 w^0_{RB2}(z,t)}{\partial z^2\,\partial t^2}+D_w^{2,0}\frac{\partial^2 w^0_{RB2}(z,t)}{\partial z^2}+D_w^{0,2}\frac{\partial^2 w^0_{RB2}(z,t)}{\partial t^2}$$

$$+D_\psi^{1,2}\frac{\partial^3\psi^0_{RB2}(z,t)}{\partial z\,\partial t^2}+D_\psi^{1,0}\frac{\partial\psi^0_{RB2}(z,t)}{\partial z}+D_\psi^{3,0}\frac{\partial^3\psi^0_{RB2}(z,t)}{\partial z^3}+K\left(w^0_{RB2}(z,t)-w^0_{RB1}(z,t)\right)=f_2(z,t), \tag{3.3.18}$$

$$D_w^{3,0}\frac{\partial^3 w^0_{RB2}(z,t)}{\partial z^3}+D_w^{1,2}\frac{\partial^3 w^0_{RB2}(z,t)}{\partial z\,\partial t^2}+D_w^{1,0}\frac{\partial w^0_{RB2}(z,t)}{\partial z}+D_\psi^{2,0}\frac{\partial^2\psi^0_{RB2}(z,t)}{\partial z^2}$$

$$+D_\psi^{0,2}\frac{\partial^2\psi^0_{RB2}(z,t)}{\partial t^2}+D_\psi^{0,0}\psi^0_{RB2}(z,t)=0, \tag{3.3.19}$$

where

$$C_w^{4,0}=\frac{1}{448}b_1{h_1}^7\alpha^2E,\ C_w^{2,2}=-\frac{1}{448}b_1{h_1}^7\alpha^2\rho,\ C_w^{2,0}=-\frac{1}{80}b_1G\beta^2{h_1}^5+\frac{1}{6}bG\beta{h_1}^3-b_1Gh_1+F_1,$$

$$C_w^{0,2}=b_1h_1\rho, C_\psi^{1,2}=\frac{1}{80}b_1{h_1}^5\alpha\rho-\frac{1}{448}b_1{h_1}^7\alpha^2\rho, C_\psi^{1,0}=-\frac{1}{80}b_1G\beta^2{h_1}^5+\frac{1}{6}b_1G\beta{h_1}^3-b_1Gh_1,$$

$$C_\psi^{3,0}=\frac{1}{448}b_1{h_1}^7\alpha^2E-\frac{1}{80}b_1{h_1}^5\alpha E, C_w^{3,0}=\frac{1}{80}b_1{h_1}^5\alpha E-\frac{1}{448}b_1{h_1}^7\alpha^2E,$$

$$C_w^{1,2}=\frac{1}{448}b_1{h_1}^7\alpha^2\rho-\frac{1}{80}b_1{h_1}^5\alpha\rho, C_w^{1,0}=\frac{1}{80}b_1G\beta^2{h_1}^5-\frac{1}{6}b_1G\beta{h_1}^3+b_1Gh_1,$$

$$C_\psi^{2,0}=-\frac{1}{448}b_1\alpha^2E{h_1}^7+\frac{1}{40}b_1\alpha E{h_1}^5-\frac{1}{12}b_1E{h_1}^3,$$

$$C_\psi^{0,2}=\frac{1}{448}b_1\alpha^2\rho{h_1}^7-\frac{1}{40}b_1\alpha\rho{h_1}^5+\frac{1}{12}b_1\rho{h_1}^3, C_\psi^{0,0}=\frac{1}{80}b_1\beta^2Gh_1{}^5-\frac{1}{6}b_1\beta G{h_1}^3+b_1Gh_1, \tag{3.3.20}$$

$$D_w^{4,0}=\frac{1}{448}b_2{h_2}^7\alpha^2E,\ D_w^{2,2}=-\frac{1}{448}b_2{h_2}^7\alpha^2\rho,\ D_w^{2,0}=-\frac{1}{80}b_2G\beta^2{h_2}^5+\frac{1}{6}bG\beta{h_2}^3-b_2Gh_2+F_2,$$
$$D_w^{0,2}=b_2h_2\rho, D_\psi^{1,2}=\frac{1}{80}b_2{h_2}^5\alpha\rho-\frac{1}{448}b_2{h_2}^7\alpha^2\rho, D_\psi^{1,0}=-\frac{1}{80}b_2G\beta^2{h_2}^5+\frac{1}{6}b_2G\beta{h_2}^3-b_2Gh_2,$$
$$D_\psi^{3,0}=\frac{1}{448}b_2{h_2}^7\alpha^2E-\frac{1}{80}b_2{h_2}^5\alpha E, D_w^{3,0}=\frac{1}{80}b_2{h_2}^5\alpha E-\frac{1}{448}b_2{h_2}^7\alpha^2E,$$
$$D_w^{1,2}=\frac{1}{448}b_2{h_2}^7\alpha^2\rho-\frac{1}{80}b_2{h_2}^5\alpha\rho, D_w^{1,0}=\frac{1}{80}b_2G\beta^2{h_2}^5-\frac{1}{6}b_2G\beta{h_2}^3+b_2Gh_2,$$
$$D_\psi^{2,0}=-\frac{1}{448}b_2\alpha^2E{h_2}^7+\frac{1}{40}b_2\alpha E{h_2}^5-\frac{1}{12}b_2E{h_2}^3,$$
$$D_\psi^{0,2}=\frac{1}{448}b_2\alpha^2\rho{h_2}^7-\frac{1}{40}b_2\alpha\rho{h_2}^5+\frac{1}{12}b_2\rho{h_2}^3, D_\psi^{0,0}=\frac{1}{80}b_2\beta^2G{h_2}^5-\frac{1}{6}b_2\beta G{h_2}^3+b_2Gh_2. \tag{3.3.21}$$

Boundary conditions for the system of two elastically connected simply supported Reddy-Bickford beams based on $(2.3.22-2.3.24)$ are given by

$$w_{RBi}^0(0,t)=0,\qquad w_{RBi}^0(l,t)=0,\qquad i=1,2, \tag{3.3.22}$$

$$\frac{d^2w_{RBi}^0(0,t)}{dz^2}=\frac{d^2w_{RBi}^0(l,t)}{dz^2}=0,\qquad i=1,2, \tag{3.3.23}$$

$$\frac{d\psi_{RBi}^0(0,t)}{dz}=\frac{d\psi_{RBi}^0(l,t)}{dz}=0,\qquad i=1,2. \tag{3.3.24}$$

Considering the harmonic motion of beam's points, we assume the solutions to the equations (3.3.16-3.3.19) as the product of functions

$$w_{RBi}^0(z,t)=\sum_{n=1}^{\infty}Z_n(z)\tilde{\tilde{S}}_{in}(t),\quad \psi_{RBi}^0(z,t)=\sum_{n=1}^{\infty}\Psi_n(z)\tilde{\tilde{S}}_{in(r)}(t),\quad i=1,2, \tag{3.3.25}$$

where $\tilde{\tilde{S}}_{in}(t)$ and $\tilde{\tilde{S}}_{in(r)}(t)$ are the unknown time functions, whereas $Z_n(z)$ and $\Psi_n(z)$ are mode shape functions

$$Z_n(z)=\sin(k_nz),\quad \Psi_n(z)=\cos(k_nz), k_n=n\pi/l,\qquad n=1,2,3,\ldots \tag{3.3.26}$$

By substituting the assumed solutions (3.3.25) into equations of transverse system vibration (3.3.16-3.3.19), multiplying them by eigenfunctions, then integrating them from 0 to l along the beam and using the orthogonality condition, we have

$$\left[\tilde{\tilde{\mathbf{M}}}\right]\left\{\ddot{\tilde{\tilde{\mathbf{S}}}}\right\}+\left[\tilde{\tilde{\mathbf{K}}}_{\mathbf{s}}\right]\left\{\tilde{\tilde{\mathbf{S}}}\right\}=\{\mathbf{F}\}, \tag{3.3.27}$$

where

$$\left\{\ddot{\tilde{\tilde{\mathbf{S}}}}\right\}=\begin{Bmatrix}\ddot{\tilde{\tilde{S}}}_{1n}(t)\\ \ddot{\tilde{\tilde{S}}}_{2n}(t)\\ \ddot{\tilde{\tilde{S}}}_{1n(r)}(t)\\ \ddot{\tilde{\tilde{S}}}_{2n(r)}(t)\end{Bmatrix},\left\{\tilde{\tilde{\mathbf{S}}}\right\}=\begin{Bmatrix}\tilde{\tilde{S}}_{1n}(t)\\ \tilde{\tilde{S}}_{2n}(t)\\ \tilde{\tilde{S}}_{1n(r)}(t)\\ \tilde{\tilde{S}}_{2n(r)}(t)\end{Bmatrix},\{\mathbf{F}\}=\begin{Bmatrix}\frac{2}{l}\int_0^l Z_n f_1(z,t)dz\\ \frac{2}{l}\int_0^l Z_n f_2(z,t)dz\\ 0\\ 0\end{Bmatrix}.$$

Matrixes $\left[\widetilde{\widetilde{\mathbf{M}}}\right]$ and $\left[\widetilde{\widetilde{\mathbf{K}}}_{\mathbf{s}}\right]$ are given in the Appendix 3.3.1. The squares of system's natural frequencies $\widetilde{\widetilde{\omega}}_{1n}$,$\widetilde{\widetilde{\omega}}_{2n}$, $\widetilde{\widetilde{\omega}}_{3n}$ and $\widetilde{\widetilde{\omega}}_{4n}$ represent eigenvalues of the matrix $\left[\widetilde{\widetilde{\mathbf{M}}}\right]^{-1}\left[\widetilde{\widetilde{\mathbf{K}}}_{\mathbf{s}}\right]$. Non-homogeneous system of differential equations with corresponding generalized coordinates $\left\{\widetilde{\widetilde{\mathbf{S}}}\right\}$ may be translated into the system of main coordinates $\tilde{p}_{jn}(t)$, $j = 1,2,3,4$, by introducing modal matrixes of the system $\left[\widetilde{\widetilde{\mathbf{P}}}\right] = \left[\widetilde{\widetilde{\mathbf{X}}}_1\widetilde{\widetilde{\mathbf{X}}}_2\widetilde{\widetilde{\mathbf{X}}}_3\widetilde{\widetilde{\mathbf{X}}}_4\right]$, the columns of which represent normalized mode shapes.

$$\left\{\widetilde{\widetilde{\mathbf{S}}}(t)\right\} = \sum_{j=1}^{4} \tilde{\tilde{p}}_{jn}(t)\left\{\widetilde{\widetilde{\mathbf{X}}}_j\right\}. \tag{3.3.28}$$

Transformation (3.3.28) is equivalent to linear transformation between generalized and main system coordinates

$$\left\{\widetilde{\widetilde{\mathbf{S}}}(t)\right\} = \left[\widetilde{\widetilde{\mathbf{P}}}\right]\{\tilde{\tilde{\mathbf{p}}}(t)\}. \tag{3.3.29}$$

By substituting the equations (3.3.28) into the system (3.3.27), we get

$$\sum_{j=1}^{4} \ddot{\tilde{\tilde{p}}}_{jn}(t)\left[\widetilde{\widetilde{\mathbf{M}}}\right]\{\widetilde{\mathbf{X}}_j\} + \sum_{j=1}^{4} \tilde{\tilde{p}}_{jn}(t)\left[\widetilde{\widetilde{\mathbf{K}}}_{\boldsymbol{S}}\right]\left\{\widetilde{\widetilde{\mathbf{X}}}_j\right\} = \{\mathbf{F}\}. \tag{3.3.30}$$

If both sides of the expression are multiplied by a scalar $\{\mathbf{X}_r\}$ for arbitrary r=1,2,3,4, we get

$$\sum_{j=1}^{4} \ddot{\tilde{\tilde{p}}}_{jn}(t)\left(\left\{\widetilde{\widetilde{\mathbf{X}}}_r\right\}, \left[\widetilde{\widetilde{\mathbf{M}}}\right]\left\{\widetilde{\widetilde{\mathbf{X}}}_j\right\}\right) + \sum_{j=1}^{4} \tilde{\tilde{p}}_{jn}(t)\left(\left\{\widetilde{\widetilde{\mathbf{X}}}_r\right\}, \left[\widetilde{\widetilde{\mathbf{K}}}_{\boldsymbol{S}}\right]\left\{\widetilde{\widetilde{\mathbf{X}}}_j\right\}\right) = \left(\left\{\widetilde{\widetilde{\mathbf{X}}}_r\right\}, \{\mathbf{F}\}\right). \tag{3.3.31}$$

By applying the mode-shape orthogonality condition we get a single member in each sum that is different from zero, namely for r=j. As mode shapes are normalized, the equation (3.3.31) becomes

$$\ddot{\tilde{\tilde{p}}}_{rn}(t) + \widetilde{\widetilde{\omega}}_{nr}^2\tilde{\tilde{p}}_{rn}(t) = \tilde{\tilde{g}}_{rn}(t), \qquad r = 1,2,3,4., \tag{3.3.32}$$

where $\tilde{\tilde{g}}_{rn}(t) = \left(\left\{\widetilde{\widetilde{\mathbf{X}}}_r\right\}, \{\tilde{\mathbf{F}}\}\right)$. If initial conditions are defined by main coordinates $\tilde{\tilde{p}}_{rn}(0) = 0, \dot{\tilde{\tilde{p}}}_{rn}(0) = 0,$ the solutions can be written in the form of convolution integral

$$\tilde{\tilde{p}}_{rn}(t) = \frac{1}{\widetilde{\widetilde{\omega}}_{rn}}\int_0^t \tilde{\tilde{g}}_{rn}(s)\sin\left[\widetilde{\widetilde{\omega}}_{rn}(t-s)\right]ds. \tag{3.3.33}$$

By substituting the obtained solutions (3.3.33) into the equation of coordinate transformation (3.3.29), we get

$$\left\{\tilde{\bar{\mathbf{S}}}\right\} = \begin{Bmatrix} \tilde{\bar{S}}_{1n}(t) \\ \tilde{\bar{S}}_{2n}(t) \\ \tilde{\bar{S}}_{1n(r)}(t) \\ \tilde{\bar{S}}_{2n(r)}(t) \end{Bmatrix} = \begin{Bmatrix} \tilde{\bar{X}}_{11}(\tilde{\omega}_{n1})\tilde{\bar{p}}_{1n}(t) + \tilde{\bar{X}}_{12}(\tilde{\omega}_{n2})\tilde{\bar{p}}_{2n}(t) + \tilde{\bar{X}}_{13}(\tilde{\omega}_{n3})\tilde{\bar{p}}_{3n}(t) + \tilde{\bar{X}}_{14}(\tilde{\omega}_{n4})\tilde{\bar{p}}_{4n}(t) \\ \tilde{\bar{X}}_{21}(\tilde{\omega}_{n1})\tilde{\bar{p}}_{1n}(t) + \tilde{\bar{X}}_{22}(\tilde{\omega}_{n2})\tilde{\bar{p}}_{2n}(t) + \tilde{\bar{X}}_{23}(\tilde{\omega}_{n3})\tilde{\bar{p}}_{3n}(t) + \tilde{\bar{X}}_{24}(\tilde{\omega}_{n4})\tilde{\bar{p}}_{4n}(t) \\ \tilde{\bar{X}}_{31}(\tilde{\omega}_{n1})\tilde{\bar{p}}_{1n}(t) + \tilde{\bar{X}}_{32}(\tilde{\omega}_{n2})\tilde{\bar{p}}_{2n}(t) + \tilde{\bar{X}}_{33}(\tilde{\omega}_{n3})\tilde{\bar{p}}_{3n}(t) + \tilde{\bar{X}}_{34}(\tilde{\omega}_{n4})\tilde{\bar{p}}_{4n}(t) \\ \tilde{\bar{X}}_{41}(\tilde{\omega}_{n1})\tilde{\bar{p}}_{1n}(t) + \tilde{\bar{X}}_{42}(\tilde{\omega}_{n2})\tilde{\bar{p}}_{2n}(t) + \tilde{\bar{X}}_{43}(\tilde{\omega}_{n3})\tilde{\bar{p}}_{3n}(t) + \tilde{\bar{X}}_{44}(\tilde{\omega}_{n4})\tilde{\bar{p}}_{4n}(t) \end{Bmatrix}. \tag{3.3.34}$$

The time functions thus obtained can now be substituted into assumed solutions (3.3.25) from where general solutions for forced transverse vibration of two elastically connected Timoshenko beams follow

$$w^0_{RB1}(z,t) = \sum_{n=1}^{\infty} \sin(k_n z)\left[\tilde{\bar{X}}_{11}(\tilde{\omega}_{n1})\tilde{\bar{p}}_{1n}(t) + \tilde{\bar{X}}_{12}(\tilde{\omega}_{n2})\tilde{\bar{p}}_{2n}(t) + \tilde{\bar{X}}_{13}(\tilde{\omega}_{n3})\tilde{\bar{p}}_{3n}(t) + \tilde{\bar{X}}_{14}(\tilde{\omega}_{n4})\tilde{\bar{p}}_{4n}(t)\right], \tag{3.3.35}$$

$$w^0_{RB2}(z,t) = \sum_{n=1}^{\infty} \sin(k_n z)\left[\tilde{\bar{X}}_{21}(\tilde{\omega}_{n1})\tilde{\bar{p}}_{1n}(t) + \tilde{\bar{X}}_{22}(\tilde{\omega}_{n2})\tilde{\bar{p}}_{2n}(t) + \tilde{\bar{X}}_{23}(\tilde{\omega}_{n3})\tilde{\bar{p}}_{3n}(t) + \tilde{\bar{X}}_{24}(\tilde{\omega}_{n4})\tilde{\bar{p}}_{4n}(t)\right], \tag{3.3.36}$$

$$\psi^0_{RB1}(z,t) = \sum_{n=1}^{\infty} \cos(k_n z)\left[\tilde{\bar{X}}_{31}(\tilde{\omega}_{n1})\tilde{\bar{p}}_{1n}(t) + \tilde{\bar{X}}_{32}(\tilde{\omega}_{n2})\tilde{\bar{p}}_{2n}(t) + \tilde{\bar{X}}_{33}(\tilde{\omega}_{n3})\tilde{\bar{p}}_{3n}(t) + \tilde{\bar{X}}_{34}(\tilde{\omega}_{n4})\tilde{\bar{p}}_{4n}(t)\right], \tag{3.3.37}$$

$$\psi^0_{RB2}(z,t) = \sum_{n=1}^{\infty} \cos(k_n z)\left[\tilde{\bar{X}}_{41}(\tilde{\omega}_{n1})\tilde{\bar{p}}_{1n}(t) + \tilde{\bar{X}}_{42}(\tilde{\omega}_{n2})\tilde{\bar{p}}_{2n}(t) + \tilde{\bar{X}}_{43}(\tilde{\omega}_{n3})\tilde{\bar{p}}_{3n}(t) + \tilde{\bar{X}}_{44}(\tilde{\omega}_{n4})\tilde{\bar{p}}_{4n}(t)\right]. \tag{3.3.38}$$

General solutions for forced vibration are necessary for determining the conditions for the behavior of the system as a dynamic absorber and examining the system's amplitudes under the influence of axial compression forces and different types of forcing. Modal matrix of the system $\left[\tilde{\bar{\mathbf{P}}}\right]$ is shown in analytical form in Appendix 3.3.1.

3.4 Particular Solutions for Special Cases of Forced Vibrations for the System of Two Elastically Connected Beams

The established general solutions for forced vibration of two elastically connected beams can be used to determine particular solutions for forced vibrations of the system subjected to continuous harmonic (Figure 3.4.1), uniform harmonic (Figure 3.4.2) and concentrated harmonic (Figure 3.4.3) loads.

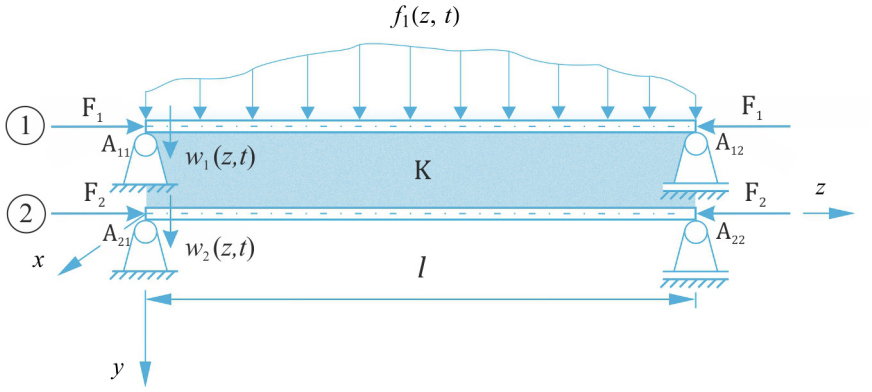

Fig. 3.4.1 The system of beams under the influence of arbitrarily continuous harmonic excitation

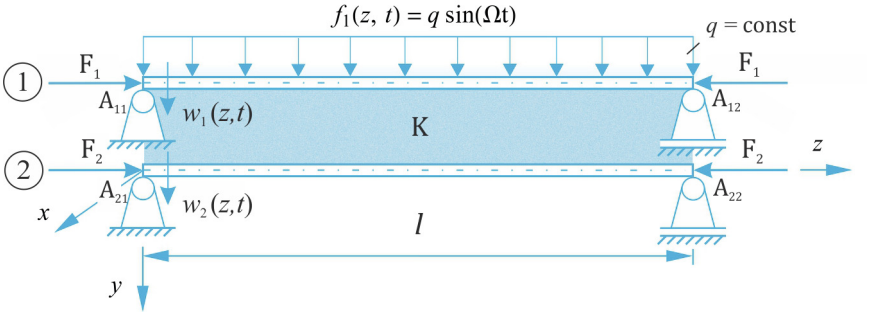

Fig. 3.4.2 The system of beams under the influence of uniform harmonic excitation

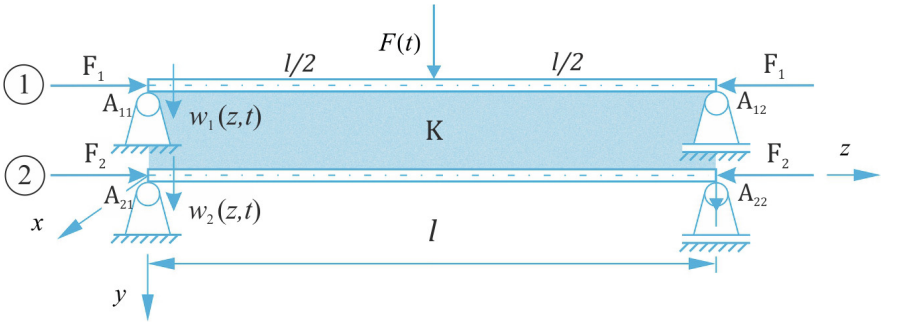

Fig. 3.4.3 The system of beams under the influence of concentrated harmonic excitation

The physical cases of harmonic excitation shown in Figures 3.4.1-3.4.3 have the following form

1) Arbitrarily continuous harmonic excitation

$$f_1(z,t) = q(z)\sin(\Omega t), \qquad f_2(z,t) = 0, \tag{3.4.1}$$

2) Uniformly continuous harmonic excitation

$$f_1(z,t) = q\sin(\Omega t), \qquad f_2(z,t) = 0, \tag{3.4.2}$$

3) Concentrated harmonic excitation

$$f_1(z,t) = F\sin(\Omega t)\delta(z-0.5l), \qquad f_2(z,t) = 0, \tag{3.4.3}$$

where $q(z)$,q, F, Ω and $\delta(z)$ represent arbitrary function of spatial coordinate z, the amplitude of uniform action, the frequency of harmonic concentrated force and Dirac delta function respectively. By substituting the equations (3.4.1), (3.4.2) and (3.4.3) into general solutions for forced vibration of Rayleigh, Timoshenko and Reddy-Bickford systems, we get particular solutions.

3.4.1 Particular Solutions for Forced Vibration of the System of Two Elastically Connected Rayleigh Beams

By substituting the equations (3.4.1), (3.4.2) and (3.4.3) into general solutions (3.1.25-3.1.26), we get

$$Y_{n1}(t) = \frac{\alpha_{n2}}{(\alpha_{n2}-\alpha_{n1})}k_R\sin(\Omega t), \quad n = 1,2,3,\ldots, \tag{3.4.4}$$

$$Y_{n2}(t) = \frac{\alpha_{n1}}{(\alpha_{n1}-\alpha_{n2})}k_R\sin(\Omega t), \quad n = 1,2,3,\ldots, \tag{3.4.5}$$

Substituting the equations (3.4.4) and (3.4.5) into general solutions to the equations (3.1.27) and (3.1.28), yields

$$w_{R1}^0(z,t) = \sum_{n=1}^{\infty}\sin(k_n z)\left[A_{n1}\sin(\Omega t) + \sum_{i=1}^{2}B_{ni}\sin(\omega_{ni}t)\right], \quad n = 1,2,3,\ldots, \tag{3.4.6}$$

$$w_{R2}^0(z,t) = \sum_{n=1}^{\infty}\sin(k_n z)\left[A_{n2}\sin(\Omega t) + \sum_{i=1}^{2}\alpha_{ni}B_{ni}\sin(\omega_{ni}t)\right], \quad n = 1,2,3,\ldots, \tag{3.4.7}$$

where

$$A_{n1} = \frac{k_R}{\alpha_{n2}-\alpha_{n1}}\left[\frac{\alpha_{n2}}{\omega_{n1}^2-\Omega^2} - \frac{\alpha_{n1}}{\omega_{n2}^2-\Omega^2}\right], \quad A_{n2} = \frac{k_R}{\alpha_{n2}-\alpha_{n1}}\left[\frac{\alpha_{n1}\alpha_{n2}}{\omega_{n1}^2-\Omega^2} - \frac{\alpha_{n1}\alpha_{n2}}{\omega_{n2}^2-\Omega^2}\right],$$

$$B_{n1} = k_R\frac{\alpha_{n2}}{\alpha_{n2}-\alpha_{n1}}\left[\frac{\Omega}{\omega_{n1}(\Omega^2-\omega_{n1}^2)}\right], \qquad B_{n2} = k_R\frac{\alpha_{n1}}{\alpha_{n2}-\alpha_{n1}}\left[\frac{\Omega}{\omega_{n2}(\omega_{n2}^2-\Omega^2)}\right].$$

Depending on the type of forcing in the general solutions, only the parameter k_R for which the following applies, changes

case 1) $k_R = 2M_1 \int_0^l q(z)\sin(k_n z)\,dz\,, \quad n = 1,2,3,\ldots$

case 2) $k_R = M_1 \dfrac{4lq}{n\pi}, n = 1,2,3,\ldots$

case 3) $k_R = 2FM_1 \sin\left(\dfrac{n\pi}{2}\right), \quad n = 1,2,3,\ldots$

Hence, the forced vibration of the mechanical system is of the following form

$$w_{R1}^0(z,t) = \sin(\Omega t)\sum_{n=1}^{\infty} A_{n1}\sin(k_n z)\,, \quad n = 1,2,3,\ldots, \tag{3.4.8}$$

$$w_{R2}^0(z,t) = \sin(\Omega t)\sum_{n=1}^{\infty} A_{n2}\sin(k_n z)\,, \quad n = 1,2,3,\ldots,. \tag{3.4.9}$$

where A_{n1}, A_{n2} represent the amplitudes of the normal vibration mode. The conditions of resonance and dynamic vibration absorption are as follows

$a)$ Resonance: $\Omega = \omega_{ni}, \qquad n = 1,3,5,\ldots$

$b)$ Dynamic vibration absorption: $\Omega^2 = \dfrac{\alpha_{n2}\omega_{n2}^2 - \alpha_{n1}\omega_{n1}^2}{\alpha_{n2} - \alpha_{n1}}, \quad A_{n1} = 0,$

$$A_{n2} = k_R \frac{\alpha_{n1} - \alpha_{n2}}{\omega_{n1}^2 - \omega_{n2}^2}, \qquad n = 1,2,3,\ldots$$

3.4.2 Particular Solutions for Forced Vibration for the System of Two Elastically Connected Timoshenko Beams

Let us find particular solutions for forced vibration of the coupled Timoshenko beam system under the influence of different types of excitation. By substituting the equations (3.4.1), (3.4.2) and (3.4.3) into general equations of forced vibration (3.2.32) and (3.2.35), we get

$$w_{T1}^0(z,t) = \sum_{n=1}^{\infty} \sin(k_n z)\left[\widetilde{A}_{n1}\sin(\Omega t) + \sum_{r=1}^{4} \widetilde{B}_{nr}\sin(\widetilde{\omega}_{nr} t)\right], \quad n = 1,2,3,\ldots, \tag{3.4.10}$$

$$w_{T2}^{0}(z,t) = \sum_{n=1}^{\infty} \sin(k_n z)\left[\widetilde{A}_{n2}\sin(\Omega t) + \sum_{r=1}^{4} \widetilde{C}_{nr}\sin(\widetilde{\omega}_{nr} t)\right], \quad n = 1,2,3,\ldots, \tag{3.4.11}$$

$$\psi_{T1}^{0}(z,t) = \sum_{n=1}^{\infty} \cos(k_n z)\left[\widetilde{A}_{n3}\sin(\Omega t) + \sum_{r=1}^{4} \widetilde{D}_{nr}\sin(\widetilde{\omega}_{nr} t)\right], \quad n = 1,2,3,\ldots, \tag{3.4.12}$$

$$\psi_{T2}^{0}(z,t) = \sum_{n=1}^{\infty} \cos(k_n z)\left[\tilde{A}_{n4}\sin(\Omega t) + \sum_{r=1}^{4} \tilde{E}_{nr}\sin(\widetilde{\omega}_{nr} t)\right], \quad n = 1,2,3,\ldots, \tag{3.4.13}$$

where

$$\tilde{A}_{n1} = k_T\left(\frac{\tilde{X}_{11}^2}{\widetilde{\omega}_{1n}^2 - \Omega^2} + \frac{\tilde{X}_{12}^2}{\widetilde{\omega}_{2n}^2 - \Omega^2} + \frac{\tilde{X}_{13}^2}{\widetilde{\omega}_{3n}^2 - \Omega^2} + \frac{\tilde{X}_{14}^2}{\widetilde{\omega}_{4n}^2 - \Omega^2}\right),$$

$$\tilde{A}_{n2} = k_T\left(\frac{\tilde{X}_{11}\tilde{X}_{21}}{\widetilde{\omega}_{1n}^2 - \Omega^2} + \frac{\tilde{X}_{12}\tilde{X}_{22}}{\widetilde{\omega}_{2n}^2 - \Omega^2} + \frac{\tilde{X}_{13}\tilde{X}_{23}}{\widetilde{\omega}_{3n}^2 - \Omega^2} + \frac{\tilde{X}_{14}\tilde{X}_{24}}{\widetilde{\omega}_{4n}^2 - \Omega^2}\right),$$

$$\tilde{A}_{n3} = k_T\left(\frac{\tilde{X}_{11}\tilde{X}_{31}}{\widetilde{\omega}_{1n}^2 - \Omega^2} + \frac{\tilde{X}_{12}\tilde{X}_{32}}{\widetilde{\omega}_{2n}^2 - \Omega^2} + \frac{\tilde{X}_{13}\tilde{X}_{33}}{\widetilde{\omega}_{3n}^2 - \Omega^2} + \frac{\tilde{X}_{14}\tilde{X}_{34}}{\widetilde{\omega}_{4n}^2 - \Omega^2}\right),$$

$$\tilde{A}_{n4} = k_T\left(\frac{\tilde{X}_{11}\tilde{X}_{41}}{\widetilde{\omega}_{1n}^2 - \Omega^2} + \frac{\tilde{X}_{12}\tilde{X}_{42}}{\widetilde{\omega}_{2n}^2 - \Omega^2} + \frac{\tilde{X}_{13}\tilde{X}_{43}}{\widetilde{\omega}_{3n}^2 - \Omega^2} + \frac{\tilde{X}_{14}\tilde{X}_{44}}{\widetilde{\omega}_{4n}^2 - \Omega^2}\right),$$

$$\tilde{B}_{1n} = k_T\tilde{X}_{11}^2\left[\frac{\Omega}{\widetilde{\omega}_{1n}(\Omega^2 - \widetilde{\omega}_{1n}^2)}\right], \qquad \tilde{B}_{2n} = k_T\tilde{X}_{12}^2\left[\frac{\Omega}{\widetilde{\omega}_{2n}(\Omega^2 - \widetilde{\omega}_{2n}^2)}\right],$$

$$\tilde{B}_{3n} = k_T\tilde{X}_{13}^2\left[\frac{\Omega}{\widetilde{\omega}_{3n}(\Omega^2 - \widetilde{\omega}_{3n}^2)}\right], \qquad \tilde{B}_{4n} = k_T\tilde{X}_{14}^2\left[\frac{\Omega}{\widetilde{\omega}_{4n}(\Omega^2 - \widetilde{\omega}_{4n}^2)}\right],$$

$$\tilde{C}_{1n} = k_T\tilde{X}_{11}\tilde{X}_{21}\left[\frac{\Omega}{\widetilde{\omega}_{1n}(\Omega^2 - \widetilde{\omega}_{1n}^2)}\right], \qquad \tilde{C}_{2n} = k_T\tilde{X}_{12}\tilde{X}_{22}\left[\frac{\Omega}{\widetilde{\omega}_{2n}(\Omega^2 - \widetilde{\omega}_{2n}^2)}\right],$$

$$\tilde{C}_{3n} = k_T\tilde{X}_{13}\tilde{X}_{23}\left[\frac{\Omega}{\widetilde{\omega}_{3n}(\Omega^2 - \widetilde{\omega}_{3n}^2)}\right], \qquad \tilde{C}_{4n} = k_T\tilde{X}_{14}\tilde{X}_{24}\left[\frac{\Omega}{\widetilde{\omega}_{4n}(\Omega^2 - \widetilde{\omega}_{4n}^2)}\right],$$

$$\widetilde{D}_{1n} = k_T\tilde{X}_{11}\tilde{X}_{31}\left[\frac{\Omega}{\widetilde{\omega}_{1n}(\Omega^2 - \widetilde{\omega}_{1n}^2)}\right], \qquad \widetilde{D}_{2n} = k_T\tilde{X}_{12}\tilde{X}_{32}\left[\frac{\Omega}{\widetilde{\omega}_{2n}(\Omega^2 - \widetilde{\omega}_{2n}^2)}\right],$$

$$\widetilde{D}_{3n} = k_T\tilde{X}_{13}\tilde{X}_{33}\left[\frac{\Omega}{\widetilde{\omega}_{3n}(\Omega^2 - \widetilde{\omega}_{3n}^2)}\right], \qquad \widetilde{D}_{4n} = k_T\tilde{X}_{14}\tilde{X}_{34}\left[\frac{\Omega}{\widetilde{\omega}_{4n}(\Omega^2 - \widetilde{\omega}_{4n}^2)}\right],$$

$$\tilde{E}_{1n} = k_T\tilde{X}_{11}\tilde{X}_{41}\left[\frac{\Omega}{\widetilde{\omega}_{1n}(\Omega^2 - \widetilde{\omega}_{1n}^2)}\right], \qquad \tilde{E}_{2n} = k_T\tilde{X}_{12}\tilde{X}_{42}\left[\frac{\Omega}{\widetilde{\omega}_{2n}(\Omega^2 - \widetilde{\omega}_{2n}^2)}\right],$$

$$\tilde{E}_{3n} = k_T\tilde{X}_{13}\tilde{X}_{43}\left[\frac{\Omega}{\widetilde{\omega}_{3n}(\Omega^2 - \widetilde{\omega}_{3n}^2)}\right], \qquad \tilde{E}_{4n} = k_T\tilde{X}_{14}\tilde{X}_{44}\left[\frac{\Omega}{\widetilde{\omega}_{4n}(\Omega^2 - \widetilde{\omega}_{4n}^2)}\right],$$

case 1) $k_T = \frac{2}{l}\int_0^l q(z)\sin(k_n z)\,dz\,, \quad n = 1,2,3,\ldots$

case 2) $k_T = \frac{4q}{n\pi}, n = 1,2,3,\ldots$

case 3) $k_T = \frac{2}{l}F\sin\left(\frac{n\pi}{2}\right), \quad n = 1,2,3,\ldots$

Particular solutions for forced vibration of mechanical system are given as

$$w_{T1}^0(z,t) = \sin(\Omega t)\sum_{n=1}^{\infty}\widetilde{A}_{n1}\sin(k_n z)\,, \quad n = 1,3,5,\ldots, \tag{3.4.14}$$

$$w_{T2}^0(z,t) = \sin(\Omega t)\sum_{n=1}^{\infty}\widetilde{A}_{n2}\sin(k_n z)\,, \quad n = 1,3,5,\ldots,. \tag{3.4.15}$$

$$\psi_{T1}^0(z,t) = \sin(\Omega t)\sum_{n=1}^{\infty}\widetilde{A}_{n3}\cos(k_n z)\,, \quad n = 1,3,5,\ldots, \tag{3.4.16}$$

$$\psi_{T2}^0(z,t) = \sin(\Omega t)\sum_{n=1}^{\infty}\widetilde{A}_{n4}\cos(k_n z)\,, \quad n = 1,3,5,\ldots,. \tag{3.4.17}$$

where $\tilde{A}_{nr}$ represents the amplitudes of the normal vibration mode. The conditions of resonance and dynamic vibration absorption are as follows

$$a)\ \text{Resonance:}\ \ \Omega = \widetilde{\omega}_{rn}, \qquad n = 1,2,3,\ldots$$

$$b)\ \text{Dynamic vibration absorption}$$

Forced frequency Ω at which the system acts as a dynamic absorber is obtained from the condition that $\tilde{A}_{n1} = 0$. After factorizing the equation $k_T\left(\frac{\tilde{X}_{11}^2}{\widetilde{\omega}_{1n}^2-\Omega^2} + \frac{\tilde{X}_{12}^2}{\widetilde{\omega}_{2n}^2-\Omega^2} + \frac{\tilde{X}_{13}^2}{\widetilde{\omega}_{3n}^2-\Omega^2} + \frac{\tilde{X}_{14}^2}{\widetilde{\omega}_{4n}^2-\Omega^2}\right) = 0,$ we get a bicubic polynomial equation for unknown forced frequencies

$$\Omega^6 + a_1\Omega^4 + a_2\Omega^2 + a_3 = 0, \tag{3.4.18}$$

where

$$a_1 = -\frac{\tilde{X}_{11}{}^2(\widetilde{\omega}_{n2}{}^2 + \widetilde{\omega}_{n3}{}^2 + \widetilde{\omega}_{n4}{}^2) + \tilde{X}_{12}{}^2(\widetilde{\omega}_{n1}{}^2 + \widetilde{\omega}_{n3}{}^2 + \widetilde{\omega}_{n4}{}^2)}{\tilde{X}_{11}{}^2 + \tilde{X}_{12}{}^2 + \tilde{X}_{13}{}^2 + \tilde{X}_{14}{}^2} -$$

$$-\frac{\tilde{X}_{13}{}^2(\widetilde{\omega}_{n1}{}^2 + \widetilde{\omega}_{n2}{}^2 + \widetilde{\omega}_{n4}{}^2) + \tilde{X}_{14}{}^2(\widetilde{\omega}_{n1}{}^2 + \widetilde{\omega}_{n2}{}^2 + \widetilde{\omega}_{n3}{}^2)}{\tilde{X}_{11}{}^2 + \tilde{X}_{12}{}^2 + \tilde{X}_{13}{}^2 + \tilde{X}_{14}{}^2},$$

$$a_2 = \frac{\tilde{\omega}_{n4}{}^2[\tilde{X}_{11}{}^2(\tilde{\omega}_{n2}{}^2 + \tilde{\omega}_{n3}{}^2) + \tilde{X}_{12}{}^2(\tilde{\omega}_{n1}{}^2 + \tilde{\omega}_{n3}{}^2)] + \tilde{\omega}_{n3}{}^2(\tilde{X}_{11}{}^2\tilde{\omega}_{n2}{}^2 + \tilde{X}_{12}{}^2\tilde{\omega}_{n1}{}^2)}{\tilde{X}_{11}{}^2 + \tilde{X}_{12}{}^2 + \tilde{X}_{13}{}^2 + \tilde{X}_{14}{}^2} +$$

$$\frac{+\tilde{X}_{13}{}^2[\tilde{\omega}_{n1}{}^2(\tilde{\omega}_{n2}{}^2 + \tilde{\omega}_{n4}{}^2) + \tilde{\omega}_{n2}{}^2\tilde{\omega}_{n4}{}^2] + \tilde{X}_{14}{}^2[\tilde{\omega}_{n3}{}^2(\tilde{\omega}_{n1}{}^2 + \tilde{\omega}_{n2}{}^2) + \tilde{\omega}_{n1}{}^2\tilde{\omega}_{n2}{}^2]}{\tilde{X}_{11}{}^2 + \tilde{X}_{12}{}^2 + \tilde{X}_{13}{}^2 + \tilde{X}_{14}{}^2},$$

$$a_3 = -\frac{\tilde{\omega}_{n4}{}^2[\tilde{\omega}_{n3}{}^2(\tilde{X}_{11}{}^2\tilde{\omega}_{n2}{}^2 + \tilde{X}_{12}{}^2\tilde{\omega}_{n1}{}^2) + \tilde{X}_{13}{}^2\tilde{\omega}_{n1}{}^2\tilde{\omega}_{n2}{}^2] + \tilde{X}_{14}{}^2\tilde{\omega}_{n1}{}^2\tilde{\omega}_{n2}{}^2\tilde{\omega}_{n3}{}^2}{\tilde{X}_{11}{}^2 + \tilde{X}_{12}{}^2 + \tilde{X}_{13}{}^2 + \tilde{X}_{14}{}^2}.$$

from where three solutions for forcing frequencies for which the amplitude of the first beam equals zero, follow.

$$\begin{Bmatrix} \tilde{\Omega}_1^2 \\ \tilde{\Omega}_2^2 \\ \tilde{\Omega}_3^2 \end{Bmatrix} = -\frac{\tilde{a}_1}{3} + 2\sqrt{-\frac{\tilde{p}}{3}} \begin{Bmatrix} \cos\left(\frac{\tilde{\theta}}{3}\right) \\ \cos\left(\frac{\tilde{\theta}+2\pi}{3}\right) \\ \cos\left(\frac{\tilde{\theta}+4\pi}{3}\right) \end{Bmatrix}, \tag{3.4.19}$$

on condition that $D = \frac{\tilde{q}^2}{4} + \frac{\tilde{p}^3}{27} < 0$ and where

$$\tilde{p} = \tilde{a}_2 - \frac{\tilde{a}_1^2}{3}, \quad \tilde{\tilde{q}} = \tilde{\tilde{a}}_3 - \frac{\tilde{a}_1\tilde{a}_2}{3} + \frac{2\tilde{a}_1^3}{27}, \quad \tilde{\theta} = \cos^{-1}\left[-\frac{\tilde{q}}{2}\left(-\frac{\tilde{p}}{3}\right)^{-\frac{3}{2}}\right].$$

3.4.3 Particular Solutions for Forced Vibration for the System of Two Elastically Connected Reddy-Bickford Beams

Particular solutions for forced vibrations for the system of coupled Reddy-Bickford beams under the influence of different types of forcing are determined by substituting the equations (3.4.1), (3.4.2) and (3.4.3) into general equations for forced vibration (3.3.35-3.3.38) which yields

$$w_{RB1}^0(z,t) = \sum_{n=1}^{\infty} \sin(k_n z)\left[\tilde{\tilde{A}}_{n1}\sin(\Omega t) + \sum_{r=1}^{4} \tilde{\tilde{B}}_{nr}\sin(\tilde{\tilde{\omega}}_{nr}t)\right], \quad n = 1,2,3,\ldots, \tag{3.4.20}$$

$$w_{RB2}^0(z,t) = \sum_{n=1}^{\infty} \sin(k_n z)\left[\tilde{\tilde{A}}_{n2}\sin(\Omega t) + \sum_{r=1}^{4} \tilde{\tilde{C}}_{nr}\sin(\tilde{\tilde{\omega}}_{nr}t)\right], \quad n = 1,2,3,\ldots, \tag{3.4.21}$$

$$\psi_{RB}^0(z,t) = \sum_{n=1}^{\infty} \cos(k_n z)\left[\tilde{\tilde{A}}_{n3}\sin(\Omega t) + \sum_{r=1}^{4} \tilde{\tilde{D}}_{nr}\sin(\tilde{\tilde{\omega}}_{nr}t)\right], \quad n = 1,2,3,\ldots, \tag{3.4.22}$$

$$\psi_{RB}^{0}(z,t)=\sum_{n=1}^{\infty}\cos(k_n z)\left[\tilde{\tilde{A}}_{n4}\sin(\Omega t)+\sum_{r=1}^{4}\tilde{\tilde{E}}_{nr}\sin\left(\tilde{\tilde{\omega}}_{nr}t\right)\right],\quad n=1,2,3,\ldots, \tag{3.4.23}$$

where

$$\tilde{\tilde{A}}_{n1}=k_{RB}\left(\frac{\tilde{\tilde{X}}_{11}^{2}}{\tilde{\tilde{\omega}}_{1n}^{2}-\Omega^{2}}+\frac{\tilde{\tilde{X}}_{12}^{2}}{\tilde{\tilde{\omega}}_{2n}^{2}-\Omega^{2}}+\frac{\tilde{\tilde{X}}_{13}^{2}}{\tilde{\tilde{\omega}}_{3n}^{2}-\Omega^{2}}+\frac{\tilde{\tilde{X}}_{14}^{2}}{\tilde{\tilde{\omega}}_{4n}^{2}-\Omega^{2}}\right),$$

$$\tilde{\tilde{A}}_{n2}=k_{RB}\left(\frac{\tilde{\tilde{X}}_{11}\tilde{\tilde{X}}_{21}}{\tilde{\tilde{\omega}}_{1n}^{2}-\Omega^{2}}+\frac{\tilde{\tilde{X}}_{12}\tilde{\tilde{X}}_{22}}{\tilde{\tilde{\omega}}_{2n}^{2}-\Omega^{2}}+\frac{\tilde{\tilde{X}}_{13}\tilde{\tilde{X}}_{23}}{\tilde{\tilde{\omega}}_{3n}^{2}-\Omega^{2}}+\frac{\tilde{\tilde{X}}_{14}\tilde{\tilde{X}}_{24}}{\tilde{\tilde{\omega}}_{4n}^{2}-\Omega^{2}}\right),$$

$$\tilde{\tilde{A}}_{n3}=k_{RB}\left(\frac{\tilde{\tilde{X}}_{11}\tilde{X}_{31}}{\tilde{\tilde{\omega}}_{1n}^{2}-\Omega^{2}}+\frac{\tilde{X}_{12}\tilde{X}_{32}}{\tilde{\tilde{\omega}}_{2n}^{2}-\Omega^{2}}+\frac{\tilde{X}_{13}\tilde{X}_{33}}{\tilde{\tilde{\omega}}_{3n}^{2}-\Omega^{2}}+\frac{\tilde{X}_{14}\tilde{X}_{34}}{\tilde{\tilde{\omega}}_{4n}^{2}-\Omega^{2}}\right),$$

$$\tilde{\tilde{A}}_{n4}=k_{RB}\left(\frac{\tilde{X}_{11}\tilde{X}_{41}}{\tilde{\tilde{\omega}}_{1n}^{2}-\Omega^{2}}+\frac{\tilde{X}_{12}\tilde{X}_{42}}{\tilde{\tilde{\omega}}_{2n}^{2}-\Omega^{2}}+\frac{\tilde{X}_{13}\tilde{X}_{43}}{\tilde{\tilde{\omega}}_{3n}^{2}-\Omega^{2}}+\frac{\tilde{X}_{14}\tilde{X}_{44}}{\tilde{\tilde{\omega}}_{4n}^{2}-\Omega^{2}}\right),$$

$$\tilde{\tilde{B}}_{1n}=k_T\tilde{X}_{11}^{2}\left[\frac{\Omega}{\tilde{\tilde{\omega}}_{1n}(\Omega^{2}-\tilde{\tilde{\omega}}_{1n}^{2})}\right],\qquad \tilde{\tilde{B}}_{2n}=k_{RB}\tilde{X}_{12}^{2}\left[\frac{\Omega}{\tilde{\tilde{\omega}}_{2n}(\Omega^{2}-\tilde{\tilde{\omega}}_{2n}^{2})}\right],$$

$$\tilde{\tilde{B}}_{3n}=k_{RB}\tilde{X}_{13}^{2}\left[\frac{\Omega}{\tilde{\omega}_{3n}(\Omega^{2}-\tilde{\tilde{\omega}}_{3n}^{2})}\right],\qquad \tilde{\tilde{B}}_{4n}=k_{RB}\tilde{X}_{14}^{2}\left[\frac{\Omega}{\tilde{\tilde{\omega}}_{4n}(\Omega^{2}-\tilde{\tilde{\omega}}_{4n}^{2})}\right],$$

$$\tilde{\tilde{C}}_{1n}=k_{RB}\tilde{\tilde{X}}_{11}\tilde{\tilde{X}}_{21}\left[\frac{\Omega}{\tilde{\tilde{\omega}}_{1n}(\Omega^{2}-\tilde{\tilde{\omega}}_{1n}^{2})}\right],\qquad \tilde{\tilde{C}}_{2n}=k_{RB}\tilde{X}_{12}\tilde{X}_{22}\left[\frac{\Omega}{\tilde{\tilde{\omega}}_{2n}(\Omega^{2}-\tilde{\tilde{\omega}}_{2n}^{2})}\right],$$

$$\tilde{\tilde{C}}_{3n}=k_{RB}\tilde{\tilde{X}}_{13}\tilde{\tilde{X}}_{23}\left[\frac{\Omega}{\tilde{\tilde{\omega}}_{3n}(\Omega^{2}-\tilde{\tilde{\omega}}_{3n}^{2})}\right],\qquad \tilde{\tilde{C}}_{4n}=k_{RB}\tilde{\tilde{X}}_{14}\tilde{\tilde{X}}_{24}\left[\frac{\Omega}{\tilde{\tilde{\omega}}_{4n}(\Omega^{2}-\tilde{\tilde{\omega}}_{4n}^{2})}\right],$$

$$\tilde{\tilde{D}}_{1n}=k_{RB}\tilde{\tilde{X}}_{11}\tilde{\tilde{X}}_{31}\left[\frac{\Omega}{\tilde{\tilde{\omega}}_{1n}(\Omega^{2}-\tilde{\tilde{\omega}}_{1n}^{2})}\right],\qquad \tilde{\tilde{D}}_{2n}=k_{RB}\tilde{\tilde{X}}_{12}\tilde{\tilde{X}}_{32}\left[\frac{\Omega}{\tilde{\tilde{\omega}}_{2n}(\Omega^{2}-\tilde{\tilde{\omega}}_{2n}^{2})}\right],$$

$$\tilde{\tilde{D}}_{3n}=k_{RB}\tilde{\tilde{X}}_{13}\tilde{\tilde{X}}_{33}\left[\frac{\Omega}{\tilde{\tilde{\omega}}_{3n}(\Omega^{2}-\tilde{\tilde{\omega}}_{3n}^{2})}\right],\qquad \tilde{\tilde{D}}_{4n}=k_{RB}\tilde{\tilde{X}}_{14}\tilde{\tilde{X}}_{34}\left[\frac{\Omega}{\tilde{\tilde{\omega}}_{4n}(\Omega^{2}-\tilde{\tilde{\omega}}_{4n}^{2})}\right],$$

$$\tilde{\tilde{E}}_{1n}=k_{RB}\tilde{X}_{11}\tilde{X}_{41}\left[\frac{\Omega}{\tilde{\tilde{\omega}}_{1n}(\Omega^{2}-\tilde{\tilde{\omega}}_{1n}^{2})}\right],\qquad \tilde{\tilde{E}}_{2n}=k_{RB}\tilde{\tilde{X}}_{12}\tilde{\tilde{X}}_{42}\left[\frac{\Omega}{\tilde{\tilde{\omega}}_{2n}(\Omega^{2}-\tilde{\tilde{\omega}}_{2n}^{2})}\right],$$

$$\tilde{\tilde{E}}_{3n}=k_{RB}\tilde{\tilde{X}}_{13}\tilde{\tilde{X}}_{43}\left[\frac{\Omega}{\tilde{\tilde{\omega}}_{3n}(\Omega^{2}-\tilde{\tilde{\omega}}_{3n}^{2})}\right],\qquad \tilde{\tilde{E}}_{4n}=k_{RB}\tilde{\tilde{X}}_{14}\tilde{\tilde{X}}_{44}\left[\frac{\Omega}{\tilde{\tilde{\omega}}_{4n}(\Omega^{2}-\tilde{\tilde{\omega}}_{4n}^{2})}\right],$$

case 1) $k_{RB}=k_T=\dfrac{2}{l}\displaystyle\int_0^{l}q(z)\sin(k_n z)\,dz,\quad n=1,2,3,\ldots$

case 2) $k_{RB}=k_T=\dfrac{4q}{n\pi}, n=1,2,3,\ldots$

case 3) $k_{RB}=\ k_T=\dfrac{2}{l}F\sin\left(\dfrac{n\pi}{2}\right),\quad n=1,2,3,\ldots$

Particular solutions for forced vibration of mechanical system are expressed as

$$w_{RB1}^{0}(z,t) = \sin(\Omega t)\sum_{n=1}^{\infty}\tilde{\tilde{A}}_{n1}\sin(k_n z), \quad n = 1,2,3,\ldots, \tag{3.4.24}$$

$$w_{RB2}^{0}(z,t) = \sin(\Omega t)\sum_{n=1}^{\infty}\tilde{\tilde{A}}_{n2}\sin(k_n z), \quad n = 1,2,3,\ldots,. \tag{3.4.25}$$

$$\psi_{RB1}^{0}(z,t) = \sin(\Omega t)\sum_{n=1}^{\infty}\tilde{\tilde{A}}_{n3}\cos(k_n z), \quad n = 1,2,3,\ldots, \tag{3.4.26}$$

$$\psi_{RB2}^{0}(z,t) = \sin(\Omega t)\sum_{n=1}^{\infty}\tilde{\tilde{A}}_{n4}\cos(k_n z), \quad n = 1,2,3,\ldots,. \tag{3.4.27}$$

where $\tilde{\tilde{A}}_{nr}$ are the amplitudes of the normal vibration mode. The conditions of resonance and dynamic vibration absorption are

$$a)\ \text{Resonance}: \quad \Omega = \tilde{\tilde{\omega}}_{rn}, \qquad n = 1,2,3,\ldots$$

$$b)\ \text{Dynamic vibration absorption}$$

The forcing frequency Ω on which the system acts as a dynamic absorber is obtained as in the case of the Timoshenko beam system, from where three solutions for forcing frequencies follow

$$\begin{Bmatrix}\tilde{\tilde{\Omega}}_1^2\\ \tilde{\tilde{\Omega}}_2^2\\ \tilde{\tilde{\Omega}}_3^2\end{Bmatrix} = -\frac{\tilde{\tilde{a}}_1}{3} + 2\sqrt{-\frac{\tilde{\tilde{p}}}{3}}\begin{Bmatrix}\cos\left(\frac{\tilde{\tilde{\theta}}}{3}\right)\\ \cos\left(\frac{\tilde{\tilde{\theta}}+2\pi}{3}\right)\\ \cos\left(\frac{\tilde{\tilde{\theta}}+4\pi}{3}\right)\end{Bmatrix}, \tag{3.4.28}$$

where

$$\tilde{\tilde{a}}_1 = -\frac{\tilde{\tilde{X}}_{11}{}^2(\tilde{\tilde{\omega}}_{n2}{}^2 + \tilde{\tilde{\omega}}_{n3}{}^2 + \tilde{\tilde{\omega}}_{n4}{}^2) + \tilde{\tilde{X}}_{12}{}^2(\tilde{\tilde{\omega}}_{n1}{}^2 + \tilde{\tilde{\omega}}_{n3}{}^2 + \tilde{\tilde{\omega}}_{n4}{}^2)}{\tilde{\tilde{X}}_{11}{}^2 + \tilde{\tilde{X}}_{12}{}^2 + \tilde{\tilde{X}}_{13}{}^2 + \tilde{\tilde{X}}_{14}{}^2} -$$

$$-\frac{\tilde{\tilde{X}}_{13}{}^2(\tilde{\tilde{\omega}}_{n1}{}^2 + \tilde{\tilde{\omega}}_{n2}{}^2 + \tilde{\tilde{\omega}}_{n4}{}^2) + \tilde{\tilde{X}}_{14}{}^2(\tilde{\tilde{\omega}}_{n1}{}^2 + \tilde{\tilde{\omega}}_{n2}{}^2 + \tilde{\tilde{\omega}}_{n3}{}^2)}{\tilde{\tilde{X}}_{11}{}^2 + \tilde{\tilde{X}}_{12}{}^2 + \tilde{\tilde{X}}_{13}{}^2 + \tilde{\tilde{X}}_{14}{}^2},$$

$$\tilde{\tilde{a}}_2 = \frac{\tilde{\tilde{\omega}}_{n4}{}^2[\tilde{\tilde{X}}_{11}{}^2\left(\tilde{\tilde{\omega}}_{n2}{}^2+\tilde{\tilde{\omega}}_{n3}{}^2\right)+\tilde{\tilde{X}}_{12}{}^2\left(\tilde{\tilde{\omega}}_{n1}{}^2+\tilde{\tilde{\omega}}_{n3}{}^2\right)]+\tilde{\tilde{\omega}}_{n3}{}^2(\tilde{\tilde{X}}_{11}{}^2\tilde{\tilde{\omega}}_{n2}{}^2+\tilde{\tilde{X}}_{12}{}^2\tilde{\tilde{\omega}}_{n1}{}^2)}{\tilde{\tilde{X}}_{11}{}^2+\tilde{\tilde{X}}_{12}{}^2+\tilde{\tilde{X}}_{13}{}^2+\tilde{\tilde{X}}_{14}{}^2}+$$

$$\frac{+\tilde{\tilde{X}}_{13}{}^2[\tilde{\tilde{\omega}}_{n1}{}^2(\tilde{\tilde{\omega}}_{n2}{}^2+\tilde{\tilde{\omega}}_{n4}{}^2)+\tilde{\tilde{\omega}}_{n2}{}^2\tilde{\tilde{\omega}}_{n4}{}^2]+\tilde{\tilde{X}}_{14}{}^2[\tilde{\tilde{\omega}}_{n3}{}^2(\tilde{\tilde{\omega}}_{n1}{}^2+\tilde{\tilde{\omega}}_{n2}{}^2)+\tilde{\tilde{\omega}}_{n1}{}^2\tilde{\tilde{\omega}}_{n2}{}^2]}{\tilde{\tilde{X}}_{11}{}^2+\tilde{\tilde{X}}_{12}{}^2+\tilde{\tilde{X}}_{13}{}^2+\tilde{\tilde{X}}_{14}{}^2},$$

$$\tilde{\tilde{a}}_3 = -\frac{\tilde{\tilde{\omega}}_{n4}{}^2[\tilde{\tilde{\omega}}_{n3}{}^2(\tilde{\tilde{X}}_{11}{}^2\tilde{\tilde{\omega}}_{n2}{}^2+\tilde{\tilde{X}}_{12}{}^2\tilde{\tilde{\omega}}_{n1}{}^2)+\tilde{\tilde{X}}_{13}{}^2\tilde{\tilde{\omega}}_{n1}{}^2\tilde{\tilde{\omega}}_{n2}{}^2]+\tilde{\tilde{X}}_{14}{}^2\tilde{\tilde{\omega}}_{n1}{}^2\tilde{\tilde{\omega}}_{n2}{}^2\tilde{\tilde{\omega}}_{n3}{}^2}{\tilde{\tilde{X}}_{11}{}^2+\tilde{\tilde{X}}_{12}{}^2+\tilde{\tilde{X}}_{13}{}^2+\tilde{\tilde{X}}_{14}{}^2}.$$

$$\tilde{\tilde{p}} = \tilde{\tilde{a}}_2 - \frac{\tilde{\tilde{a}}_1^2}{3},\quad \tilde{\tilde{q}} = \tilde{\tilde{a}}_3 - \frac{\tilde{\tilde{a}}_1\tilde{\tilde{a}}_2}{3} + \frac{2\tilde{\tilde{a}}_1^3}{27},\quad \tilde{\tilde{\theta}} = \cos^{-1}\left[-\frac{\tilde{\tilde{q}}}{2}\left(-\frac{\tilde{\tilde{p}}}{3}\right)^{-\frac{3}{2}}\right].$$

3.5 Numerical Analysis

The purpose of taking into account the effects of rotary inertia and transverse shear is to show the differences in the amplitudes occurring at the action of axial forces on thicker beams. These influences increase the differences in the approximation of solutions and must be considered when the rotation of the beams' cross-sections occurs due to shear forces. The numerical experiment used the two-beam model with identical material and geometric properties.

$$E = 1\times10^{10}\mathrm{Nm}^{-2},\quad \nu = 0.34,\quad G = 0.417*10^{10}\mathrm{Nm}^{-2},\quad k = \frac{5}{6},\quad K = 2\times10^{5}\mathrm{Nm}^{-2}$$

$$\rho = 2\times10^{3}\mathrm{kgm}^{-3}, A = 5\times10^{-2}\mathrm{m}^2,\quad I = \frac{bh^3}{12} = 4\times10^{-4}\mathrm{m}^4,$$

$$l = 10\ \mathrm{m},\quad b = \frac{1}{8}\sqrt{\frac{5}{3}}\mathrm{m},\ h = h_1 = \frac{2}{5}\sqrt{\frac{3}{5}}\mathrm{m}. \tag{3.5.1}$$

Let us introduce the quantity χ – axial force factor on the first beam in the function of its critical value, ζ- axial force factor on the second beam in the function of axial force on the first beam and amplitude ratios with and without the action of axial forces φ_1, φ_2 in the following form

$$F_1 = \chi F^{kr},\quad 0\le\chi\le1,\quad F_2 = \zeta F_1,\quad 0\le\zeta\le1,\quad \varphi_1 = \frac{A_{n1}}{A_{0,n1}},\quad \varphi_2 = \frac{A_{n2}}{A_{0,n2}},$$

ref. [51] Euler, Rayleigh: $F^{cr} = \dfrac{EI\pi^2}{l^2}$, ref. [52] Timoshenko: $F^{cr} = \dfrac{\frac{EI\pi^2}{l^2}}{1+\frac{EI\pi^2}{GAkl^2}}$,

$$\text{ref. [31] Reddy} - \text{Bickford: } F^{cr} = \frac{EI\pi^2\left(840G+\frac{Eh^2\pi^2}{l^2}\right)}{l^2\left(840G+\frac{85Eh^2\pi^2}{l^2}\right)}. \tag{3.5.2}$$

In case of uniformly continuous harmonic excitation, the amplitudes of normal forced vibration of the beam system can be established for system parameters based on determined analytical expressions. The amplitude ratios $\varphi_1$and φ_2 at an excitation with following characteristics $\Omega = 0.6\omega_{nII}$, $q = 1$ are shown in Figures 3.5.1 - 3.5.16. The obtained results were compared to the results for forced vibration of the system of elastically connected Euler beams, ref. Zhang et al. [5]. It can be noted in all Figures that the amplitude ratio for the second beam is higher compared to that of the first. By comparing the obtained results in the same vibration mode for different values of axial compression ($\zeta = 0.1, \zeta = 0.9$), it may be concluded that the influence of axial force on the second beam slightly affects the difference in vibration amplitude ratios of both beams.

In case of doubly thicker beams (3.5.9-3.5.16), we see that with the increase of the vibration mode, the difference in the amplitude ratio increases at a faster rate between the used models, with the Timoshenko and Reddy-Bickford's model providing a much better approximation. Therefore, it is appropriate to use analytically determined results given in this chapter for such model of the two elastically connected thicker beams. The figures 3.5.17-3.5.18 show amplitude-frequency characteristics of the vibration of two elastically connected beams joined by a Winkler layer. It can be clearly seen from the Figures when the resonance occurs and when the system acts as a dynamic absorber. The differences in the obtained solutions show the importance of applying the theories that take into account the rotary inertia and transverse shear, the effects of which increase with the rise of the forced vibration mode of the system.

Case for $h = h_1$

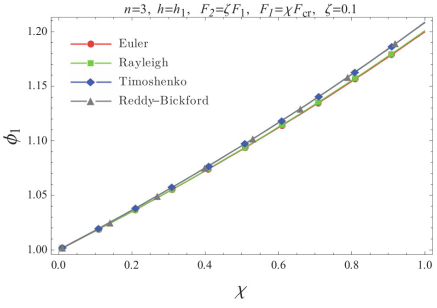

Fig.3.5.1 φ_1; $(n = 3, \zeta = 0.1)$

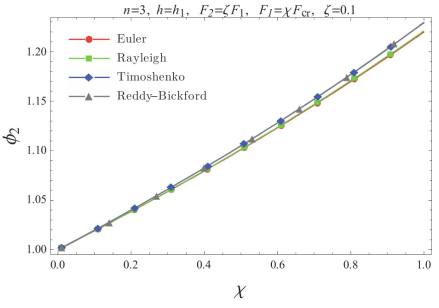

Fig. 3.5.2 φ_2; $(n = 3, \zeta = 0.1)$

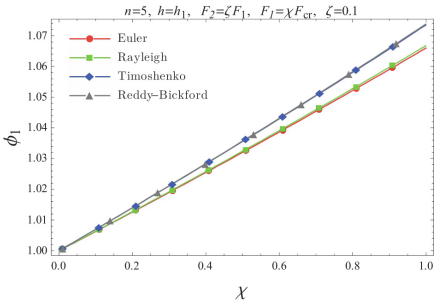

Fig. 3.5.3 φ_1; $(n = 5, \zeta = 0.1)$

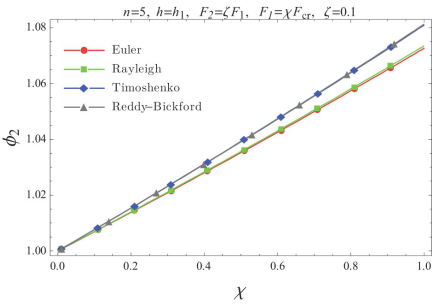

Fig. 3.5.4 φ_2; $(n = 5, \zeta = 0.1)$

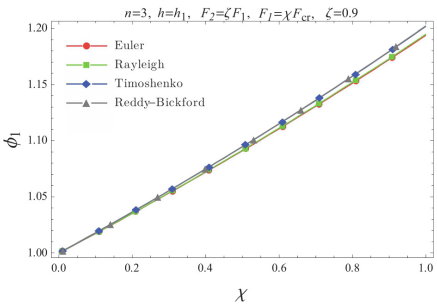

Fig. 3.5.5 φ_1; $(n = 3, \zeta = 0.9)$

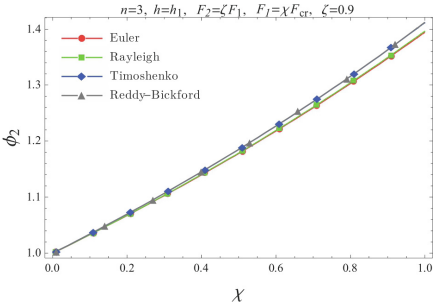

Fig. 3.5.6 φ_2; $(n = 3, \zeta = 0.9)$

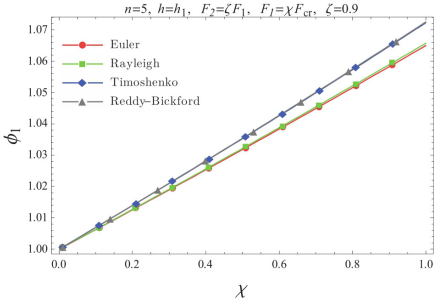

Fig. 3.5.7 φ_1; $(n = 5, \zeta = 0.9)$

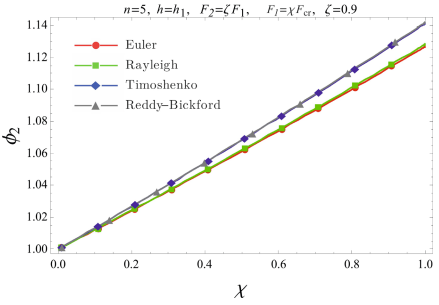

Fig. 3.5.8 φ_2; $(n = 5, \zeta = 0.9)$

Case $h = 2h_1$

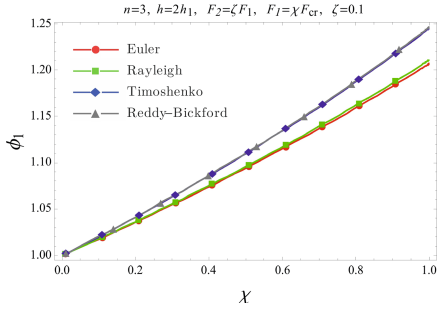

Fig. 3.5.9 φ_1; ($n = 3, \zeta = 0.1$)

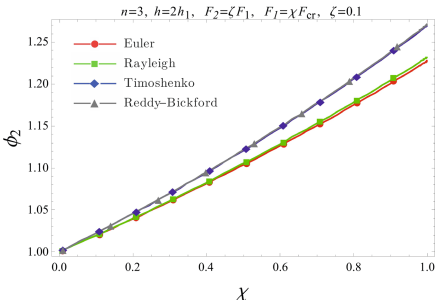

Fig. 3.5.10 φ_2; ($n = 3, \zeta = 0.1$)

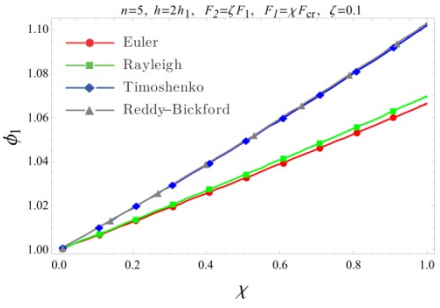

Fig. 3.5.11 φ_1; ($n = 5, \zeta = 0.1$)

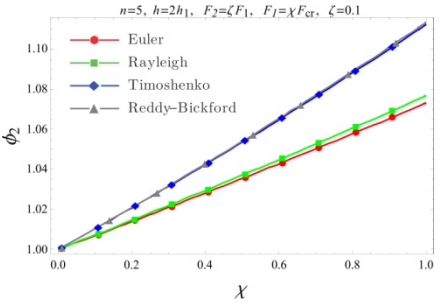

Fig. 3.5.12 φ_2; ($n = 5, \zeta = 0.1$)

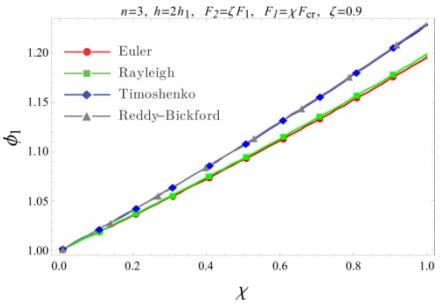

Fig. 3.5.13 φ_1; ($n = 3, \zeta = 0.9$)

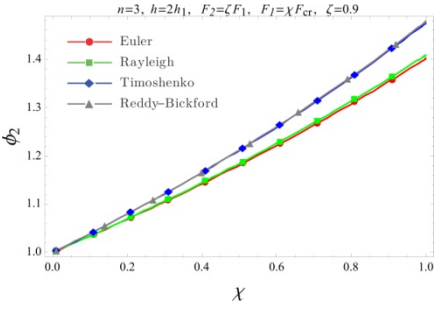

Fig. 3.5.14 φ_2; ($n = 3, \zeta = 0.9$)

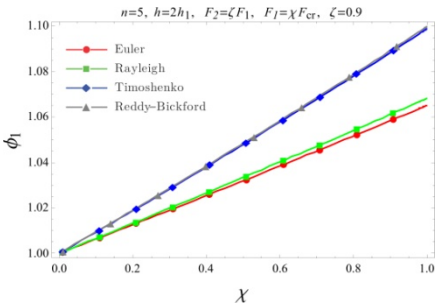

Fig. 3. 5. 15 φ_1; ($n = 5, \zeta = 0.9$)

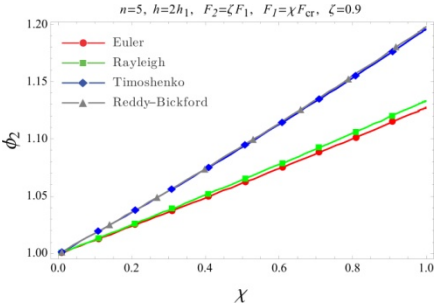

Fig. 3.5.16 φ_2; ($n = 5, \zeta = 0.9$)

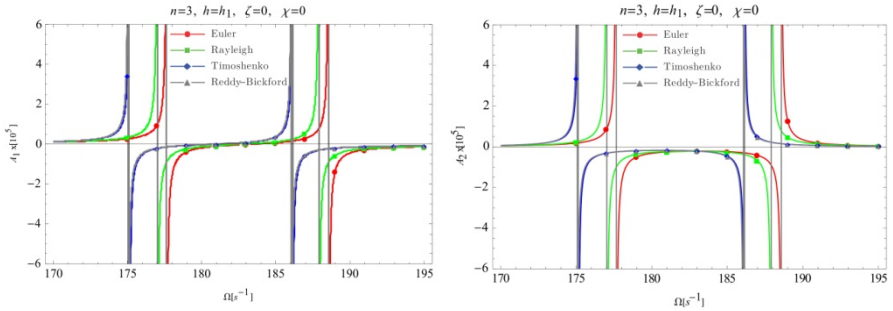

Fig. 3.5.17 h=h_1, n=3

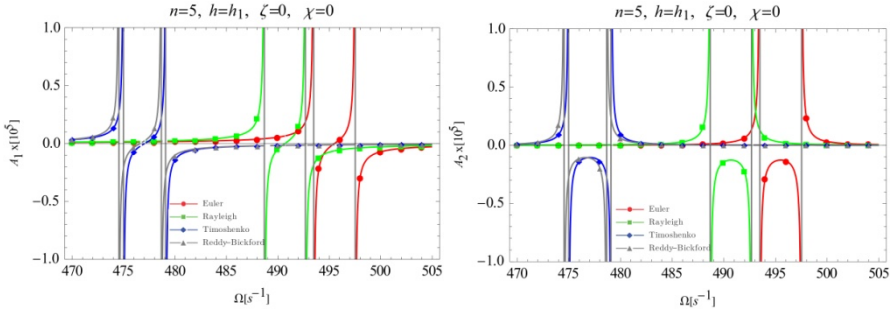

Fig. 3.5.18 h=h_1, n=5

Chapter 4

Static and Stochastic Stability of an Elastically Connected Beam System on an Elastic Foundation

Chapter 4 considers the static and stochastic stability of the elastically connected three beams on an elastic foundation. It is derived a new set of partial differential equations for static analysis of deflections and critical buckling force of the complex mechanical system and it is presented comparison study of the static stability between mechanical systems with one, two and three beams on an elastic foundation. It is analytically determined critical buckling force for each system individually. It is concluded that the system is the most stable in the case of the one beam on elastic foundation.

In the case of the stochastic stability of the three elastically connected beams on an elastic foundation, the model is given as a system of the three coupled oscillators. Stochastic stability conditions are expressed by the Lyapunov exponent and moment Lyapunov exponents. It is determined the new set of transformation for getting Itô differential equations which can be applied for any system of three coupled oscillators. The method of regular perturbation is used to determine the asymptotic expressions for these exponents in the presence of small intensity noises. Analytical results are presented for the almost sure and moment stability of a stochastic dynamical system. The results are applied to study the moment stability of the complex structure with the influence of the white noise excitation due to the axial compressive stochastic load.

4.1 Critical Buckling Force of Three Elastically Connected Timoshenko Beams on an Elastic Foundation

Let us analyze the case of three elastically connected Timoshenko beams of the same length l, on an elastic Winkler-type foundation with the stiffness modulus K and the influence of identical axial loads F, Stojanović et al. [14]. Partial differential equations of motion for points of the system shown in Figure 4.1.1 are derived by applying the principle of virtual work for beams with identical geometric and material properties.

V. Stojanović and P. Kozić, *Vibrations and Stability of Complex Beam Systems,*
Springer Tracts in Mechanical Engineering, DOI: 10.1007/978-3-319-13767-4_4

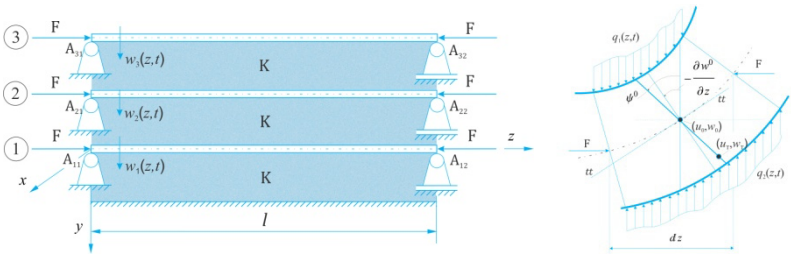

(a) (b)

Fig. 4.1.1 a) Three-beam system on an elastic foundation b) An elementary deformed beam part

Let us mark the functions of longitudinal and transverse motions and the angle between the beam's cross-section and y–axis as $u_{T1}(y,z,t)$, $w_{T1}(y,z)$, $\psi^0_{T1}(z)$, $u_{T2}(y,z)$, $w_{T2}(y,z)$, $\psi^0_{T2}(z)$, $u_{T3}(y,z)$,$w_{T3}(y,z)$ and $\psi^0_{T3}(z)$ respectively. For a clockwise angle of the cross-section ψ^0_T ref. [14, 26], the motion of beam points is expressed as

$$u_{Ti}(y,z) = u^0_{Ti}(z) - y\psi^0_{Ti}(z), \quad w_{Ti}(y,z) = w^0_{Ti}(z), \quad i = 1,2,3. \tag{4.1.1}$$

Deformation in the function of motion and the relation between stress and deformation according to the Hooke's law are

$$\varepsilon_{zi}(y,z) = \frac{\partial u^0_{Ti}(z)}{\partial z} - y\frac{\partial \psi^0_{Ti}(z)}{\partial z}, \quad \gamma_{zyi}(z) = \frac{\partial w^0_{Ti}(z)}{\partial z} - \psi^0_{Ti}(z), \tag{4.1.2}$$

$$\begin{Bmatrix}\sigma_{zi}\\ \tau_{zyi}\end{Bmatrix} = \begin{bmatrix}E & 0\\ 0 & kG\end{bmatrix}\begin{Bmatrix}\varepsilon_{zi}\\ \gamma_{zyi}\end{Bmatrix}, \quad i = 1,2,3. \tag{4.1.3}$$

Virtual work of internal and external forces is given by

$$\delta W_{Vi} = -b\int_0^l \int_{-\frac{h}{2}}^{\frac{h}{2}} \left[\sigma_{zi}(z)\delta\varepsilon_{zi}(z) + \tau_{zyi}\delta\gamma_{zyi}(z)\right]dydz, \quad i = 1,2,3. \tag{4.1.4}$$

$$\delta W_{ex1} = \int_0^l \left[\delta w^0_{T1}(z)K\left(w^0_{T2}(z) - 2w^0_{T1}(z)\right) + F\frac{\partial w^0_{T1}(z)}{\partial z}\frac{\partial \delta w^0_{T1}(z)}{\partial z}\right]dz, \tag{4.1.5}$$

$$\delta W_{ex2} = \int_0^l \left[\delta w^0_{T2}(z)K\left(w^0_{T1}(z) - 2w^0_{T2}(z) + w^0_{T3}(z)\right) + F\frac{\partial w^0_{T2}(z)}{\partial z}\frac{\partial \delta w^0_{T2}(z)}{\partial z}\right]dz, \tag{4.1.6}$$

$$\delta W_{ex3} = \int_0^l \left[\delta w^0_{T3}(z)K\left(w^0_{T2}(z) - w^0_{T3}(z)\right) + F\frac{\partial w^0_{T3}(z)}{\partial z}\frac{\partial \delta w^0_{T3}(z)}{\partial z}\right]dz, \tag{4.1.7}$$

By substituting the equations (4.1.4-4.1.7) into a general equation of virtual work principle without the action of inertial forces $\delta W_{Vi} + \delta W_{exi} = 0$, $i = 1,2,3$ and applying the Green's theorem, partial differential equations of beam point motion in the static region are obtained

$$-kGA\left(\frac{\partial^2 w_1}{\partial z^2} - \frac{\partial \psi_1}{\partial z}\right) + F\frac{\partial^2 w_1}{\partial z^2} + 2Kw_1 - Kw_2 = 0, \quad -EI_x\frac{\partial^2 \psi_1}{\partial z^2} - kGA\left(\frac{\partial w_1}{\partial z} - \psi_1\right) = 0, \tag{4.1.8}$$

$$-kGA\left(\frac{\partial^2 w_2}{\partial z^2}-\frac{\partial \psi_2}{\partial z}\right)+F\frac{\partial^2 w_2}{\partial z^2}-Kw_1+2Kw_2-Kw_3=0,\quad -EI_x\frac{\partial^2 \psi_2}{\partial z^2}-kGA\left(\frac{\partial w_2}{\partial z}-\psi_2\right)=0, \tag{4.1.9}$$

$$-kGA\left(\frac{\partial^2 w_3}{\partial z^2}-\frac{\partial \psi_3}{\partial z}\right)+F\frac{\partial^2 w_3}{\partial z^2}-Kw_2+Kw_3=0,\qquad EI_x\frac{\partial^2 \psi_3}{\partial z^2}-kGA\left(\frac{\partial w_3}{\partial z}-\psi_3\right)=0, \tag{4.1.10}$$

By eliminating ψ_i from the equations (4.1.8 - 4.1.10), we get the system of three partial differential equations of the fourth degree

$$EI\left(1-\frac{F}{kAG}\right)\frac{\partial^4 w_1}{\partial z^4}+\left(F-2\frac{KEI}{kAG}\right)\frac{\partial^2 w_1}{\partial z^2}+\frac{KEI}{kAG}\frac{\partial^2 w_2}{\partial z^2}+2Kw_1-Kw_2=0, \tag{4.1.11}$$

$$EI\left(1-\frac{F}{kAG}\right)\frac{\partial^4 w_2}{\partial z^4}+\frac{KEI}{kAG}\frac{\partial^2 w_1}{\partial z^2}+\left(F-\frac{KEI}{kAG}\right)\frac{\partial^2 w_2}{\partial z^2}+\frac{KEI}{kAG}\frac{\partial^2 w_3}{\partial z^2}-Kw_1+2Kw_2-Kw_3=0, \tag{4.1.12}$$

$$EI\left(1-\frac{F}{kAG}\right)\frac{\partial^4 w_3}{\partial z^4}+\frac{KEI}{kAG}\frac{\partial^2 w_2}{\partial z^2}+\left(F-\frac{KEI}{kAG}\right)\frac{\partial^2 w_3}{\partial z^2}-Kw_2+Kw_3=0. \tag{4.1.13}$$

As the beams are simply supported, we apply the boundary conditions for which the following applies

$$w_i(0)=\frac{d^2 w_i(0)}{dz^2}=\frac{d^2 w_i(l)}{dz^2}=w_i(l)=0. \tag{4.1.14}$$

We can assume the deflection of the beam as the order

$$w_i(z)=\sum_{n=1}^{\infty}A_{ni}Z_n(z),\qquad i=1,2. \tag{4.1.15}$$

where the function $Z_n(z)$ is given by

$$Z_n(z)=\sin(k_n z),\qquad k_n=n\pi/l,\qquad n=1,2,3,\ldots \tag{4.1.16}$$

By substituting the assumed solutions (4.1.15) into equations (4.1.11-4.1.13), we obtain a homogeneous system of algebraic equations that can be written in the matrix form

$$\begin{bmatrix} x+2RK & -KR & 0 \\ -KR & x+2RK & -KR \\ 0 & -KR & x+RK \end{bmatrix}\begin{Bmatrix} A_{n1} \\ A_{n2} \\ A_{n3} \end{Bmatrix}=\begin{Bmatrix} 0 \\ 0 \\ 0 \end{Bmatrix}, \tag{4.1.17}$$

where

$$R=1+\frac{EI}{GAk}k_n^2,\quad x=k_n^2(EIk_n^2-FR). \tag{4.1.18}$$

The existence of non-trivial solutions requires that the matrix determinant in the equation (4.1.17) equals zero, which yields a characteristic third degree equation expressed as

$$x^3+5RKx^2+6(RK)^2x+(RK)^3=0, \tag{4.1.19}$$

where

$$a_0=1,\quad a_1=5RK,\quad a_2=6(RK)^2,\quad a_3=(RK)^3.$$

The solutions of the third degree polynomial equation (4.1.19) are

$$x_1 = -\frac{5}{3}RK + 2\sqrt{-\frac{p}{3}}cos\left(\frac{\theta}{3}\right) = -0{,}198062RK,$$
$$x_2 = -\frac{5}{3}RK + 2\sqrt{-\frac{p}{3}}cos\left(\frac{\theta+2\pi}{3}\right) = -1{,}55496RK,$$
$$x_3 = -\frac{5}{3}RK + 2\sqrt{-\frac{p}{3}}cos\left(\frac{\theta+4\pi}{3}\right) = -3{,}24698RK, \qquad (4.1.20)$$

where

$$p = \frac{a_2}{a_o} - \frac{a_1^2}{3a_0^2}, \quad q = \frac{a_3}{a_o} - \frac{a_1 a_2}{3a_0^2} + \frac{2a_1^3}{27a_0^3}, \quad D = \frac{q^2}{4} + \frac{p^3}{27} < 0, \quad \theta = cos^{-1}\left[-\frac{q}{2}\left(-\frac{p}{3}\right)^{-\frac{3}{2}}\right].$$

If we substitute possible solutions (4.1.20) into the expression (4.1.18), we will obtain three values for force F, the lowest of which represents the critical buckling force and has the following form

$$F_b^{cr} = \frac{0.198062\,Kl^2}{\pi^2 n^2} + \frac{EI\pi^2 n^2}{l^2\left(1 + \frac{EI}{GAk}\frac{\pi^2 n^2}{l^2}\right)}. \qquad (4.1.21)$$

For $K = 0$ in the equation (4.1.21), we have

$$P_n = \frac{EI\pi^2 n^2}{l^2\left(1 + \frac{EI}{GAk}\frac{\pi^2 n^2}{l^2}\right)}, \qquad (4.1.22)$$

which represents the critical buckling force of the *n*-th mode for the Timoshenko beam [27]. For $= 1$, the equation (4.1.22) is reduced to

$$P = \frac{EI\pi^2}{l^2\left(1 + \frac{EI}{GAk}\frac{\pi^2}{l^2}\right)}. \qquad (4.1.23)$$

which is the lowest value of the force affecting the beam in the stability region. We will verify the solutions to the equation (4.1.19) using the trigonometric method [28]. Let us assume the solutions to the system of homogeneous algebraic equations (4.1.17) are non-trivial

$$A_{nk} = Nsink\varphi, \qquad N \neq 0, \qquad sink\varphi \neq 0, \qquad k = 1{,}2{,}3. \qquad (4.1.24)$$

By substituting the assumed solutions (4.1.24) into the equation system (4.1.17), we get

$$-KR \cdot Nsin\varphi + (x + 2RK) \cdot Nsin2\varphi - KR \cdot Nsin3\varphi = 0. \qquad (4.1.25)$$

By solving the equation (4.1.25) for variable *x,* we have

$$x = 2KR(cos\varphi - 1). \qquad (4.1.26)$$

By substituting the assumed solution (4.1.24) and x in the expression (4.1.26) into the first equation of the system (4.1.17), we get the following identity

$$(x + 2RK) \cdot A_{n1} - KR \cdot A_{n2} \equiv 0, \quad \Rightarrow \quad (2KRcos\varphi - 2KR + 2KR) \cdot Nsin\varphi - KRNsin2\varphi = 0, \qquad (4.1.27)$$

whereas from the third equation of the system (4.1.17), we get

$$-KR\cdot A_{n2}+(x+RK)\cdot A_{n3}=0 \quad \Rightarrow \quad -KR\cdot N sin2\varphi+(2KRcos\varphi-KR)\cdot N sin3\varphi=0. \tag{4.1.28}$$

Expansion and transformation of the equation (4.1.28) yields

$$sin4\varphi-sin3\varphi=0, \quad \Leftrightarrow \quad 2\,sin\left(\frac{4\varphi-3\varphi}{2}\right)cos\left(\frac{4\varphi+3\varphi}{2}\right)=0. \tag{4.1.29}$$

The solutions to the trigonometric equation (4.1.29) are

$$sin\left(\frac{\varphi}{2}\right)=0 \ \vee \ cos\left(\frac{7\varphi}{2}\right)=0 \ \Rightarrow \ \varphi=2n\pi \vee \frac{7\varphi}{2}=s\pi-\frac{\pi}{2} \ \Rightarrow \ \varphi_s=\frac{2s-1}{7}\pi, \ \ s=1,2,3,\ldots n. \tag{4.1.30}$$

The equation (4.1.17) may be rewritten in the following form for different values of φ_s

$$x_s=2KR\left(cos\varphi_s-1\right)=k_n^2(EIk_n^2-FR), \quad s=1,2,3,\ldots n. \tag{4.1.31}$$

Buckling forces in the equation (4.1.32) are determined as

$$F_s=2\frac{Kl^2}{\pi^2n^2}\left(1-cos\varphi_s\right)+\frac{EI\pi^2n^2}{l^2\left(1+\frac{EI}{GAk}\frac{\pi^2n^2}{l^2}\right)}, \quad s=1,2,3,\ldots n, \tag{4.1.32}$$

from where by substituting $\varphi_s=\frac{2s-1}{7}\pi$ for $s=1,2,3$ into the expression (4.1.33) for F_s respective buckling forces follow

$$F_1=2\frac{Kl^2}{\pi^2n^2}\left(1-cos\frac{\pi}{7}\right)+\frac{EI\pi^2n^2}{l^2\left(1+\frac{EI}{GAk}\frac{\pi^2n^2}{l^2}\right)}=0.1980622\frac{Kl^2}{\pi^2n^2}+\frac{EI\pi^2n^2}{l^2\left(1+\frac{EI}{GAk}\frac{\pi^2n^2}{l^2}\right)}\approx F_b^I,$$

$$F_2=2\frac{Kl^2}{\pi^2n^2}\left(1-cos\frac{3\pi}{7}\right)+\frac{EI\pi^2n^2}{l^2\left(1+\frac{EI}{GAk}\frac{\pi^2n^2}{l^2}\right)}=1.554958\frac{Kl^2}{\pi^2n^2}+\frac{EI\pi^2n^2}{l^2\left(1+\frac{EI}{GAk}\frac{\pi^2n^2}{l^2}\right)}\approx F_b^{II},$$

$$F_3=2\frac{Kl^2}{\pi^2n^2}\left(1-cos\frac{5\pi}{7}\right)=3.2469796\frac{Kl^2}{\pi^2n^2}+\frac{EI\pi^2n^2}{l^2\left(1+\frac{EI}{GAk}\frac{\pi^2n^2}{l^2}\right)}\approx F_b^{III}. \tag{4.1.33}$$

4.2 Critical Buckling Force of Two Elastically Connected Timoshenko Beams on an Elastic Foundation

Let us analyze the case of two elastically connected Timoshenko beams on the elastic foundation. Both beams are under the influence of equal axial compression forces, reference [14].

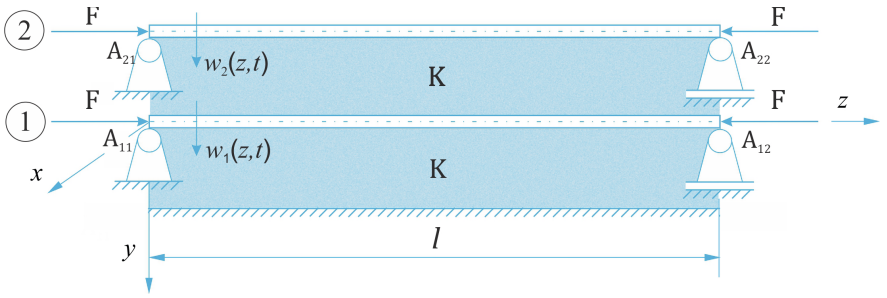

Fig. 4.2.1 Two-beam system on an elastic Winkler layer

The equation (4.1.17) in the matrix form is now reduced to the following

$$\begin{bmatrix} x+2RK & -KR \\ -KR & x+RK \end{bmatrix} \begin{Bmatrix} A_{n1} \\ A_{n2} \end{Bmatrix} = 0. \tag{4.2.1}$$

By expanding the determinant (4.2.1), we get the equation

$$x^2 + 3RKx + (RK)^2 = 0, \tag{4.2.2}$$

with following solutions

$$x_{1/2} = \frac{-3RK \pm RK\sqrt{5}}{2} \quad \Rightarrow \quad x_1 = \frac{-3RK + RK\sqrt{5}}{2} = -0.382RK,$$

$$x_2 = \frac{-3RK - RK\sqrt{5}}{2} = -2.618RK.$$

The lower value represents the critical buckling force for the n-th mode of system vibration and is given by

$$F_b^{cr} = \frac{0.382\,Kl^2}{\pi^2 n^2} + \frac{EI\pi^2 n^2}{l^2\left(1 + \frac{EI}{GAk}\frac{\pi^2 n^2}{l^2}\right)}. \tag{4.2.3}$$

4.3 Critical Buckling Force of Timoshenko Beams on an Elastic Surface

In case of a single beam on an elastic surface, the equation (4.1.17) in the matrix form is reduced to the following

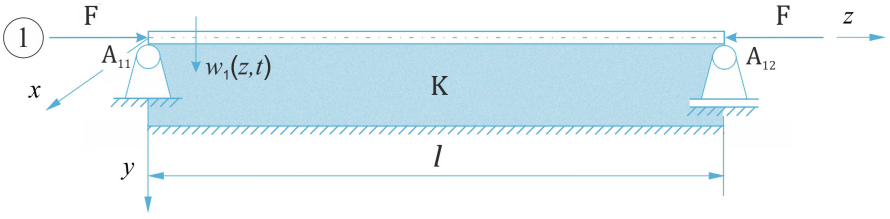

Fig. 4.3.1 The beam on an elastic Winkler-type foundation

$$(x + RK)A_{n1} = 0. \tag{4.3.1}$$

By solving the equation (4.3.1) for the *n*-th vibration mode, we obtain the expression for critical buckling load in the form

$$F_b^{kr} = \frac{Kl^2}{\pi^2 n^2} + \frac{EI\pi^2 n^2}{l^2\left(1 + \frac{EI}{GAk}\frac{\pi^2 n^2}{l^2}\right)}. \tag{4.3.2}$$

4.4 Numerical Analysis

The values of the physical parameters for the system used in the numerical experiment

$$E = 1 \times 10^{10}\ Nm^{-2},\ G = 0.417 \times 10^{10} Nm^{-2},\ k = 5/6,\ K_0 = 2 \times 10^5\ Nm^{-2},\\ l = 10\ m,\ A = 5 \times 10^{-2} m^2,\quad I = 4 \times 10^{-4} m^4, \rho = 2 \times 10^3\ kgm^{-3}. \tag{4.4.1}$$

After introducing the non-dimensional parameter as the ratio of cross-section thickness to beam length $\xi = h/l$, the area of the cross-section and the moment of inertia may be written as

$$A = h^2 = (\xi l)^2,\quad I = I_x = \frac{h^4}{12} = \frac{(\xi l)^4}{12}. \tag{4.4.2}$$

Figure 4.4.1 illustrates the change in the relative ratio of critical forces to critical force in the function of non-dimensional parameter ξ for a different number of beams and different stiffness. From Figure 4.4.1 we can conclude that the relative critical force ratio decreases with the increase of beam thickness, whereas with the increase of the beam number for the lowest stiffness of the Winkler layer, the critical force ratio decreases in beams of lesser thickness. From the critical force ratio, we conclude that the system is the most stable in case of a single beam on an elastic foundation and that the stability decreases with the increase of the beam number. The same tendency of the relative critical force ratio for different modes can be seen in Figure 4.4.2. The change in the region of the system's static stability in the function of the beam number and the Winkler layer stiffness with the change in beam thickness is shown in Figure 4.4.3.

The points marked in Figure 4.4.4 show the values of physical parameters for which the system has the same critical force value in different modes. Thus, the point A12 in Figure 4.4.4 represents the bifurcation point for a single-beam system, i.e. the value of the beam thickness to length ratio, for which the system has the same absolute value of critical force in the first and second mode. With the increase of beam thickness from A12, the system becomes more stable in the second mode. Point A13 presents the point in which for the value of beam thickness to length ratio the system has the same absolute value of critical force in the first and the third mode. The same holds for points B12, B13 that refer to the double-beam system and points C12, C13 referring to the three-beam system. With the increase of the beam number, it may be concluded that the system becomes more sensitive to the influence of elastic layer stiffness since lesser thickness of beams is required, for which the systems are characterized by the same critical force in different modes.

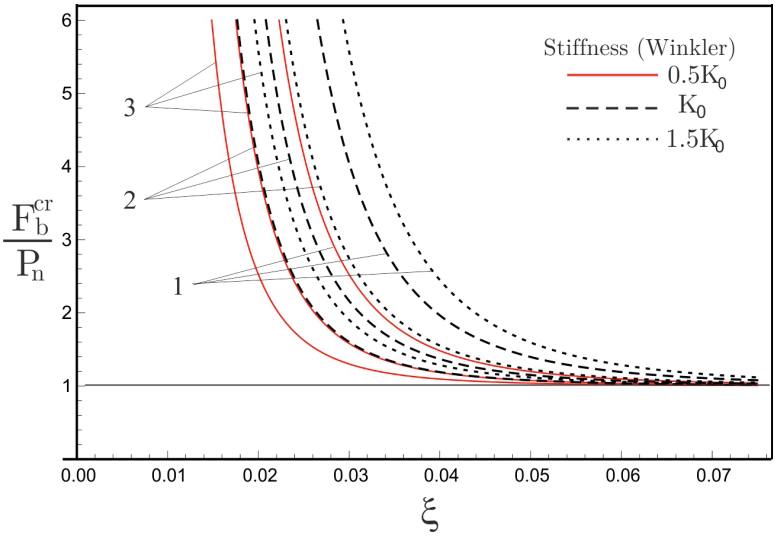

Fig. 4.4.1 The influence of beam thickness on critical force ratio F_b^{cr}/P_n (K =$0.5K_0, K_0, 1.5K_0$)

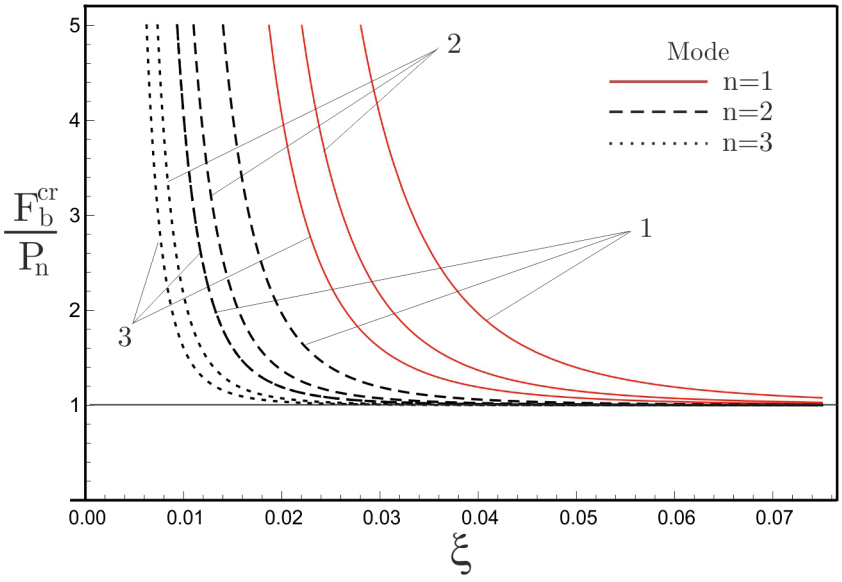

Fig. 4.4.2 The influence of thickness and the number of beams on critical force ratio F_b^{cr}/P_n (n=1,2,3)

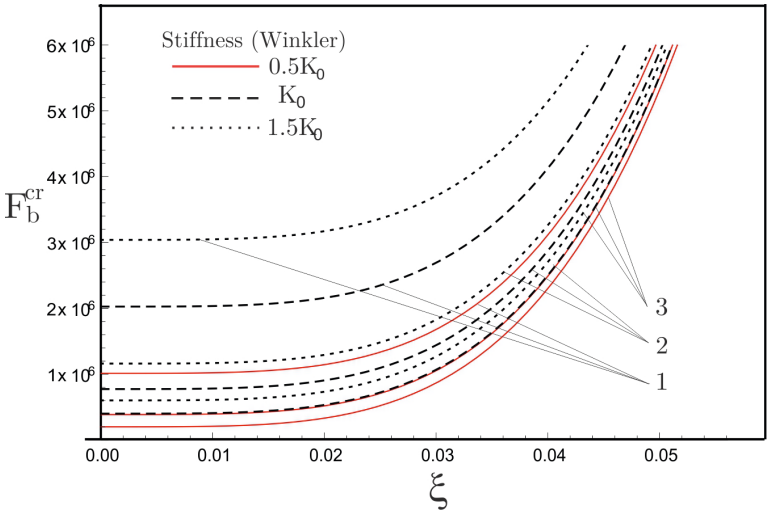

Fig. 4.4.3 The influence of thickness and the number of beams on critical force F_b^{cr} (K =$0.5K_0, K_0, 1.5K_0$)

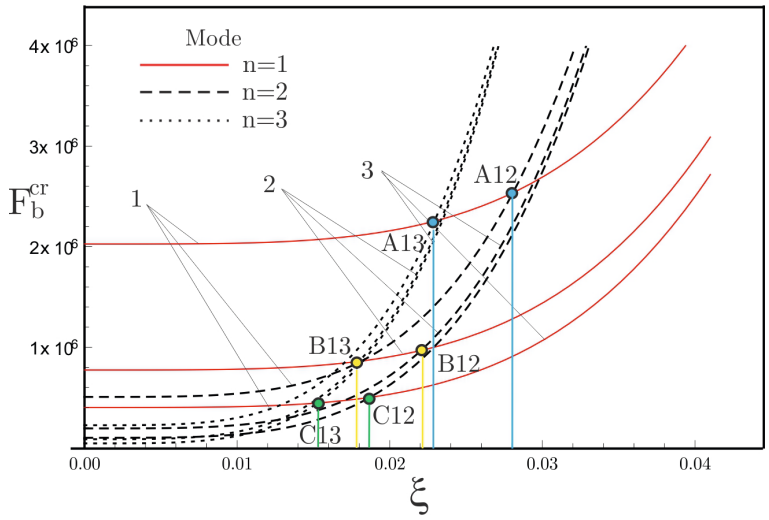

Fig. 4.4.4 The influence of thickness and the number of beams on critical force F_b^{cr} (n=1,2,3)

4.5 Stochastic Stability of Three Elastically Connected Beams on an Elastic Foundation

Physical problems of real engineering can lead to the further investigation of the transverse vibration instability of a complex system on elastic foundation

subjected to stochastic compressive axial loading [54]. It is assumed that the three beams of the system are under the stochastic excitation. The rotary inertia and shear deformation should be negligible in motion of the beams is governed by the partial differential equations $(4.5.1-4.5.3)$. This theory is based on the assumption that plane cross-sections of a beam remain plane during flexure and that the radius of curvature of a bent beam is larger than the beam's depth. It is valid only if the ratio of the depth to the length of the beam is small. We can obtain the general equations for transverse vibrations of elastically connected beams shown in Fig. 4.1.1

$$EI_1\frac{\partial^4 w_1}{\partial z^4}+\rho A_1\frac{\partial^2 w_1}{\partial t^2}+\varepsilon c_0\left(2\frac{\partial w_1}{\partial t}-\frac{\partial w_2}{\partial t}\right)+F_1(t)\frac{\partial^2 w_1}{\partial z^2}+\varepsilon K(2w_1-w_2)=0, \tag{4.5.1}$$

$$EI_2\frac{\partial^4 w_2}{\partial z^4}+\rho A_2\frac{\partial^2 w_2}{\partial t^2}+\varepsilon c_0\left(2\frac{\partial w_2}{\partial t}-\frac{\partial w_1}{\partial t}-\frac{\partial w_3}{\partial t}\right)+F_2(t)\frac{\partial^2 w_2}{\partial z^2}+\varepsilon K(2w_2-w_1-w_3)=0, \tag{4.5.2}$$

$$EI_3\frac{\partial^4 w_3}{\partial z^4}+\rho A_3\frac{\partial^2 w_3}{\partial t^2}+\varepsilon c_0\left(\frac{\partial w_3}{\partial t}-\frac{\partial w_2}{\partial t}\right)+F_3(t)\frac{\partial^2 w_3}{\partial z^2}+\varepsilon K(w_3-w_2)=0. \tag{4.5.3}$$

where w_1, w_2 and w_3 are transverse beam deflections which are positive if downward, I_1, I_2 and I_3 are the second moments of inertia of the beams, A_1, A_2 and A_3 are the cross-sectional area of the beams, and E and ρ, Young's modulus and the mass density. Thus c_0 represent the damping coefficients per unit axial length, respectively, and K is the stiffness modulus of a Winkler elastic layer. $F_1(t)$, $F_2(t)$ and $F_3(t)$ are stochastically varying static loads. Simply supported ends for the same length l of the beams are satisfied with boundary conditions $w_i(0,t)=w_i(l,t)=\partial^2 w_i(0,t)/\partial z^2=\partial^2 w_i(l,t)/\partial z^2=0,\ i=1,2,3.$ Using Galerkin method only for fundamental modes are considered, boundary conditions are satisfied by taking and substituting $w_i(z,t)=T_i(t)\sin(\pi z/l),\ (i=1,2,3.)$ into equations of motion. Unknown time functions can be expressed as

$$\ddot{T}_1+\frac{c_0\varepsilon}{\rho A_1}(2\dot{T}_1-\dot{T}_2)+\left(\frac{EI_1}{\rho A_1}\frac{\pi^4}{l^4}+\frac{2K\varepsilon}{\rho A_1}-\frac{\pi^2}{\rho A_1 l^2}F_1(t)\right)T_1-\frac{2K\varepsilon}{\rho A_1}T_2=0, \tag{4.5.4}$$

$$\ddot{T}_2+\frac{c_0\varepsilon}{\rho A_2}(2\dot{T}_2-\dot{T}_3-\dot{T}_1)+\left(\frac{EI_2}{\rho A_2}\frac{\pi^4}{l^4}+\frac{2K\varepsilon}{\rho A_2}-\frac{\pi^2}{\rho A_2 l^2}F_2(t)\right)T_2-\frac{K\varepsilon}{\rho A_2}T_3-\frac{K\varepsilon}{\rho A_2}T_1=0, \tag{4.5.5}$$

$$\ddot{T}_3+\frac{c_0\varepsilon}{\rho A_3}\dot{T}_3-\frac{c_0\varepsilon}{\rho A_3}\dot{T}_2+\left(\frac{EI_3}{\rho A_3}\frac{\pi^4}{l^4}+\frac{K\varepsilon}{\rho A_3}-\frac{\pi^2}{\rho A_3 l^2}F_3(t)\right)T_3-\frac{K\varepsilon}{\rho A_3}T_2=0. \tag{4.5.6}$$

Using the further substitutions

$$\omega_1^2=\frac{EI_1}{\rho A_1}\frac{\pi^4}{l^4},\ \omega_2^2=\frac{EI_2}{\rho A_2}\frac{\pi^4}{l^4},\ \omega_3^2=\frac{EI_3}{\rho A_3}\frac{\pi^4}{l^4},\ \beta_1=\frac{c_0}{\rho A_1}\ ,\ \beta_2=\frac{c_0}{\rho A_2},\ \beta_3=\frac{c_0}{\rho A_3}\ ,$$

$$K_1=\frac{\pi^2}{\rho A_1 l^2},\ K_2=\frac{\pi^2}{\rho A_2 l^2},K_3=\frac{\pi^2}{\rho A_3 l^2},H_1=\frac{K}{\rho A_1},\ H_2=\frac{K}{\rho A_2},\ H_3=\frac{K}{\rho A_3},$$

and assume that the compressive axial forces are stochastic white-noise processes with small intensity $F_1(t) = F_2(t) = F_3(t) = \sqrt{\varepsilon}\,\gamma(t)$ we have oscillatory system in form

$$\frac{\mathrm{d}^2T_1}{\mathrm{d}t^2} + \omega_1^2 T_1 + \varepsilon\beta_1\left(2\frac{\mathrm{d}T_1}{\mathrm{d}t} - \frac{\mathrm{d}T_2}{\mathrm{d}t}\right) + \varepsilon H_1(2T_1 - T_2) - \sqrt{\varepsilon}K_1\gamma(t)T_1 = 0,$$

$$\frac{\mathrm{d}^2T_2}{\mathrm{d}t^2} + \omega_2^2 T_2 + \varepsilon\beta_2\left(2\frac{\mathrm{d}T_2}{\mathrm{d}t} - \frac{\mathrm{d}T_3}{\mathrm{d}t} - \frac{\mathrm{d}T_1}{\mathrm{d}t}\right) + \varepsilon H_2(2T_2 - T_3 - T_1) - \sqrt{\varepsilon}K_2\gamma(t)T_2 = 0,$$

$$\frac{\mathrm{d}^2T_3}{\mathrm{d}t^2} + \omega_3^2 T_3 + \varepsilon\beta_3\left(\frac{\mathrm{d}T_3}{\mathrm{d}t} - \frac{\mathrm{d}T_2}{\mathrm{d}t}\right) + \varepsilon H_3(T_3 - T_2) - \sqrt{\varepsilon}K_3\gamma(t)T_3 = 0. \qquad (4.5.7)$$

System consist of unknown generalized coordinates in functions of time T_i, natural frequencies ω_i and viscous damping coefficients $\varepsilon\beta_i, (i = 1,2,3)$. The stochastic term $\sqrt{\varepsilon}\,\gamma(t)$presents a white-noise process with small intensity. Dynamic stability of a oscillatory system can be known in case to determine the maximal Lyapunov exponent and the pth moment Lyapunov exponent which is described

$$\lambda_T = \lim_{t\to\infty}\frac{1}{t}\log\|\boldsymbol{T}(t;T_0)\|,$$

Where $\boldsymbol{T}(t;T_0)$is the solution process of a linear dynamical system. The almost-sure stability depends upon the sign of the maximal Lyapunov exponent which is an exponential growth rate of the solution of the randomly perturbed dynamical system. A negative sign of the maximal Lyapunov exponent implies the almost-sure stability whereas a non-negative value indicates instability. The exponential growth rate $E\left[\left\|\boldsymbol{T}(t;T_0,\dot{T}_0)\right\|^p\right]$ is provided by the moment Lyapunov exponent defined as

$$\Lambda_T(p) = \lim_{t\to\infty}\frac{1}{t}\log E[\|\boldsymbol{T}(t;T_0)\|^p],$$

Where $E[\,]$ denotes the expectation. If $\Lambda_T(p) < 0$, then by definition $E\left[\left\|\boldsymbol{T}(t;T_0,\dot{T}_0)\right\|^p\right] \to 0$ as $t \to 0$ and this is referred to as pth moment stability. Although the moment Lyapunov exponents are important in the study of the dynamic stability of the stochastic systems, the actual evaluations of the moment Lyapunov exponents are very difficult and the almost-sure and moment stability of the equilibrium state $T = \dot{T} = 0$ of Eq. (32). Using the transformation $T_1 = x_1$, $\dot{T}_1 = \omega_1 x_2$, $T_2 = x_3$, $\dot{T}_2 = \omega_2 x_4$, $T_3 = x_5$, $\dot{T}_3 = \omega_3 x_6$ the equation (1) can be represented in the first-order form by Stratonovich differential equations

$$d\begin{Bmatrix} x_1 \\ x_2 \\ x_3 \\ x_4 \\ x_5 \\ x_6 \end{Bmatrix} = \begin{Bmatrix} x_1 \\ x_2 \\ x_3 \\ x_4 \\ x_5 \\ x_6 \end{Bmatrix} dt$$

$$d\begin{Bmatrix} x_1 \\ x_2 \\ x_3 \\ x_4 \\ x_5 \\ x_6 \end{Bmatrix} = \begin{bmatrix} 0 & \omega_1 & 0 & 0 & 0 & 0 \\ -2h_1\varepsilon - \omega_1 & -2\varepsilon\beta_1 & \varepsilon h_1 & \varepsilon\beta_1\omega_2/\omega_1 & 0 & 0 \\ 0 & 0 & 0 & \omega_2 & 0 & 0 \\ h_2\varepsilon & \varepsilon\beta_2\omega_1/\omega_2 & -2h_2\varepsilon - \omega_2 & -2\varepsilon\beta_2 & h_2\varepsilon & \varepsilon\beta_2\omega_3/\omega_2 \\ 0 & 0 & 0 & 0 & 0 & \omega_3 \\ 0 & 0 & \varepsilon h_3 & \varepsilon\beta_3\omega_2/\omega_3 & -\varepsilon h_3 - \omega_3 & -\varepsilon\beta_3 \end{bmatrix} \begin{Bmatrix} x_1 \\ x_2 \\ x_3 \\ x_4 \\ x_5 \\ x_6 \end{Bmatrix} dt$$

$$+\sqrt{\varepsilon}\begin{bmatrix} 0 & 0 & 0 & 0 & 0 & 0 \\ k_1 & 0 & 0 & 0 & 0 & 0 \\ 0 & 0 & 0 & 0 & 0 & 0 \\ 0 & 0 & k_2 & 0 & 0 & 0 \\ 0 & 0 & 0 & 0 & 0 & 0 \\ 0 & 0 & 0 & 0 & k_3 & 0 \end{bmatrix} \begin{Bmatrix} x_1 \\ x_2 \\ x_3 \\ x_4 \\ x_5 \\ x_6 \end{Bmatrix} \circ d\gamma(t), \tag{4.5.8}$$

where $h_1 = H_1/\omega_1$, $h_2 = H_2/\omega_2$, $h_3 = H_3/\omega_3$, $k_1 = K_1/\omega_1$, $k_2 = K_2/\omega_2$, $k_3 = K_3/\omega_3$. $\gamma(t)$ is the white-noise process with zero mean and autocorrelation function

$$R_{\gamma\gamma}(t_1, t_2) = E[\gamma(t_1)\gamma(t_1)] = \sigma^2\delta(t_2 - t_1), \tag{4.5.9}$$

where σ is the intensity of the random process $\gamma(t)$, $\delta()$ is the Dirac delta function and $E[\,]$ denotes expectation. Using corresponding transformation

$$x_1 = a\cos\varphi_1\cos\varphi_2\cos\theta_1, x_2 = -a\cos\varphi_1\cos\varphi_2\sin\theta_1\ , x_3 = a\cos\varphi_1\sin\varphi_2\cos\theta_2,$$

$$x_4 = -a\cos\varphi_1\sin\varphi_2\sin\theta_2,\ x_5 = a\sin\varphi_1\cos\theta_3,\ x_6 = -a\sin\varphi_1\sin\theta_3,$$

$$P = a^p = (x_1^2 + x_2^2 + x_3^2 + x_4^2 + x_5^2 + x_6^2)^{\frac{p}{2}},$$

$$-\infty < p < \infty, \qquad 0 \le \theta_i \le 2\pi, \qquad 0 \le \varphi_j \le \frac{\pi}{2}, \qquad i = 1,2,3, \qquad j = 1,2.$$

Itô's rule get the set of equations for the pth power of the norm of the response and phase variables. Trigonometric transformation represents a as anorm of the response, where θ_1, θ_2 and θ_3 are the angles of the three oscillators and φ_1 and φ_2 describe the coupling or exchange of energy between the oscillators.

$$d\theta_1 = m_1(\theta_1, \theta_2, \theta_3, \varphi_1, \varphi_2)dt + \sigma_{11}(\theta_1, \theta_2, \theta_3, \varphi_1, \varphi_2)dW(t),$$
$$d\theta_2 = m_2(\theta_1, \theta_2, \theta_3, \varphi_1, \varphi_2)dt + \sigma_{21}(\theta_1, \theta_2, \theta_3, \varphi_1, \varphi_2)dW(t),$$
$$d\theta_3 = m_3(\theta_1, \theta_2, \theta_3, \varphi_1, \varphi_2)dt + \sigma_{31}(\theta_1, \theta_2, \theta_3, \varphi_1, \varphi_2)dW(t),$$
$$d\varphi_1 = m_4(\theta_1, \theta_2, \theta_3, \varphi_1, \varphi_2)dt + \sigma_{41}(\theta_1, \theta_2, \theta_3, \varphi_1, \varphi_2)dW(t),$$
$$d\varphi_2 = m_5(\theta_1, \theta_2, \theta_3, \varphi_1, \varphi_2)dt + \sigma_{51}(\theta_1, \theta_2, \theta_3, \varphi_1, \varphi_2)dW(t),$$

$$dP = Pm_6(\theta_1, \theta_2, \theta_3, \varphi_1, \varphi_2)dt + P\sigma_{61}(\theta_1, \theta_2, \theta_3, \varphi_1, \varphi_2)dW(t). \tag{4.5.10}$$

where $W(t)$ is the standard Weiner process and

$$m_1(\theta_1, \theta_2, \theta_3, \varphi_1, \varphi_2) = \omega_1 - \varepsilon\beta_1\left(\sin 2\theta_1 - \frac{\omega_2}{\omega_1}\cos\theta_1\sin\theta_2\tan\varphi_2\right)$$
$$+\varepsilon h_1(1 + \cos 2\theta_1 - \cos\theta_1\cos\theta_2\tan\varphi_2)$$
$$-\varepsilon\frac{k_1^2\sigma^2}{8}(\cos 3\theta_1\sin\theta_1 + 2\sin 2\theta_1 + \cos\theta_1\sin 3\theta_1), \tag{4.5.11}$$

$$\sigma_{11}(\theta_1,\theta_2,\theta_3,\varphi_1,\varphi_2) = -\sqrt{\varepsilon}k_1\sigma\cos^2\theta_1, \tag{4.5.12}$$

$$m_2(\theta_1,\theta_2,\theta_3,\varphi_1,\varphi_2) = \omega_2 - \varepsilon\beta_2\left(\sin 2\theta_2 - \frac{\omega_1}{\omega_2}\cos\theta_2\cot\varphi_2\sin\theta_1 - \frac{\omega_3}{\omega_2}\cos\theta_2\sin\theta_3\frac{\tan\varphi_1}{\sin\varphi_2}\right)$$
$$+\varepsilon h_2\left(1+\cos 2\theta_2 - \cos\theta_1\cos\theta_2\cot\varphi_2 - \frac{\tan\varphi_1}{\sin\varphi_2}\cos\theta_2\sin\theta_3\right)$$
$$-\varepsilon\frac{k_2^2\sigma^2}{8}(\cos 3\theta_2\sin\theta_2 + 2\sin 2\theta_2 + \cos\theta_2\sin 3\theta_2), \tag{4.5.13}$$

$$\sigma_{21}(\theta_1,\theta_2,\theta_3,\varphi_1,\varphi_2) = -\sqrt{\varepsilon}k_2\sigma\cos^2\theta_2, \tag{4.5.14}$$

$$m_3(\theta_1,\theta_2,\theta_3,\varphi_1,\varphi_2) = \frac{\omega_3}{16}\left(13+\cos 2\theta_3 + \frac{5+4\cos 2\theta_3 - \cos 4\theta_3}{2(1+\cos 2\theta_3)}\right)$$
$$-\frac{\varepsilon\beta_3}{8}\left[3\sin 2\theta_3 + \tan\theta_3(1+\cos 2\theta_3) - 4\frac{\omega_2}{\omega_3}\sin\varphi_2\cot\varphi_1\sin\theta_2\left(\cos\theta_3 + \frac{1}{\cos\theta_3} - \tan\theta_3\right)\right]$$
$$+\frac{\varepsilon h_3}{2}\left(1+\cos 2\theta_3 - \cos\theta_2\cos\theta_3\cot\varphi_1\sin\varphi_2 - \frac{\cos\theta_2}{\cos\theta_3}\cot\varphi_1\sin\varphi_2\right.$$
$$\left.+\cos\theta_2\cot\varphi_1\sin\theta_3\sin\varphi_2\tan\theta_3\right)$$
$$-\varepsilon\frac{k_3^2\sigma^2}{8}(\cos 3\theta_3\sin\theta_3 + 2\sin 2\theta_3 + \cos\theta_3\sin 3\theta_3), \tag{4.5.15}$$

$$\sigma_{31}(\theta_1,\theta_2,\theta_3,\varphi_1,\varphi_2) = -\sqrt{\varepsilon}k_3\sigma\cos^2\theta_3, \tag{4.5.16}$$

$$m_4(\theta_1,\theta_2,\theta_3,\varphi_1,\varphi_2) = \varepsilon\left\langle\frac{h_1}{4}[\cos\theta_2\sin\theta_1\sin 2\varphi_1\sin 2\varphi_2 - \sin 2\theta_1(\cos 2\varphi_2\sin 2\varphi_1 + \sin 2\varphi_1)]\right.$$
$$+\frac{\beta_1}{4}\left\{\sin 2\varphi_1\left[(1-\cos 2\theta_1)(1+\cos 2\varphi_2) - \frac{\omega_2}{\omega_1}\sin\theta_1\sin\theta_1\sin 2\varphi_2\right]\right\}$$
$$+\frac{h_2}{4}[\sin 2\varphi_1(\cos 2\varphi_2\sin 2\theta_2 - \sin 2\theta_2 + \sin 2\varphi_2\cos\theta_1\sin\theta_2) + 2\sin\theta_2\cos\theta_3\sin\varphi_2(1-\cos 2\varphi_1)]$$
$$+\frac{\beta_2}{4}\left\{\sin 2\varphi_1\left[(1-\cos 2\theta_2)(1-\cos 2\varphi_2) - \frac{2\omega_3}{\omega_2}(1-\cos 2\varphi_1)\sin\theta_2\sin\theta_3\sin\varphi_2\right.\right.$$
$$\left.\left.-\frac{\omega_1}{\omega_2}\sin\theta_1\sin\theta_2\sin 2\varphi_1\sin 2\varphi_2\right]\right\} + \frac{h_3}{4}[\sin 2\theta_3\sin 2\varphi_1 - 2\cos\theta_2\sin\theta_3\sin\varphi_2(1+\cos 2\varphi_1)]$$
$$+\frac{\beta_3}{4}\left[\sin 2\varphi_1(\cos 2\theta_3 - 1) + \frac{2\omega_2}{\omega_3}\sin\theta_2\sin\theta_3\sin 2\varphi_2(1+\cos 2\varphi_1)\right]$$
$$+\frac{\sigma^2}{64}\{2k_1^2\cos^2\varphi_2[\sin 4\varphi_1\sin^2 2\theta_1\cos^2\varphi_2 - 8\cos^2\theta_1\sin 2\varphi_1(\cos^2\theta_1 - \cos 2\varphi_2\sin^2\theta_1)]$$
$$+2k_2^2\sin^2\varphi_2[\sin 4\varphi_1\sin^2 2\theta_2\sin^2\varphi_2 - 8\cos^2\theta_2\sin 2\varphi_1(\cos^2\theta_2 + \cos 2\varphi_2\sin^2\theta_2)]$$
$$+16k_3^2\sin 2\varphi_1\cos^2\theta_3(\cos 2\theta_3 + \cos 2\varphi_1\sin^2\theta_3) + k_1k_2\sin^2 2\varphi_2\sin 2\theta_1\sin 2\theta_2(4\sin 2\varphi_1 + \sin 4\varphi_1)$$
$$\left.-4k_1k_3\cos^2\varphi_2\sin 4\varphi_1\sin 2\theta_1\sin 2\theta_3 - 4k_2k_3\sin^2\varphi_2\sin 4\varphi_1\sin 2\theta_2\sin 2\theta_3\}\right\rangle, \tag{4.5.17}$$

$$\sigma_{41}(\theta_1,\theta_2,\theta_3,\varphi_1,\varphi_2) = \frac{\sqrt{\varepsilon}\sigma}{8}\sin 2\varphi_1\,[k_1\sin 2\theta_1(1+\cos 2\varphi_2)$$
$$+k_2\sin 2\theta_2(1-\cos 2\varphi_2) - 2k_3\sin 2\theta_3\sin 2\varphi_1], \tag{4.5.18}$$

$$m_5(\theta_1,\theta_2,\theta_3,\varphi_1,\varphi_2) =$$
$$= \varepsilon\langle h_1[\sin\theta_1\sin\varphi_2(\cos\theta_2\sin\varphi_2 - 2\cos\theta_1\cos\varphi_2)] + \beta_1[\sin\theta_1\sin\varphi_2(2\cos\varphi_2\sin\theta_1 - \frac{\omega_2}{\omega_1}\sin\theta_2\sin\varphi_2)]$$
$$-h_2\Big[\sin\theta_2\cos\varphi_2(\cos\theta_1\cos\varphi_2 - 2\cos\theta_2\sin\varphi_2 + \cos\theta_3\tan\varphi_1)] + \beta_2\Big[\sin\theta_2\Big(\frac{\omega_1}{\omega_2}\cos^2\varphi_2\sin\theta_1$$
$$-\sin\theta_2\sin 2\varphi_2 + \frac{\omega_3}{\omega_2}\cos\varphi_2\sin\theta_3\tan\varphi_1)] - \frac{\sigma^2}{16}\{[4k_1^2\cos^2\theta_1\sin 2\varphi_2(\cos 2\theta_1 - \cos 2\varphi_2\sin^2\theta_1)]$$
$$-[4k_2^2\cos^2\theta_2\times\sin 2\varphi_2(\cos 2\theta_2 + \cos 2\varphi_2\sin^2\theta_2)] + [k_1k_2\sin 2\theta_1\sin 2\theta_2\sin 4\varphi_2]\}\rangle, \quad (4.5.19)$$

$$\sigma_{51}(\theta_1,\theta_2,\theta_3,\varphi_1,\varphi_2) = \frac{\sqrt{\varepsilon}\sigma}{4}\sin 2\varphi_2\,[k_1\sin 2\theta_1 - k_2\sin 2\theta_2], \quad (4.5.20)$$

$$m_6(\theta_1,\theta_2,\theta_3,\varphi_1,\varphi_2) =$$
$$= \varepsilon p\{h_1[\cos^2\varphi_1\cos\varphi_2\sin\theta_1(2\cos\theta_1\cos\varphi_2 - \cos\theta_2\sin\varphi_2)] + \beta_1[\cos^2\varphi_1\cos\varphi_2\sin\theta_1$$
$$\times\Big(\frac{\omega_2}{\omega_1}\sin\theta_2\sin\varphi_2 - 2\cos\varphi_2\sin\theta_1)]$$
$$+\frac{h_2}{2}[\sin\varphi_2\sin\theta_2(-\cos\theta_3\sin 2\varphi_1 - 2\cos^2\varphi_1(\cos\theta_1\cos\varphi_2 - 2\cos\theta_2$$
$$\times\sin\varphi_2))] + \frac{\beta_2}{2}\Big[\sin\varphi_2\sin\theta_2\Big(\frac{\omega_3}{\omega_2}\sin\theta_2\sin 2\varphi_1 + 2\cos^2\varphi_1\Big(\frac{\omega_1}{\omega_2}\cos\varphi_2\sin\theta_1 - 2\sin\theta_2\sin\varphi_2\Big)\Big)\Big]$$
$$+\frac{\sigma^2k_1^2}{128}\cos^2\varphi_1(2\cos^2\theta_1\cos 2\varphi_2(10+3p+4(2+p)-(p-2)\cos 2\theta_1(3+4\cos 2\varphi_2)) + (p-2)\sin^2 2\theta_1$$
$$(8\cos 2\varphi_1\cos^4\varphi_2 + \cos 4\varphi_2)$$
$$+\frac{\sigma^2k_2^2}{128}\cos^2\varphi_1(2\cos^2\theta_2\cos 2\varphi_2(10+3p-4(2+p)+(p-2)\cos 2\theta_2)$$
$$\times(4\cos 2\varphi_2 - 3)) + (\mathrm{p}-2)\sin^2 2\theta_2(\cos 4\varphi_2 + 8\cos 4\varphi_1\sin^4\varphi_2))$$
$$+\frac{\sigma^2k_3^2}{64}(2\cos^2\theta_3(4\cos 2\varphi_1 - 3)\cos 2\theta_3$$
$$\times(p-2) + 3p + 2 - 4p\cos 2\varphi_1) + (p-2)\cos 4\varphi_1\sin^2 2\theta_3 + \frac{\sigma^2k_1k_2}{16}(p-2)$$
$$\sin 2\theta_1\sin 2\theta_2\cos^4\varphi_1\sin^2 2\varphi_2 +$$
$$+\frac{\sigma^2k_1k_3}{16}(p-2)\sin 2\theta_1\sin 2\theta_3\cos^2\varphi_2\sin^2 2\varphi_1 + \frac{\sigma^2k_1k_3}{16}(p-2)\sin 2\theta_2\sin 2\theta_3\sin^2\varphi_2\sin^2 2\varphi_1\},$$
(4.5.21)

$$\sigma_{61}(\theta_1,\theta_2,\theta_3,\varphi_1,\varphi_2) =$$
$$= \frac{-p\sqrt{\varepsilon}\sigma}{2}(k_1\sin 2\theta_1\cos^2\varphi_1\cos^2\varphi_2 + k_2\sin 2\theta_2\cos^2\varphi_1\sin^2\varphi_2 + k_3\sin 2\theta_3\sin^2\varphi_1). \quad (4.5.22)$$

Applying a linear stochastic transformation

$$S = T(\theta_1,\theta_2,\theta_3,\varphi_1,\varphi_2)P, \qquad P = \frac{S}{T(\theta_1,\theta_2,\theta_3,\varphi_1,\varphi_2)}, \quad (4.5.23)$$

introducing the new norm process S by means of the scalar function $T(\theta_1,\theta_2,\theta_3,\varphi_1,\varphi_2)$ which is defined on the stationary phase process φ_j, the Itô equation for the new pth norm process S can be obtained from Itô's Lemma

$$dS = P\left[\frac{1}{2}\left(\sigma_{11}^2\frac{\partial^2 T}{\partial\theta_1^2}+\sigma_{21}^2\frac{\partial^2 T}{\partial\theta_2^2}+\sigma_{31}^2\frac{\partial^2 T}{\partial\theta_3^2}+\sigma_{41}^2\frac{\partial^2 T}{\partial\varphi_1^2}+\sigma_{51}^2\frac{\partial^2 T}{\partial\varphi_2^2}\right)+\sigma_{11}\sigma_{21}\frac{\partial^2 T}{\partial\theta_1\partial\theta_2}+\sigma_{11}\sigma_{31}\frac{\partial^2 T}{\partial\theta_1\partial\theta_3}\right.$$
$$+\sigma_{11}\sigma_{41}\frac{\partial^2 T}{\partial\theta_1\partial\varphi_1}++\sigma_{31}\sigma_{51}\frac{\partial^2 T}{\partial\theta_3\partial\varphi_2}+\sigma_{41}\sigma_{51}\frac{\partial^2 T}{\partial\varphi_1\partial\varphi_2}+m_1\frac{\partial T}{\partial\theta_1}+m_2\frac{\partial T}{\partial\theta_2}+$$
$$m_3\frac{\partial T}{\partial\theta_3}+m_4\frac{\partial T}{\partial\varphi_1}+m_5\frac{\partial T}{\partial\varphi_2}+m_6T+\sigma_{11}\sigma_{61}\frac{\partial T}{\partial\theta_1}++\sigma_{21}\sigma_{61}\frac{\partial T}{\partial\theta_2}+\sigma_{31}\sigma_{61}\frac{\partial T}{\partial\theta_3}$$
$$\left.+\sigma_{41}\sigma_{61}\frac{\partial T}{\partial\varphi_1}+\sigma_{51}\sigma_{61}\frac{\partial T}{\partial\varphi_2}\right]dT+P\left(\sigma_{11}\frac{\partial T}{\partial\theta_1}+\sigma_{21}\frac{\partial T}{\partial\theta_2}+\sigma_{31}\frac{\partial T}{\partial\theta_3}+\sigma_{41}\frac{\partial T}{\partial\varphi_1}+\sigma_{51}\frac{\partial T}{\partial\varphi_2}\sigma_{61}T\right)dW(t). \tag{4.5.24}$$

In the case that transformation function $T(\varphi_j)$ is bounded and non-singular, both processes P and S possess the same stability behavior. Therefore, transformation function $T(\varphi_j)$ is chosen so that the drift term, of the Itô differential Eq. does not depend on the phase process φ_j, so that

$$dS = \Lambda(p)Sdt+\frac{S}{T}\left(\sigma_{11}\frac{\partial T}{\partial\theta_1}+\sigma_{21}\frac{\partial T}{\partial\theta_2}+\sigma_{31}\frac{\partial T}{\partial\theta_3}+\sigma_{41}\frac{\partial T}{\partial\varphi_1}+\sigma_{51}\frac{\partial T}{\partial\varphi_2}+\sigma_{61}T\right)dW(t). \tag{4.5.25}$$

Transformation function $T(\theta_1,\theta_2,\theta_3,\varphi_1,\varphi_2)$ is given by the following equation

$$[L_0+\varepsilon L_1]T(\theta_1,\theta_2,\theta_3,\varphi_1,\varphi_2)=\Lambda(p)T(\theta_1,\theta_2,\theta_3,\varphi_1,\varphi_2). \tag{4.5.26}$$

Where L_0 and L_1 are the differential operators in the forms

$$L_0=\omega_1\frac{\partial}{\partial\theta_1}+\omega_2\frac{\partial}{\partial\theta_2}+\omega_3\frac{\partial}{\partial\theta_3},$$
$$L_1=a_1\frac{\partial^2}{\partial\theta_1^2}+a_2\frac{\partial^2}{\partial\theta_2^2}+a_3\frac{\partial^2}{\partial\theta_3^2}+a_4\frac{\partial^2}{\partial\varphi_1^2}+a_5\frac{\partial^2}{\partial\varphi_2^2}+a_6\frac{\partial^2}{\partial\theta_1\partial\theta_2}+a_7\frac{\partial^2}{\partial\theta_1\partial\theta_3}+a_8\frac{\partial^2}{\partial\theta_1\partial\varphi_1}+a_9\frac{\partial^2}{\partial\theta_1\partial\varphi_2}$$
$$+a_{10}\frac{\partial^2}{\partial\theta_2\partial\theta_3}+a_{11}\frac{\partial^2}{\partial\theta_2\partial\varphi_1}+a_{12}\frac{\partial^2}{\partial\theta_2\partial\varphi_2}+a_{13}\frac{\partial^2}{\partial\theta_3\partial\varphi_1}+a_{14}\frac{\partial^2}{\partial\theta_3\partial\varphi_2}+a_{15}\frac{\partial^2}{\partial\varphi_1\partial\varphi_2}+b_1\frac{\partial}{\partial\theta_1}$$
$$+b_2\frac{\partial}{\partial\theta_2}+b_3\frac{\partial}{\partial\theta_3}+b_4\frac{\partial}{\partial\varphi_1}+b_5\frac{\partial}{\partial\varphi_2}+c. \tag{4.5.27}$$

4.6 Moment Lyapunov Exponents

Applying the method of regular perturbation, both the moment Lyapunov exponent $\Lambda(p)$ and the eigenfunction $T(\theta_1,\theta_2,\theta_3,\varphi_1,\varphi_2)$ are expanded in power series of ε to obtain a weak noise expansion of the Lyapunov exponent of a system with stochastic excitation described by six-dimensional components as

$$\Lambda(p)=\Lambda_0(p)+\varepsilon\Lambda_1(p)+\varepsilon^2\Lambda_2(p)+\cdots+\varepsilon^n\Lambda_n(p)+\cdots,$$
$$T(\theta_1,\theta_2,\theta_3,\varphi_1,\varphi_2)=T_0(\theta_1,\theta_2,\theta_3,\varphi_1,\varphi_2)+\varepsilon T_1(\theta_1,\theta_2,\theta_3,\varphi_1,\varphi_2)+\varepsilon^2T_2(\theta_1,\theta_2,\theta_3,\varphi_1,\varphi_2)+\cdots$$
$$+\varepsilon^2T_2(\theta_1,\theta_2,\theta_3,\varphi_1,\varphi_2)+\cdots+\varepsilon^nT_n(\theta_1,\theta_2,\theta_3,\varphi_1,\varphi_2)+\cdots. \tag{4.6.1}$$

Equating terms of the equal powers of ε the following equations may be written as

$$\begin{aligned}
\varepsilon^0:\ & L_0T_0(\theta_1,\theta_2,\theta_3,\varphi_1,\varphi_2) = \Lambda_0(p)T_0(\theta_1,\theta_2,\theta_3,\varphi_1,\varphi_2),\\
\varepsilon^1:\ & L_0T_1(\theta_1,\theta_2,\theta_3,\varphi_1,\varphi_2) + L_1T_0(\theta_1,\theta_2,\theta_3,\varphi_1,\varphi_2)\\
&= \Lambda_0(p)T_1(\theta_1,\theta_2,\theta_3,\varphi_1,\varphi_2) + \Lambda_1(p)T_0(\theta_1,\theta_2,\theta_3,\varphi_1,\varphi_2),\\
\varepsilon^2:\ & L_0T_2(\theta_1,\theta_2,\theta_3,\varphi_1,\varphi_2) + L_1T_1(\theta_1,\theta_2,\theta_3,\varphi_1,\varphi_2)\\
&= \Lambda_0(p)T_2(\theta_1,\theta_2,\theta_3,\varphi_1,\varphi_2) + \Lambda_1(p)T_1(\theta_1,\theta_2,\theta_3,\varphi_1,\varphi_2)\\
&\quad +\Lambda_2(p)T_0(\theta_1,\theta_2,\theta_3,\varphi_1,\varphi_2),\\
\varepsilon^3:\ & L_0T_3(\theta_1,\theta_2,\theta_3,\varphi_1,\varphi_2) + L_1T_2(\theta_1,\theta_2,\theta_3,\varphi_1,\varphi_2)\\
&= \Lambda_0(p)T_3(\theta_1,\theta_2,\theta_3,\varphi_1,\varphi_2) + \Lambda_1(p)T_2(\theta_1,\theta_2,\theta_3,\varphi_1,\varphi_2)\\
&\quad +\Lambda_2(p)T_1(\theta_1,\theta_2,\theta_3,\varphi_1,\varphi_2) + \Lambda_3(p)T_0(\theta_1,\theta_2,\theta_3,\varphi_1,\varphi_2),\\
&\dots,\\
\varepsilon^n:\ & L_0T_n(\theta_1,\theta_2,\theta_3,\varphi_1,\varphi_2) + L_1T_{n-1}(\theta_1,\theta_2,\theta_3,\varphi_1,\varphi_2)\\
&= \Lambda_0(p)T_n(\theta_1,\theta_2,\theta_3,\varphi_1,\varphi_2) + \Lambda_1(p)T_{n-1}(\theta_1,\theta_2,\theta_3,\varphi_1,\varphi_2)\\
&\quad +\cdots+\Lambda_n(p)T_0(\theta_1,\theta_2,\theta_3,\varphi_1,\varphi_2),
\end{aligned} \tag{4.6.2}$$

where each function $T_s(\theta_1,\theta_2,\theta_3,\varphi_1,\varphi_2), s = 1,2,3,\dots$ must be positive and periodic in the range $0 \le \theta_i \le 2\pi$.

4.6.1 Zeroth Order Perturbation

The zeroth order perturbation equation is $L_0T_0 = \Lambda_0(p)T_0$ and can be written as

$$\begin{aligned}
\omega_1\frac{\partial T_0(\theta_1,\theta_2,\theta_3,\varphi_1,\varphi_2)}{\partial\theta_1} + \omega_2\frac{\partial T_0(\theta_1,\theta_2,\theta_3,\varphi_1,\varphi_2)}{\partial\theta_2} + \omega_3\frac{\partial T_0(\theta_1,\theta_2,\theta_3,\varphi_1,\varphi_2)}{\partial\theta_3}\\
= \Lambda_0(p)T_0(\theta_1,\theta_2,\theta_3,\varphi_1,\varphi_2).
\end{aligned} \tag{4.6.3}$$

Eq. (4.6.3) can be easily solved from the moment Lyapunov exponent characteristic which results $\Lambda_n(0) = 0$ for $n = 0,1,2,3,\dots$because of $\Lambda(0) = \Lambda_0(0) + \varepsilon\Lambda_1(0) + \varepsilon^2\Lambda_2(0) + \cdots + \varepsilon^n\Lambda_n(0) = 0$. The eigenvalue $\Lambda_0(p)$ is independent of p. Hence $\Lambda_0(0) = 0$ leads to $\Lambda_0(p) = 0$. The solutions have a periodic solution if and only if

$$\Lambda_0(p) = 0,\ T_0(\theta_1,\theta_2,\theta_3,\varphi_1,\varphi_2) = 1. \tag{4.6.4}$$

4.6.2 First Order Perturbation

Equation given from first-order perturbation is

$$\begin{aligned}
&L_0T_1(\theta_1,\theta_2,\theta_3,\varphi_1,\varphi_2) + L_1T_0(\theta_1,\theta_2,\theta_3,\varphi_1,\varphi_2)\\
&= \Lambda_0(p)T_1(\theta_1,\theta_2,\theta_3,\varphi_1,\varphi_2) + \Lambda_1(p)T_0(\theta_1,\theta_2,\theta_3,\varphi_1,\varphi_2),
\end{aligned} \tag{4.6.5}$$

and Eq. (4.6.5) has a periodic solution if and only if

$$\int_0^{2\pi}\int_0^{2\pi}\int_0^{2\pi}\int_0^{\pi/2}\int_0^{\pi/2}[L_1\cdot 1-\Lambda_1(p)]\,d\varphi_1 d\varphi_2 d\theta_1 d\theta_2 d\theta_3=0, \tag{4.6.6}$$

which yields

$$\begin{aligned}\Lambda_1(p)&=\frac{1}{2\pi^5}\int_0^{2\pi}\int_0^{2\pi}\int_0^{2\pi}\int_0^{\pi/2}\int_0^{\pi/2}[c(\theta_1,\theta_2,\theta_3,\varphi_1,\varphi_2)]\,d\varphi_1 d\varphi_2 d\theta_1 d\theta_2 d\theta_3\\&=\sigma^2\left[\frac{k_1^2+k_2^2}{1024}p(9p+46)+\frac{k_3^2}{128}p(3p+10)\right]-\frac{p}{4}(\beta_1+\beta_2+\beta_3).\end{aligned} \tag{4.6.7}$$

The first-order perturbation equation can be rewritten as

$$\begin{aligned}&\omega_1\frac{\partial T_1(\theta_1,\theta_2,\theta_3,\varphi_1,\varphi_2)}{\partial\theta_1}+\omega_2\frac{\partial T_1(\theta_1,\theta_2,\theta_3,\varphi_1,\varphi_2)}{\partial\theta_2}+\omega_3\frac{\partial T_1(\theta_1,\theta_2,\theta_3,\varphi_1,\varphi_2)}{\partial\theta_3}\\&\qquad+c(\theta_1,\theta_2,\theta_3,\varphi_1,\varphi_2)=\Lambda_1(p).\end{aligned} \tag{4.6.8}$$

It is important to take into consideration commensurable frequencies where exists a relation of the form of $m_1\omega_1=m_2\omega_2=m_3\omega_3$ where m_1,m_2 and m_3 are integers and expressions for second and third frequency are $\omega_2=l_1\omega_1$ and $\omega_3=l_2\omega_1$ respectively. The function $c(\theta_1,\theta_2,\theta_3,\varphi_1,\varphi_2)$ can be written in the form

$$\begin{aligned}&c(\theta_1,\theta_2,\theta_3,\varphi_1,\varphi_2)=\Lambda_1(p)+f_0(\theta_1,\theta_2,\theta_3)+f_1(\theta_1,\theta_2,\theta_3)\cos 2\varphi_1+f_2(\theta_1,\theta_2,\theta_3)\cos 2\varphi_2\\&+f_3(\theta_1,\theta_2,\theta_3)\cos 4\varphi_1+f_4(\theta_1,\theta_2,\theta_3)\cos 4\varphi_2+f_5(\theta_1,\theta_2,\theta_3)\sin 2\varphi_2+f_6(\theta_1,\theta_2,\theta_3)\cos 2\varphi_1\cos 2\varphi_2\\&+f_7(\theta_1,\theta_2,\theta_3)\cos 2\varphi_1\sin 2\varphi_2+f_8(\theta_1,\theta_2,\theta_3)\cos 2\varphi_1\cos 4\varphi_2+f_9(\theta_1,\theta_2,\theta_3)\cos 4\varphi_1\cos 2\varphi_2\\&+f_{10}(\theta_1,\theta_2,\theta_3)\cos 4\varphi_1\cos 4\varphi_2+f_{11}(\theta_1,\theta_2,\theta_3)\sin 2\varphi_1\sin\varphi_2.\end{aligned} \tag{4.6.9}$$

Functions $f_r(\theta_1,\theta_2,\theta_3)$ are periodic in θ_1,θ_2 and θ_3 and given as

$$f_r(\theta_1,\theta_2,\theta_3)=\lfloor\mathbf{U}\rfloor\{\mathbf{s}_r\},\quad r=0,1,\ldots,11, \tag{4.6.10}$$

Where $\lfloor\mathbf{U}\rfloor$ is the vector in the form

$$\lfloor\mathbf{U}\rfloor=\lfloor h_1\quad\beta_1\quad h_2\quad\beta_2\quad h_3\quad\beta_3\quad\sigma^2k_1^2\quad\sigma^2k_2^2\quad\sigma^2k_3^2\quad\sigma^2k_1k_2\quad\sigma^2k_1k_3\quad\sigma^2k_2k_3\rfloor,$$

The combination of coefficients φ_1 and φ_2 suggests that function $T_1(\theta_1,\theta_2,\theta_3,\varphi_1,\varphi_2)$ can be written as

$$\begin{aligned}&T_1(\theta_1,\theta_2,\theta_3,\varphi_1,\varphi_2)=T_{10}(\theta_1,\theta_2,\theta_3)+T_{11}(\theta_1,\theta_2,\theta_3)\cos 2\varphi_1+T_{12}(\theta_1,\theta_2,\theta_3)\cos 2\varphi_2\\&+T_{13}(\theta_1,\theta_2,\theta_3)\cos 4\varphi_1+T_{14}(\theta_1,\theta_2,\theta_3)\cos 4\varphi_2+T_{15}(\theta_1,\theta_2,\theta_3)\sin 2\varphi_2\\&+T_{16}(\theta_1,\theta_2,\theta_3)\cos 2\varphi_1\cos 2\varphi_2+T_{17}(\theta_1,\theta_2,\theta_3)\cos 2\varphi_1\sin 2\varphi_2+T_{18}(\theta_1,\theta_2,\theta_3)\cos 2\varphi_1\cos 4\varphi_2\\&+T_{110}(\theta_1,\theta_2,\theta_3)\cos 4\varphi_1\cos 4\varphi_2+T_{111}(\theta_1,\theta_2,\theta_3)\sin 2\varphi_1\sin\varphi_2+T_{19}(\theta_1,\theta_2,\theta_3)\cos 4\varphi_1\cos 2\varphi_2.\end{aligned}$$

Equating terms of the equal trigonometry function to give set of partial differential equations

$$\omega_1 \frac{\partial T_{1r}(\theta_1,\theta_2,\theta_3)}{\partial \theta_1} + \omega_2 \frac{\partial T_{1r}(\theta_1,\theta_2,\theta_3)}{\partial \theta_2} + \omega_3 \frac{\partial T_{1r}(\theta_1,\theta_2,\theta_3)}{\partial \theta_3} + f_r(\theta_1,\theta_2,\theta_3) = 0, r = 0,1,\dots,11. \tag{4.6.11}$$

The functions $T_{1r}(\theta_1,\theta_2,\theta_3)$ can be written as

$$T_{1r}(\theta_1,\theta_2,\theta_3) = [\mathbf{U}]\{\mathbf{v}_r\} + C_r(\theta_2 - l_1\theta_1, \theta_3 - l_2\theta_1), \quad r = 0,1,\dots,11, \tag{4.6.12}$$

Here $C_r(\theta_2 - l_1\theta_1, \theta_3 - l_2\theta_1)$ are the same arbitrary functions of three variables for which we make assumptions as follows

$$C_r(\theta_2 - l_1\theta_1, \theta_3 - l_2\theta_1) = A_{1r} + B_{1r}\sin(2\theta_2 - 2l_1\theta_1) + C_{1r}\sin(4\theta_2 - 4l_1\theta_1)$$
$$+D_{1r}\sin(2\theta_3 - 2l_2\theta_1) + E_{1r}\sin(4\theta_3 - 4l_2\theta_1), r = 0,1,\dots,11. \tag{4.6.13}$$

As each function $T_{1r}(\theta_1,\theta_2,\theta_3), r = 0,1,\dots,11$ must be positive and periodic, unknown constants A_{1r}, B_{1r}, C_{1r}, D_{1r}, E_{1r} can be determined using conditions

$$T_{1r}(0,0,0) = T_{1r}(0,0,2\pi) = T_{1r}(0,2\pi,0) = T_{1r}(2\pi,0,0) = T_{1r}(2\pi,2\pi,0) = T_{1r}(0,2\pi,2\pi)$$
$$= T_{1r}(2\pi,0,2\pi) = T_{1r}(2\pi,2\pi,2\pi) = 0, \tag{4.6.14}$$

$$\frac{\partial T_{1r}(0,0,0)}{\partial \theta_1} = \frac{\partial T_{1r}(2\pi,0,0)}{\partial \theta_1}, \frac{\partial T_{1r}(0,0,0)}{\partial \theta_2} = \frac{\partial T_{1r}(0,2\pi,0)}{\partial \theta_2}, \frac{\partial T_{1r}(0,0,0)}{\partial \theta_3}$$
$$= \frac{\partial T_{1r}(0,0,2\pi)}{\partial \theta_3}, r = 0,1,\dots,11. \tag{4.6.15}$$

4.6.3 Second Order Perturbation

The second-order perturbation equation must satisfied the condition of periodic function $T_2(\theta_1,\theta_2,\theta_3,\varphi_1,\varphi_2)$ in θ_1,θ_2 and θ_3 given as

$$L_0T_2(\theta_1,\theta_2,\theta_3,\varphi_1,\varphi_2) + L_1T_2(\theta_1,\theta_2,\theta_3,\varphi_1,\varphi_2) = \Lambda_1(p)T_1(\theta_1,\theta_2,\theta_3,\varphi_1,\varphi_2) + \Lambda_2(p). \tag{4.6.16}$$

We have

$$\Lambda_2(p) = \frac{1}{2\pi^5}\int_0^{2\pi}\int_0^{2\pi}\int_0^{2\pi}\int_0^{\pi/2}\int_0^{\pi/2}\left\{a_1\frac{\partial^2 T_1}{\partial\theta_1^2} + a_2\frac{\partial^2 T_1}{\partial\theta_2^2} + a_3\frac{\partial^2 T_1}{\partial\theta_3^2} + a_4\frac{\partial^2 T_1}{\partial\varphi_1^2} + a_5\frac{\partial^2 T_1}{\partial\varphi_2^2} + a_6\frac{\partial^2 T_1}{\partial\theta_1\partial\theta_2}\right.$$
$$+a_7\frac{\partial^2 T_1}{\partial\theta_1\partial\theta_3} + a_8\frac{\partial^2 T_1}{\partial\theta_1\partial\varphi_1} + a_9\frac{\partial^2 T_1}{\partial\theta_1\partial\varphi_2} + a_{10}\frac{\partial^2 T_1}{\partial\theta_2\partial\theta_3} + a_{11}\frac{\partial^2 T_1}{\partial\theta_2\partial\varphi_1} + a_{12}\frac{\partial^2 T_1}{\partial\theta_2\partial\varphi_2} + a_{13}\frac{\partial^2 T_1}{\partial\theta_3\partial\varphi_1}$$
$$+a_{14}\frac{\partial^2 T_1}{\partial\theta_3\partial\varphi_2} + a_{15}\frac{\partial^2 T_1}{\partial\varphi_1\partial\varphi_2} + b_1\frac{\partial T_1}{\partial\theta_1} + b_2\frac{\partial T_1}{\partial\theta_2}b_3\frac{\partial T_1}{\partial\theta_3} + b_4\frac{\partial T_1}{\partial\varphi_1}$$
$$\left.+b_5\frac{\partial T_1(\theta_1,\theta_2,\theta_3,\varphi_1,\varphi_2)}{\partial\varphi_2} + [c - \Lambda_1(p)]T_1\right\}d\varphi_1 d\varphi_2 d\theta_1 d\theta_2 d\theta_3. \tag{4.6.17}$$

$\Lambda_2(p)$ can be obtained symbolically. After integrating, the solution has the following form

$$\Lambda_2(p) = \\ = \frac{\Lambda_{20}(p) + \Lambda_{21}(p)\sin 4l_2\pi + \Lambda_{22}(p)\cos 4l_2\pi + \Lambda_{23}(p)\cos 3l_2\pi \sin l_2\pi + \Lambda_{24}(p)\cos l_2\pi \sin 3l_2\pi}{\omega_1(l_1^2-1)(l_2^2-1)(l_1^2-l_2^2)(2+\cos 4l_2\pi)}. \tag{4.6.18}$$

The weak noise expansion of the moment Lyapunov exponent in the second-order perturbation for the stochastic system is determined in the form

$$\Lambda(p) = \varepsilon\Lambda_1(p) + \varepsilon^2\Lambda_2(p) + O(\varepsilon^3). \tag{4.6.19}$$

The Lyapunov exponent can be obtained by using a property of the moment Lyapunov exponent

$$\lambda = \left.\frac{d\Lambda(p)}{dp}\right|_{p=0} = \varepsilon\lambda_1 + \varepsilon^2\lambda_2 + O(\varepsilon^3) = \varepsilon\left\{\left[\frac{23}{512}(k_1^2+k_2^2) + \frac{5}{64}k_3^2\right]\sigma^2 - \frac{1}{4}(\beta_1+\beta_2+\beta_3)\right\} \\ +\varepsilon^2\frac{\lambda_{20} + \lambda_{21}\sin 4l_2\pi + \lambda_{22}\cos 4l_2\pi + \lambda_{23}\cos 3l_2\pi \sin l_2\pi + \lambda_{24}\cos l_2\pi \sin 3l_2\pi}{\omega_1(l_1^2-1)(l_2^2-1)(l_1^2-l_2^2)(2+\cos 4l_2\pi)} + O(\varepsilon^3), \tag{4.6.20}$$

4.6.4 Stochastic Stability Conditions

The values used for the parameters of the stochastic system in the calculations for determining Moment Lyapunov exponent and Lyapunov exponent are given as follows

$$E = 1\times 10^{10}\ Nm^{-2},\quad K = 2\times 10^{5}\ Nm^{-2},\quad \rho = 2\times 10^{3}\ kgm^{-3}, \\ l = 10\ m,\ \ A_1 = A_2 = A_3 = 5\times 10^{-2}\ m^2,\ \ I_1 = 4\times 10^{-4}m^4, I_2 = \frac{25}{4}\times 10^{-4}m^4,\ \ I_3 = \frac{35}{4}\times 10^{-4}m^4, \tag{4.6.21}$$

where we assume for the simplicity that

$$H_1 = H_2 = H_3 = \frac{K}{\rho A},\ K_1 = K_2 = K_3 = \frac{\pi^2}{l^2\rho A}. \tag{4.6.22}$$

We determined analytically the pth moment stability boundary in the first-order perturbation for various values $p = 1,2,4$, respectively with the definition of the moment stability $\Lambda(p) < 0$. Using the results for the moment Lyapunov exponent from first order perturbation, $\Lambda(p) = \varepsilon\Lambda_1(p) + O(\varepsilon^2)$ we obtained

$$\Lambda(1) < 0 \xrightarrow{pert.\ 1} c_0 > \left[\frac{55}{768}(k_1^2+k_2^2) + \frac{13}{96}k_3^2\right]\sigma^2\rho A, \\ \Lambda(2) < 0 \xrightarrow{pert.\ 1} c_0 > \frac{1}{12}(k_1^2+k_2^2+2k_3^2)\,\sigma^2\rho A, \\ \Lambda(4) < 0 \xrightarrow{pert.\ 1} c_0 > \left[\frac{41}{384}(k_1^2+k_2^2) + \frac{11}{48}k_3^2\right]\sigma^2\rho A. \tag{4.6.23}$$

Almost-sure stability boundary of the oscillatory system can be determined in the first-order perturbation from known that oscillatory stochastic system is

asymptotically stable only if the Lyapunov exponent $\lambda < 0$. From expression $\lambda = \varepsilon\lambda_1 + O(\varepsilon^2)$ we have

$$\lambda < 0 \overset{pert.\ 1}{\Longrightarrow} c_0 > \left[\frac{23}{384}(k_1^2 + k_2^2) + \frac{5}{48}k_3^2\right]\sigma^2\rho A. \tag{4.6.24}$$

Following the same procedure using the values of natural frequencies $\omega_1 = 19.739\ s^{-1}, \omega_2 = 24.674 s^{-1}$ and $\omega_3 = 29.194 s^{-1}$ calculated for the parameters of the system we determined the moment stability boundary in the second-order perturbation in form of equations

$$\begin{aligned} &\Lambda(1) < 0 \overset{pert.\ 2}{\Longrightarrow} 0.0004287 + 0.02258090c_0 + 1.50619 \times 10^{-6}c_0^2 > 0, \\ &\Lambda(2) < 0 \overset{pert.\ 2}{\Longrightarrow} 0.00099457 + 0.0453544c_0 + 4.0165 \times 10^{-6}c_0^2 > 0, \\ &\Lambda(4) < 0 \overset{pert.\ 2}{\Longrightarrow} 0.0025176 + 0.0914795c_0 + 0.00001204\, c_0^2 > 0. \end{aligned} \tag{4.6.25}$$

We determined the almost-sure stability boundary in the second-order perturbation by the same procedure applied to $\lambda = \varepsilon\lambda_1 + \varepsilon^2\lambda_2 + O(\varepsilon^3)$ and we have condition

$$\lambda < 0 \overset{pert.\ 2}{\Longrightarrow} 0.0003586 + 0.022485c_0 + 1.00412 \times 10^{-6}c_0^2 > 0 \tag{4.6.26}$$

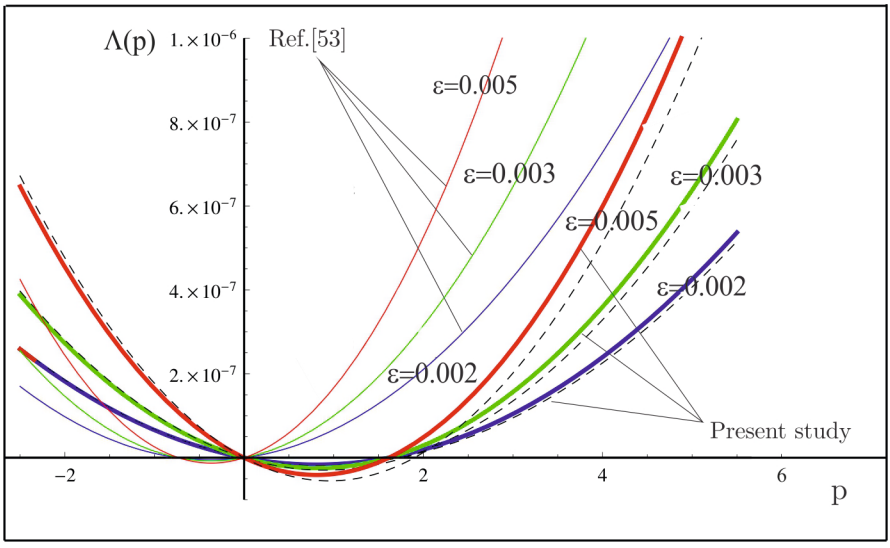

Fig. 4.6.1 Moment Lyapunov exponent $\Lambda(p)$ for $\sigma = \sqrt{200 \times 10^3}$, $d_1 = d_2 = c_0 = 0.01$, thin lines - double beam [53], thick lines – three beam system on elastic foundation, dashed lines – second perturbation of the three beam system.

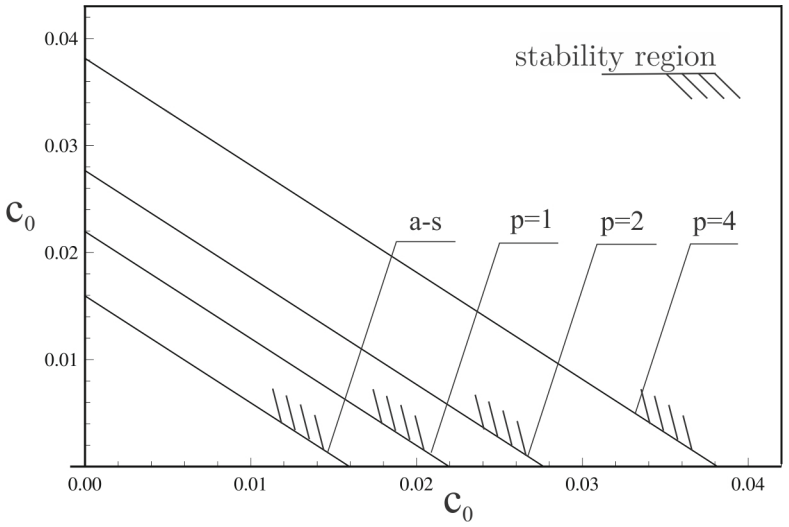

Fig. 4.6.2 Stability regions for almost-sure (a-s) and pth moment stability for $\varepsilon = 0.002$.

Variation of moment Lyapunov exponent for double beam and three beam system on elastic foundation is presented on Fig. 4.6.1. Values for the double beam system in numerical experiment are chosen from present study for the properties of the beams 1 and 2 and compared with results for moment Lyapunov exponent for the three beam system on elastic foundation. The main point of the presented results on Fig 4.6.1. is that the stochastic stability of three beam system on elastic foundation is higher then for the double beam system without foundation. We compared stability when one more beam and elastic foundation is included with simple double-beam system. Our investigation shows that regardless because we increased the number of freedom of the system with one more beam, elastic foundation has significant influence on increasing the region of the stochastic stability, and the system considered in the present work is more stable because the values of $\Lambda(p)$ is negative on the bigger region of the p. Negative values of the $\Lambda(p)$ shows when the system is stable. Fig. 4.6.2. just shows moment stability boundaries for first perturbation with respect to the damping coefficients. We can conclude that the stability region is increasing with increasing the damping coefficient what was expected.

Chapter 5
The Effects of Rotary Inertia and Transverse Shear on the Vibrations and Stability of the Elastically Connected Timoshenko Beam-System on Elastic Foundation

Chapter 5 analyzed free vibration of the multiple elastically connected beams of Timoshenko's type on an elastic foundation under the influence of axial forces. Analytical solutions for the natural frequencies and the critical buckling forces are determined by the trigonometric method and verified numerically. It is shown that the fundamental natural frequency in the first mode of the multiple beam system tends to the value of the natural frequency of the system with one beam resting on an elastic foundation with the tendency of increasing the number of connected beams with the same stiffness of the layers between.

5.1 Free Vibration of Elastically Connected Timoshenko Beams

Let us consider the system of m elastically connected Timoshenko beams of the same length l, elastically connected by Winkler-type layers with the stiffness modulus $K_{ii}, (ii = 0, 1, \ldots, m-1)$ under the influence of axial compression forces of the intensity F, reference [15].

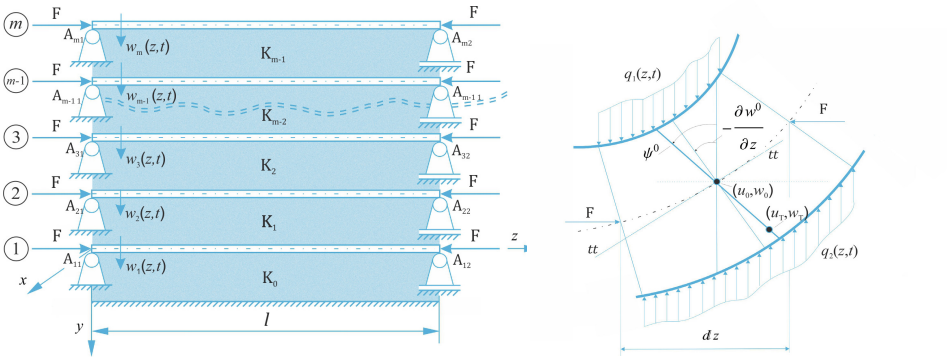

Fig. 5.1.1 a) The system of elastically connected beams on an elastic foundation b) Elementary deformed beam part

V. Stojanović and P. Kozić, *Vibrations and Stability of Complex Beam Systems*,
Springer Tracts in Mechanical Engineering, DOI: 10.1007/978-3-319-13767-4_5

Let the functions of longitudinal and transverse motion as well as the angle between the beam's cross section and y–axis be $u_{T\tilde{\imath}}(y,z,t)$,$w_{T\,\tilde{\imath}}(y,z)$,$\psi^0_{T\,\tilde{\imath}}(z)$, $\tilde{\imath}=1,2,\dots,m$. For a clockwise angle ψ^0 of the cross-section as shown in Figure 5.1.1 b) pursuant to the derived equations in reference [15], we define the motion of beam points as

$$u_{T\tilde{\imath}}(y,z,t)=u^0_{T\tilde{\imath}}(z,t)-y\psi^0_{T\tilde{\imath}}(z,t),\quad w_{T\tilde{\imath}}(y,z,t)=w^0_{T\tilde{\imath}}(z,t),\quad \tilde{\imath}=1,2,\dots,m. \tag{5.1.1}$$

Deformation in the function of motion and the relation between stress and deformation according to Hooke's law are given by

$$\varepsilon_{z\tilde{\imath}}(y,z,t)=\frac{\partial u^0_{T\tilde{\imath}}(z,t)}{\partial z}-y\frac{\partial \psi^0_{T\tilde{\imath}}(z,t)}{\partial z},\quad \gamma_{zy\tilde{\imath}}(z,t)=\frac{\partial w^0_{T\tilde{\imath}}(z,t)}{\partial z}-\psi^0_{T\tilde{\imath}}(z,t), \tag{5.1.2}$$

$$\begin{Bmatrix}\sigma_{z\tilde{\imath}}\\ \tau_{zy\tilde{\imath}}\end{Bmatrix}=\begin{bmatrix}E_{\tilde{\imath}} & 0\\ 0 & kG_{\tilde{\imath}}\end{bmatrix}\begin{Bmatrix}\varepsilon_{z\tilde{\imath}}\\ \gamma_{zy\tilde{\imath}}\end{Bmatrix},\quad \tilde{\imath}=1,2,\dots,m. \tag{5.1.3}$$

Virtual work of inertial forces is given by

$$\delta W_{in\tilde{\imath}}=-\rho_{\tilde{\imath}}b_{\tilde{\imath}}\int_0^l\int_{-\frac{h_{\tilde{\imath}}}{2}}^{\frac{h_{\tilde{\imath}}}{2}}\left[\frac{\partial^2 w_{T\tilde{\imath}}(y,z,t)}{\partial t^2}\delta w_{T\tilde{\imath}}(y,z,t)+\frac{\partial^2 u_{T\tilde{\imath}}(y,z,t)}{\partial t^2}\delta u_{T\tilde{\imath}}(y,z,t)\right]dydz. \tag{5.1.4}$$

Virtual work of internal forces is

$$\delta W_{V\tilde{\imath}}=-b_{\tilde{\imath}}\int_0^l\int_{-\frac{h_1}{2}}^{\frac{h_1}{2}}\left[\sigma_{z\tilde{\imath}}(z,t)\delta\varepsilon_{z\tilde{\imath}}(z,t)+\tau_{zy\tilde{\imath}}(z,t)\delta\gamma_{zy\tilde{\imath}}(z,t)\right]dydz. \tag{5.1.5}$$

Virtual work of external work is expressed as

$$\delta W_{ex1}=\int_0^l\left\{\delta w^0_{T1}(z,t)\left[-K_0w^0_{T1}(z,t)+K_1\left(w^0_{T2}(z,t)-w^0_{T1}(z,t)\right)\right]+F\frac{\partial w^0_{T1}(z,t)}{\partial z}\frac{\partial\delta w^0_{T1}(z,t)}{\partial z}\right\}dz, \tag{5.1.6}$$

$$\delta W_{exi}=\int_0^l\left\{\delta w^0_{Ti}(z,t)\left[-K_{i-1}\left(w^0_{Ti}(z,t)-w^0_{Ti-1}(z,t)\right)+K_i\left(w^0_{Ti+1}(z,t)-w^0_{Ti}(z,t)\right)\right]+\right.$$

$$\left.+F\frac{\partial w^0_{Ti}(z,t)}{\partial z}\frac{\partial\delta w^0_{Ti}(z,t)}{\partial z}\right\}dz,\qquad i=2,3,\dots,m-1, \tag{5.1.7}$$

$$\delta W_{exm}=\int_0^l\left\{\delta w^0_{Tm}(z,t)\left[-K_{m-1}\left(w^0_{Tm}(z,t)-w^0_{Tm-1}(z,t)\right)\right]\right.$$

$$\left.+F\frac{\partial w^0_{Tm}(z,t)}{\partial z}\frac{\partial\delta w^0_{Tm}(z,t)}{\partial z}\right\}dz, \tag{5.1.8}$$

Substituting the equations (5.1.4-5.1.8) into a general equation of the virtual work principle $\delta W_{in\tilde{\imath}}+\delta W_{V\tilde{\imath}}+\delta W_{ex\tilde{\imath}}=0$, $\tilde{\imath}=1,2,\dots m$, and applying the Green's theorem, we get the coupled system of partial differential equations of vibration in the following form

$$\rho_1A_1\frac{\partial^2w_1}{\partial t^2}-kG_1A_1\left(\frac{\partial^2w_1}{\partial z^2}-\frac{\partial\psi_1}{\partial z}\right)+F\frac{\partial^2w_1}{\partial z^2}+K_0w_1-K_1(w_2-w_1)=0, \tag{5.1.9}$$

$$\rho_1 I_{x1}\frac{\partial^2 \psi_1}{\partial t^2} - E_1 I_{x1}\frac{\partial^2 \psi_1}{\partial z^2} - kG_1 A_1\left(\frac{\partial w_1}{\partial z} - \psi_1\right) = 0, \tag{5.1.10}$$

$$\rho_i A_i\frac{\partial^2 w_i}{\partial t^2} - kG_i A_i\left(\frac{\partial^2 w_i}{\partial z^2} - \frac{\partial \psi_i}{\partial z}\right) + F\frac{\partial^2 w_i}{\partial z^2} + K_{i-1}(w_i - w_{i-1}) - K_i(w_{i+1} - w_i) = 0, \tag{5.1.11}$$

$$\rho_i I_{xi}\frac{\partial^2 \psi_i}{\partial t^2} - E_i I_{xi}\frac{\partial^2 \psi_i}{\partial z^2} - kG_i A_i\left(\frac{\partial w_i}{\partial z} - \psi_i\right) = 0, \quad i = 2, 3, \cdots m-1, \tag{5.1.12}$$

$$\rho_m A_m\frac{\partial^2 w_m}{\partial t^2} - kG_m A_m\left(\frac{\partial^2 w_m}{\partial z^2} - \frac{\partial \psi_m}{\partial z}\right) + F\frac{\partial^2 w_m}{\partial z^2} + K_{m-1}(w_m - w_{m-1}) = 0, \tag{5.1.13}$$

$$\rho_m I_{xm}\frac{\partial^2 \psi_m}{\partial t^2} - E_m I_{xm}\frac{\partial^2 \psi_m}{\partial z^2} - kG_m A_m\left(\frac{\partial w_m}{\partial z} - \psi_m\right) = 0, \tag{5.1.14}$$

The system of coupled differential equations (5.1.9-5.1.14) is reduced to the following form after the elimination of the variable ψ_m

$$E_1 I_1\left(1 - \frac{F}{kA_1 G_1}\right)\frac{\partial^4 w_1}{\partial z^4} + \left[\rho_1 A_1 + (K_0 + K_1)\frac{\rho_1 I_1}{kA_1 G_1}\right]\frac{\partial^2 w_1}{\partial t^2} - \frac{K_1 \rho_1 I_1}{kA_1 G_1}\frac{\partial^2 w_2}{\partial t^2}$$
$$+ \left[F - (K_0 + K_1)\frac{E_1 I_1}{kA_1 G_1}\right]\frac{\partial^2 w_1}{\partial z^2} + K_1\frac{E_1 I_1}{kA_1 G_1}\frac{\partial^2 w_2}{\partial z^2}$$

$$-\rho_1 I_1\left[1 + \frac{E_1}{kG_1} - \frac{F}{kA_1 G_1}\right]\frac{\partial^4 w_1}{\partial z^2 \partial t^2} + \frac{\rho_1^2 I_1}{kG_1}\frac{\partial^4 w_1}{\partial t^4} + (K_0 + K_1)w_1 - K_1 w_2 = 0, \tag{5.1.15}$$

$$E_i I_i\left(1 - \frac{F}{kA_i G_i}\right)\frac{\partial^4 w_i}{\partial z^4} - \frac{K_{i-1}\rho_i I_i}{kA_i G_i}\frac{\partial^2 w_{i-1}}{\partial t^2} + \left[\rho_i A_i + (K_{i-1} + K_i)\frac{\rho_i I_i}{kA_i G_i}\right]\frac{\partial^2 w_i}{\partial t^2} - \frac{K_i \rho_i I_i}{kA_i G_i}\frac{\partial^2 w_{i+1}}{\partial t^2}$$

$$+ \frac{K_{i-1}E_i I_i}{kA_i G_i}\frac{\partial^2 w_{i-1}}{\partial z^2} + \left[F - (K_{i-1} + K_i)\frac{E_i I_i}{kA_i G_i}\right]\frac{\partial^2 w_i}{\partial z^2} + \frac{K_i E_i I_i}{kA_i G_i}\frac{\partial^2 w_{i+1}}{\partial z^2} - \rho_i I_i\left[1 + \frac{E_i}{kG_i} - \frac{F}{kA_i G_i}\right]\frac{\partial^4 w_i}{\partial z^2 \partial t^2}$$

$$+ \frac{\rho_i^2 I_i}{kG_i}\frac{\partial^4 w_{i+1}}{\partial t^4} - K_{i-1}w_{i-1} + (K_{i-1} + K_i)w_i - K_i w_{i+1} = 0, \quad i = 2, 3, \cdots m-1, \tag{5.1.16}$$

$$E_m I_m\left(1 - \frac{F}{kA_m G_m}\right)\frac{\partial^4 w_m}{\partial z^4} - \frac{K_{m-1}\rho_m I_m}{kA_m G_m}\frac{\partial^2 w_{m-1}}{\partial t^2} + \left[\rho_m A_m + \frac{K_{m-1}\rho_m I_m}{kA_m G_m}\right]\frac{\partial^2 w_m}{\partial t^2}$$
$$+ \frac{K_{m-1}E_m I_m}{kA_m G_m}\frac{\partial^2 w_{m-1}}{\partial z^2} + \left[F - \frac{K_{m-1}E_m I_m}{kA_m G_m}\right]\frac{\partial^2 w_m}{\partial z^2} - \rho_m I_m\left[1 + \frac{E_m}{kG_m} - \frac{F}{kA_m G_m}\right]\frac{\partial^4 w_m}{\partial z^2 \partial t^2}$$

$$+ \frac{\rho_m^2 I_m}{kG_m}\frac{\partial^4 w_m}{\partial t^4} - K_{m-1}w_{m-1} + K_{m-1}w_m = 0. \tag{5.1.17}$$

Initial and boundary conditions for simply supported beams are

$$w_{\tilde{\imath}}(z,0) = w_{\tilde{\imath}0}(z), \quad \dot{w}_{\tilde{\imath}}(z,0) = v_{\tilde{\imath}0}(z), \quad \psi_{\tilde{\imath}}(z,0) = \psi_{\tilde{\imath}0}(z), \quad \dot{\psi}_{\tilde{\imath}}(z,0) = \omega_{\tilde{\imath}0}(z), \tag{5.1.18}$$

$$w_{\tilde{\imath}}(0,t) = w_{\tilde{\imath}}(l,t) = w''_{\tilde{\imath}}(0,t) = w''_{\tilde{\imath}}(l,t) = 0, \quad \tilde{\imath} = 1,2,3\cdots m. \tag{5.1.19}$$

If we assume harmonic beam motion, we may express the transverse beam motions as the product of the functions

$$w_{\tilde{\imath}}(z,t) = \sum_{n=1}^{\infty} Z_n(z) T_{\tilde{\imath}n}(t), \qquad \tilde{\imath} = 1,2,\ldots m \tag{5.1.20}$$

where $T_{\tilde{\imath}n}(t)$, $\tilde{\imath} = 1,2,3\cdots m$, denotes unknown time functions and $Z_n(z)$ is the mode shape function which satisfies boundary conditions for simply supported beams

$$Z_n(z) = \sin(k_n z), \qquad k_n = n\pi/l, \qquad n = 1,2,3,\cdots. \tag{5.1.21}$$

If we substitute the assumed transverse motions (5.1.20) into equations (5.1.15-5.1.17), we get

$$\sum_{n=1}^{\infty}\left\{\frac{1}{C_{s1}^2}\frac{d^4T_{1n}}{dt^4} + \left[1 + C_{r1}^2\left(1 + \frac{C_{b1}^2}{C_{s1}^2C_{r1}^4}\right)k_n^2 + \frac{1}{C_{s1}^2}\left(H_0^* + H_1 - F\eta_{1n}\right)\right]\frac{d^2T_{1n}}{dt^2} - \frac{H_1}{C_{s1}^2}\frac{d^2T_{2n}}{dt^2}\right.$$
$$\left. + \left[C_{b1}^2k_n^4 + \left(H_0^* + H_1 - F\eta_{1n}\right)\left(1 + \frac{C_{b1}^2}{C_{s1}^2C_{r1}^2}k_n^2\right)\right]T_{1n} - H_1\left(1 + \frac{C_{b1}^2}{C_{s1}^2C_{r1}^2}k_n^2\right)T_{2n}\right\}Z_n = 0, \tag{5.1.22}$$

$$\sum_{n=1}^{\infty}\left\{\frac{1}{C_{si}^2}\frac{d^4T_{in}}{dt^4} - \frac{H_{i-1}^*}{C_{si}^2}\frac{d^2T_{(i-1)n}}{dt^2} + \left[1 + C_{ri}^2\left(1 + \frac{C_{bi}^2}{C_{si}^2C_{ri}^4}\right)k_n^2 + \frac{1}{C_{si}^2}\left(H_{i-1}^* + H_i - F\eta_{in}\right)\right]\frac{d^2T_{in}}{dt^2}\right.$$
$$- \frac{H_i}{C_{si}^2}\frac{d^2T_{(i+1)n}}{dt^2} - H_{(i-1)}^*\left(1 + \frac{C_{bi}^2}{C_{si}^2C_{ri}^2}k_n^2\right)T_{(i-1)n} + \left[C_{bi}^2k_n^4 + \left(H_{i-1}^* + H_i - F\eta_{in}\right)\left(1 + \frac{C_{bi}^2}{C_{si}^2C_{ri}^2}k_n^2\right)\right]T_{in}$$
$$\left. - H_i\left(1 + \frac{C_{bi}^2}{C_{si}^2C_{ri}^2}k_n^2\right)T_{(i+1)n}\right\}Z_n = 0, \quad i = 2,3,\cdots m-1, \tag{5.1.23}$$

$$\sum_{n=1}^{\infty}\left\{\frac{1}{C_{sm}^2}\frac{d^4T_{mn}}{dt^4} - \frac{H_{m-1}^*}{C_{sm}^2}\frac{d^2T_{(m-1)n}}{dt^2} + \left[1 + C_{rm}^2\left(1 + \frac{C_{bm}^2}{C_{sm}^2C_{rm}^4}\right)k_n^2 + \frac{1}{C_{sm}^2}\left(H_{m-1}^* - F\eta_{mn}\right)\right]\frac{d^2T_{mn}}{dt^2}\right.$$
$$\left. - H_{m-1}^*\left(1 + \frac{C_{bm}^2}{C_{sm}^2C_{rm}^2}k_n^2\right)T_{(m-1)n} + \left[C_{bm}^2k_n^4 + \left(H_{m-1}^* - F\eta_{mn}\right)\left(1 + \frac{C_{bm}^2}{C_{sm}^2C_{rm}^2}k_n^2\right)\right]T_{mn}\right\}Z_n = 0, \tag{5.1.24}$$

where

$$H_{\tilde{\imath}-1}^{*}=\frac{K_{\tilde{\imath}-1}}{\rho_{\tilde{\imath}}A_{\tilde{\imath}}},\qquad H_{\tilde{\imath}}=\frac{K_{\tilde{\imath}}}{\rho_{\tilde{\imath}}A_{\tilde{\imath}}},\qquad \eta_{\tilde{\imath}n}=\frac{k_n^2}{\rho_{\tilde{\imath}}A_{\tilde{\imath}}},$$

$$C_{b\tilde{\imath}}=\sqrt{\frac{E_{\tilde{\imath}}I_{\tilde{\imath}}}{\rho_{\tilde{\imath}}A_{\tilde{\imath}}}},\qquad C_{s\tilde{\imath}}=\sqrt{\frac{G_{\tilde{\imath}}A_{\tilde{\imath}}k}{\rho_{\tilde{\imath}}I_{\tilde{\imath}}}},\qquad C_{r\tilde{\imath}}=\sqrt{\frac{I_{\tilde{\imath}}}{A_{\tilde{\imath}}}},\quad \tilde{\imath}=1,2,3,\cdots m.$$

We assume the solutions to the equations (5.1.22 -5.1.24) in the following form

$$T_{\tilde{\imath}n}=A_{\tilde{\imath}n}e^{j\omega_n t},\quad \tilde{\imath}=1,2,3,\cdots m,\qquad j=\sqrt{-1}, \tag{5.1.25}$$

where ω_n is the natural frequency of the system. If we substitute the solutions (5.1.25) into differential equations (5.1.22-5.1.24), we get a homogeneous system of algebraic equations for unknowns $A_{n1},\ A_{n2},\ A_{n3},\ \cdots\ A_{nm}$ in the form

$$\left\{\frac{\omega_n^4}{C_{s1}^2}-\left[1+C_{r1}^2\left(1+\frac{C_{b1}^2}{C_{s1}^2C_{r1}^2}\right)k_n^2+\frac{1}{C_{s1}^2}\left(H_0^*+H_1-F\,\eta_{1n}\right)\right]\omega_n^2\right.$$

$$\left.+C_{b1}^2k_n^4+\left(H_0^*+H_1-F\,\eta_{1n}\right)\left(1+\frac{C_{b1}^2}{C_{s1}^2C_{r1}^2}k_n^2\right)\right\}A_{1n}+H_1\left[\frac{\omega_n^2}{C_{s1}^2}-\left(1+\frac{C_{b1}^2}{C_{s1}^2C_{r1}^2}k_n^2\right)\right]A_{2n}=0 \tag{5.1.26}$$

$$H_{i-1}^{*}\left[\frac{\omega_n^2}{C_{si}^2}-\left(1+\frac{C_{bi}^2}{C_{si}^2C_{ri}^2}k_n^2\right)\right]A_{(i-1)n}+\left\{\frac{\omega_n^4}{C_{si}^2}-\left[1+C_{ri}^2\left(1+\frac{C_{bi}^2}{C_{si}^2C_{ri}^2}\right)k_n^2+\frac{1}{C_{si}^2}\left(H_{i-1}^*+H_i-F\,\eta_{in}\right)\right]\omega_n^2\right.$$

$$\left.+\left[C_{bi}^2k_n^4+\left(H_{i-1}^*+H_i-F\,\eta_{in}\right)\left(1+\frac{C_{bi}^2}{C_{si}^2C_{ri}^2}k_n^2\right)\right]\right\}A_{in}+H_i\left[\frac{\omega_n^2}{C_{si}^2}-\left(1+\frac{C_{bi}^2}{C_{si}^2C_{ri}^2}k_n^2\right)\right]A_{(i+1)n}=0, \tag{5.1.27}$$

$$H_{m-1}^{*}\left[\frac{\omega_n^2}{C_{sm}^2}-\left(1+\frac{C_{bm}^2}{C_{sm}^2C_{rm}^2}k_n^2\right)\right]A_{(m-1)n}+\left\{\frac{\omega_n^4}{C_{sm}^2}-\left[1+C_{rm}^2\left(1+\frac{C_{bm}^2}{C_{sm}^2C_{rm}^2}\right)k_n^2\right.\right.$$

$$\left.\left.+\frac{1}{C_{sm}^2}\left(H_{m-1}^*-F\,\eta_{mn}\right)\right]\omega_n^2+\left[C_{bm}^2k_n^4+\left(H_{m-1}^*-F\,\eta_{mn}\right)\left(1+\frac{C_{bm}^2}{C_{sm}^2C_{rm}^2}k_n^2\right)\right]\right\}A_{mn}=0. \tag{5.1.28}$$

For determining analytical solutions, we assume the beams have identical material and geometric properties. The homogeneous system of algebraic equations (5.1.26-5.1.28) can then be written as a matrix equation

$$\begin{bmatrix}
S_n & -u_n & 0 & \cdots & 0 & 0 & 0 & \cdots & 0 & 0 & 0\\
-u_n & S_n & -u_n & \cdots & 0 & 0 & 0 & \cdots & 0 & 0 & 0\\
\cdots & \cdots & \cdots & \cdots & \cdots & \cdots & \cdots & \cdots & \cdots & \cdots & \cdots\\
0 & 0 & 0 & \cdots & S_n & -u_n & 0 & \cdots & 0 & 0 & 0\\
0 & 0 & 0 & \cdots & -u_n & S_n & -u_n & \cdots & 0 & 0 & 0\\
0 & 0 & 0 & \cdots & 0 & -u_n & S_n & \cdots & 0 & 0 & 0\\
\cdots & \cdots & \cdots & \cdots & \cdots & \cdots & \cdots & \cdots & \cdots & \cdots & \cdots\\
0 & 0 & 0 & \cdots & 0 & 0 & 0 & \cdots & -u_n & S_n & -u_n\\
0 & 0 & 0 & \cdots & 0 & 0 & 0 & \cdots & 0 & -u_n & S_n-u_n
\end{bmatrix}
\begin{Bmatrix}
A_{n1}\\ A_{n2}\\ A_{n3}\\ \cdots\\ A_{n(\tilde{\imath}-1)}\\ A_{n\tilde{\imath}}\\ A_{n(\tilde{\imath}+1)}\\ \cdots\\ A_{n(m-2)}\\ A_{n(m-1)}\\ A_{nm}
\end{Bmatrix}=
\begin{Bmatrix}
0\\0\\0\\ \cdots\\0\\0\\0\\ \cdots\\0\\0\\0
\end{Bmatrix}, \tag{5.1.29}$$

where

$$H_{i-1}^{*}=\frac{K_{i-1}}{\rho_i A_i}=H,\qquad H_i=\frac{K_i}{\rho_i A_i}=H,\qquad \eta_{in}=\frac{k_n^2}{\rho_i A_i}=\eta_n,\quad i=1,2,3,\cdots m,$$

$$C_{bi}=\sqrt{\frac{E_i I_i}{\rho_i A_i}}=C_b,\qquad C_{si}=\sqrt{\frac{G_i A_i k}{\rho_i I_i}}=C_s,\qquad C_{ri}=\sqrt{\frac{I_i}{A_i}}=C_r\,,\quad i=1,2,3,\cdots m,$$

$$S_n=\frac{\omega_n^4}{C_s^2}-\left[1+C_r^2\left(1+\frac{C_b^2}{C_s^2C_r^4}\right)k_n^2+\frac{1}{C_s^2}(2H-F\eta_n)\right]\omega_n^2+\left[C_b^2k_n^4+(2H-F\eta_n)\left(1+\frac{C_b^2}{C_s^2C_r^2}k_n^2\right)\right],$$

$$u_n=H\left[-\frac{\omega_n^2}{C_s^2}+\left(1+\frac{C_b^2}{C_s^2C_r^2}k_n^2\right)\right].$$

The solutions to the system of homogenous algebraic equations (5.1.26 -5.1.28) are different from trivial ones only if the matrix m x m determinant in the equation (5.1.29) equals zero. In that case, the solution we obtain is a polynomial of the $4m$ -th degree, the solutions to which can be determined only numerically for specific data.

If the connected beam system consists of more than three beams, solutions can be obtained by way of the trigonometric method we used for verifying the analytical solutions in Chapter 4. According to the trigonometric method, Raskovic [28], the unknowns A_{ni} are assumed as

$$A_{n\tilde{\imath}}=N\sin(\tilde{\imath}\varphi),\quad \tilde{\imath}=1,2,3\cdots m. \tag{5.1.30}$$

From substituting (5.1.30) into $\tilde{\imath}$-th equation of the system (5.1.29), for $\tilde{\imath}=1,2,3\cdots m$, it follows that

$$-u_nN\sin(\tilde{\imath}-1)\varphi+S_nN\sin(\tilde{\imath}\varphi)-u_nN\sin(\tilde{\imath}+1)\varphi=0, \tag{5.1.31}$$

i.e.

$$(S_n-2u_n\cos\varphi)N\sin(\tilde{\imath}\varphi)=0, \tag{5.1.32}$$

the equation (5.1.32) is satisfied when $N\neq 0$ and $\sin(\tilde{\imath}\varphi)\neq 0$ as the unknowns $A_{\tilde{\imath}n}\neq 0$, hence it must follow that

$$S_n-2u_n\cos\varphi=0\quad\Rightarrow\quad S_n=2u_n\cos\varphi. \tag{5.1.33}$$

By substituting unknowns S_n and u_n into the equation (5.1.33), we get a frequency equation which is a 4$^{\text{th}}$ degree polynomial for the unknown ω_n. If we substitute $A_{n1}=N\sin\varphi$ and $A_{n2}=N\sin2\varphi$ into the first equation of the system (5.1.29), we have

$$S_nN\sin\varphi-u_nN\sin2\varphi=0\quad\Rightarrow\quad(S_n-2u_n\cos\varphi)N\sin\varphi\equiv 0. \tag{5.1.34}$$

The unknown φ is determined from the last equation of the system (5.1.29). By substituting $A_{(m-1)n}$ and A_{mn}, we get:

$$-u_n N\sin[(m-1)\varphi] + (S_n - u_n)N\sin(m\varphi) = 0, \tag{5.1.35}$$

i.e.

$$Nu_n \sin\left(\frac{\varphi}{2}\right)\cos\left(\frac{2m+1}{2}\varphi\right) = 0. \tag{5.1.36}$$

The solutions to the equation (5.1.36) are

$$sin\left(\frac{\varphi}{2}\right) = 0 \vee cos\left(\frac{2m+1}{2}\varphi\right) = 0 \quad \Rightarrow \quad \varphi_s = \frac{2s-1}{2m+1}\pi, \quad s = 1,2,3,\cdots m, \tag{5.1.37}$$

as $N \neq 0$, $u_n \neq 0$ and $sin\left(\frac{\varphi}{2}\right) \neq 0$. By substituting the solution (5.1.37) into (5.1.33), we get a frequency equation in the following form

$$\frac{\omega_{n,s}^4}{C_s^2} - \left[1 + C_r^2\left(1 + \frac{C_b^2}{C_s^2 C_r^4}\right)k_n^2 + \frac{1}{C_s^2}(2H - F\eta_n)\right]\omega_{n,s}^2 + \left[C_b^2 k_n^4 + (2H - F\eta_n)\left(1 + \frac{C_b^2}{C_s^2 C_r^2}k_n^2\right)\right]$$
$$= 2H\left[-\frac{\omega_{n,s}^2}{C_s^2} + \left(1 + \frac{C_b^2}{C_s^2 C_r^2}k_n^2\right)\right]\cos\left(\frac{2s-1}{2m+1}\pi\right), \tag{5.1.38}$$

i.e.

$$\omega_{n,s}^4 - \left\{C_s^2(R_n + C_r^2 k_n^2) + 4H\sin^2\left[\frac{2s-1}{2(2m+1)}\pi\right] - F\eta_n\right\}\omega_{n,s}^2$$
$$+C_s^2\left\{C_b^2 k_n^4 + 4HR_n\sin^2\left[\frac{2s-1}{2(2m+1)}\pi\right] - F\eta_n R_n\right\} = 0, s = 1,2,3\cdots m, \tag{5.1.39}$$

where

$$R_n = 1 + \frac{C_b^2}{C_s^2 C_r^2}k_n^2.$$

The equation (5.1.39) is biquadratic so the squares of natural frequencies follow in the form

$$\left[\omega_{n,s}^2\right]_l = \frac{1}{2}\left\{\left[C_s^2(R_n + C_r^2 k_n^2) + 4H\sin^2\left(\frac{2s-1}{2(2m+1)}\pi\right) - F\eta_n\right]\right.$$
$$\left.-\sqrt{\left[C_s^2(R_n + C_r^2 k_n^2) + 4H\sin^2\left(\frac{2s-1}{2(2m+1)}\pi\right) - F\eta_n\right]^2 - 4C_s^2\left[C_b^2 k_n^4 + 4HR_n\sin^2\left(\frac{2s-1}{2(2m+1)}\pi\right) - F\eta_n R_n\right]}\right\}, \tag{5.1.40}$$

$$\left[\omega_{n,s}^2\right]_h = \frac{1}{2}\left\{\left[C_s^2(R_n + C_r^2 k_n^2) + 4H\sin^2\left(\frac{2s-1}{2(2m+1)}\pi\right) - F\eta_n\right]\right.$$
$$\left.+\sqrt{\left[C_s^2(R_n + C_r^2 k_n^2) + 4H\sin^2\left(\frac{2s-1}{2(2m+1)}\pi\right) - F\eta_n\right]^2 - 4C_s^2\left[C_b^2 k_n^4 + 4HR_n\sin^2\left(\frac{2s-1}{2(2m+1)}\pi\right) - F\eta_n R_n\right]}\right\}, \tag{5.1.41}$$

$$s = 1,2,3\cdots m.$$

where $\left[\omega_{n,s}\right]_l$ represents a lower and $\left[\omega_{n,s}\right]_h$ a higher natural frequency. Static stability of the system depending on the stiffness of elastic layers can be examined based on the equation (5.1.39). The system will be in a state of indifferent equilibrium if subjected to axial forces under the influence of which the natural frequency of the system equals zero. If we apply this condition ($\omega_{n,s} = 0$), from the equation (5.1.39), it follows

$$C_b^2 k_n^4 + 4HR_n \sin^2\left[\frac{2s-1}{2(2m+1)}\pi\right] - F\eta_n R_n = 0, \quad s = 1,2,3\cdots m. \tag{5.1.42}$$

From the equation (5.1.42), it follows that the minimum value of the solution for unknown axial force F is the critical force of the system of m elastically connected beams corresponding to the n-th mode, ref. Stojanović et al. [*15*]

$$F_b^{kr} = \min_{\substack{n=1,2,3\cdots \\ s=1,2,3\cdots m}} \left\{\frac{C_b^2 k_n^4}{R_n \eta_n} + 4\frac{H}{\eta_n}\sin^2\left[\frac{2s-1}{2(2m+1)}\pi\right]\right\} \Leftrightarrow F_b^{kr} = \min_{\substack{n=1,2,3\cdots \\ s=1,2,3\cdots m}} \left\{\frac{EI\pi^2 n^2}{l^2\left(1+\frac{EI}{GAk}\frac{\pi^2 n^2}{l^2}\right)} + 4\frac{Kl^2}{\pi^2 n^2}\sin^2\left[\frac{2s-1}{2(2m+1)}\pi\right]\right\}, \tag{5.1.43}$$

For $K = 0$ from the equation (5.1.43) it follows that

$$P_n = \frac{EI\pi^2 n^2}{l^2\left(1+\frac{EI}{GAk}\frac{\pi^2 n^2}{l^2}\right)}. \tag{5.1.44}$$

P_n is the critical buckling load of a single Timoshenko beam corresponding to the n-th mode. Its minimum value at which buckling takes place is obtained for n=1

$$P = \frac{EI\pi^2}{\left(1+\frac{EI}{GAk}\frac{\pi^2}{l^2}\right)l^2}. \tag{5.1.45}$$

5.2 Numerical Analysis in the Frequency Domain of the System of Elastically Connected Timoshenko Beams

Numerical analysis compares the results obtained for systems composed of 3, 5, 7 and 9 elastically connected Timoshenko beams with identical material properties

$$E = 1\times 10^{10}\mathrm{Nm}^{-2}, \quad G = 0.417\times 10^{10}\ \mathrm{Nm}^{-2}, \quad k = 5/6, \quad K_0 = 2\times 10^5\mathrm{Nm}^{-2},$$

$$\rho = 2\times 10^3\mathrm{kgm}^{-3}, \quad l = 10\ \mathrm{m}, \quad A = 5\times 10^{-2}\mathrm{m}^2, \quad I = 4\times 10^{-4}\mathrm{m}^4. \tag{5.2.1}$$

Table 5.2.1 shows natural frequencies of the system for different number of elastically connected Timoshenko beams obtained by way of trigonometric method or numerically. It can be concluded that with the increase of the beam number, the lowest natural frequency tends to the value of the frequency of a single beam with no elastic layers.

Table 5.2.1 Natural frequencies $[s^{-1}]$ of elastically connected Timoshenko beams for $n = 1,\ F = 0$ i $m = 3, 5, 7$ i 9

ref.[15]	$[\omega_{n,s}]_l$	Trigonometric method (5.1.40)	Numerical solution to the equation (5.1.29)
$m = 3$	$\omega_{1,1}$	28.0046632875	28.0046632873
	$\omega_{1,2}$	59.1263182936	59.1263182935
	$\omega_{1,3}$	82.9295278423	82.9295278423
$m = 5$	$\omega_{1,1}$	23.4595097487	23.4595097486
	$\omega_{1,2}$	42.0466472348	42.0466472347
	$\omega_{1,3}$	61.7777785430	61.7777785429
	$\omega_{1,4}$	77.7538496710	77.7538496709
	$\omega_{1,5}$	88.0208916175	88.0208916176
$m = 7$	$\omega_{1,1}$	21.8125810709	21.8125810709
	$\omega_{1,2}$	33.9378813493	33.9378813494
	$\omega_{1,3}$	48.8556749524	48.8556749523
	$\omega_{1,4}$	62.9882585212	62.9882585213
	$\omega_{1,5}$	74.9693492803	74.9693492802
	$\omega_{1,6}$	84.0221781219	84.0221781219
	$\omega_{1,7}$	89.6471858944	89.6471858945
$m = 9$	$\omega_{1,1}$	21.0466074643	21.0466074644
	$\omega_{1,2}$	29.4987136192	29.4987136191
	$\omega_{1,3}$	40.9671530516	40.9671530516
	$\omega_{1,4}$	52.7236801181	52.7236801181
	$\omega_{1,5}$	63.6808309227	63.6808309228
	$\omega_{1,6}$	73.2562413513	73.2562413513
	$\omega_{1,7}$	81.0640517350	81.0640517351
	$\omega_{1,8}$	86.8296550265	86.8296550263
	$\omega_{1,9}$	90.3637299233	90.3637299234

Based on the obtained results shown in Table 5.2.1, it can be noted that the difference between numerical and analytical solutions obtained by way of trigonometric method is negligibly small. Let us now consider the influence of axial compression force $\lambda = F/F_b^{cr}$ and the stiffness of elastic layers $K = 0.5K_0,\ K_0,\ 1.5K_0$ on the lowest natural frequency of the system composed of one, three, or five elastically connected Timoshenko beams. Analytical forms of

frequencies based on the expression (5.1.40) for $m = 1, 3, 5$ beams in the first mode are given by

$$\left[\omega_{1,1}^2\right]_l = \frac{1}{2}\left\{\left[C_s^2(R_1 + C_r^2 k_1^2) + 4H\sin^2\frac{\pi}{6} - F\eta_1\right]\right.$$
$$\left. - \sqrt{\left[C_s^2(R_1 + C_r^2 k_1^2) + 4H\sin^2\frac{\pi}{6} - F\eta_1\right]^2 - 4C_s^2\left[C_b^2 k_1^4 + 4HR_1\sin^2\frac{\pi}{6} - F\eta_1 R_1\right]}\right\}, \quad (5.2.2)$$

$$\left[\omega_{1,1}^2\right]_l = \frac{1}{2}\left\{\left[C_s^2(R_1 + C_r^2 k_1^2) + 4H\sin^2\frac{\pi}{14} - F\eta_1\right]\right.$$
$$\left. - \sqrt{\left[C_s^2(R_1 + C_r^2 k_1^2) + 4H\sin^2\frac{\pi}{14} - F\eta_1\right]^2 - 4C_s^2\left[C_b^2 k_1^4 + 4HR_1\sin^2\frac{\pi}{14} - F\eta_1 R_1\right]}\right\}, \quad (5.2.3)$$

$$\left[\omega_{1,1}^2\right]_l = \frac{1}{2}\left\{\left[C_s^2(R_1 + C_r^2 k_1^2) + 4H\sin^2\frac{\pi}{22} - F\eta_1\right]\right.$$
$$\left. - \sqrt{\left[C_s^2(R_1 + C_r^2 k_1^2) + 4H\sin^2\frac{\pi}{22} - F\eta_1\right]^2 - 4C_s^2\left[C_b^2 k_1^4 + 4HR_1\sin^2\frac{\pi}{22} - F\eta_1 R_1\right]}\right\}. \quad (5.2.4)$$

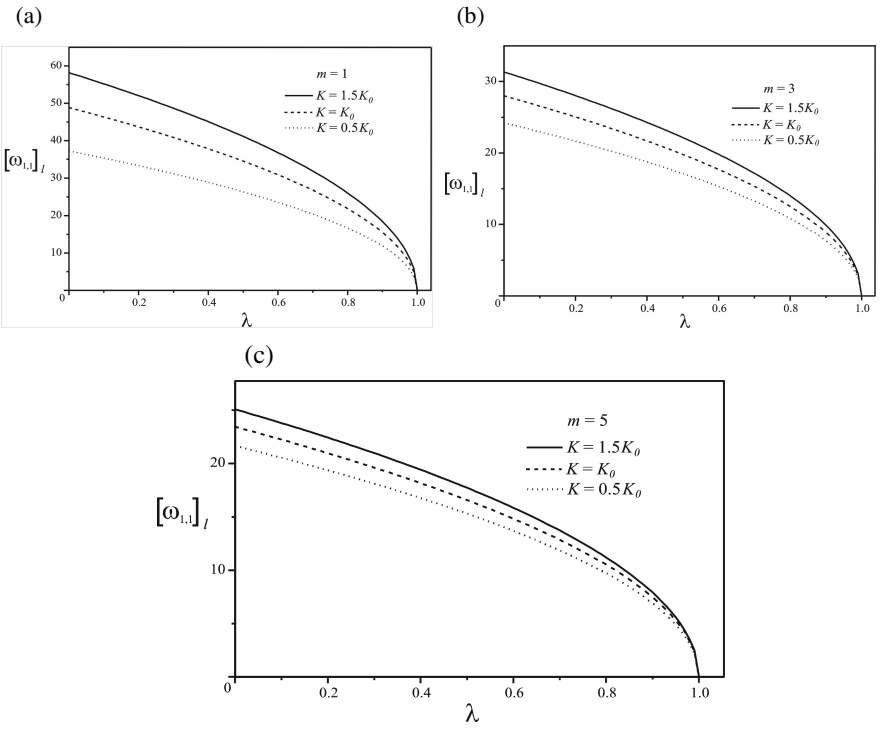

Fig. 5.2.1 The influence of elastic layer stiffness on the lowest natural frequency a) $m = 1$; b) $m = 3$; c) $m = 5$.

Based on the changes in natural frequencies shown in Figure 5.2.1, it can be concluded that the increase of the number of beams results in the decrease of natural frequencies. For the same stiffness of elastic layers in the system with a higher beam number, natural frequencies become close which can be significant in the analysis of geometric non-linear vibration of elastically connected beams. The advantage of derived analytical expressions for the system of elastically connected beams can serve as a starting point for obtaining an insight into the changes in vibrations which occur with the change of geometric and material properties of beams. It is not necessary to create a mathematical model every time – the results are easily obtained by changing physical parameters and the number of elastically connected beams in expressions.

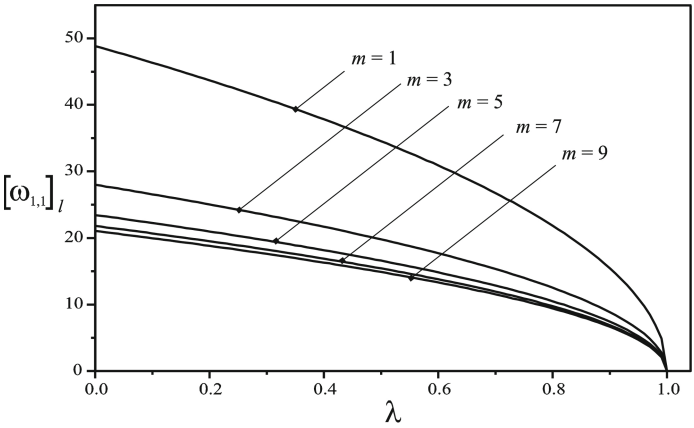

Fig. 5.2.2 The influence of beam number on the lowest natural frequency in the function of axial compression force for $K=K_0$

5.3 Numerical Analysis in the Static Stability Region for the System of Elastically Connected Timoshenko Beams

If we substitute $m = 1,3,5$ in the equation (5.1.42) for minimum values $s = 1$ and $n = 1$, we get analytical expressions for critical buckling force for a system consisting of one, three or five elastically connected Timoshenko beams,

$$F_b^{cr} = \frac{C_b^2 k_1^4}{R_1 \eta_1} + 4\frac{H}{\eta_1}\sin^2\frac{\pi}{6}, \tag{5.3.1}$$

$$F_b^{cr} = \frac{C_b^2 k_1^4}{R_1 \eta_1} + 4\frac{H}{\eta_1}\sin^2\frac{\pi}{14}, \tag{5.3.2}$$

$$F_b^{cr} = \frac{C_b^2 k_1^4}{R_1 \eta_1} + 4\frac{H}{\eta_1}\sin^2\frac{\pi}{22}, \tag{5.3.3}$$

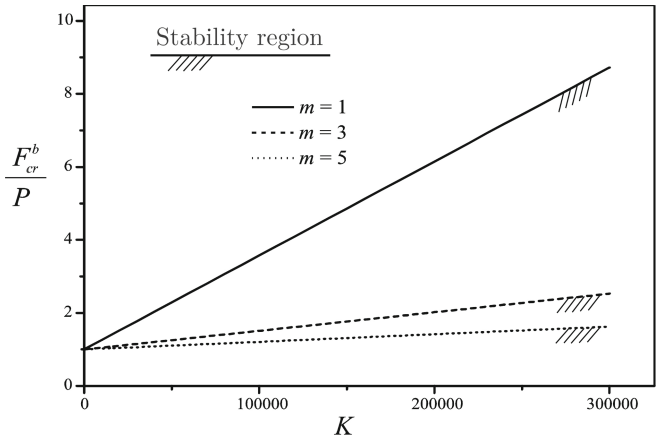

Fig. 5.3.1 The influence of beam number on critical buckling force F_b^{cr} in the function of stiffness of Winkler elastic layers

Figure 5.3.1 shows the static stability regions for a system consisting of one, three or five elastically connected Timoshenko beams. Based on the data shown in Figure 5.3.1, it can be concluded that the system is most stable in case of a single beam on an elastic foundation with the decrease of the region as the number of elastically connected beams rises.

Chapter 6

The Effects of Rotary Inertia and Transverse Shear on Vibrations and Stability of the System of Elastically Connected Reddy-Bickford Beams on Elastic Foundation

Chapters 6 analyzed free vibration of the multiple elastically connected beam system of Reddy-Bickford's type on an elastic foundation under the influence of axial forces with the comparison of the frequency and stability theoretical research for all four types of the beam's theory. Analytical solutions for the natural frequencies and the critical buckling forces are determined by the trigonometric method and verified numerically as in case in the previous chapter. In the case of the Reddy-Bickford's model, it is shown that the natural frequency provides the best solution approximation.

6.1 Free Vibration of the System of Elastically Connected Reddy-Bickford Beams

Let us examine the system of m elastically connected Reddy-Bickford beams of the same length l, under the influence of axial compression forces of the same intensity F, reference [15].

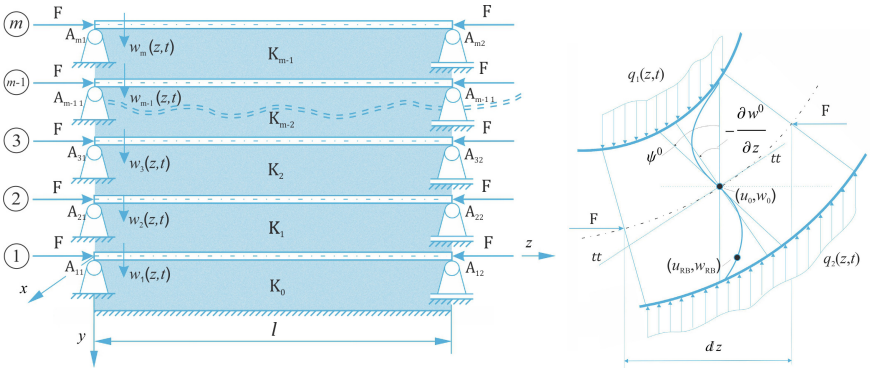

a) b)

Fig. 6.1.1 a) The system of elastically connected beams on an elastic foundation b) Elementary deformed beam part

V. Stojanović and P. Kozić, *Vibrations and Stability of Complex Beam Systems*,
Springer Tracts in Mechanical Engineering, DOI: 10.1007/978-3-319-13767-4_6

Let the functions of longitudinal and transverse motion and the angle between the tangent of the deformed cross-section of the beam on the neutral line of y – axis be $u_{RB\tilde{\imath}}(y,z,t)$, $w_{RB\tilde{\imath}}(y,z)$, $\psi^0_{RB\tilde{\imath}}(z)$, $\tilde{\imath}=1,2,\dots,m$ respectively. For the angle ψ^0_{RB} shown in Figure 6.1.1 b) based on the derived equations in references [15], [29-31], we define the functions of motions as

$$u_{RB\tilde{\imath}}(y,z,t)=u^0_{RB\tilde{\imath}}(z,t)+y\psi^0_{RB\tilde{\imath}}(z,t)-\alpha y^3\left(\psi^0_{RB\tilde{\imath}}(z,t)+\frac{\partial w^0_{RB\tilde{\imath}}(z,t)}{\partial z}\right),$$
$$w_{RB\tilde{\imath}}(y,z,t)=w^0_{RB\tilde{\imath}}(z,t),\qquad \tilde{\imath}=1,2,\dots,m. \tag{6.1.1}$$

Deformation in the function of motions and the relation between the stress and deformation according to Hooke's law are

$$\varepsilon_{z\tilde{\imath}}(y,z,t)=\frac{\partial u^0_{RB\tilde{\imath}}(z,t)}{\partial z}+y\frac{\partial \psi^0_{RB\tilde{\imath}}(z,t)}{\partial z}-\alpha y^3\left(\frac{\partial \psi^0_{RB\tilde{\imath}}(z,t)}{\partial z}+\frac{\partial^2 w^0_{RB\tilde{\imath}}(z,t)}{\partial z^2}\right), \tag{6.1.2}$$

$$\gamma_{zy\tilde{\imath}}(y,z,t)=\psi^0_{RB\tilde{\imath}}(z,t)+\frac{\partial w^0_{RB\tilde{\imath}}(z,t)}{\partial z}-\beta y^2\left(\psi^0_{RB\tilde{\imath}}(z,t)+\frac{\partial w^0_{RB\tilde{\imath}}(z,t)}{\partial z}\right), \tag{6.1.3}$$

$$\begin{Bmatrix}\sigma_{z\tilde{\imath}}\\ \tau_{zy\tilde{\imath}}\end{Bmatrix}=\begin{bmatrix}E_{\tilde{\imath}} & 0\\ 0 & G_{\tilde{\imath}}\end{bmatrix}\begin{Bmatrix}\varepsilon_{z\tilde{\imath}}\\ \gamma_{zy\tilde{\imath}}\end{Bmatrix},\quad \tilde{\imath}=1,2,\dots,m. \tag{6.1.4}$$

Virtual work of inertial forces is

$$\delta W_{in\tilde{\imath}}=-\rho_{\tilde{\imath}}b_{\tilde{\imath}}\int_0^l\int_{-\frac{h_{\tilde{\imath}}}{2}}^{\frac{h_{\tilde{\imath}}}{2}}\left[\frac{\partial^2 w_{RB\tilde{\imath}}(y,z,t)}{\partial t^2}\delta w_{RB\tilde{\imath}}(y,z,t)+\frac{\partial^2 u_{RB\tilde{\imath}}(y,z,t)}{\partial t^2}\delta u_{RB\tilde{\imath}}(y,z,t)\right]dydz. \tag{6.1.5}$$

Virtual work of internal forces is given by

$$\delta W_{V\tilde{\imath}}=-b_{\tilde{\imath}}\int_0^l\int_{-\frac{h_1}{2}}^{\frac{h_1}{2}}\left[\sigma_{z\tilde{\imath}}(z,t)\delta\varepsilon_{z\tilde{\imath}}(z,t)+\tau_{zy\tilde{\imath}}(z,t)\delta\gamma_{zy\tilde{\imath}}(z,t)\right]dydz. \tag{6.1.6}$$

Virtual work of external forces is expressed as

$$\delta W_{ex1}=\int_0^l\left\{\delta w^0_{RB1}(z,t)\left[-K_0w^0_{RB1}(z,t)+K_1\left(w^0_{RB2}(z,t)-w^0_{RB1}(z,t)\right)\right]+\right.$$
$$\left.+F\frac{\partial w^0_{RB1}(z,t)}{\partial z}\frac{\partial\delta w^0_{RB1}(z,t)}{\partial z}\right\}dz, \tag{6.1.7}$$

$$\delta W_{exi}=\int_0^l\left\{\delta w^0_{RBi}(z,t)\left[-K_{i-1}\left(w^0_{RBi}(z,t)-w^0_{RBi-1}(z,t)\right)+K_i\left(w^0_{RBi+1}(z,t)-w^0_{RBi}(z,t)\right)\right]+\right.$$
$$\left.+F\frac{\partial w^0_{RBi}(z,t)}{\partial z}\frac{\partial\delta w^0_{RBi}(z,t)}{\partial z}\right\}dz,\quad i=2,3,\dots,m-1. \tag{6.1.8}$$

$$\delta W_{exm} = \int_0^l \left\{ \delta w_{RBm}^0(z,t) \left[-K_{m-1}\left(w_{RBm}^0(z,t) - w_{RBm-1}^0(z,t) \right) \right] + F + \frac{\partial w_{RBm}^0(z,t)}{\partial z} \frac{\partial \delta w_{RBm}^0(z,t)}{\partial z} \right\} dz, \tag{6.1.9}$$

By substituting the equations (6.1.5-6.1.9) into a general equation of virtual work principle $\delta W_{in\tilde{\imath}} + \delta W_{V\tilde{\imath}} + \delta W_{ex\tilde{\imath}} = 0,\ \tilde{\imath} = 1,2,\dots m,$ and applying the Green's theorem, we get a coupled system of partial differential equations of vibration in the following form

$$C_{w1}^{4,0}\frac{\partial^4 w_1}{\partial z^4} + C_{w1}^{2,2}\frac{\partial^4 w_1}{\partial z^2\,\partial t^2} + C_{w1}^{2,0}\frac{\partial^2 w_1}{\partial z^2} + C_{w1}^{0,2}\frac{\partial^2 w_1}{\partial t^2} + C_{\psi 1}^{1,2}\frac{\partial^3 \psi_1}{\partial z\,\partial t^2} + C_{\psi 1}^{1,0}\frac{\partial \psi_1}{\partial z} + C_{\psi 1}^{3,0}\frac{\partial^3 \psi_1}{\partial z^3} + K_0 w_1 - K_1(w_2 - w_1) = 0, \tag{6.1.10}$$

$$C_{w1}^{3,0}\frac{\partial^3 w_1}{\partial z^3} + C_{w1}^{1,2}\frac{\partial^3 w_1}{\partial z\,\partial t^2} + C_{w1}^{1,0}\frac{\partial w_1}{\partial z} + C_{\psi 1}^{2,0}\frac{\partial^2 \psi_1(z,t)}{\partial z^2} + C_{\psi 1}^{0,2}\frac{\partial^2 \psi_1(z,t)}{\partial t^2} + C_{\psi 1}^{0,0}\psi_1 = 0, \tag{6.1.11}$$

$$C_{wi}^{4,0}\frac{\partial^4 w_i}{\partial z^4} + C_{wi}^{2,2}\frac{\partial^4 w_i}{\partial z^2\,\partial t^2} + C_{wi}^{2,0}\frac{\partial^2 w_i}{\partial z^2} + C_{wi}^{0,2}\frac{\partial^2 w_i}{\partial t^2} + C_{\psi i}^{1,2}\frac{\partial^3 \psi_i}{\partial z\,\partial t^2} + C_{\psi i}^{1,0}\frac{\partial \psi_i}{\partial z} + C_{\psi i}^{3,0}\frac{\partial^3 \psi_i}{\partial z^3} + K_{i-1}(w_i - w_{i-1}) - K_i(w_{i+1} - w_i) = 0, \quad i = 2,3,\cdots m-1, \tag{6.1.12}$$

$$C_{wi}^{3,0}\frac{\partial^3 w_i}{\partial z^3} + C_{wi}^{1,2}\frac{\partial^3 w_i}{\partial z\,\partial t^2} + C_{wi}^{1,0}\frac{\partial w_i}{\partial z} + C_{\psi i}^{2,0}\frac{\partial^2 \psi_i}{\partial z^2} + C_{\psi i}^{0,2}\frac{\partial^2 \psi_i}{\partial t^2} + C_{\psi i}^{0,0}\psi_i = 0, \tag{6.1.13}$$

$$C_{wm}^{4,0}\frac{\partial^4 w_m}{\partial z^4} + C_{wm}^{2,2}\frac{\partial^4 w_m}{\partial z^2\,\partial t^2} + C_{wm}^{2,0}\frac{\partial^2 w_m}{\partial z^2} + C_{wm}^{0,2}\frac{\partial^2 w_m}{\partial t^2} + C_{\psi m}^{1,2}\frac{\partial^3 \psi_m}{\partial z\,\partial t^2} + C_{\psi m}^{1,0}\frac{\partial \psi_m}{\partial z} + C_{\psi m}^{3,0}\frac{\partial^3 \psi_m}{\partial z^3} + K_{m-1}(w_m - w_{m-1}) = 0, \tag{6.1.14}$$

$$C_{wm}^{3,0}\frac{\partial^3 w_m}{\partial z^3} + C_{wm}^{1,2}\frac{\partial^3 w_m}{\partial z\,\partial t^2} + C_{wm}^{1,0}\frac{\partial w_m}{\partial z} + C_{\psi m}^{2,0}\frac{\partial^2 \psi_m}{\partial z^2} + C_{\psi m}^{0,2}\frac{\partial^2 \psi_m}{\partial t^2} + C_{\psi m}^{0,0}\psi_m = 0, \tag{6.1.15}$$

where for $\tilde{\imath} = 1,2,\dots,m$, we have

$$C_{w\tilde{\imath}}^{4,0} = \frac{1}{448}b_{\tilde{\imath}}h_{\tilde{\imath}}{}^7\alpha^2 E_{\tilde{\imath}},\ C_{w\tilde{\imath}}^{2,2} = -\frac{1}{448}b_{\tilde{\imath}}h_{\tilde{\imath}}{}^7\alpha^2\rho_{\tilde{\imath}},\ C_{w}^{2,0} = -\frac{1}{80}b_{\tilde{\imath}}G_{\tilde{\imath}}\beta^2 h_{\tilde{\imath}}{}^5 + \frac{1}{6}b_{\tilde{\imath}}G_{\tilde{\imath}}\beta h_{\tilde{\imath}}{}^3 - b_{\tilde{\imath}}G_{\tilde{\imath}}h_{\tilde{\imath}} + F,$$
$$C_{w\tilde{\imath}}^{0,2} = b_{\tilde{\imath}}h_{\tilde{\imath}}\rho_{\tilde{\imath}}, C_{\psi\tilde{\imath}}^{1,2} = \frac{1}{80}b_{\tilde{\imath}}h_{\tilde{\imath}}{}^5\alpha\rho_{\tilde{\imath}} - \frac{1}{448}b_{\tilde{\imath}}h_{\tilde{\imath}}{}^7\alpha^2\rho_{\tilde{\imath}}, C_{\psi\tilde{\imath}}^{1,0} = -\frac{1}{80}b_{\tilde{\imath}}G_{\tilde{\imath}}\beta^2 h_{\tilde{\imath}}{}^5 + \frac{1}{6}b_{\tilde{\imath}}G_{\tilde{\imath}}\beta h_{\tilde{\imath}}{}^3 - b_{\tilde{\imath}}G_{\tilde{\imath}}h_{\tilde{\imath}},$$
$$C_{\psi\tilde{\imath}}^{3,0} = \frac{1}{448}b_{\tilde{\imath}}h_{\tilde{\imath}}{}^7\alpha^2 E_{\tilde{\imath}} - \frac{1}{80}b_{\tilde{\imath}}h_{\tilde{\imath}}{}^5\alpha E_{\tilde{\imath}}, C_{w\tilde{\imath}}^{3,0} = \frac{1}{80}b_{\tilde{\imath}}h_{\tilde{\imath}}{}^5\alpha E_{\tilde{\imath}} - \frac{1}{448}b_{\tilde{\imath}}h_{\tilde{\imath}}{}^7\alpha^2 E_{\tilde{\imath}},$$
$$C_{w\tilde{\imath}}^{1,2} = \frac{1}{448}b_{\tilde{\imath}}h_{\tilde{\imath}}{}^7\alpha^2\rho - \frac{1}{80}b_{\tilde{\imath}}h_{\tilde{\imath}}{}^5\alpha\rho_{\tilde{\imath}},$$
$$C_{w\tilde{\imath}}^{1,0} = \frac{1}{80}b_{\tilde{\imath}}G_{\tilde{\imath}}\beta^2 h_{\tilde{\imath}}{}^5 - \frac{1}{6}b_{\tilde{\imath}}G_{\tilde{\imath}}\beta h_{\tilde{\imath}}{}^3 + b_{\tilde{\imath}}G_{\tilde{\imath}}h_{\tilde{\imath}}, C_{\psi\tilde{\imath}}^{2,0} = -\frac{1}{448}b_{\tilde{\imath}}\alpha^2 E_{\tilde{\imath}}h_{\tilde{\imath}}{}^7 + \frac{1}{40}b_{\tilde{\imath}}\alpha E_{\tilde{\imath}}h_{\tilde{\imath}}{}^5 - \frac{1}{12}b_{\tilde{\imath}}E_{\tilde{\imath}}h_{\tilde{\imath}}{}^3,$$
$$C_{\psi\tilde{\imath}}^{0,2} = \frac{1}{448}b_{\tilde{\imath}}\alpha^2\rho_{\tilde{\imath}}h_{\tilde{\imath}}{}^7 - \frac{1}{40}b_{\tilde{\imath}}\alpha\rho_{\tilde{\imath}}h_{\tilde{\imath}}{}^5 + \frac{1}{12}b_{\tilde{\imath}}\rho_{\tilde{\imath}}h_1{}^3,\ C_{\psi\tilde{\imath}}^{0,0} = \frac{1}{80}b_{\tilde{\imath}}\beta^2 G_{\tilde{\imath}}h_{\tilde{\imath}}{}^5 - \frac{1}{6}b_{\tilde{\imath}}\beta G_{\tilde{\imath}}h_{\tilde{\imath}}{}^3 + b_{\tilde{\imath}}G_{\tilde{\imath}}h_{\tilde{\imath}}, \tag{6.1.16}$$

For the elimination of the variable ψ_m we use an application developed within the *Mathematica* 9-software – Appendix 6.1.1. After applying the software and eliminating the variable ψ_m, the system of $2m$ partial differential equations (6.1.10-6.1.15) is reduced to the system of m partial differential equations in the form

$$C(1)_{w1}^{6,0}\frac{\partial^6 w_1}{\partial z^6}+C(1)_{w1}^{4,2}\frac{\partial^6 w_1}{\partial z^4\partial t^2}+C(1)_{w1}^{4,0}\frac{\partial^4 w_1}{\partial z^4}+C(1)_{w1}^{2,4}\frac{\partial^6 w_1}{\partial z^2\partial t^4}+C(1)_{w1}^{2,2}\frac{\partial^4 w_1}{\partial z^2\partial t^2}+C(1)_{w2}^{2,0}\frac{\partial^2 w_2}{\partial z^2}$$

$$+C(1)_{w1}^{2,0}\frac{\partial^2 w_1}{\partial z^2}+C(1)_{w1}^{0,4}\frac{\partial^4 w_1}{\partial t^4}+C(1)_{w2}^{0,2}\frac{\partial^2 w_2}{\partial t^2}+C(1)_{w1}^{0,2}\frac{\partial^2 w_1}{\partial t^2}+(K_0+K_1)w_1-K_1w_2=0, \quad (6.1.17)$$

$$C(i)_{wi}^{6,0}\frac{\partial^6 w_i}{\partial z^6}+C(i)_{wi}^{4,2}\frac{\partial^6 w_i}{\partial z^4\partial t^2}+C(i)_{w\,i+1}^{4,0}\frac{\partial^4 w_{i+1}}{\partial z^4}+C(i)_{w\,i+1}^{2,4}\frac{\partial^6 w_i}{\partial z^4\partial t^2}+C(i)_{wi}^{2,2}\frac{\partial^2 w_i}{\partial z^2\partial t^2}+C(i)_{wi}^{4,0}\frac{\partial^4 w_i}{\partial z^4}$$

$$+C(i)_{w\,i+1}^{2,0}\frac{\partial^2 w_{i+1}}{\partial z^2}+C(i)_{wi}^{2,0}\frac{\partial^2 w_i}{\partial z^2}+C(i)_{w\,i-1}^{2,0}\frac{\partial^2 w_{i-1}}{\partial z^2}+C(i)_{wi}^{0,4}\frac{\partial^4 w_i}{\partial t^4}+C(i)_{w\,i+1}^{0,2}\frac{\partial^2 w_{i+1}}{\partial t^2}$$

$$+C(i)_{wi}^{0,2}\frac{\partial^2 w_i}{\partial t^2}+C(i)_{w\,i-1}^{0,2}\frac{\partial^2 w_{i-1}}{\partial t^2}-K_{i-1}w_{i-1}+(K_{i-1}+K_i)w_i-K_iw_{i+1}=0,\ \ i=2,3,\cdots m-1, \quad (6.1.18)$$

$$C(m)_{wm}^{6,0}\frac{\partial^6 w_m}{\partial z^6}+C(m)_{wm}^{4,2}\frac{\partial^6 w_m}{\partial z^4\partial t^2}+C(m)_{wm}^{4,0}\frac{\partial^4 w_m}{\partial z^4}+C(m)_{wm}^{2,4}\frac{\partial^6 w_1}{\partial z^2\partial t^4}+C(m)_{wm}^{2,2}\frac{\partial^2 w_m}{\partial z^2\partial t^2}$$

$$+C(m)_{wm}^{2,0}\frac{\partial^2 w_m}{\partial z^2}+C(m)_{w\,m-1}^{2,0}\frac{\partial^2 w_{m-1}}{\partial z^2}+C(m)_{w\,m}^{0,4}\frac{\partial^4 w_m}{\partial t^4}+C(m)_{wm}^{0,2}\frac{\partial^2 w_m}{\partial t^2}+C(m)_{wm-1}^{0,2}\frac{\partial^2 w_{m-1}}{\partial t^2}$$

$$-K_{m-1}w_{m-1}+K_{m-1}w_m=0. \quad (6.1.19)$$

The simplified form of the coefficients $C(\tilde{\imath})_{w\tilde{\imath}}^{*,*}$, $\tilde{\imath}=1,2,\dots,m$ is given in Appendix 6.1.2.

Let us assume that, as in the previous chapter for the case of the Timoshenko connected beam system, the beams have identical material and geometric properties.

$$A_i=A,\quad E_i=E,\quad G_i=G,\qquad K_{i-1}=K,\qquad K_m=0,\quad \rho_i=\rho\,,\tilde{\imath}=1,2,3,\cdots m. \quad (6.1.20)$$

Initial and boundary conditions of simply supported beams based on $(2.3.22-2.3.24)$ are

$$w_{\tilde{\imath}}(z,0)=w_{\tilde{\imath}0}(z),\qquad \dot{w}_{\tilde{\imath}}(z,0)=v_{\tilde{\imath}0}(z),\qquad \psi_{\tilde{\imath}}(z,0)=\psi_{\tilde{\imath}0}(z),\qquad \dot{\psi}_{\tilde{\imath}}(z,0)=\omega_{\tilde{\imath}0}(z),$$

$$w_{\tilde{\imath}}(0,t)=w_{\tilde{\imath}}(l,t)=w''_{\tilde{\imath}}(0,t)=w''_{\tilde{\imath}}(l,t)=0,\qquad \tilde{\imath}=1,2,3\cdots m. \quad (6.1.21)$$

If we assume harmonic beam movement, transverse beam motions can be written as the product of mode shape functions and unknown time functions in the following form

$$w_{\tilde{\imath}}(z,t)=\sum_{n=1}^{\infty}Z_n(z)T_{\tilde{\imath}n}(t),\qquad T_{\tilde{\imath}n}=A_{\tilde{\imath}n}e^{j\omega_n t}\,,\quad \tilde{\imath}=1,2,3,\cdots m,\qquad j=\sqrt{-1}. \quad (6.1.22)$$

The function Z_n meets boundary conditions for simply supported beams if expressed as

$$Z_n(z) = \sin(k_n z), \qquad k_n = n\pi/l, \qquad n = 1, 2, 3, \cdots. \tag{6.1.23}$$

If we substitute the assumed transverse motions (6.1.22) into equations (6.1.17-6.1.19), we obtain the homogeneous system of algebraic equations for unknowns $A_{n1},\ A_{n2},\ A_{n3},\ \cdots\ A_{nm}$ in the form

$$\begin{bmatrix} S_n & -u_n & 0 & \cdots & 0 & 0 & 0 & \cdots & 0 & 0 & 0 \\ -u_n & S_n & -u_n & \cdots & 0 & 0 & 0 & \cdots & 0 & 0 & 0 \\ \cdots & \cdots & \cdots & \cdots & \cdots & \cdots & \cdots & \cdots & \cdots & \cdots & \cdots \\ 0 & 0 & 0 & \cdots & S_n & -u_n & 0 & \cdots & 0 & 0 & 0 \\ 0 & 0 & 0 & \cdots & -u_n & S_n & -u_n & \cdots & 0 & 0 & 0 \\ 0 & 0 & 0 & \cdots & 0 & -u_n & S_n & \cdots & 0 & 0 & 0 \\ \cdots & \cdots & \cdots & \cdots & \cdots & \cdots & \cdots & \cdots & \cdots & \cdots & \cdots \\ 0 & 0 & 0 & \cdots & 0 & 0 & 0 & \cdots & -u_n & S_n & -u_n \\ 0 & 0 & 0 & \cdots & 0 & 0 & 0 & \cdots & 0 & -u_n & S_n - u_n \end{bmatrix} \begin{Bmatrix} A_{n1} \\ A_{n2} \\ A_{n3} \\ \cdots \\ A_{n(\bar{\imath}-1)} \\ A_{n\bar{\imath}} \\ A_{n(\bar{\imath}+1)} \\ \cdots \\ A_{n(m-2)} \\ A_{n(m-1)} \\ A_{nm} \end{Bmatrix} = \begin{Bmatrix} 0 \\ 0 \\ 0 \\ \cdots \\ 0 \\ 0 \\ 0 \\ \cdots \\ 0 \\ 0 \\ 0 \end{Bmatrix}, \tag{6.1.24}$$

where

$$S_n = \left(C_{(4)S}\omega_n^4 + C_{(2)S}\omega_n^2 + C_{(0)S}\right), \qquad u_n = C_{(2)u}\omega_n^2 + C_{(0)u}, \tag{6.1.25}$$

$$C_{(4)S} = -3bh^3\rho^2\left\{\alpha h^2\left[\alpha h^2\left(h^2 {k_n}^2 + 75\right) - 840\right] + 2800\right\},$$

$$C_{(2)S} = h\rho\{b[3Eh^2{k_n}^2[\alpha h^2(2\alpha h^4{k_n}^2 + 75\alpha h^2 - 840) + 2800] + 35G[\beta h^2(3\beta h^2 - 40) + 240)(h^2{k_n}^2 + 12)] - 15h[3\alpha h^2(5\alpha h^2 - 56) + 560](F{k_n}^2 - 2K)\},$$

$$C_{(0)S} = -3\alpha^2 bE^2h^9{k_n}^6 + 5Eh^2{k_n}^4\{3F[3\alpha h^2(5\alpha h^2 - 56) + 560] - 7bGh[\beta h^2(3\beta h^2 - 40) + 240]\} - 30K\left\{Eh^2{k_n}^2[3\alpha h^2(5\alpha h^2 - 56) + 560] + 28G[\beta h^2(3\beta h^2 - 40) + 240]\right\} + 420FGk_n{}^2[\beta h^2(3\beta h^2 - 40) + 240],$$

$$C_{(2)u} = 15h^2K\rho[3\alpha h^2(5\alpha h^2 - 56) + 560],$$
$$C_{(0)u} = -15K\left\{Eh^2{k_n}^2[3\alpha h^2(5\alpha h^2 - 56) + 560] + 28G[\beta h^2(3\beta h^2 - 40) + 240]\right\}.$$

The solutions to the homogeneous system (6.1.24) are different from trivial ones only if the matrix m x m determinant in the equation (6.1.24) equals zero. In that case, as a solution a polynomial of the $4m$-th degree is obtained, the solutions of which can be determined only numerically for specific data. The solution we obtained in case of m elastically connected Timoshenko beams shall be used for forming a trigonometric frequency equation from the following relations

$$S_n - 2u_n\cos\varphi = 0 \quad \Rightarrow \quad S_n = 2u_n\cos\varphi, \quad \varphi(s,m) = \frac{2s-1}{2m+1}\pi, \quad s = 1,2,3,\cdots m, \tag{6.1.26}$$

where m is the number of elastically connected beams while s represents the ordinal number of frequency. From the relations (6.1.25) and (6.1.26) this follows

$$\left(C_{(4)S}\omega_n^4 + C_{(2)S}\omega_n^2 + C_{(0)S}\right) = -2\left(C_{(2)u}\omega_n^2 + C_{(0)u}\right)\cos\left(\frac{2s-1}{2m+1}\pi\right), \quad (6.1.27)$$

i.e. the biquadratic equation in the form

$$C_{(4)S}\omega_n^4 + \left[C_{(2)S} + 2C_{(2)u}\cos\left(\frac{2s-1}{2m+1}\pi\right)\right]\omega_n^2 + C_{(0)S} + 2C_{(0)u}\cos\left(\frac{2s-1}{2m+1}\pi\right) = 0. \quad (6.1.28)$$

From the expression (6.1.27) follow the solutions given as the squares of natural frequencies

$$\left[\omega_{n,s}^2\right]_l = \frac{-\left[C_{(2)S} + 2C_{(2)u}\cos\left(\frac{2s-1}{2m+1}\pi\right)\right]}{2C_{(4)S}} - \frac{\sqrt{\left[C_{(2)S} + 2C_{(2)u}\cos\left(\frac{2s-1}{2m+1}\pi\right)\right]^2 - 4C_{(4)S}\left[C_{(0)S} + 2C_{(0)u}\cos\left(\frac{2s-1}{2m+1}\pi\right)\right]}}{2C_{(4)S}}, \quad (6.1.29)$$

$$\left[\omega_{n,s}^2\right]_h = \frac{-\left[C_{(2)S} + 2C_{(2)u}\cos\left(\frac{2s-1}{2m+1}\pi\right)\right]}{2C_{(4)S}} + \frac{\sqrt{\left[C_{(2)S} + 2C_{(2)u}\cos\left(\frac{2s-1}{2m+1}\pi\right)\right]^2 - 4C_{(4)S}\left[C_{(0)S} + 2C_{(0)u}\cos\left(\frac{2s-1}{2m+1}\pi\right)\right]}}{2C_{(4)S}}, s = 1,2,3\cdots m. \quad (6.1.30)$$

where $\left[\omega_{n,s}\right]_l$ represents a lower and $\left[\omega_{n,s}\right]_h$ a higher natural frequency. Static stability of the system depending on the stiffness of elastic layers may be examined based on the equation (6.1.27). The system shall be in the state of indifferent equilibrium when affected by axial forces under the influence of which the natural frequency of the system equals zero. If we apply this condition ($\omega_n = 0$), from the equation (6.1.27) it follows that the minimum value of the solution for the unknown axial force F is the critical force of the system of m elastically connected beams which corresponds to the n-th mode and is expressed as

$$F_b^{cr} = \min_{\substack{n=1,2,3\cdots \\ s=1,2,3\cdots m}} \frac{EI_x k_n^2(Eh^2k_n^2 + 840G)}{85Eh^2k_n^2 + 840G} + \frac{2K}{k_n^2}\left[1 - \cos\left(\frac{2s-1}{2m+1}\pi\right)\right], s = 1,2,3\cdots m. \quad (6.1.31)$$

For $K = 0$, this follows from the equation (6.1.30)

$$P_n = \frac{EI_x k_n^2(Eh^2k_n^2 + 840G)}{85Eh^2k_n^2 + 840G}, \quad (6.1.32)$$

In the expression (6.1.31) I_x and P_n represent the moment of inertia of the beam's cross-section for x–axis and the critical buckling load of a single Reddy-Bickford

beam which corresponds to the *n*-th mode. Its minimum value at which buckling occurs is obtained for *n*=1, ref. [31], and equals

$$P = \frac{EI\pi^2\left(840G + \frac{Eh^2\pi^2}{l^2}\right)}{l^2\left(840G + \frac{85Eh^2\pi^2}{l^2}\right)}. \tag{6.1.33}$$

6.2 Numerical Analysis and the Results in the Static and Frequency Domain for the System of Elastically Connected Reddy-Bickford's Beams

In the numerical analysis of the system, the results for 3, 5, 7 and 9 elastically connected beams with the same material properties were compared to show the significance of taking into account the effects of rotary inertia and the transverse shear particularly in thicker beams.

$$E = 1\times10^{10}\mathrm{Nm}^{-2}, \nu = 0.34, G = \frac{E}{2(1+\nu)}, k = \frac{5+5\nu}{6+5\nu} \text{ ref. [24]}, \quad K = K_0 = K_1 = 2\times10^5\mathrm{Nm}^{-2}$$

$$\rho = 2\times10^3\mathrm{kgm}^{-3}, \ A = 5\times10^{-2}\mathrm{m}^2 \ I = 4\times10^{-4}\mathrm{m}^4 \tag{6.2.1}$$

$$l = 10\ \mathrm{m}, \quad b = \frac{1}{8}\sqrt{\frac{5}{3}}\mathrm{m}, \qquad h_1 = \frac{2}{5}\sqrt{\frac{3}{5}}\mathrm{m}.$$

Tables 6.2.1-6.2.3 show the values of natural frequencies of the system in the function of the number of elastically connected beams, their thickness, the stiffness of Winkler's layers and vibration modes. By eliminating the effects of transverse shear and rotary inertia with transverse shear from the equation system (5.1.29) provided that the beams have the same material properties and are connected by elastic Winkler layers with the same stiffness, we obtain the expressions for natural frequencies of elastically connected Rayleigh and Euler beams respectively as

$$Rayleigh \quad \left[\omega_{n,s}^2\right]_l = \sqrt{\frac{C_b^2k_n^4 - F\eta^2 + 2H\left[1-\cos\left(\frac{2s-1}{2(2m+1)}\pi\right)\right]}{1+C_r^2k_n^2}}, \tag{6.2.2}$$

$$Euler \quad \left[\omega_{n,s}^2\right]_l = \sqrt{\frac{EIk_n^4 - Fk_n^2 + 2K\left[1-\cos\left(\frac{2s-1}{2(2m+1)}\pi\right)\right]}{\rho A}}. \tag{6.2.3}$$

Based on analytical expressions (5.1.40) for the frequencies of Timoshenko beams and (6.1.28) for Reddy-Bickford beams as well as the expressions (6.2.2) and (6.2.3), we obtain the values of natural frequencies as shown in the tables (6.2.1-6.2.3).

Table 6.2.1 Natural frequencies $[s^{-1}]$ of elastically connected beams $n = 1,\ h = h_1,\ K = K_0,\ F = 0$

	ω	Euler	Rayleigh	Timoshenko	Reddy – Bickford
$m = 3$	$\omega_{1,1}$	28.031426872	28.020367058	28.003561651	28.002821765
	$\omega_{1,2}$	59.157016729	59.133676296	59.125802235	59.125455645
	$\omega_{1,3}$	82.967436814	82.934701967	82.929164958	82.928921239
$m = 5$	$\omega_{1,1}$	23.487538604	23.478271583	23.458193420	23.457309327
	$\omega_{1,2}$	42.073666685	42.057066497	42.045916431	42.045425613
	$\omega_{1,3}$	61.809198434	61.784811580	61.777285278	61.776953996
	$\omega_{1,4}$	77.790079162	77.759387044	77.753461310	77.753200481
	$\omega_{1,5}$	88.060493386	88.025749070	88.020550942	88.020322140
$m = 7$	$\omega_{1,1}$	21.841381852	21.832764322	21.811164921	21.810213778
	$\omega_{1,2}$	33.964222155	33.950821553	33.936973666	33.936364049
	$\omega_{1,3}$	48.883907005	48.864619833	48.855047581	48.854626231
	$\omega_{1,4}$	63.020016749	62.995152167	62.987775034	62.987450318
	$\omega_{1,5}$	75.004695464	74.975102320	74.968945793	74.968674806
	$\omega_{1,6}$	84.060447236	84.027281140	84.021820224	84.021579855
	$\omega_{1,7}$	89.687335754	89.651949566	89.646851796	89.646627411
$m = 9$	$\omega_{1,1}$	21.075842819	21.067527333	21.045139576	21.044153681
	$\omega_{1,2}$	29.525266456	29.513617246	29.497668145	29.496965979
	$\omega_{1,3}$	40.994024901	40.977850686	40.966402718	40.965898783
	$\omega_{1,4}$	52.752769268	52.731955634	52.723099701	52.722709887
	$\omega_{1,5}$	63.712785077	63.687647162	63.680352865	63.680031795
	$\omega_{1,6}$	73.291052064	73.262135039	73.255828000	73.255550387
	$\omega_{1,7}$	81.101350153	81.069351570	81.063680034	81.063430394
	$\omega_{1,8}$	86.868857490	86.834583335	86.829309382	86.829077242
	$\omega_{1,9}$	90.404122311	90.368453315	90.363398650	90.363176162

Table 6.2.2 Natural frequencies $[s^{-1}]$ of elastically connected beams $n = 1,\ h = 5h_1,$ $K = K_0,\ F = 0$

	ω	Euler	Rayleigh	Timoshenko	Reddy – Bickford
$m = 3$	$\omega_{1,1}$	99.096589290	98.132790386	95.40454845252	95.29121980836
	$\omega_{1,2}$	101.798292501	100.808217227	98.16012190987	98.05020502668
	$\omega_{1,3}$	105.069981178	104.048085939	101.49149714614	101.3854652178
$m = 5$	$\omega_{1,1}$	98.860076494	97.898577878	95.16310932326	95.04947262192
	$\omega_{1,2}$	100.085066399	99.111653711	96.41324130255	96.30118348187
	$\omega_{1,3}$	102.112963098	101.119827384	98.48078910939	98.37125723554
	$\omega_{1,4}$	104.274834518	103.260672759	100.68237420869	100.57542156451
	$\omega_{1,5}$	105.895759734	104.865833094	102.33144489069	102.22635387173
$m = 7$	$\omega_{1,1}$	98.784568748	97.823804509	95.08602145955	94.97228608059
	$\omega_{1,2}$	99.467057400	98.499655377	95.78266327808	95.66981405117
	$\omega_{1,3}$	100.702080928	99.722667247	97.04257516993	96.93129725168
	$\omega_{1,4}$	102.260873909	101.266299636	98.63149925523	98.52214749443
	$\omega_{1,5}$	103.865888042	102.855703637	100.26610997272	100.15867806020
	$\omega_{1,6}$	105.243591674	104.220007925	101.66811549425	101.56228266034
	$\omega_{1,7}$	106.168476816	105.135897770	102.60876553273	102.50398190177
$m = 9$	$\omega_{1,1}$	98.751304096	97.790863384	95.05205955721	94.93828065546
	$\omega_{1,2}$	99.183315645	98.218673253	95.49307250817	95.37985643507
	$\omega_{1,3}$	99.995419125	99.022878333	96.32178515768	96.20961317796
	$\omega_{1,4}$	101.091803642	100.108599575	97.43996296681	97.32917248273
	$\omega_{1,5}$	102.346693288	101.351284348	98.71893719109	98.60968968300
	$\omega_{1,6}$	103.620931732	102.613129736	100.01672755385	99.90900666616
	$\omega_{1,7}$	104.778182986	103.759125733	101.19460836013	101.08824024895
	$\omega_{1,8}$	105.698729940	104.670719582	102.13106586866	102.02575174257
	$\omega_{1,9}$	106.289994339	105.256233431	102.73232232681	102.62767513291

Table 6.2.3 Natural frequencies $[s^{-1}]$ of elastically connected beams $n = 1,\ h = h_1,\ K = 2K_0,\ F = 0$

	ω	Euler	Rayleigh	Timoshenko	Reddy – Bickford
$m = 3$	$\omega_{1,1}$	34.378560483	34.364996403	34.351317052	34.350714857
	$\omega_{1,2}$	81.298640164	81.266563741	81.260906711	81.260657710
	$\omega_{1,3}$	115.661379807	115.615745547	115.611878846	115.611708644
$m = 5$	$\omega_{1,1}$	26.715025271	26.704484843	26.686845653	26.686069033
	$\omega_{1,2}$	56.131546322	56.109399590	56.101089263	56.100723467
	$\omega_{1,3}$	85.153494690	85.119897332	85.114510608	85.114273505
	$\omega_{1,4}$	108.226412987	108.183712197	108.179551202	108.179368048
	$\omega_{1,5}$	122.962045472	122.913530730	122.909919911	122.9097609709
$m = 7$	$\omega_{1,1}$	23.758273470	23.748899630	23.729051486	23.728177531
	$\omega_{1,2}$	43.789272763	43.771995681	43.761288976	43.760817679
	$\omega_{1,3}$	66.254330908	66.228190226	66.221185217	66.220876882
	$\omega_{1,4}$	86.910348394	86.876057868	86.870786589	86.870554567
	$\omega_{1,5}$	104.219826900	104.178706910	104.174370694	104.174179828
	$\omega_{1,6}$	117.229182437	117.182929599	117.179120402	117.178952731
	$\omega_{1,7}$	125.291659839	125.242225946	125.238690813	125.2385352044
$m = 9$	$\omega_{1,1}$	22.332620467	22.323809119	22.302687139	22.301757041
	$\omega_{1,2}$	36.794651167	36.780133817	36.767361943	36.766799711
	$\omega_{1,3}$	54.510400761	54.488893652	54.480329887	54.479952934
	$\omega_{1,4}$	71.944930098	71.916544187	71.910113991	71.909830958
	$\omega_{1,5}$	87.914740518	87.880053709	87.874846414	87.874617208
	$\omega_{1,6}$	101.752249416	101.71210301	101.707652291	101.7074563850
	$\omega_{1,7}$	112.983280308	112.938702692	112.934734250	112.9345595710
	$\omega_{1,8}$	121.254939855	121.207098652	121.203430623	121.2032691656
	$\omega_{1,9}$	126.317751317	126.267912579	126.264409944	126.2642557652

Figure 6.2.1 shows the change in natural frequencies of the system according to the influence of axial compression forces defined by a non-dimensional parameter $\lambda = F/F_b^{kr}$ and the number of elastically connected beams of different types: Euler, Rayleigh, Timoshenko and Reddy-Bickford. It can be inferred that with the increase of the beam number, natural frequency of the system decreases. It can also be noted that there is a significant difference in the approximate solutions depending on the beam type, or the beam theory used. In the numerical experiment the results of which are shown in a set of Figures 6.2.7a-f, the thicker beam was considered where the influence of rotary inertia and transverse shear is stronger, hence the difference in the approximate solutions for the first natural frequency. In the Figure 6.2.1 b) in case of three elastically connected beams, it can be seen that the influence of transverse shear is minor compared to the

influence of transverse shear and rotary inertia, i.e. the Rayleigh model provides good approximate solutions, which is not the case for more than three elastically connected beams where the effects of transverse shear increase, hence better approximation of solutions are provided by Timoshenko and Reddy-Bickford model. It can be noted that with the increase of the axial compression forces, the differences in approximate solutions decrease. Thus, in the case of a single beam on an elastic foundation affected by axial forces 70% higher than the critical value, the effects of transverse shear on natural frequencies vanish, therefore, in such cases Rayleigh model may be used for thicker beams.

Figures 6.2.2a-b show the change in natural frequencies of the system according to the effects of axial compression forces of Reddy-Bickford beams depending on their number. Figures 6.2.3 and 6.2.4 show the changes in natural frequencies of the system depending on beams' thickness defined by a non-dimensional parameter $\xi = h/l.$. In Figure 6.2.3 a) it can be noted that all the theories give roughly the same values for approximate results up to the value $\xi = 0.2$, but when it comes to cross-sections of greater thickness, the differences in approximate solution increase. With the increase of the number of beams, the models of the Timoshenko and Reddy-Bickford system provide very similar results. In case of a single beam on an elastic foundation, Figure 6.2.3 a), Reddy-Bickford's model provides the best solution approximation.

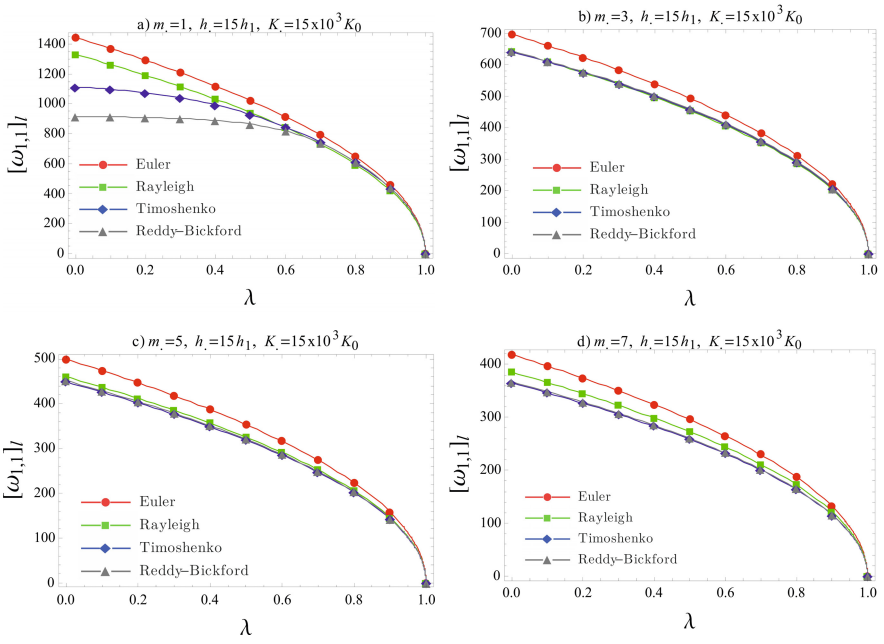

Fig. 6.2.1 The influence of axial compression λ change on the lowest natural frequency of the beam with a thickness of h=$15h_1$ a) $m = 1$; b) $m = 3$; c) $m = 5$ d) $m = 7$;

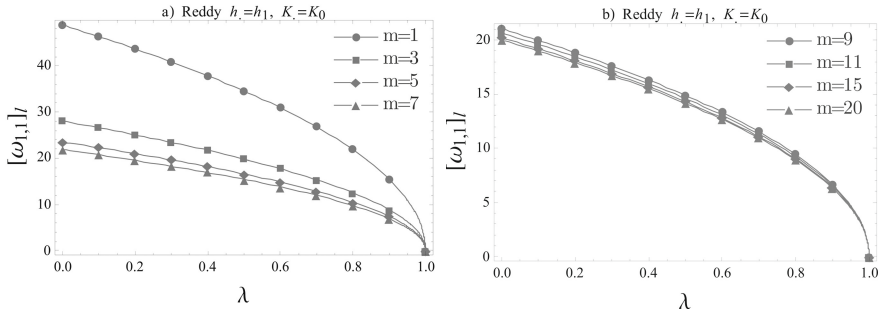

Fig. 6.2.2 The influence of compressive axial forces λ on the lowest natural frequency of the beam with a thickness of $h=h_1$ a) $m = 1, 3, 5, 7$; b) $m = 9, 11, 15, 20$

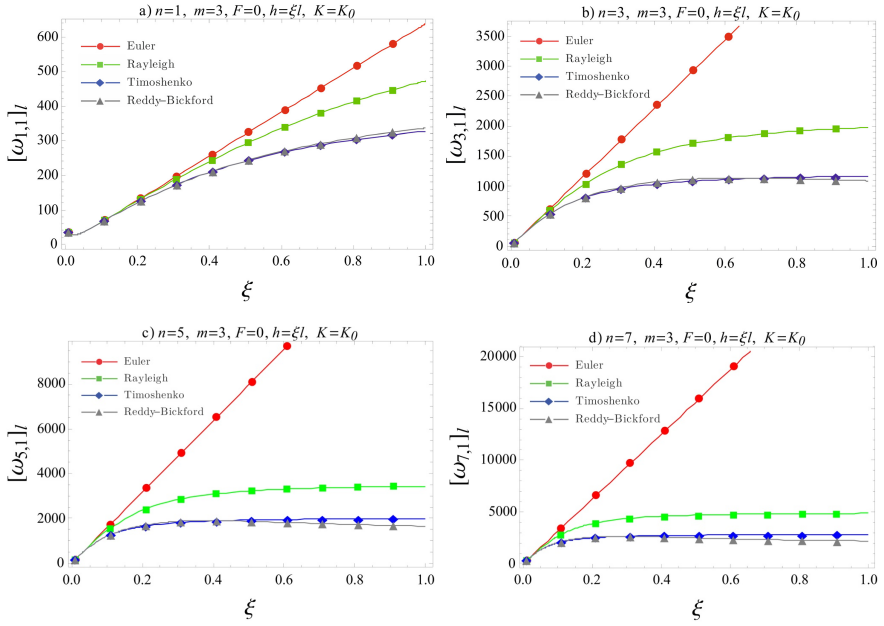

Fig. 6.2.3 The influence of the parameter ξ on the beam's lowest natural frequency a) $m = 1$; b) $m = 3$; c) $m = 5$; d) $m = 7$

Figures 6.2.4a show the region of beam thickness in which all theories provide good approximations according to the vibration mode for the case of three elastically connected beams. It can also be noted that with the increase of the vibration mode, the differences in approximation of frequencies rise, while the zone of beam thickness in which all theories provide good approximate results decreases. This phenomenon is the most significant in the Euler and Reddy-Bickford model.

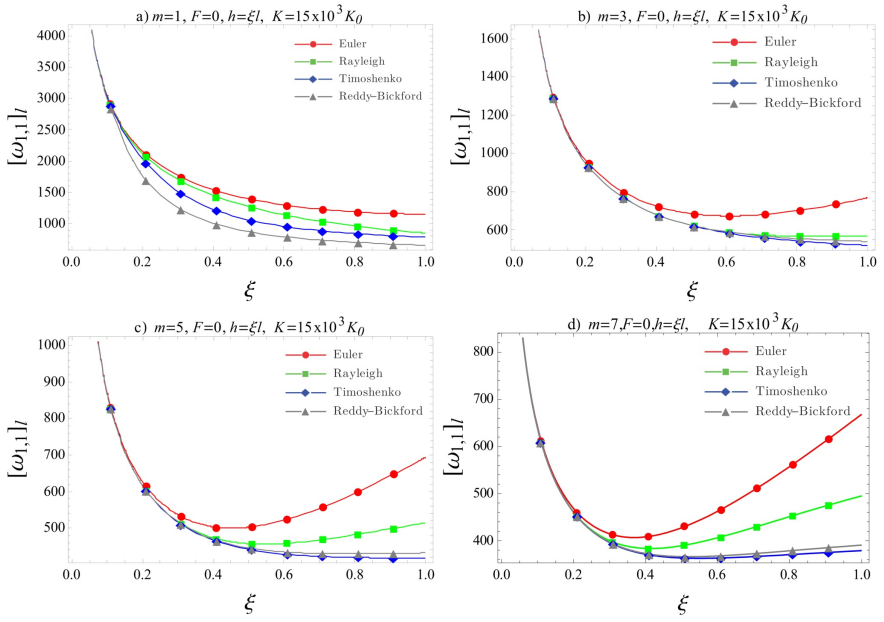

Fig. 6.2.4 The influence of parameter ξ on the beam's lowest natural frequency for different modes n a) $n = 1$; b) $n = 3$; c) $n = 5$; d) $n = 7$

Figure 6.3.1 shows the static stability regions of a system consisting of one, three and five elastically connected beams of different types. The differences in the approximation of solutions across the used model types are small, although it should be noted that the system is most stable in case of a single beam on an elastic foundation.

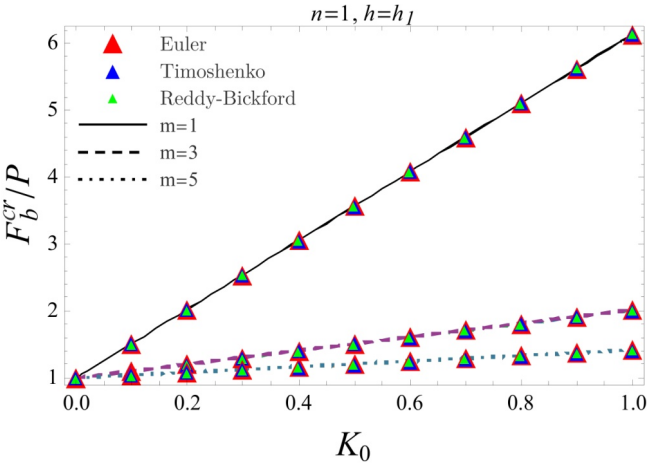

Fig. 6.2.5 The influence of beam number on critical buckling force F_b^{cr}/P in the function of the Winkler's elastic layer stiffness

Appendix 6.1.2- Coefficients in partial differential equations (6.1.17-6.1.19)

$$C(1)_{w1}^{0,2} \quad \frac{h_1\rho_1\{28b_1G_1[\beta{h_1}^2(3\beta{h_1}^2-40)+240]+h_1[3\alpha{h_1}^2(5\alpha{h_1}^2-56)+560](K_0+K_1)\}}{28G_1[\beta{h_1}^2(3\beta{h_1}^2-40)+240]}$$

$$C(1)_{w2}^{0,2} \quad \frac{{h_1}^2K_1\rho_1[3\alpha{h_1}^2(56-5\alpha{h_1}^2)-560]}{28G_1[\beta{h_1}^2(3\beta{h_1}^2-40)+240]}$$

$$C(1)_{w1}^{0,4} \quad \frac{b_1{h_1}^3\rho_1{}^2[3\alpha{h_1}^2(5\alpha{h_1}^2-56)+560]}{28G_1[\beta{h_1}^2(3\beta{h_1}^2-40)+240]}$$

$$C(1)_{w1}^{2,0} \quad F+\frac{E_1{h_1}^2[3\alpha{h_1}^2(56-5\alpha{h_1}^2)-560](K_0+K_1)}{28G_1[\beta{h_1}^2(3\beta{h_1}^2-40)+240]}$$

$$C(1)_{w2}^{2,0} \quad \frac{E_1{h_1}^2K_1[3\alpha{h_1}^2(5\alpha{h_1}^2-56)+560]}{28G_1[\beta{h_1}^2(3\beta{h_1}^2-40)+240]}$$

$$C(1)_{w1}^{2,2} \quad \frac{{h_1}^2\rho_1\{3F[3\alpha{h_1}^2(5\alpha{h_1}^2-56)+560]+b_1{h_1}^3[9\alpha E_1(56-5\alpha{h_1}^2)+7\beta G_1(40-3\beta{h_1}^2)]-1680b_1h_1(E_1+G_1)\}}{84G_1[\beta{h_1}^2(3\beta{h_1}^2-40)+240]}$$

$$C(1)_{w1}^{2,4} \quad -\frac{\alpha^2b_1{h_1}^9\rho_1{}^2}{140G_1[\beta{h_1}^2(3\beta{h_1}^2-40)+240]}$$

$$C(1)_{w1}^{4,0} \quad \frac{1}{84}E_1{h_1}^2\{7b_1h_1-\frac{3F[3\alpha{h_1}^2(5\alpha{h_1}^2-56)+560]}{G_1[\beta{h_1}^2(3\beta{h_1}^2-40)+240]}\}$$

$$C(1)_{w1}^{4,2} \quad \frac{\alpha^2b_1E_1{h_1}^9\rho_1}{70G_1[\beta{h_1}^2(3\beta{h_1}^2-40)+240]}$$

$$C(1)_{w1}^{6,0} \quad -\frac{\alpha^2b_1E_1{}^2{h_1}^9}{140G_1[\beta{h_1}^2(3\beta{h_1}^2-40)+240]}$$

$$C(i)_{wi}^{0,2} \quad \frac{h_i\rho_i\{28b_iG_i[\beta{h_i}^2(3\beta{h_i}^2-40)+240]+h_i[3\alpha{h_i}^2(5\alpha{h_i}^2-56)+560](K_i+K_{i-1})\}}{28G_i[\beta{h_i}^2(3\beta{h_i}^2-40)+240]}$$

$$C(i)_{wi-1}^{0,2} \quad \frac{{h_i}^2K_{i-1}\rho_i[3\alpha{h_i}^2(56-5\alpha{h_i}^2)-560]}{28G_i[\beta{h_i}^2(3\beta{h_i}^2-40)+240]}$$

$$C(i)_{wi+1}^{0,2} \quad \frac{{h_i}^2K_i\rho_i[3\alpha{h_i}^2(56-5\alpha{h_i}^2)-560]}{28G_i[\beta{h_i}^2(3\beta{h_i}^2-40)+240]}$$

$$C(i)_{wi}^{0,4} \quad \frac{b_i{h_i}^3\rho_i{}^2[3\alpha{h_i}^2(5\alpha{h_i}^2-56)+560]}{28G_i[\beta{h_i}^2(3\beta{h_i}^2-40)+240]}$$

$$C(i)_{wi}^{2,0} \quad F+\frac{E_i{h_i}^2[3\alpha{h_i}^2(56-5\alpha{h_i}^2)-560](K_i+K_{i-1})}{28G_i(\beta{h_i}^2(3\beta{h_i}^2-40)+240)}$$

$$C(i)_{wi-1}^{2,0} \quad \frac{E_i{h_i}^2K_{i-1}[3\alpha{h_i}^2(5\alpha{h_i}^2-56)+560]}{28G_i[\beta{h_i}^2(3\beta{h_i}^2-40)+240]}$$

$$C(i)_{wi+1}^{2,0} \quad \frac{E_i{h_i}^2K_i[3\alpha{h_i}^2(5\alpha{h_i}^2-56)+560]}{28G_i[\beta{h_i}^2(3\beta{h_i}^2-40)+240]}$$

$$C(i)_{wi}^{2,2} \quad \frac{{h_i}^2\rho_i\{3F[3\alpha{h_i}^2(5\alpha{h_i}^2-56)+560]+b_i{h_i}^3[9\alpha E_i(56-5\alpha{h_i}^2)+7\beta G_i(40-3\beta{h_i}^2)]-1680b_ih_i(E_i+G_i)\}}{84G_i[\beta{h_i}^2(3\beta{h_i}^2-40)+240]}$$

$$C(i)_{wi}^{2,4} \quad -\frac{\alpha^2b_i{h_i}^9\rho_i{}^2}{140G_i[\beta{h_i}^2(3\beta{h_i}^2-40)+240]}$$

$$C(i)_{wi}^{4,0} \quad \frac{1}{84}E_i{h_i}^2\{7b_ih_i-\frac{3F(3\alpha{h_i}^2(5\alpha{h_i}^2-56)+560)}{G_i[\beta{h_i}^2(3\beta{h_i}^2-40)+240]}\}$$

$$C(i)_{wi}^{4,2} \quad \frac{\alpha^2b_iE_i{h_i}^9\rho_i}{70G_i[\beta{h_i}^2(3\beta{h_i}^2-40)+240]}$$

$$C(i)_{wi}^{6,0} \quad -\frac{\alpha^2b_iE_i{}^2{h_i}^9}{140G_i[\beta{h_i}^2(3\beta{h_i}^2-40)+240]}$$

$$C(m)_w^{0,2} \quad \frac{h_m\rho_m\{28b_mG_m[\beta {h_m}^2(3\beta {h_m}^2-40)+240]+h_mK_0[3\alpha {h_m}^2(5\alpha {h_m}^2-56)+560]\}}{28G_m[\beta {h_m}^2(3\beta {h_m}^2-40)+240]}$$

$$C(m)_{wm-1}^{0,2} \quad \frac{{h_m}^2K_0\rho_m[3\alpha {h_m}^2(56-5\alpha {h_m}^2)-560]}{28G_m[\beta {h_m}^2(3\beta {h_m}^2-40)+240]}$$

$$C(m)_w^{0,4} \quad \frac{{b_mh_m}^3{\rho_m}^2[3\alpha {h_m}^2(5\alpha {h_m}^2-56)+560]}{28G_m[\beta {h_m}^2(3\beta {h_m}^2-40)+240]}$$

$$C(m)_w^{2,0} \quad F+\frac{E_m{h_m}^2K_0[3\alpha {h_m}^2(56-5\alpha {h_m}^2)-560]}{28G_m[\beta {h_m}^2(3\beta {h_m}^2-40)+240]}$$

$$C(m)_{wm-1}^{2,0} \quad \frac{E_m{h_m}^2K_0[3\alpha {h_m}^2(5\alpha {h_m}^2-56)+560]}{28G_m[\beta {h_m}^2(3\beta {h_m}^2-40)+240]}$$

$$C(m)_w^{2,2} \quad \frac{{h_m}^2\rho_m\{3F[3\alpha {h_m}^2(5\alpha {h_m}^2-56)+560]+b_m{h_m}^3[9\alpha E_m(56-5\alpha {h_m}^2)+7\beta G_m(40-3\beta {h_m}^2)]-1680b_mh_m(E_m+G_m)\}}{84G_m[\beta {h_m}^2(3\beta {h_m}^2-40)+240]}$$

$$C(m)_w^{2,4} \quad -\frac{\alpha^2b_m{h_m}^9{\rho_m}^2}{140G_m[\beta {h_m}^2(3\beta {h_m}^2-40)+240]}$$

$$C(m)_w^{4,0} \quad \frac{1}{84}E_m{h_m}^2\{7b_mh_m-\frac{3F(3\alpha {h_m}^2(5\alpha {h_m}^2-56)+560)}{G_m(\beta {h_m}^2(3\beta {h_m}^2-40)+240)}\}$$

$$C(m)_w^{4,2} \quad \frac{\alpha^2b_mE_m{h_m}^9\rho_m}{70G_m[\beta {h_m}^2(3\beta {h_m}^2-40)+240]}$$

$$C(m)_w^{6,0} \quad -\frac{\alpha^2b_m{E_m}^2{h_m}^9}{140G_m[\beta {h_m}^2(3\beta {h_m}^2-40)+240]}$$

Chapter 7

Geometrically Non-linear Vibrations of Timoshenko Damaged Beams Using the New *p*–Version of Finite Element Method

Chapter 7 presents geometrically nonlinear forced vibrations of damaged Timoshenko beams. In the study it is developed new *p*-version of finite element method for damaged beams. The advantage of the new method is compared with the traditional *p*-version of finite element method and provides better approximations of solutions with a small number of degrees of freedom used in numerical analysis.

Scientific contribution was made in two fields - computational mechanics and non-linear vibrations of beams. It is concluded that traditional method can't give good approximations of solutions in the case of very small width of the damage. This benefit is also shown in comparison with obtained results in the commercial software Ansys. A new p-version finite element is suggested to deal with geometrically non-linear vibrations of damaged Timoshenko beams. The novelty of the p-element comes from the use of new displacement shape functions, which are function of the damage location and, therefore, provide for more efficient models, where accuracy is improved at lower computational cost. In numerical tests in the linear regime, coupling between cross sectional rotation and longitudinal vibrations is discovered, with longitudinal displacements suddenly changing direction at the damage location and with a peculiar change in the cross section rotation at the same place. Geometrically nonlinear, forced vibrations are then investigated in the time domain using Newmark's method and further couplings between displacement components are found.

7.1 Development of the New *p*–Version of Finite Element Method

The development of supercomputers and numerical methods have allowed scholars to investigate non-linear mathematical models in a more precise way. Particularly, the finite element method has extensively been used for creating non-linear discretized structure of beams and plates. The finite element method is based on determining approximate solutions by solving the appropriate polynomial functions, ref. Petyt [32]. In general, the structure is divided into smaller elements defining the local function form. Shape functions are simple

V. Stojanović and P. Kozić, *Vibrations and Stability of Complex Beam Systems,*
Springer Tracts in Mechanical Engineering, DOI: 10.1007/978-3-319-13767-4_7

polynomials with the fixed, lower p degree where the accuracy of approximate solution increases with the increased number of elements in the model. Increasing the number of elements results in the decrease of their width h. Another way to improve the precision of approximation is for the network to remain unchanged while the number of shape functions increases, which implies the increase of their degree p, hence the name the p –version of the finite element method, ref. Ribeiro [32]. The reasons for its wide use lie in its main advantages over classic models which are as follows:

a) it does not require the change in a formed network for increasing the accuracy of solutions,
b) the matrix with non-linear members of lower degree polynomial may be used for the derivatives of non-linear member matrixes with an improved new approximation
c) linear member matrixes in p-version of the method are diagonal and easier to use than matrixes with already conditioned members of a classic finite element method,
d) joining the polynomial elements of different degree is simple and enables easy introduction of additional degrees of freedom where necessary,
e) simple structures can be modeled with a single element, which eliminates the problems of internal element continuity as well as their need for connecting,
f) the possibility of choosing the number and the type of shape functions for different displacement allows a better insight into an interaction between individual component vibrations (component longitudinal vibration, component transverse vibration and component vibration of the cross-section rotation),
g) with the p - version of the finite element method it is possible to get a greater accuracy of solutions without the increase of the elements in the structure but only increasing the degree of polynomials which constitute the mode shapes.

As a consequence of these characteristics, the p -version of the finite element method requires less time to model and examine the structure compared to conventional finite element method. This is a huge advantage in non-linear analysis where the iterative calculation procedure requires determining the matrix of non-linear members in each step. Quicker convergence towards the accurate solution thanks to the p –version of the finite element method has been confirmed in static linear analysis of beams, plates and shells in the paper, Szabó et Sahrmann [34], non-linear geometric static analysis of composite plates, Han et al. [35] as well as the analysis of free and forced vibration of different structures [36-43].

The new p –version of the finite element method came as a result of research into geometric non-linear vibration of damaged beams. The conventional p–version of the finite element method did not allow the recognition of a sufficiently small discontinuity in the beam's cross section regardless of increasing the degree of polynomial shape functions of displacement within the finite element. In order to make this possible, it was necessary to introduce new shape functions of displacement which satisfy the boundary conditions and depend on the location

and the size of damage on the beam. Figure 7.1.1 shows a model of a homogenous, elastic, isotropic beam with the length$L$, width b and thickness$h$. The present damage constitutes a cut in the rectangular cross-section along the entire beam width with the depthh_1. The size of damage along the local coordinate axis ξ is defined by the starting point l_1 and the end l_2 of the cross-section's discontinuity.

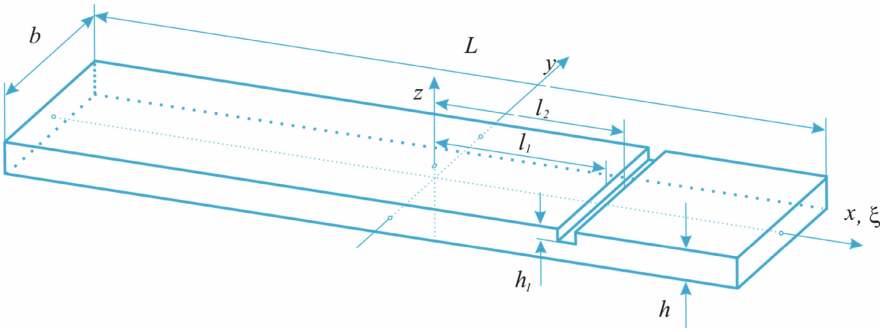

Fig. 7.1.1 The model of a damaged beam with local and global coordinate system

Unlike the classical finite element method, the number of elements used in the p–version depends on the geometry of an analyzed structure. Thus in an example of frame beam, ref. Ribeiro [44] three elements were used. The increase of result accuracy in the classic finite element method in places of structure's changed geometry is achieved by increasing the number of elements in its surrounding. However, regardless of the above mentioned basic features of the finite element method p–version, it will be shown that, regardless of the change in the beam's geometry due to damage, it is possible to get an accurate model by introducing new shape functions of displacement, ref. Stojanovic et al. [22]. The relationship between local and global coordinates is given by the following expression

$$\xi = \frac{2x}{L}. \tag{7.1.1}$$

If we label the functions of longitudinal and transverse displacement corresponding to the global coordinate system as $u(x,z,t)$ and $w(x,z,t)$, then the following relations apply

$$u(x,z,t) = u^0(x,t) + z\theta^0(x,t), \quad w(x,z,t) = w^0(x,t), \tag{7.1.2}$$

where $u^0(x,t)$ and $w^0(x,t)$ represent longitudinal and transverse displacement of the beam's point $(x, z = 0, t)$ belonging to the x–axis. The cross-section rotation $\theta^0(x,t)$ is defined by the change of an angle between the z-axis and the beam's cross section in the xz plane around the y - axis. Considering von

Kármán model of geometric non-linearity, deformation along the x axis $\varepsilon_x(x,t)$ and the deformation caused by transverse shear $\gamma_{xz}(x,t)$ are given by

$$\varepsilon_x(x,z,t) = \frac{\partial u^0(x,t)}{\partial x} + \frac{1}{2}\left(\frac{\partial w^0(x,t)}{\partial x}\right)^2 + \mathrm{z}\frac{\partial \theta^0(x,t)}{\partial x}, \tag{7.1.3}$$

$$\gamma_{xz}(x,t) = \frac{\partial w^0(x,t)}{\partial x} + \theta^0(x,t). \tag{7.1.4}$$

In each element, vector $\mathbf{d_0}(\xi,t)$, comprised of the motion component can be expressed as a combination of hierarchical shape functions

$$\mathbf{d_0}(\xi,t) = \mathbf{N}(\xi)\,\mathbf{q}(t) <=> \begin{Bmatrix} u^0(\xi,t) \\ w^0(\xi,t) \\ \theta^0(\xi,t) \end{Bmatrix} = \begin{bmatrix} \mathbf{N}^u(\xi)^{\mathrm{T}} & \mathbf{0} & \mathbf{0} \\ \mathbf{0} & \mathbf{N}^w(\xi)^{\mathrm{T}} & \mathbf{0} \\ \mathbf{0} & \mathbf{0} & \mathbf{N}^\theta(\xi)^{\mathrm{T}} \end{bmatrix} \begin{Bmatrix} \mathbf{q_u}(t) \\ \mathbf{q_w}(t) \\ \mathbf{q_\theta}(t) \end{Bmatrix} \tag{7.1.5}$$

where $\mathbf{q_u}(t)$- is a vector of longitudinal generalized displacement, $\mathbf{q_w}(t)$- a vector of transverse generalized displacement and $\mathbf{q_\theta}(t)$- a vector of generalized rotation of the cross-section around the y-axis. $\mathbf{N}(\xi)$is a matrix shape function comprised of vectors of longitudinal, transverse and rotation shape functions. The increase of the number of these functions in the model increases the accuracy of model discretization. Total number of shape functions implemented in a single element model presents the degree of system's freedom.

By introducing two new functions into the p-version of the finite element method, we get a new system of shape functions which allows the recognition of the expected increased beam flexibility in the narrow domain of damage. The two new shape functions introduced into the model are labeled "d" in the index and depend on the location of the damage centre $L_1 = \frac{l_1+l_2}{2}$, , Figure 7.1.1. The orders of vectors of longitudinal, transverse and rotational displacement of the beam's cross-sections with discontinuity now have the following form

$$\begin{aligned} \boldsymbol{N}^u(\xi)^{\mathrm{T}} &= \left[f_1^d(L,L_1,\xi) f_2^d(L,L_1,\xi) \mid f_1(\xi)\ f_2(\xi) f_3(\xi)\ \ldots\ f_{pu}(\xi)\right], \\ \boldsymbol{N}^w(\xi)^{\mathrm{T}} &= \left[f_1^d(L,L_1,\xi) f_2^d(L,L_1,\xi) \mid f_1(\xi)\ f_2(\xi) f_3(\xi)\ \ldots\ f_{pw}(\xi)\right], \\ \boldsymbol{N}^\theta(\xi)^{\mathrm{T}} &= \left[f_1^d(L,L_1,\xi) f_2^d(L,L_1,\xi) \mid f_1(\xi)\ f_2(\xi) f_3(\xi)\ \ldots\ f_{p\theta}(\xi)\right], \end{aligned} \tag{7.1.6}$$

where pu, pw and $p\theta$ represent the number of longitudinal, transverse and rotation shape functions to which the functions $f_1^d(L,L_1,\xi)$ and $f_2^d(L,L_1,\xi)$have been added. The first four functions are given by

$$f_1(\xi) = \frac{1}{2} - \frac{3}{4}\xi + \frac{1}{4}\xi^3,\ \ f_2(\xi) = \frac{1}{4} - \frac{1}{4}\xi - \frac{1}{4}\xi^2 + \frac{1}{4}\xi^3,$$

$$f_3(\xi)=\frac{1}{2}+\frac{3}{4}\xi-\frac{1}{4}\xi^3,\ \ f_4(\xi)=-\frac{1}{4}-\frac{1}{4}\xi+\frac{1}{4}\xi^2+\frac{1}{4}\xi^3. \tag{7.1.7}$$

The remaining shape functions are obtained by way of a formula, ref. Petyt [32], p.298.

$$f_r(\xi)=\sum_{n=0}^{\mathrm{INT}\left(\frac{r}{2}\right)}\frac{(-1)^n(2r-2n-7)!!}{2^n n!\,(r-2n-1)!}\xi^{r-2n-1}, r>4, \tag{7.1.8}$$

where $r!!=r(r-2)\ldots(2\ or\ 1)$, $0!!=(-1)!!=1$ and INT $(r/2)$ are integers of $r/2$. Shape functions $f_r(\xi)$ satisfy boundary conditions for doubly clamped beams (functions and their first derivatives are at the boundaries of the zero element). Functions f_1-f_4 of the third-degree polynomial, also known as Hermite's polynomials [33], are usually included when it is necessary to change boundary conditions in other types of beam support and are used for constructing and creating a function. New implemented functions $f_1^d(L,L_1,\xi)$ and $f_2^d(L,L_1,\xi)$ in analytical form are as follows

$$f_1^d(L,L_1,\xi)=\begin{cases}\dfrac{(1+\xi)^2[6L_1+L(1-2\xi)]}{8L}, & -1\le\xi\le\dfrac{2L_1}{L},\\[2ex] \dfrac{(L+2L_1)^3(\xi-1)^2(L-6L_1+2L\xi)}{8L(L-2L_1)^3}, & 2L_1/L\le\xi\le 1,\end{cases} \tag{7.1.9}$$

$$f_2^d(L,L_1,\xi)=\begin{cases}\dfrac{1}{4}(1+\xi)^2\left(\xi-\dfrac{2L_1}{L}\right), & -1\le\xi\le 2L_1/L\\[2ex] \dfrac{(L+2L_1)^2(\xi-1)^2(\xi-\frac{2L_1}{L})}{4(L-2L_1)^2}, & 2L_1/L\le\xi\le 1.\end{cases} \tag{7.1.10}$$

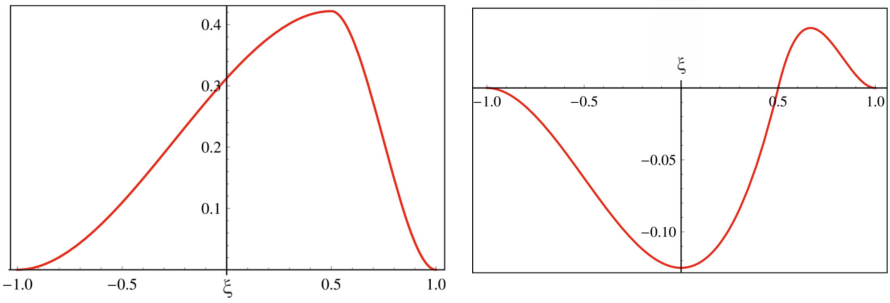

$f_1^{\mathrm{d}}(L,L_1,\xi)$ $f_2^{\mathrm{d}}(L,L_1,\xi)$

Fig. 7.1.2 Displacement shape functions

As an example of a non-dimensional damage location given in the ratio of a global to local coordinate system $(L=\frac{2x}{\xi})$, $L_1=0.5$, the newly introduced

functions of mode shapes are shown in Figure 7.2.1. The function $f_1^d(L, L_1, \xi)$ is introduced with its maximum at the place of the damage centre, while the function $f_2^d(L, L_1, \xi)$ has been introduced with its zero in the place of the damage centre. By including these two functions into the element, the continuity condition still applies.

We assume the beam's is elastic and isotropic hence the Hooke's law applies

$$\boldsymbol{\sigma} = \mathbf{D}\boldsymbol{\varepsilon} \Leftrightarrow \begin{Bmatrix} \sigma_x \\ \tau_{xz} \end{Bmatrix} = \begin{bmatrix} E & 0 \\ 0 & kG \end{bmatrix} \begin{Bmatrix} \varepsilon_x \\ \gamma_{xz} \end{Bmatrix}, \tag{7.1.11}$$

where $\mathbf{D}$ is the matrix of elastic coefficients, $\boldsymbol{\sigma}$ and $\boldsymbol{\varepsilon}$ are vectors of stress and deformation, E is Young's modulus, G is shear modulus given by $E/[2(1+\nu)]$, where ν is the Poisson's ratio. In the numerical experiment, the shear factor was used which yielded the best correspondence with experimental results, ref. [24] in the form of k=(5+5 ν)/(6+5 ν). Longitudinal deformation may be written as

$$\varepsilon_x = \lfloor 1 \quad z \rfloor \left(\begin{Bmatrix} \varepsilon_0^p \\ \varepsilon_0^b \end{Bmatrix} + \begin{Bmatrix} \varepsilon_L^p \\ 0 \end{Bmatrix} \right). \tag{7.1.12}$$

In the equation (7.1.12), the deformation consists of a linear and non-linear part, where ε_0^p and z ε_0^b represent the respective linear longitudinal and linear deformation due to buckling, while ε_L^p represents geometric non-linear longitudinal deformation. In the shown model they can be written as

$$\varepsilon_0^p = \boldsymbol{N}_{,\xi}^{u\,\mathrm{T}} \mathbf{q}_\mathbf{u} \frac{2}{L},\ \varepsilon_0^b = \boldsymbol{N}_{,\xi}^{\theta\,\mathrm{T}} \mathbf{q}_\boldsymbol{\theta} \frac{2}{L},\ \varepsilon_L^p = \frac{2}{L^2} \mathbf{q}_\mathbf{w}{}^{\mathrm{T}} \boldsymbol{N}_{,\xi}^{w} \boldsymbol{N}_{,\xi}^{w\,\mathrm{T}} \mathbf{q}_\mathbf{w},\ \gamma_{xz} = \left\lfloor \frac{2}{L} \boldsymbol{N}_{,\xi}^{w\,T} \quad \boldsymbol{N}^{\theta\,T} \right\rfloor \begin{Bmatrix} \mathbf{q}_\mathbf{w} \\ \mathbf{q}_\boldsymbol{\theta} \end{Bmatrix}, \tag{7.1.13}$$

where "$,\xi$" is the first derivative of the variable for ξ. Integrating normal and shear stress and the moment of normal stress in the expressions (7.1.11), we get the forces in perpendicular and tangent direction respectively, as well as the moment in the following form

$$T_x = \begin{cases} \displaystyle\int_{-\frac{h}{2}}^{\frac{h}{2}} \sigma_x \mathrm{d}z, & x \in \left[-\frac{L}{2}, l_1\right] \cup \left[l_2, \frac{L}{2}\right] \\ \displaystyle\int_{-\frac{h}{2}}^{\frac{h}{2}-h_1} \sigma_x \mathrm{d}z, & x \in [l_1, l_2] \end{cases}, \tag{7.1.14}$$

$$Q_x = \begin{cases} \displaystyle\int_{-\frac{h}{2}}^{\frac{h}{2}} \tau_{xz} \mathrm{d}z, & x \in \left[-\frac{L}{2}, l_1\right] \cup \left[l_2, \frac{L}{2}\right] \\ \displaystyle\int_{-\frac{h}{2}}^{\frac{h}{2}-h_1} \tau_{xz} \mathrm{d}z, & x \in [l_1, l_2] \end{cases}, \tag{7.1.15}$$

$$M_x = \begin{cases} \displaystyle\int_{-h/2}^{h/2} \sigma_x\, z\, \mathrm{d}z, & x \in \left[-\frac{L}{2}, l_1\right] \cup \left[l_2, \frac{L}{2}\right] \\ \displaystyle\int_{-h/2}^{\frac{h}{2}-h_1} \sigma_x\, z\, \mathrm{d}z, & x \in [l_1, l_2] \end{cases}. \tag{7.1.16}$$

By substituting the quantities marked in expressions (7.1.13) into equations (7.1.14-7.1.16), we determine the relation between the forces and the moment on the one hand and the deformation on the other hand

$$\begin{Bmatrix} T \\ M \end{Bmatrix} = \begin{bmatrix} A & B \\ B & D \end{bmatrix} \left(\begin{Bmatrix} \varepsilon_0^p \\ \varepsilon_0^b \end{Bmatrix} + \begin{Bmatrix} \varepsilon_L^p \\ 0 \end{Bmatrix} \right),$$

$$Q_x = \begin{cases} \dfrac{Eh\lambda}{2(1+\nu)}\gamma_{xz}, & x \in \left[-\dfrac{L}{2}, l_1\right] \cup \left[l_2, \dfrac{L}{2}\right] \\ \dfrac{E(h-h_1)\lambda}{2(1+\nu)}\gamma_{xz}, & x \in [l_1, l_2] \end{cases},$$

$$A, B, D = \int_z (1, z, z^2) E \, \mathrm{dz}, \tag{7.1.17}$$

where A is the coefficient of extension, B the coupling coefficient between the bending and extension deformation (occurring as a consequence of beam damage, in other cases of classic beams it equals zero) and D the bending coefficient which have the following form

$$A = \begin{cases} Eh, & x \in \left[-\dfrac{L}{2}, l_1\right] \cup \left[l_2, \dfrac{L}{2}\right], \\ E(h-h_1), & x \in [l_1, l_2] \end{cases}$$

$$B = \begin{cases} 0, & x \in \left[-\dfrac{L}{2}, l_1\right] \cup \left[l_2, \dfrac{L}{2}\right] \\ \dfrac{Eh_1(h_1-h)}{2}, & x \in [l_1, l_2] \end{cases}, \tag{7.1.18}$$

$$D = \begin{cases} \dfrac{Eh^3}{12}, & x \in \left[-\dfrac{L}{2}, l_1\right] \cup \left[l_2, \dfrac{L}{2}\right] \\ \dfrac{E[h^3 + (h-2h_1)^3]}{24}, & x \in [l_1, l_2] \end{cases},$$

We can notice that B is different from zero on the beam part with the change of shape with the damage in the form of a geometric change on the beam. Equations of motion are derived based on the principle of virtual work for which the following holds

$$\delta W_{in} + \delta W_V + \delta W_{ex} = 0, \tag{7.1.19}$$

where $\delta W_{in}, \delta W_V$ and δW_{ex} are virtual work of inertial, internal and external forces on virtual displacement $\delta \mathbf{d}$ in the form

$$\delta \mathbf{d} = \begin{Bmatrix} \delta \mathrm{u} \\ \delta \mathrm{w} \\ \delta\theta \end{Bmatrix} = \mathbf{N}\, \delta \mathbf{q}. \tag{7.1.20}$$

Virtual work of internal forces is

$$\delta W_V = -\int_V \delta\boldsymbol{\varepsilon}^{\mathrm{T}}\boldsymbol{\sigma}\mathrm{d}V =$$

$$= -b\int_L \left(\begin{Bmatrix}\delta\varepsilon_0^p\\ \delta\varepsilon_0^b\end{Bmatrix}^{\mathrm{T}} + \begin{Bmatrix}\delta\varepsilon_L^p\\ 0\end{Bmatrix}^{\mathrm{T}}\right)\begin{bmatrix}A & B\\ B & D\end{bmatrix}\left(\begin{Bmatrix}\varepsilon_0^p\\ \varepsilon_0^b\end{Bmatrix} + \begin{Bmatrix}\varepsilon_L^p\\ 0\end{Bmatrix}\right)\mathrm{d}x - b\int_{-\frac{L}{2}}^{l_1}\delta\gamma_{xz}\frac{Eh\lambda}{2(1+\nu)}\gamma_{xz}\,\mathrm{d}x - \quad (7.1.21)$$

$$-b\int_{l_1}^{l_2}\delta\gamma_{xz}\frac{E(h-h_1)\lambda}{2(1+\nu)}\gamma_{xz}\,\mathrm{d}x - \int_{l_2}^{L/2}\delta\gamma_{xz}\frac{Eh\lambda}{2(1+\nu)}\gamma_{xz}\,\mathrm{d}x = \delta\mathbf{q}^{\mathrm{T}}\mathbf{K}(\mathbf{q})\mathbf{q},$$

where $\delta\boldsymbol{\varepsilon}$ is the vector of virtual deformation. Virtual work of inertial forces is given by

$$\delta W_{in} = -\int_V \rho\delta\mathbf{d}^{\mathrm{T}}\ddot{\mathbf{d}}\mathrm{d}V =$$

$$= -b\int_{-h/2}^{h/2}\int_{-L/2}^{l_1}\rho(\delta u\ddot{u} + \delta w\ddot{w})\,\mathrm{d}x\,\mathrm{d}z - b\int_{-h/2}^{(h/2)-h_1}\int_{l_1}^{l_2}\rho(\delta u\ddot{u} + \delta w\ddot{w})\,\mathrm{d}x\,\mathrm{d}z - \quad (7.1.22)$$

$$-b\int_{-h/2}^{h/2}\int_{l_2}^{L/2}\rho(\delta u\ddot{u} + \delta w\ddot{w})\,\mathrm{d}x\,\mathrm{d}z = \delta\mathbf{q}^{\mathrm{T}}\mathbf{M}\ddot{\mathbf{q}},$$

where $\ddot{\mathbf{d}}$ is component acceleration of the beam point. Virtual work of external forces is

$$\delta W_{ex} = \int_L \left(\left[P_u^j(t)\delta(x-x_j) + P_u^d(x,t)\right]\delta u(x,t) + \left[P_w^j(t)\delta(x-x_j) + P_w^d(x,t)\right]\delta w(x,t)\right)\mathrm{d}x +$$

$$+\int_L \left[M^j(t)\delta(x-x_j) + M^d(x,t)\right]\delta\theta(x,t)\,\mathrm{d}x = \left[\delta\mathbf{q}_{\mathbf{u}}^{\mathrm{T}}\ \ \delta\mathbf{q}_{\mathbf{w}}^{\mathrm{T}}\ \ \delta\mathbf{q}_{\boldsymbol{\theta}}^{\mathrm{T}}\right]\begin{Bmatrix}\mathbf{F}_{\mathbf{u}}^{\mathbf{E}}(t)\\ \mathbf{F}_{\mathbf{w}}^{\mathbf{E}}(t)\\ \mathbf{M}^{\mathbf{E}}(t)\end{Bmatrix}. \quad (7.1.23)$$

If we substitute the equations (7.1.21-7.1.23) into the equation (7.1.19), we get a non-linear system of partial differential equations for forced vibrations of the damaged Timoshenko beam in the following form

$$\begin{bmatrix}\mathbf{M}^l & \mathbf{0} & \mathbf{0}\\ \mathbf{0} & \mathbf{M}^b & \mathbf{0}\\ \mathbf{0} & \mathbf{0} & \mathbf{M}^r\end{bmatrix}\begin{Bmatrix}\ddot{\mathbf{q}}_{\mathbf{u}}\\ \ddot{\mathbf{q}}_{\mathbf{w}}\\ \ddot{\mathbf{q}}_{\boldsymbol{\theta}}\end{Bmatrix} + \begin{bmatrix}\mathbf{0} & \mathbf{0} & \mathbf{M}^{lr}\\ \mathbf{0} & \mathbf{0} & \mathbf{0}\\ \mathbf{M}^{lr\,\mathrm{T}} & \mathbf{0} & \mathbf{0}\end{bmatrix}\begin{Bmatrix}\ddot{\mathbf{q}}_{\mathbf{u}}\\ \ddot{\mathbf{q}}_{\mathbf{w}}\\ \ddot{\mathbf{q}}_{\boldsymbol{\theta}}\end{Bmatrix} +$$

$$+\begin{bmatrix}\mathbf{K}_\ell^l & \mathbf{0} & \mathbf{0}\\ \mathbf{0} & \mathbf{K}_\ell^{\gamma_{11}} & \mathbf{K}_\ell^{\gamma_{12}}\\ \mathbf{0} & \mathbf{K}_\ell^{\gamma_{21}} & \mathbf{K}_\ell^b + \mathbf{K}_\ell^{\gamma_{22}}\end{bmatrix}\begin{Bmatrix}\mathbf{q}_{\mathbf{u}}\\ \mathbf{q}_{\mathbf{w}}\\ \mathbf{q}_{\boldsymbol{\theta}}\end{Bmatrix} + \begin{bmatrix}\mathbf{0} & \mathbf{0} & \mathbf{K}_\ell^{lr}\\ \mathbf{0} & \mathbf{0} & \mathbf{0}\\ \mathbf{K}_\ell^{lr\,\mathrm{T}} & \mathbf{0} & \mathbf{0}\end{bmatrix}\begin{Bmatrix}\mathbf{q}_{\mathbf{u}}\\ \mathbf{q}_{\mathbf{w}}\\ \mathbf{q}_{\boldsymbol{\theta}}\end{Bmatrix} + \quad (7.1.24)$$

$$+\begin{bmatrix}\mathbf{0} & \mathbf{K}_{n\ell}^2(\mathbf{q}_{\mathbf{w}}) & \mathbf{0}\\ \mathbf{K}_{n\ell}^3(\mathbf{q}_{\mathbf{w}}) & \mathbf{K}_{n\ell}^4(\mathbf{q}_{\mathbf{w}}) & \mathbf{0}\\ \mathbf{0} & \mathbf{0} & \mathbf{0}\end{bmatrix}\begin{Bmatrix}\mathbf{q}_{\mathbf{u}}\\ \mathbf{q}_{\mathbf{w}}\\ \mathbf{q}_{\boldsymbol{\theta}}\end{Bmatrix} + \begin{bmatrix}\mathbf{0} & \mathbf{0} & \mathbf{0}\\ \mathbf{0} & \mathbf{0} & \mathbf{K}_{n\ell}^{br}(\mathbf{q}_{\mathbf{w}})\\ \mathbf{0} & \mathbf{K}_{n\ell}^{br\,\mathrm{T}}(\mathbf{q}_{\mathbf{w}}) & \mathbf{0}\end{bmatrix}\begin{Bmatrix}\mathbf{q}_{\mathbf{u}}\\ \mathbf{q}_{\mathbf{w}}\\ \mathbf{q}_{\boldsymbol{\theta}}\end{Bmatrix} = \begin{Bmatrix}\mathbf{F}_{\mathbf{u}}^{\mathbf{E}}\\ \mathbf{F}_{\mathbf{w}}^{\mathbf{E}}\\ \mathbf{M}^{\mathbf{E}}\end{Bmatrix},$$

where $\{\mathbf{F}_{\mathbf{u}}^{\mathbf{E}}(t),\ \mathbf{F}_{\mathbf{w}}^{\mathbf{E}}(t),\ \mathbf{M}^{\mathbf{E}}(t)\}$ is the vector of generalized external forces. Matrixes $\mathbf{M}$ and $\mathbf{K}_\ell$ are comprised of constants, $\mathbf{K}_{n\ell}^2, \mathbf{K}_{n\ell}^3$ and $\mathbf{K}_{n\ell}^{br}$ matrix

members depend linearly on the solution while the matrix $\mathbf{K}_{\mathrm{n}\ell}^{\mathbf{4}}$ members depend squarely on the solution (i.e. in the general form they present the members of cubic non-linearity). The labels in the indexes l, b, r and γ represent the effects of longitudinal displacement, deflection, component rotational displacement of beams' cross-sections and shear respectively. The label lr in the index represents the coupling of longitudinal and rotational displacement which occurs in mass and stiffness matrixes as a consequence of beam damage. The br label represents the coupling of transverse and rotational displacement of the cross-section which also occurs in the matrix with non-linear members. If we introduce the Rayleigh damping type defined by coefficients α and β, we obtain

$$(\mathbf{M}+\mathbf{M}^{c})\ddot{\mathbf{q}}(t)+\alpha(\mathbf{K}_{\ell}+\mathbf{K}_{\ell}^{c})\dot{\mathbf{q}}(t)+\beta(\mathbf{M}+\mathbf{M}^{c})\dot{\mathbf{q}}(t)+ \\ +\{\mathbf{K}_{\ell}+\mathbf{K}_{\ell}^{c}+\mathbf{K}_{\mathrm{n}\ell}[\mathbf{q}(t)]+\mathbf{K}_{\mathrm{n}\ell}^{c}[\mathbf{q}(t)]\}\mathbf{q}(t)=\mathbf{F}(t). \tag{7.1.25}$$

The matrixes $\mathbf{M}^{c}$, $\mathbf{K}_{\ell}^{c}$ and $\mathbf{K}_{\mathrm{n}\ell}^{c}(\mathbf{q}(t))$ represent the coupling of motion between independent displacement occurring due to discontinuity in the cross-section. Mass and stiffness matrices with linear and non-linear members are given in Appendix 7.1.1.

7.2 Mode Shapes of Component Longitudinal and Transverse Vibration and Component Vibration Mode Shapes of Beams' Cross-Sections

The *p*-version model of the finite element method was applied to a doubly clamped beam whose characteristics have been given in the papers [17], [45], [46]. Depending on the damage depth in the numerical experiment, the following cases were considered:

Case 1.1. Ref. [13]

$L = 1330$ mm, $b = 25.3$ mm, $h = 25.3$ mm, $E = 203.91$ GNm^{-2}, $\rho = 7800$ kgm^{-3}.

Damage position: $l_1 = 222.5$ mm, $l_2 = 247.5$ mm, $w_d = 1.87\%$.

Damage depth: a) 4 mm b) 8 mm c) 12 mm.

Case 2.1 Ref. [35],[36]

$L = 406$ mm, $b = 20$ mm, $h = 2$ mm, $E = 7.172$ GNm^{-2}, $\rho = 2800$ kg m^{-3}.

2.1.1. Damage position: $l_1 = 68$ mm, $l_2 = 75.5$ mm, $w_d = 1.7\%$.
Damage depth: a) 0.3 mm b) 0.6 mm c) 0.9 mm.

2.1.2. Damage position: $l_1 = -5$ mm, $l_2 = 5$ mm, $w_d = 2.4\%$.
Damage depth: a) 0.9 mm

Case 2.2. Ref [35]

$L = 406$ mm, $b = 20$ mm, $h = 20.3$ mm, $E = 7.172$ GNm^{-2}, $\rho = 2800$ kg m^{-3}.
Damage position: $l_1 = 68$ mm, $l_2 = 75.5$ mm, $w_d = 1.7\%$.
Damage depth: a) 5mm b) 9 mm

In the numerical experiment, w_d represents the relative damage length of shown in percentages. The beams with such geometric and material characteristics were chosen in order to verify the obtained results against experimental findings already existing in literature. Experimental results obtained in the paper by Sinha [17] were compared to the obtained results for the case of damage occurring in the same place. Experimental results obtained for a non-damaged beam, ref. Wolf [46] were numerically compared with the results for the same beam in non-linear vibration mode, ref. Ribeiro [45]. We verified the known numerical and experimental results using the new *p*-version of the finite element method on the same beam model assuming the damage depth in the model to be zero. In the paper [45], the non-damaged thicker beam (*L*/*h*=20) was analyzed and its characteristics used for considering the vibration of thicker beams with damage. The Ansys software pack [47] was used for the comparison of models in terms of vibration freedom degree.

The results in Tables 7.2.1, 7.2.2 and 7.2.3 show transverse natural beam frequencies for different damage depths. For result comparison using the Ansys software pack, the *h*–version of the "BEAM189" element was used which is based on Timoshenko's theory and has three binding points with six degrees of vibration freedom for each of them. The results shown in Ansys-created tables were obtained using the model with 300 elements. Such a dense network was used to verify the *p*–version of the finite element method although convergence is achieved by using only thirty elements. The tables also show the results obtained through traditional *p*-version of the finite element method which use the shape functions shown in paper [49] without the implemented functions f_1^d and f_1^d.

Table 7.2.1 Natural frequencies [Hz] of clamped-clamped beam for case 1.1

Mode	Non-damaged beam				4mm damage depth			
	ANSYS BEAM189	Classical *p*-FEM (15 sf)	New *p*-FEM (15 sf)	Experimental [17]	ANSYS BEAM189	Classical *p*-FEM (25 sf)	New *p*-FEM (25 sf)	Experimental [17]
1	74.979	74.986	74.986	75.313	74.923	75.012	74.924	74.688
2	206.01	206.05	206.05	207.188	204.52	205.37	204.50	205.625
3	402.04	402.21	402.21	406.250	401.65	402.00	401.79	405.625
4	660.88	661.35	661.35	667.813	658.66	660.12	658.94	666.250

Mode	8mm damage depth				12mm damage depth			
	ANSYS BEAM189	Classical *p*-FEM (26 sf)	New *p*-FEM (26sf)	Experimental [17]	ANSYS BEAM189	Classical *p*-FEM (28 sf)	New *p*-FEM (28 sf)	Experimental [17]
1	74.666	75.094	74.648	74.063	73.973	75.230	73.957	72.813
2	201.21	205.258	201.00	202.500	194.50	205.679	194.30	197.188
3	400.80	401.977	400.90	404.688	399.11	402.084	399.29	403.125
4	654.02	659.781	654.043	662.813	644.90	660.167	644.79	655.938

Table 7.2.2 Natural frequencies [Hz] of clamped-clamped beam for case 2.1

Mode	Non-damaged beam			0.3 mm damage depth 2.1.1.		
	ANSYS BEAM189	Classical *p*-FEM (15 sf)	New *p*-FEM (15sf)	ANSYS BEAM189	Classical *p*-FEM (28 sf)	New *p*-FEM (28 sf)
1	63.111	63.111	63.111	63.070	63.131	63.045
2	173.93	173.93	173.93	172.85	173.39	172.53
3	340.87	340.87	340.87	340.62	340.73	340.51
4	563.25	563.28	563.28	561.71	562.37	561.22

Mode	0.6 mm damage depth 2.1.1.			0.9 mm damage depth 2.1.1.		
	ANSYS BEAM189	Classical *p*-FEM (28sf)	New *p*-FEM (28sf)	ANSYS BEAM189	Classical *p*-FEM (28sf)	New *p*-FEM (28sf)
1	62.893	63.197	62.769	62.419	63.306	62.387
2	170.51	173.31	169.22	165.77	173.66	165.27
3	340.03	340.71	339.67	338.86	340.81	338.72
4	558.33	562.14	556.64	551.76	562.49	551.39

Mode		0.9 mm damage depth 2.1.2.	
	ANSYS BEAM189	Classical *p*-FEM (23 sf)	New *p*-FEM (23 sf)
1	59.832	63.255	60.300
2	173.88	173.93	173.92
3	318.24	339.40	321.00
4	562.61	563.26	563.25

Table 7.2.3 Natural frequencies [Hz] of a clamped-clamped beam for case 2.2

Mode	Non-damaged beam			9 mm damage depth		
	ANSYS BEAM189	Classical *p*-FEM (15 sf)	Nova *p*-FEM (15sf)	ANSYS BEAM189	Classical *p*-FEM (28sf)	New *p*-FEM (28sf)
1	629.74	629.74	629.74	623.36	631.97	623.15
2	1698.7	1698.7	1698.7	1671.3	1698.6	1620.5
3	3240.1	3240.1	3240.1	3222.9	3245.0	3227.2
4	5121.8	5121.8	5121.8	5103.6	5190.2	5047.8

The results in Tables 7.2.1-7.2.3 show that the new *p*- version of the finite element method yields accurate results with a lower number of the used vibration freedom degrees compared to the *h*–version of the commercial Ansys software. The matching with experimental results confirms the accuracy and the value of the new method. It should be noted that the traditional version of the finite element method does not allow obtaining good results in damaged beams since the frequencies higher than those for the non-damaged beams are obtained.

The change in natural frequencies does not give a complete picture on the influence of damage on structure vibration. Natural frequency can be the same for the cases of different damage location, therefore it is necessary to determine the change of other characteristics describing the vibration. One such characteristic is the change in independent components of mode shapes. With non-damaged doubly clamped beams only two component vibration modes are possible, transverse displacement of beams' centre lines and rotation of cross-sections. In case of a damaged model, anti-symmetry occurs in the beam geometry which leads to the coupling of transverse rotation and longitudinal displacement (B is different from zero – second equation 7.1.18) and is displayed through changes in mass and stiffness submatrixes of linear members. Such a model of damaged beams allows us to determine longitudinal components of mode shapes. Figure 7.2.1 shows mode shapes of longitudinal vibration for characteristic modes of a beam described in case 1.1 c). It can be seen from a diagram that sudden changes in longitudinal vibration occur in geometric place of damage. In the first and the sixth mode a maximum longitudinal displacement of the beam occurs in the place of damage onset on the side of the beam farther from the clamp. In higher modes, maximum longitudinal displacement of the beam is in the place of damage onset on the side of the beam closer to the clamp. The described occurrence of longitudinal vibration is an important dynamic feature of the model since it occurs exclusively as the consequence of beam damage.

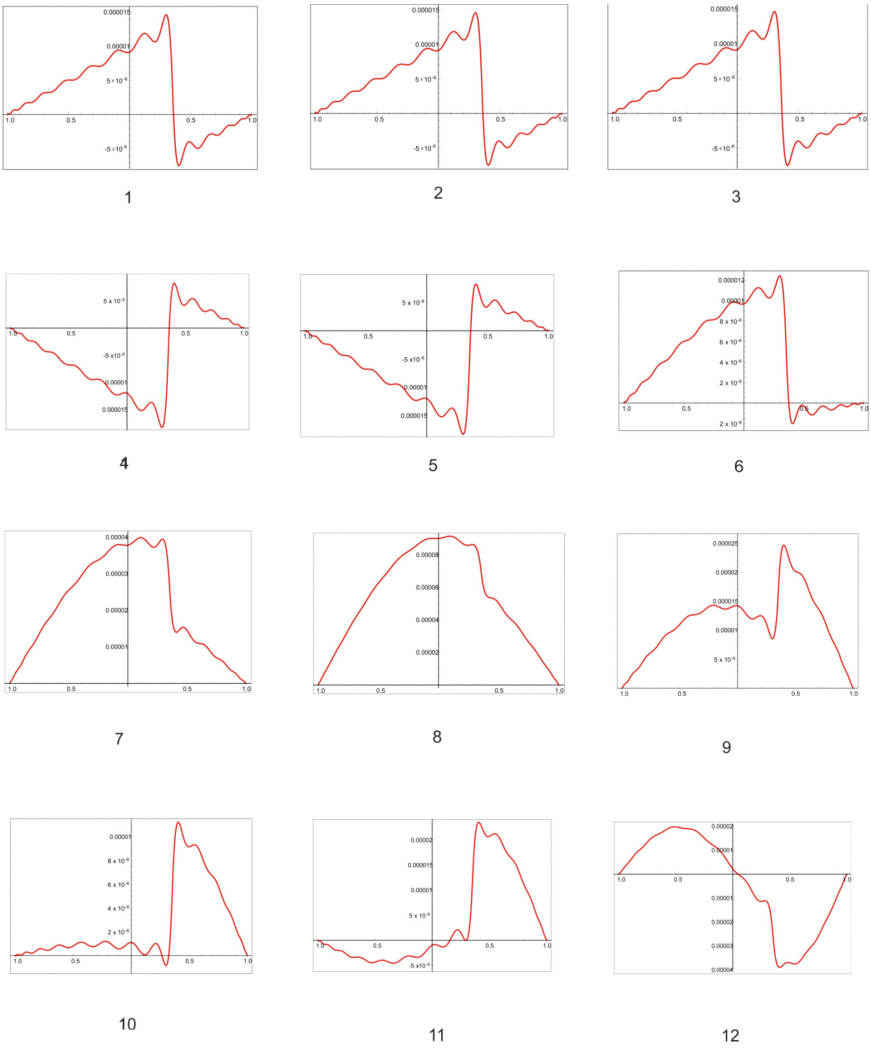

Fig. 7.2.1 Longitudinal components of mode shapes

Transverse and rotational components of beams' mode shapes (case 1.1) are shown in Figures 7.2.2-7.2.3. To facilitate the comparison, component mode shapes were normalized so that the amplitudes are equal in the occurrence point of the first local extreme on the left side of the non-damaged beam. The natural frequencies shown in table 7.1.1 correspond to the component mode shapes in Figures (7.2.2-7.2.3.). Figures clearly show the deviation in mode shapes in the place of damage location which becomes more significant in higher modes.

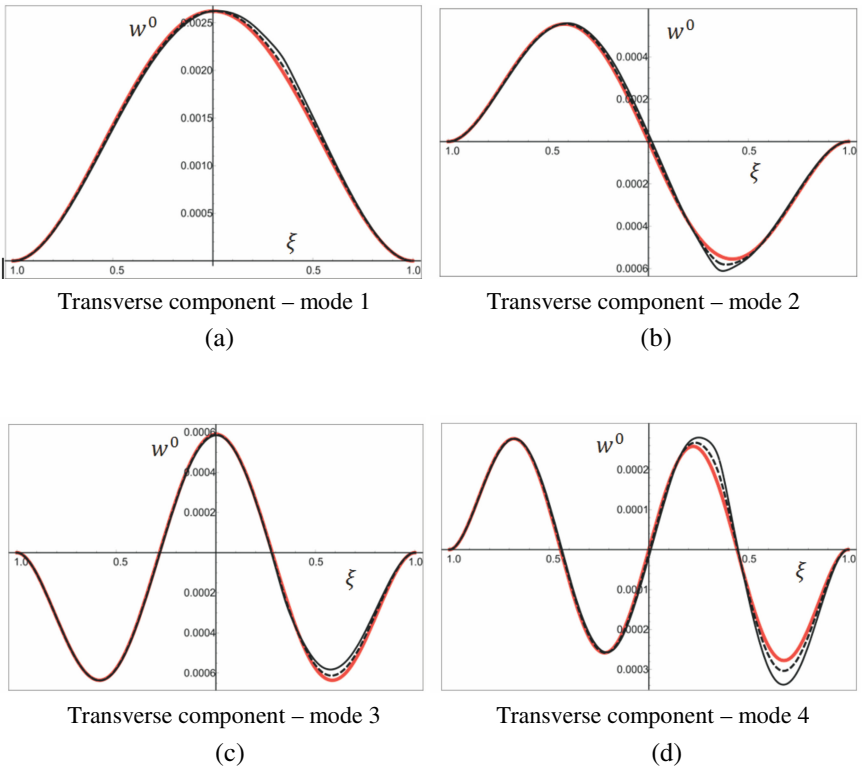

Fig. 7.2.2 Transverse component of mode shapes: Case 1.1 — non-damaged beam; ----- 8mm damage; ▬ 12mm damage

Mutual coupling of longitudinal vibration with rotational component of cross-section vibration results in new mode shapes as shown in Figure 7.2.3. The first thing we notice is that with the increase of damage depth, the amplitude of transverse vibration rises in the damaged area. It is interesting to note that the cross-section rotation angle in component rotation vibration of the cross-section in the centre of damage is the same regardless of damage depth, whereas in the area stretching from the centre of damage to its ends the cross-section rotation angle rises after which it tends afterwards the values of cross-section angles of a non-damaged beam. This is a characteristic phenomenon and occurs regardless of the vibration mode. The qualities of changes in the cross-section angle are not easily determined experimentally. If this were possible, the component mode shapes of the component rotation of beams' cross-section vibration could be used for damage detection with great accuracy.

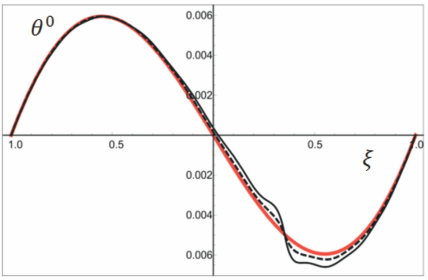

Rotational component of cross-section - mode 1
(a)

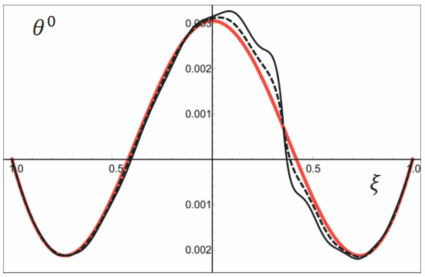

Rotational component of cross - section - mode 2
(b)

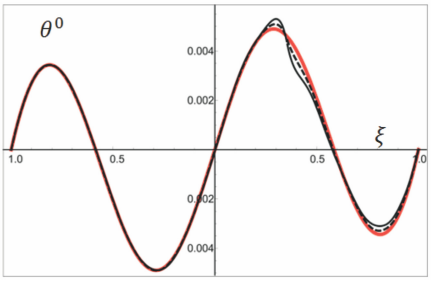

Rotational component of cross-section - mode 3
(c)

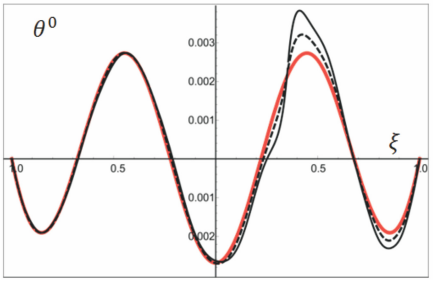

Rotational component of cross-section - mode 4
(d)

Fig. 7.2.3 Rotational components of beams' cross-sections mode shapes: Case 1.1 — non-damaged beam; ----- 8mm damage; — 12mm damage

7.3 Geometrically Non-linear Vibrations of a Damaged Timoshenko Beam in the Time Domain

Consideration of geometric non-linear vibration of a damaged beam can be applied in technical practice. In addition to numerical tools for damage detection, the dynamic behavior of the damaged structure in the time domain also has an important role. This implies determining the displacement of the damaged beams' centerline in the function of location and damage depth. The system of non-linear partial differential equations 7.1.24 was solved by Newmark method [32]. In the numerical experiment, transverse forced action on the beam was taken as a harmonic concentrated external excitation in the form $f(t) = F\cos(\omega_e\, t)$, where ω_e and F are the frequency and amplitude respectively. The new p –version of the finite element method was first tested for case 2.1 – the case of a non-damaged beam considered experimentally [46] and numerically [45]. The model of a non-damaged beam with newly implemented shape functions was derived and tested in a non-linear domain whereby damage depth equals zero. Figure 7.3.1 shows transverse displacement of the point on the centre of a non-damaged beam and the beam with

different damage depth in the case when the amplitudes of external concentrated harmonic excitation equals 0.134 N and frequency $\omega_e = \omega_{l1}$. For determining the amplitudes of a non-damaged beam in the time domain, 15 shape functions were used in the new p model. The vertical axis shows the values of transverse beam displacement divided by its thickness h, while the horizontal axis shows non-dimensional frequency. The amplitude of a non-damaged beam corresponds well to the results obtained by way of a shooting method as well as the traditional p -version of the finite element method [45]. As an example of maximum amplitude of transverse displacement of the centre point of the non-damaged beam calculated at the excitation frequency of $\omega_e = 1.02\ \omega_{l1}$ obtained by the new p-version of the finite element method is 0.425, the value which is close to the experimental result obtained in the same conditions 0.43 given in reference [46].

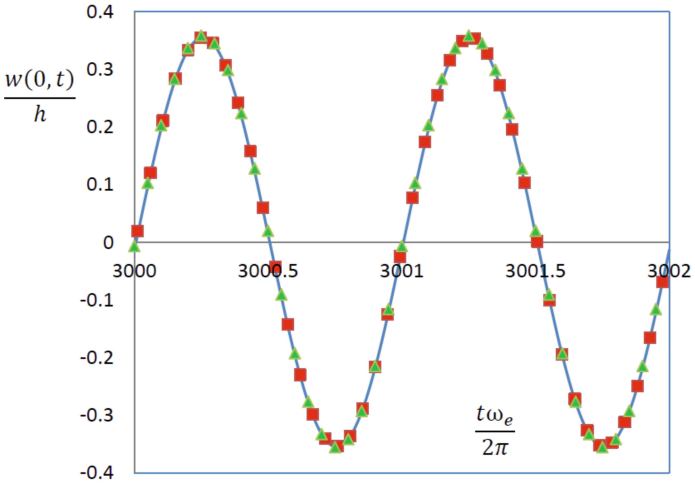

Fig. 7.3.1 Amplitude-time diagram, $x = 0$, Case - 2.1.1, external excitation - 0.134 N, $\omega_e = \omega_{l1}$, ——— non-damaged beam; ■■■ 2.1.1. b); ▲▲▲ 2.1.1. c).

The diagram 7.3.1 shows a barely noticeable difference in the amplitude size of beam's centre lines at external excitation of the beam's centre point. However, in the points of the beam's centre line closer to damage, it has stronger influence and more noticeable differences in amplitude of beam vibration appear. Figure 7.3.2 illustrates the amplitudes of two symmetrically chosen beam points in relation to vertical axis z. It can be concluded that asymmetry occurs in vibration as a consequence of the beam's changed geometry due to its damage and is visible by comparing the obtained results for the point closer to the damage centre $= 71.75$ mm. . The effect of a constant member on a beam's deflection can be seen in Fourier's spectrum diagram 7.3.5 c), which, coupled with non-linear members, increases the effect of square non-linearities and does not allow disregarding the second harmonic at vibration.

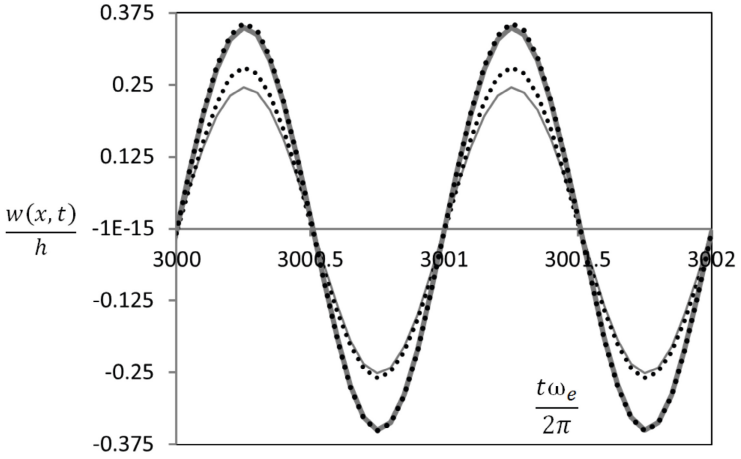

Fig. 7.3.2 Amplitude-time diagram of beam's symmetric points case 2.1.1 c), external concentrated excitation at beam's centre with the amplitude of 0.134 N, $\omega_e = \omega_{l1}$;—$x = -78$mm; ••• $x = 78$ mm; —$x = -15$ mm;●●●$x = 15$ mm

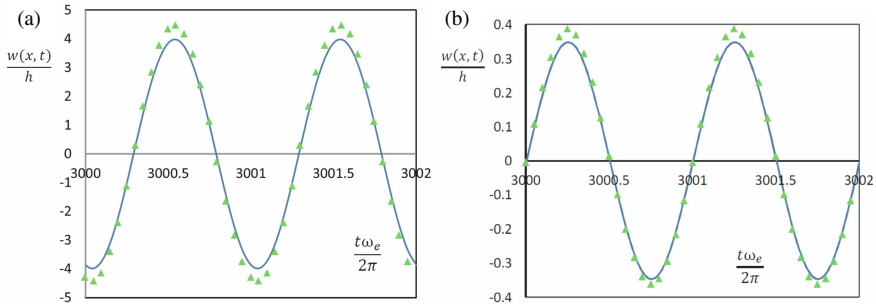

Fig. 7.3.3 Amplitude-time diagram $x = 62.4$ mm for case 2.1.1 c) external concentrated excitation $x = 62.4$mm, 0.134 N, $\omega_e = \omega_{l1}$,(a) linear mode (b) non-linear mode — non-damaged beam; ▲▲▲2.1.1 c)

Diagrams 7.3.3 a) and b) show the amplitudes at external concentrated excitation for a linear and non-linear model respectively. It is important to note that the non-linear influence is displayed through the appearance of symmetry in vibration in relation to the horizontal axis x which cannot be concluded from a linear model. Greater vibration amplitude thus occurs on the side of the damage (in this model it is the beam's top side). Such phenomenon occurs as a consequence of coupling of transverse and rotational displacement of the cross-section in the stiffness matrix of non-linear members (equation 7.1.24).

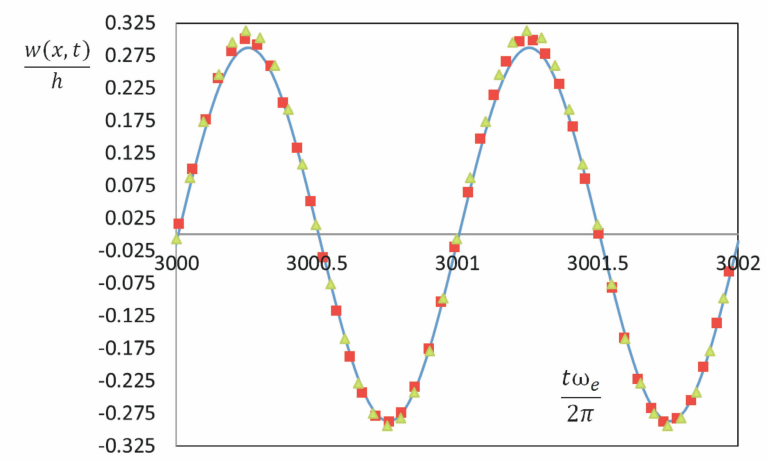

Fig. 7.3.4 Amplitude –time diagram $x = 62.4$ mm, case 2.1.1, amplitude of forcing 0.134 N, $\omega_e = \omega_{l1}$, — non-damaged beam; ▬ 2.1.1. b); ▲▲▲ 2.1.1. c)

The effect of geometric non-linearity for different values of damage depth is shown in Figures 7.3.4-7.3.5. The increase of damage depth yields increased amplitudes of transverse displacement of the beam's centre line which is more dominant in the points near damage. In the phase diagram 7.3.5 a) asymmetry in vibration as a consequence of damage and geometric non-linearity can also be noted. The points in the Poincaré diagram 7.3.5 b) show the difference between the vibration of a non-damaged beam and the beam with different damage depths.

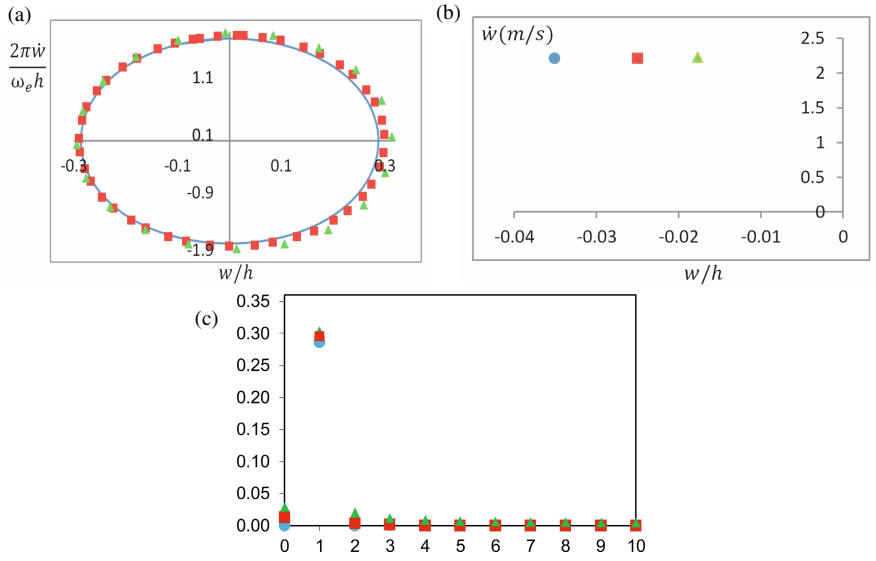

Fig. 7.3.5 Case 2.1.1 amplitude of forcing $x = 0$, 0.134N, $\omega_e = \omega_{l1}$ (a) Phase diagram $x = 62.4$ mm;(b) Poincaré diagram $x = 62.4$ mm; (c) Fourier spectrum $x = 62.4$ mm. —, ●non-damaged beam; ▬ 2.1.1. b); ▲▲▲ 2.1.1. c)

The difference between the amplitude of a beam with different depth damages increases in higher modes of forcing. Figure 7.3.6 shows the amplitude-time diagram at external excitation frequency which equals linear frequency in the third mode. It can be noted that with the parameters of such excitation a more dominant asymmetry in vibration take place, as well as the movement of the beam towards the side where the damage has been detected. With the increase of damage depth at higher vibration modes, the asymmetry in beam vibration rises.

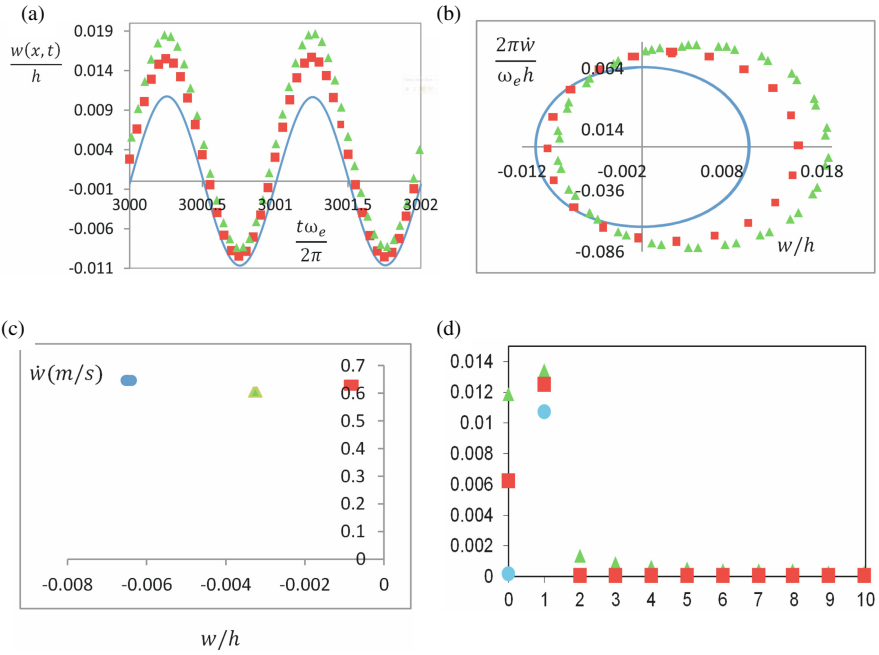

Fig. 7.3.6 Case 2.1.1 amplitude of forcing 0. 4N, x= 101.5mm, $\omega_e = \omega_{l3}$ Amplitude-time diagram ; (b) Phase diagram; (c) Poincaré diagram; (d) Fourier spectrum; (x = 62.4 mm)——, ● non-damaged beam; ■■■ 2.1.1. b); ▲▲▲ 2.1.1. c)

The new p–version of the finite element method can be applied in the consideration of thicker beams. The results obtained for a thicker beam (Figure 7.3.7) show the same qualitative effect of the geometric linearity and damage as in the case of slender beams.

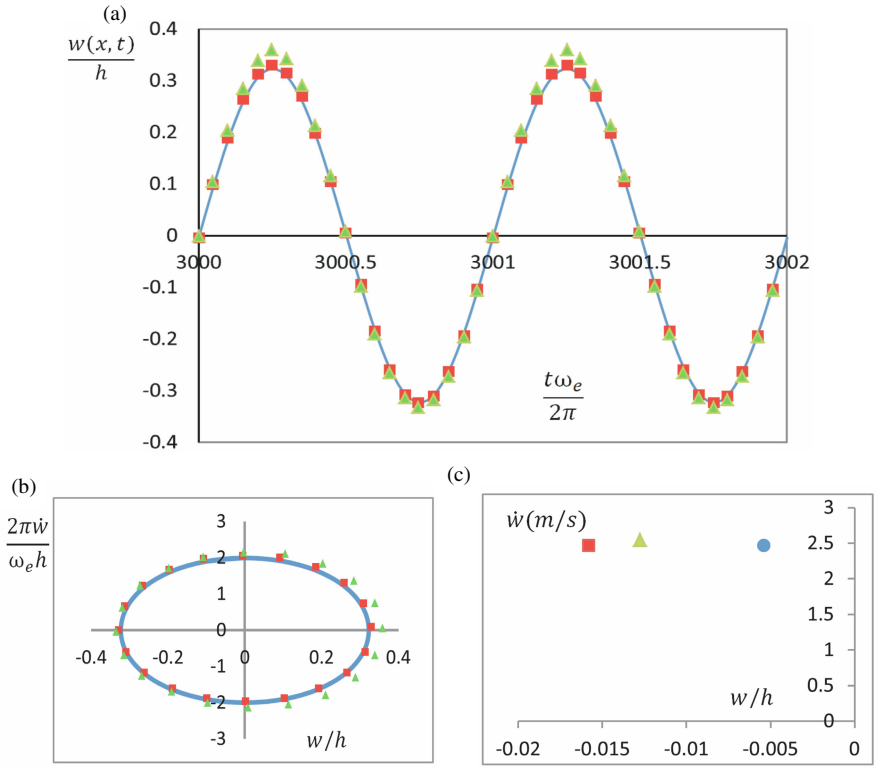

Fig. 7.3.7 Case 2.2 amplitude of forcing 2000N,x= 0, $\omega_e = \omega_{l1}$ (a) Amplitude-time diagram; (b) Phase diagram; (c) Poincaré diagram; ($x = 62.4$ mm) —, ● non-damaged beam; ■■■ 2.2 a); ▲▲▲ 2.2 b)

7.4 Free Geometric Non-linear Vibrations of the Damaged Timoshenko Beam in the Frequency Domain

Through the application of the harmonic balance method and the Continuation method [49] we can determine bifurcation points which are very common in non-linear mechanics. If we consider the system of damaged beam which is not affected by external forces $\delta W_{ex} = 0$, by applying the virtual work principle, we obtain

$$\begin{bmatrix} \mathbf{M}^l & \mathbf{0} & \mathbf{0} \\ \mathbf{0} & \mathbf{M}^b & \mathbf{0} \\ \mathbf{0} & \mathbf{0} & \mathbf{M}^r \end{bmatrix} \begin{Bmatrix} \ddot{\mathbf{q}}_\mathbf{u} \\ \ddot{\mathbf{q}}_\mathbf{w} \\ \ddot{\mathbf{q}}_\boldsymbol{\theta} \end{Bmatrix} + \begin{bmatrix} \mathbf{0} & \mathbf{0} & \mathbf{M}^{lr} \\ \mathbf{0} & \mathbf{0} & \mathbf{0} \\ \mathbf{M}^{lr\mathrm{T}} & \mathbf{0} & \mathbf{0} \end{bmatrix} \begin{Bmatrix} \ddot{\mathbf{q}}_\mathbf{u} \\ \ddot{\mathbf{q}}_\mathbf{w} \\ \ddot{\mathbf{q}}_\boldsymbol{\theta} \end{Bmatrix} +$$
$$+ \begin{bmatrix} \mathbf{K}_\ell^l & \mathbf{0} & \mathbf{0} \\ \mathbf{0} & \mathbf{K}_\ell^{\gamma_{11}} & \mathbf{K}_\ell^{\gamma_{12}} \\ \mathbf{0} & \mathbf{K}_\ell^{\gamma_{21}} & \mathbf{K}_\ell^b + \mathbf{K}_\ell^{\gamma_{22}} \end{bmatrix} \begin{Bmatrix} \mathbf{q}_\mathbf{u} \\ \mathbf{q}_\mathbf{w} \\ \mathbf{q}_\boldsymbol{\theta} \end{Bmatrix} + \begin{bmatrix} \mathbf{0} & \mathbf{0} & \mathbf{K}_\ell^{lr} \\ \mathbf{0} & \mathbf{0} & \mathbf{0} \\ \mathbf{K}_\ell^{lr\mathrm{T}} & \mathbf{0} & \mathbf{0} \end{bmatrix} \begin{Bmatrix} \mathbf{q}_\mathbf{u} \\ \mathbf{q}_\mathbf{w} \\ \mathbf{q}_\boldsymbol{\theta} \end{Bmatrix} + \tag{7.4.1}$$
$$+ \begin{bmatrix} \mathbf{0} & \mathbf{K}_{n\ell}^2(\mathbf{q}_\mathbf{w}) & \mathbf{0} \\ \mathbf{K}_{n\ell}^3(\mathbf{q}_\mathbf{w}) & \mathbf{K}_{n\ell}^4(\mathbf{q}_\mathbf{w}) & \mathbf{0} \\ \mathbf{0} & \mathbf{0} & \mathbf{0} \end{bmatrix} \begin{Bmatrix} \mathbf{q}_\mathbf{u} \\ \mathbf{q}_\mathbf{w} \\ \mathbf{q}_\boldsymbol{\theta} \end{Bmatrix} + \begin{bmatrix} \mathbf{0} & \mathbf{0} & \mathbf{0} \\ \mathbf{0} & \mathbf{0} & \mathbf{K}_{n\ell}^{br}(\mathbf{q}_\mathbf{w}) \\ \mathbf{0} & \mathbf{K}_{n\ell}^{br\mathrm{T}}(\mathbf{q}_\mathbf{w}) & \mathbf{0} \end{bmatrix} \begin{Bmatrix} \mathbf{q}_\mathbf{u} \\ \mathbf{q}_\mathbf{w} \\ \mathbf{q}_\boldsymbol{\theta} \end{Bmatrix} = \begin{Bmatrix} \mathbf{0} \\ \mathbf{0} \\ \mathbf{0} \end{Bmatrix}.$$

The products $[\mathbf{M}^{l}]\{\ddot{\mathbf{q}}_{\mathbf{u}}\}, [\mathbf{M}^{lr}]\{\ddot{\mathbf{q}}_{\boldsymbol{\theta}}\}$ and $\left[\mathbf{M}^{lr^{\mathrm{T}}}\right]\{\ddot{\mathbf{q}}_{\mathbf{u}}\}$ represent small quantities and do not affect the solutions in a non-linear mode as shown in ref. [44] and can be disregarded

$$\begin{bmatrix}\mathbf{M}^{b} & 0\\ 0 & \mathbf{M}^{r}\end{bmatrix}\begin{Bmatrix}\ddot{\mathbf{q}}_{\mathbf{w}}\\ \ddot{\mathbf{q}}_{\boldsymbol{\theta}}\end{Bmatrix}+\begin{bmatrix}\mathbf{K}_{\ell}^{\gamma_{11}} & \mathbf{K}_{\ell}^{\gamma_{12}}\\ \mathbf{K}_{\ell}^{\gamma_{12}\mathrm{T}} & \overline{\mathbf{KL}_{\mathbf{55}}}\end{bmatrix}\begin{Bmatrix}\mathbf{q}_{\mathbf{w}}\\ \mathbf{q}_{\boldsymbol{\theta}}\end{Bmatrix}+\begin{bmatrix}\mathbf{KNL}1 & \mathbf{KNL}2\\ \mathbf{KNL}3 & 0\end{bmatrix}\begin{Bmatrix}\mathbf{q}_{\mathbf{w}}\\ \mathbf{q}_{\boldsymbol{\theta}}\end{Bmatrix}=\begin{Bmatrix}\mathbf{0}\\ \mathbf{0}\end{Bmatrix}. \quad (7.4.2)$$

where

$$\overline{\mathbf{KL}_{\mathbf{55}}}=\mathbf{K}_{\ell}^{b}+\mathbf{K}_{\ell}^{\gamma_{22}}-\mathbf{K}_{\ell}^{lr^{\mathrm{T}}}\mathbf{K}_{\ell}^{l^{-1}}\mathbf{K}_{\ell}^{lr},\mathbf{KNL}1=\mathbf{K}_{n\ell}^{4}(\mathbf{q}_{\mathbf{w}})-\mathbf{K}_{n\ell}^{3}(\mathbf{q}_{\mathbf{w}})\mathbf{KL}_{\mathbf{11}}{}^{-1}\mathbf{K2}_{\mathbf{13}},$$
$$\mathbf{KNL}2=\mathbf{K}_{n\ell}^{br}-2\mathbf{K2}_{\mathbf{13}}{}^{\mathrm{T}}\mathbf{K}_{\ell}^{l^{-1}}\mathbf{K}_{\ell}^{lr},\mathbf{KNL}3=\mathbf{K}_{n\ell}^{br^{\mathrm{T}}}-\mathbf{K}_{\ell}^{lr^{\mathrm{T}}}\mathbf{K}_{\ell}^{l^{-1}}\mathbf{K}_{n\ell}^{2}(\mathbf{q}_{\mathbf{w}}).$$

The vector of generalized coordinates and their second derivative (acceleration) can be shown as a sum of first three members of a trigonometric order (first three members are sufficient based on the results of the Fourier spectrum) in the following form

$$\begin{Bmatrix}\mathbf{q}_{\mathbf{w}}(\boldsymbol{t})\\ \mathbf{q}_{\boldsymbol{\theta}}(\boldsymbol{t})\end{Bmatrix}=\frac{1}{2}\begin{Bmatrix}Q_{w_{c0}}\\ Q_{\theta_{c0}}\end{Bmatrix}+\cos(\omega t)\begin{Bmatrix}Q_{w_{c1}}\\ Q_{\theta_{c1}}\end{Bmatrix}+\cos(2\omega t)\begin{Bmatrix}Q_{w_{c2}}\\ Q_{\theta_{c2}}\end{Bmatrix}+\cos(3\omega t)\begin{Bmatrix}Q_{w_{c3}}\\ Q_{\theta_{c3}}\end{Bmatrix}, \quad (7.4.3)$$

$$\begin{Bmatrix}\ddot{\mathbf{q}}_{\mathbf{w}}(t)\\ \ddot{\mathbf{q}}_{\boldsymbol{\theta}}(t)\end{Bmatrix}=-\omega^{2}\cos(\omega t)\begin{Bmatrix}Q_{w_{c1}}\\ Q_{\theta_{c1}}\end{Bmatrix}-4\,\omega^{2}\cos(2\omega t)\begin{Bmatrix}Q_{w_{c2}}\\ Q_{\theta_{c2}}\end{Bmatrix}-9\,\omega^{2}\cos(3\omega t)\begin{Bmatrix}Q_{w_{c3}}\\ Q_{\theta_{c3}}\end{Bmatrix}. \quad (7.4.4)$$

where ω represents the system's natural frequency. The vector of new unknowns is now

$$\{Q^{HBM}\}=\begin{Bmatrix}Q_{w_{c0}}\\ Q_{w_{c1}}\\ Q_{w_{c2}}\\ Q_{w_{c3}}\\ Q_{\theta_{c0}}\\ Q_{\theta_{c1}}\\ Q_{\theta_{c2}}\\ Q_{\theta_{c3}}\end{Bmatrix}. \quad (7.4.5)$$

If we substitute the expressions (7.4.3) and (7.4.4) into the initial set of equations of motion (7.4.2), we get

$$(-\omega^{2}\mathbf{M}^{\mathrm{HBM}}+\mathbf{KL}^{\mathrm{HBM}}+\mathbf{KNL}^{\mathrm{HBM}})\{Q^{HBM}\}=\{0\}, \quad (7.4.6)$$

where

$$\mathbf{M}^{\mathrm{HBM}} = \begin{bmatrix} 0 & 0 & 0 & 0 & 0 & 0 & 0 & 0 \\ 0 & \mathbf{M}^{b} & 0 & 0 & 0 & 0 & 0 & 0 \\ 0 & 0 & 4\mathbf{M}^{b} & 0 & 0 & 0 & 0 & 0 \\ 0 & 0 & 0 & 9\mathbf{M}^{b} & 0 & 0 & 0 & 0 \\ 0 & 0 & 0 & 0 & 0 & 0 & 0 & 0 \\ 0 & 0 & 0 & 0 & 0 & \mathbf{M}^{r} & 0 & 0 \\ 0 & 0 & 0 & 0 & 0 & 0 & 4\mathbf{M}^{r} & 0 \\ 0 & 0 & 0 & 0 & 0 & 0 & 0 & 9\mathbf{M}^{r} \end{bmatrix}, \tag{7.4.7}$$

$$\mathbf{KL}^{\mathrm{HBM}} = \begin{bmatrix} (1/2)\mathbf{K}_{\ell}^{\gamma_{11}} & 0 & 0 & 0 & (1/2)\mathbf{K}_{\ell}^{\gamma_{12}} & 0 & 0 & 0 \\ 0 & \mathbf{K}_{\ell}^{\gamma_{11}} & 0 & 0 & 0 & \mathbf{K}_{\ell}^{\gamma_{12}} & 0 & 0 \\ 0 & 0 & \mathbf{K}_{\ell}^{\gamma_{11}} & 0 & 0 & 0 & \mathbf{K}_{\ell}^{\gamma_{12}} & 0 \\ 0 & 0 & 0 & \mathbf{K}_{\ell}^{\gamma_{11}} & 0 & 0 & 0 & \mathbf{K}_{\ell}^{\gamma_{12}} \\ (1/2)\mathbf{K}_{\ell}^{\gamma_{12}\mathrm{T}} & 0 & 0 & 0 & (1/2)\overline{\mathbf{KL}}_{\mathbf{55}} & 0 & 0 & 0 \\ 0 & \mathbf{K}_{\ell}^{\gamma_{12}\mathrm{T}} & 0 & 0 & 0 & \overline{\mathbf{KL}}_{\mathbf{55}} & 0 & 0 \\ 0 & 0 & \mathbf{K}_{\ell}^{\gamma_{12}\mathrm{T}} & 0 & 0 & 0 & \overline{\mathbf{KL}}_{\mathbf{55}} & 0 \\ 0 & 0 & 0 & \mathbf{K}_{\ell}^{\gamma_{12}\mathrm{T}} & 0 & 0 & 0 & \overline{\mathbf{KL}}_{\mathbf{55}} \end{bmatrix}. \tag{7.4.8}$$

Amplitude-frequency characteristic of the model's first and third harmonic is shown in Figure 7.4.1.

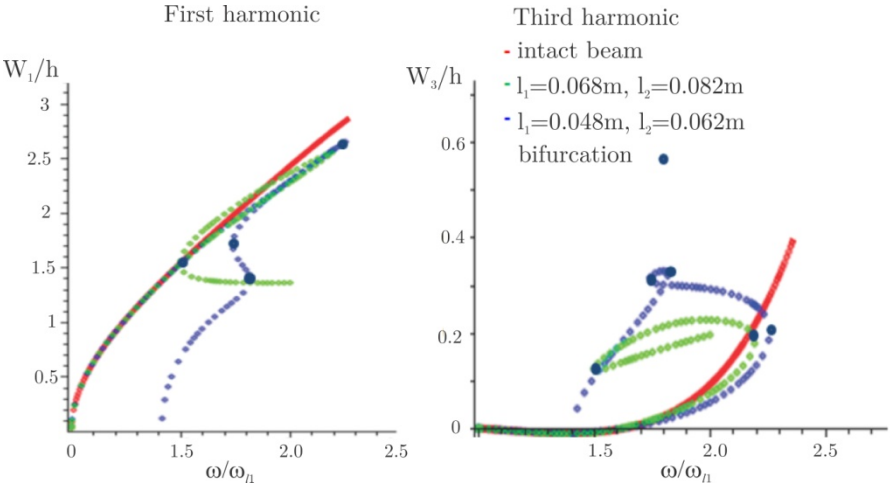

Fig. 7.4.1 Amplitude-frequency diagram for case 2.1.1

From Figure 7.4.1 it can be concluded that the interaction between the higher vibration modes for different positions of damage on the beam, results in bifurcations marked on the diagram, Stojanovic et Ribeiro [23]. Their occurrence brings the beam into a state of internal resonance, hence it is essential to know in which amplitude-frequency relation it takes place. The diagram 7.4.1 shows the locations of possible dual solutions for the first and third harmonics for the vibration of a damaged beam.

Based on the shown results, Stojanović et al. [50], we conclude that the change in geometry of the beam caused by the occurrence of damage introduces new coupling between component mode shapes in both linear and non-linear vibration mode. Certain deviations in component mode shapes can be used for creating a model for damage detection. The results obtained from the occurrence of longitudinal vibration and asymmetry in transverse vibration present novelties in displacement dynamics of damaged beam's points and can be used in the analysis of actual constructions.

Appendix 7.1.1 - Mass and stiffness matrixes of linear and non-linear members in the expression (7.1.24)

$$\mathbf{M} = \begin{bmatrix} \mathbf{M}^{l} & \mathbf{0} & \mathbf{0} \\ \mathbf{0} & \mathbf{M}^{b} & \mathbf{0} \\ \mathbf{0} & \mathbf{0} & \mathbf{M}^{r} \end{bmatrix} + \begin{bmatrix} \mathbf{0} & \mathbf{0} & \mathbf{M}^{lr} \\ \mathbf{0} & \mathbf{0} & \mathbf{0} \\ \mathbf{M}^{lr\mathrm{T}} & \mathbf{0} & \mathbf{0} \end{bmatrix},$$

where

$$\mathbf{M}^{l} = \frac{\rho hbl}{2}\int_{-1}^{\frac{2l_1}{L}} \boldsymbol{N^{u1}}^{\mathrm{T}}\boldsymbol{N^{u1}}\mathrm{d}\xi + \frac{\rho bl}{2}\int_{-\frac{h}{2}}^{\frac{h}{2}-h_1}\int_{\frac{2l_1}{L}}^{\frac{2l_1+x_c}{L}} \boldsymbol{N^{u1}}^{\mathrm{T}}\boldsymbol{N^{u1}}\mathrm{d}\xi$$

$$+\frac{\rho bl}{2}\int_{-\frac{h}{2}}^{\frac{h}{2}-h_1}\int_{\frac{2l_1+x_c}{L}}^{\frac{2l_2}{L}} \boldsymbol{N^{u2}}^{\mathrm{T}}\boldsymbol{N^{u2}}\mathrm{d}\xi + \frac{\rho hbl}{2}\int_{\frac{2l_2}{L}}^{1} \boldsymbol{N^{u2}}^{\mathrm{T}}\boldsymbol{N^{u2}}\mathrm{d}\xi,$$

$$\mathbf{M}^{b} = \frac{\rho hbl}{2}\int_{-1}^{\frac{2l_1}{L}} \boldsymbol{N^{w1}}^{\mathrm{T}}\boldsymbol{N^{w1}}\mathrm{d}\xi + \frac{\rho bl}{2}\int_{-\frac{h}{2}}^{\frac{h}{2}-h_1}\int_{\frac{2l_1}{L}}^{\frac{2l_1+x_c}{L}} \boldsymbol{N^{w1}}^{\mathrm{T}}\boldsymbol{N^{w1}}\mathrm{d}\xi\mathrm{d}z$$

$$+\frac{\rho bl}{2}\int_{-\frac{h}{2}}^{\frac{h}{2}-h_1}\int_{\frac{2l_1+x_c}{L}}^{\frac{2l_2}{L}} \boldsymbol{N^{w2}}^{\mathrm{T}}\boldsymbol{N^{w2}}\mathrm{d}\xi\mathrm{d}z + \frac{\rho hbl}{2}\int_{\frac{2l_2}{L}}^{1} \boldsymbol{N^{w2}}^{\mathrm{T}}\boldsymbol{N^{w2}}\mathrm{d}\xi,$$

$$\mathbf{M}^{r} = \frac{\rho hbl}{2}\int_{-1}^{\frac{2l_1}{L}} \boldsymbol{N^{\theta 1}}^{\mathrm{T}}\boldsymbol{N^{\theta 1}}\mathrm{d}\xi + \frac{\rho bl}{2}\int_{-\frac{h}{2}}^{\frac{h}{2}-h_1}\int_{\frac{2l_1}{L}}^{\frac{2l_1+x_c}{L}} \boldsymbol{N^{\theta 1}}^{\mathrm{T}}\boldsymbol{N^{\theta 1}}z^2\mathrm{d}\xi\mathrm{d}z$$

$$+\frac{\rho bl}{2}\int_{-\frac{h}{2}}^{\frac{h}{2}-h_1}\int_{\frac{2l_1+x_c}{L}}^{\frac{2l_2}{L}} \boldsymbol{N^{\theta 2}}^{\mathrm{T}}\boldsymbol{N^{\theta 2}}z^2\mathrm{d}\xi\mathrm{d}z + \frac{\rho hbl}{2}\int_{\frac{2l_2}{L}}^{1} \boldsymbol{N^{\theta 2}}^{\mathrm{T}}\boldsymbol{N^{\theta 2}}\mathrm{d}\xi,$$

$$\mathbf{M}^{lr} = \frac{\rho bl}{2}\int_{-\frac{h}{2}}^{\frac{h}{2}-h_1}\int_{\frac{2l_1}{L}}^{\frac{2l_1+x_c}{L}} \boldsymbol{N^{u1}}^{\mathrm{T}}\boldsymbol{N^{\theta 1}}z\,\mathrm{d}\xi\mathrm{d}z + \frac{\rho bl}{2}\int_{-\frac{h}{2}}^{\frac{h}{2}-h_1}\int_{\frac{2l_1+x_c}{L}}^{\frac{2l_2}{L}} \boldsymbol{N^{u2}}^{\mathrm{T}}\boldsymbol{N^{\theta 2}}z\,\mathrm{d}\xi\mathrm{d}z.$$

$$\mathbf{K}(\mathbf{q}) = \mathbf{K}_{\ell} + \mathbf{K}_{\ell}^{c} + \mathbf{K}_{\mathrm{n}\ell}(\mathbf{q}) + \mathbf{K}_{\mathrm{n}\ell}^{c}(\mathbf{q}) = \begin{bmatrix} \mathbf{K}_{\ell}^{l} & \mathbf{0} & \mathbf{0} \\ \mathbf{0} & \mathbf{K}_{\ell}^{\gamma_{11}} & \mathbf{K}_{\ell}^{\gamma_{12}} \\ \mathbf{0} & \mathbf{K}_{\ell}^{\gamma_{21}} & \mathbf{K}_{\ell}^{b} + \mathbf{K}_{\ell}^{\gamma_{22}} \end{bmatrix} + \begin{bmatrix} \mathbf{0} & \mathbf{0} & \mathbf{K}_{\ell}^{lr} \\ \mathbf{0} & \mathbf{0} & \mathbf{0} \\ \mathbf{K}_{\ell}^{lr\mathrm{T}} & \mathbf{0} & \mathbf{0} \end{bmatrix} +$$

$$+ \begin{bmatrix} \mathbf{0} & \mathbf{K}_{n\ell}^{2}(\mathbf{q_w}) & \mathbf{0} \\ \mathbf{K}_{n\ell}^{3}(\mathbf{q_w}) & \mathbf{K}_{n\ell}^{4}(\mathbf{q_w}) & \mathbf{0} \\ \mathbf{0} & \mathbf{0} & \mathbf{0} \end{bmatrix} + \begin{bmatrix} \mathbf{0} & \mathbf{0} & \mathbf{0} \\ \mathbf{0} & \mathbf{0} & \mathbf{K}_{n\ell}^{br}(\mathbf{q_w}) \\ \mathbf{0} & \mathbf{K}_{n\ell}^{br\mathrm{T}}(\mathbf{q_w}) & \mathbf{0} \end{bmatrix},$$

$$\mathbf{K}_{\ell}^{l}=\frac{2Ehb}{L}\int_{-1}^{\frac{2l_1}{L}}\frac{d\boldsymbol{N^{u1}}^{\mathrm{T}}}{d\xi}\frac{d\boldsymbol{N^{u1}}}{d\xi}\mathrm{d}\xi+\frac{2Eb}{L}\int_{-\frac{h}{2}}^{\frac{h}{2}-h_1}\int_{\frac{2l_1}{L}}^{\frac{2l_1+x_c}{L}}\frac{d\boldsymbol{N^{u1}}^{\mathrm{T}}}{d\xi}\frac{d\boldsymbol{N^{u1}}}{d\xi}z^2\mathrm{d}\xi\mathrm{d}z+$$

$$+\frac{2Eb}{L}\int_{-\frac{h}{2}}^{\frac{h}{2}-h_1}\int_{\frac{2l_1+x_c}{L}}^{\frac{2l_2}{L}}\frac{d\boldsymbol{N^{u2}}^{\mathrm{T}}}{d\xi}\frac{d\boldsymbol{N^{u2}}}{d\xi}z^2\mathrm{d}\xi\mathrm{d}z+\frac{2Ehb}{L}\int_{\frac{2l_2}{L}}^{1}\frac{d\boldsymbol{N^{u2}}^{\mathrm{T}}}{d\xi}\frac{d\boldsymbol{N^{u2}}}{d\xi}\mathrm{d}\xi$$

$$\mathbf{K}_{\ell}^{\gamma_{11}}=\frac{2kGhb}{L}\int_{-1}^{\frac{2l_1}{L}}\frac{d\boldsymbol{N^{w1}}^{\mathrm{T}}}{d\xi}\frac{d\boldsymbol{N^{w1}}}{d\xi}\mathrm{d}\xi+\frac{2\lambda Gb}{L}\int_{-\frac{h}{2}}^{\frac{h}{2}-h_1}\int_{\frac{2l_1}{L}}^{\frac{2l_1+x_c}{L}}\frac{d\boldsymbol{N^{w1}}^{\mathrm{T}}}{d\xi}\frac{d\boldsymbol{N^{w1}}}{d\xi}\mathrm{d}\xi\mathrm{d}z+$$

$$+\frac{2kGb}{L}\int_{-\frac{h}{2}}^{\frac{h}{2}-h_1}\int_{\frac{2l_1+x_c}{L}}^{\frac{2l_2}{L}}\frac{d\boldsymbol{N^{w2}}^{\mathrm{T}}}{d\xi}\frac{d\boldsymbol{N^{w2}}}{d\xi}\mathrm{d}\xi\mathrm{d}z+\frac{2\lambda Ghb}{L}\int_{\frac{2l_2}{L}}^{1}\frac{d\boldsymbol{N^{w2}}^{\mathrm{T}}}{d\xi}\frac{d\boldsymbol{N^{w2}}}{d\xi}\mathrm{d}\xi$$

$$\mathbf{K}_{\ell}^{\gamma_{12}}=kGhb\int_{-1}^{\frac{2l_1}{L}}\frac{d\boldsymbol{N^{w1}}^{\mathrm{T}}}{d\xi}\boldsymbol{N^{\theta 1}}\mathrm{d}\xi+kGb\int_{-\frac{h}{2}}^{\frac{h}{2}-h_1}\int_{\frac{2l_1}{L}}^{\frac{2l_1+x_c}{L}}\frac{d\boldsymbol{N^{w1}}^{\mathrm{T}}}{d\xi}\boldsymbol{N^{\theta 1}}\mathrm{d}\xi\mathrm{d}z+$$

$$kGb\int_{-\frac{h}{2}}^{\frac{h}{2}-h_1}\int_{\frac{2l_1+x_c}{L}}^{\frac{2l_2}{L}}\frac{d\boldsymbol{N^{w2}}^{\mathrm{T}}}{d\xi}\boldsymbol{N^{\theta 2}}d\xi dz+kGhb\int_{\frac{2l_2}{L}}^{1}\frac{d\boldsymbol{N^{w2}}^{\mathrm{T}}}{d\xi}\boldsymbol{N^{\theta 2}}d\xi,$$

$$\mathbf{K}_{\ell}^{\gamma_{21}}=kGhb\int_{-1}^{\frac{2l_1}{L}}\boldsymbol{N^{\theta 1}}^{\mathrm{T}}\frac{d\boldsymbol{N^{w1}}}{d\xi}d\xi+kGb\int_{-\frac{h}{2}}^{\frac{h}{2}-h_1}\int_{\frac{2l_1}{L}}^{\frac{2l_1+x_c}{L}}\boldsymbol{N^{\theta 1}}^{\mathrm{T}}\frac{d\boldsymbol{N^{w1}}}{d\xi}d\xi dz+$$

$$+kGb\int_{-\frac{h}{2}}^{\frac{h}{2}-h_1}\int_{\frac{2l_1+x_c}{L}}^{\frac{2l_2}{L}}\boldsymbol{N^{\theta 2}}^{\mathrm{T}}\frac{d\boldsymbol{N^{w2}}}{d\xi}\mathrm{d}\xi\mathrm{d}z+kGhb\int_{\frac{2l_2}{L}}^{1}\boldsymbol{N^{\theta 2}}^{\mathrm{T}}\frac{d\boldsymbol{N^{w2}}}{d\xi}\mathrm{d}\xi,$$

$$\mathbf{K}_{\ell}^{\gamma_{22}}=\frac{2kGhb}{L}\int_{-1}^{\frac{2l_1}{L}}\boldsymbol{N^{\theta 1}}^{\mathrm{T}}\boldsymbol{N^{\theta 1}}\mathrm{d}\xi+\frac{2kGb}{L}\int_{-\frac{h}{2}}^{\frac{h}{2}-h_1}\int_{\frac{2l_1}{L}}^{\frac{2l_1+x_c}{L}}\boldsymbol{N^{\theta 1}}^{\mathrm{T}}\boldsymbol{N^{\theta 1}}\mathrm{d}\xi\mathrm{d}z$$

$$+\frac{2kGb}{L}\int_{-\frac{h}{2}}^{\frac{h}{2}-h_1}\int_{\frac{2l_1+x_c}{L}}^{\frac{2l_2}{L}}\boldsymbol{N^{\theta 2}}^{\mathrm{T}}\boldsymbol{N^{\theta 2}}\mathrm{d}\xi\mathrm{d}z+\frac{2kGhb}{L}\int_{\frac{2l_2}{L}}^{1}\boldsymbol{N^{\theta 2}}^{\mathrm{T}}\boldsymbol{N^{\theta 2}}\mathrm{d}\xi,$$

$$\mathbf{K}_{\ell}^{lr}=\frac{2Eb}{L}\int_{-\frac{h}{2}}^{\frac{h}{2}-h_1}\int_{\frac{2l_1}{L}}^{\frac{2l_1+x_c}{L}}\frac{d\boldsymbol{N^{u1}}^{\mathrm{T}}}{d\xi}\frac{d\boldsymbol{N^{\theta 1}}}{d\xi}z\,\mathrm{d}\xi\mathrm{d}z+\frac{2Eb}{L}\int_{-\frac{h}{2}}^{\frac{h}{2}-h_1}\int_{\frac{2l_1+x_c}{L}}^{\frac{2l_2}{L}}\frac{d\boldsymbol{N^{u2}}^{\mathrm{T}}}{d\xi}\frac{d\boldsymbol{N^{\theta 2}}}{d\xi}z\,\mathrm{d}\xi\mathrm{d}z,$$

$$\mathbf{K}_{\ell}^{b}=\frac{2E}{L}\frac{bh^3}{12}\int_{-1}^{\frac{2l_1}{L}}\frac{d\boldsymbol{N^{\theta 1}}^{\mathrm{T}}}{d\xi}\frac{d\boldsymbol{N^{\theta 1}}}{d\xi}\mathrm{d}\xi+\frac{2Eb}{L}\int_{-\frac{h}{2}}^{\frac{h}{2}-h_1}\int_{\frac{2l_1}{L}}^{\frac{2l_1+x_c}{L}}\frac{d\boldsymbol{N^{\theta 1}}^{\mathrm{T}}}{d\xi}\frac{d\boldsymbol{N^{\theta 1}}}{d\xi}z^2\mathrm{d}\xi\mathrm{d}z+$$

$$+\frac{2Eb}{L}\int_{-\frac{h}{2}}^{\frac{h}{2}-h_1}\int_{\frac{2l_1+x_c}{L}}^{\frac{2l_2}{L}}\frac{d\boldsymbol{N^{\theta 2}}^{\mathrm{T}}}{d\xi}\frac{d\boldsymbol{N^{\theta 2}}}{d\xi}z^2\mathrm{d}\xi\mathrm{d}z+\frac{2E}{L}\frac{bh^3}{12}\int_{\frac{2l_2}{L}}^{1}\frac{d\boldsymbol{N^{\theta 2}}^{\mathrm{T}}}{d\xi}\frac{d\boldsymbol{N^{\theta 2}}}{d\xi}\mathrm{d}\xi,$$

$$\mathbf{K}_{nl}^{2}(\mathbf{q_w})=\frac{2Ebh}{L^2}\int_{-1}^{\frac{2l_1}{L}}\frac{dw_0}{d\xi}\frac{d\boldsymbol{N^{u1}}^{\mathrm{T}}}{d\xi}\frac{d\boldsymbol{N^{w1}}}{d\xi}\mathrm{d}\xi+\frac{2Eb}{L^2}\int_{-\frac{h}{2}}^{\frac{h}{2}-h_1}\int_{\frac{2l_1}{L}}^{\frac{2l_1+x_c}{L}}\frac{dw_0}{d\xi}\frac{d\boldsymbol{N^{u1}}^{\mathrm{T}}}{d\xi}\frac{d\boldsymbol{N^{w1}}}{d\xi}\mathrm{d}\xi\mathrm{d}z$$

$$+\frac{2Eb}{L^2}\int_{-\frac{h}{2}}^{\frac{h}{2}-h_1}\int_{\frac{2l_1+x_c}{L}}^{\frac{2l2}{L}}\frac{dw_0}{d\xi}\frac{d\boldsymbol{N^{u2}}^{\mathrm{T}}}{d\xi}\frac{d\boldsymbol{N^{w2}}}{d\xi}\mathrm{d}\xi\mathrm{d}z+\frac{2Ebh}{L^2}\int_{\frac{2l2}{L}}^{1}\frac{dw_0}{d\xi}\frac{d\boldsymbol{N^{u2}}^{\mathrm{T}}}{d\xi}\frac{d\boldsymbol{N^{w2}}}{d\xi}\mathrm{d}\xi,$$

$$\mathbf{K}^{\mathbf{3}}_{n\ell}(\mathbf{q_w}) = 2\mathbf{K}^{\mathbf{2}}_{n\ell}{}^{\mathrm{T}}(\mathbf{q_w}),$$

$$\mathbf{K}^{\mathbf{4}}_{n\ell}(\mathbf{q_w}) = \frac{4Ebh}{L^3}\int_{-1}^{\frac{2l_1}{L}}\left(\frac{dw_0}{d\xi}\right)^2\frac{d\boldsymbol{N^{w1}}^{\mathrm{T}}}{d\xi}\frac{d\boldsymbol{N^{w1}}}{d\xi}\mathrm{d}\xi +$$

$$+\frac{4Eb}{L^3}\int_{-\frac{h}{2}}^{\frac{h}{2}-h_1}\int_{\frac{2l_1}{L}}^{\frac{2l_1+x_c}{L}}\left(\frac{dw_0}{d\xi}\right)^2\frac{d\boldsymbol{N^{w1}}^{\mathrm{T}}}{d\xi}\frac{d\boldsymbol{N^{w1}}}{d\xi}\mathrm{d}\xi\mathrm{d}z +$$

$$+\frac{4Eb}{L^3}\int_{-\frac{h}{2}}^{\frac{h}{2}-h_1}\int_{\frac{2l_1+x_c}{L}}^{\frac{2l_2}{L}}\left(\frac{dw_0}{d\xi}\right)^2\frac{d\boldsymbol{N^{w2}}^{\mathrm{T}}}{d\xi}\frac{d\boldsymbol{N^{w2}}}{d\xi}\mathrm{d}\xi\mathrm{d}z + \frac{4Ebh}{L^3}\int_{\frac{2l_2}{L}}^{1}\left(\frac{dw_0}{d\xi}\right)^2\frac{d\boldsymbol{N^{w2}}^{\mathrm{T}}}{d\xi}\frac{d\boldsymbol{N^{w2}}}{d\xi}\mathrm{d}\xi,$$

$$\mathbf{K}^{br}_{n\ell}(\mathbf{q_w}) = \frac{4Eb}{L^2}\int_{-\frac{h}{2}}^{\frac{h}{2}-h_1}\int_{\frac{2l_1}{L}}^{\frac{2l_1+x_c}{L}}\frac{dw_0}{d\xi}\frac{d\boldsymbol{N^{w1}}^{\mathrm{T}}}{d\xi}\frac{d\boldsymbol{N^{\theta 1}}}{d\xi}z\mathrm{d}\xi\mathrm{d}z +$$

$$+\frac{4Eb}{L^2}\int_{-\frac{h}{2}}^{\frac{h}{2}-h_1}\int_{\frac{2l_1+x_c}{L}}^{\frac{2l_2}{L}}\frac{dw_0}{d\xi}\frac{d\boldsymbol{N^{w2}}^{\mathrm{T}}}{d\xi}\frac{d\boldsymbol{N^{\theta 2}}}{d\xi}z\mathrm{d}\xi dz$$

Chapter 8
Conclusion

The problems of beam vibration present a basic mechanical system encountered in mechanical engineering, civil engineering, aeronautical and transportation industry. Determining solutions of greater accuracy becomes increasingly significant in the reality of technical practice in cases the analysis of the motion of complex systems as deformable bodies with indefinite degree of vibration freedom is required. The existence of more precise approximations of solutions for certain elements allows the elimination a cumulative error effect in finding the solutions for complex dynamic systems. One model of a complex system is a system of elastically connected beams. Having regard to the influence of rotary inertia and transverse shear, the effects of which are familiar in the literature, the problem of establishing analytical solutions for linear vibrations of two or more elastically connected beams of greater thickness with indefinite degree in vibration freedom was analyzed in the present research. The problems of two elastically connected beams attracted a great deal of researchers' attention for practical reasons of determining the conditions under which the system acts as a dynamic absorber. In cases of multiple elastically connected beams, the investigation focused on the stability and establishing the analytical forms of the system's natural frequencies, the number of which increases with the increased number of connected elements resulting in a greater likelihood of a system going into the resonant state. Wide application of such mechanical systems in civil engineering, models of multistory buildings or the associated reinforcement grids, prompted the researchers to start taking a greater number of physical influences into account in formulating mathematical models that shall provide better approximations of solutions.

In addition to dynamic systems which are complex by their nature, in real technical circumstances – civil and mechanical engineering, aeronautical and transportation industry, dynamic problems of elastic bodies that are not necessarily of a complex structure but are characterized by a very complex movement (*complex is taken to mean express deviation in motion compared to classical models of mechanical systems*) start to appear particularly in a non-linear vibration mode. Damaged beams constitute one such group of practically essential mechanical systems. In most cases, the oscillatory motion of such systems can only be determined experimentally. The development of satisfactory mathematical models, numerical methods and software tools enabled a more thorough analysis

V. Stojanović and P. Kozić, *Vibrations and Stability of Complex Beam Systems,*
Springer Tracts in Mechanical Engineering, DOI: 10.1007/978-3-319-13767-4_8

of damaged beams. Thus, the obtaining of more precise solutions for system's vibration was facilitated in terms of less time-consuming calculations for the motion of mechanical systems in non-linear conditions. In the present research on non-linear oscillatory motion of damaged beams, numerical solutions were determined under the influence of rotary inertia and transverse shear by using a newly developed finite element method.

In the analysis of elastically connected beams as complex structures and damaged beams with deviations in motion, the influences of rotary inertia and transverse shear were included, allowing the investigation of thicker beam dynamics and more exact approximations of solutions for slender beams. The present paper comprises seven parts individually formed as chapters. The first chapter includes introductory remarks and the overview of research conducted thus far in the theory of elastically connected and damaged structures. It presents one of the procedures used to derive partial differential equations for describing the movement of mechanical systems and gives a summary of the applied methods. Chapters 2-6 deal with the analysis of linear vibration of elastically connected beams, while the seventh chapter focuses on geometric non-linear vibration of damaged beams with the use of the new finite element method.

Free vibration and static stability of two elastically connected beams were discussed in Chapter 2, reference Stojanovic et al. [12]. Different examples were used to show the analytically obtained results and the influences of certain mechanical parameters of the system on natural frequencies and vibration amplitude. The obtained analytical results were verified by way of their comparison with the results attained for the model with identical geometric and material properties acquired through the classical Euler-Bernoulli beam theory. This chapter formulates the equations of free vibration for two elastically connected beams joint by a Winkler layer with the influence of rotary inertia (the Rayleigh's model) and the effects of rotary inertia with transverse shear (Timoshenko's model, Reddy-Bickford's model). The final part of the chapter examines static stability of two elastically connected beams of different types and provides analytical expressions for the values of critical forces. A numerical experiment confirmed the validity of analytically obtained results by comparing them with the results of the models existing in literature. The entire Chapter 2 leads to the conclusion that the effects of rotary inertia and transverse shear must be taken into account with thicker beams, as the errors which occur multiply with the increase of the vibration mode if these are ignored. Changes in natural frequencies and the stability regions were shown for different values of the parameters pertaining to the mechanical system, according to which it can be concluded that the deformation theory of a higher order yields the most precise approximation of solutions.

Chapter 3 analyses forced vibration of two elastically connected Rayleigh, Timoshenko and Reddy-Bickford beams under the influence of axial forces. It provides analytical forms of solutions for three types of external excitation – arbitrarily continuous harmonic excitation, uniformly continuous harmonic excitation and harmonic concentrated excitation. Analytical solutions were

obtained by way of modal analysis, ref. Kelly [25]. In this chapter, partial differential equations were derived for vibrations of a forced system for three types of beam models under the influence of axial compression forces. In addition, it presents general solutions for forced vibration of a system comprising two elastically connected beams under the influence of axial compression forces having taken into account the effects of rotary inertia and transverse shear. The chapter on forced vibration for arbitrarily continuous harmonic external excitation affecting one of the beams subjected to axial compression forces, derives analytical solutions and presents the conditions of resonance and dynamic vibration absorption. Analytical solutions for forced vibration for concentrated harmonic excitation on one of the beams affected by axial compression forces are also determined. Based on the results provided in this chapter, it can be concluded that the increase of axial compression forces up to their critical value under the influence of external continuously uniform harmonic excitation, results in the increase of the beam vibration amplitude ratio. The differences in the approximations of these solutions are given according to the used beam model. Reddy-Bickford and Timoshenko model, Stojanovic et Kozic ref. [13] provided more precise solutions compared to those of Rayleigh, ref. [13] and Euler, Zhang et al. ref. [5]. The increase of vibration mode leads to increased differences in solutions and it is therefore necessary to take the effects of rotary inertia and transverse shear into account in such cases.

Chapter 4 discusses static and stochastic stability of two or three elastically connected beams as well as the case of a single Timoshenko beam on an elastic foundation. Partial differential equations for the motion of points on the beams' centre lines at deformation were derived and the critical buckling force determined for each system. It has been concluded that the system is most stable in case of a single beam on an elastic foundation.

Chapters 5 and 6 analyze free vibration of *m* elastically connected Timoshenko and Reddy-Bickford beams on an elastic foundation under the influence of axial compression forces. Analytical solutions for natural frequencies and critical forces, ref. Stojanovic et al. [15] were determined by way of trigonometric method, ref. Raskovic [28] and numerically verified. Closing remarks on numerical experiments presented in this chapter are given on the basis of results which show that the most precise approximations are provided by the Reddy-Bickford beam model which gives the lowest natural frequencies. Through Reddy-Bickford's model lower values were obtained compared to Timoshenko's model, which can be significant in beams with large cross-sections whereby it is most appropriate to use the deformation theory of a higher order.

Chapter 7 discusses forced geometric non-linear vibration of a doubly clamped Timoshenko beam with damage. The analysis used the newly developed *p*-version of the finite element method which enabled solving the problems of small width damages. The advantage of this new method over its traditional version is providing better approximations of solutions using lower number of freedom degree in numerical analysis. In addition, traditional method could not provide good approximations of solutions for small width damage regardless of the

increase of polynomial degree. This advantage was also shown in comparison with the results obtained using the Ansys commercial software. Newly formed shape functions depending on damage location may also be used in non-linear analysis of non-damaged beams. Open crack beam model was created by the geometric change on the beam which implies the open crack type with a rectangular cross-section. The changed geometry of the beam resulted in the discovery of coupling between longitudinal and rotational displacement of the beams' cross-section in mass and stiffness matrixes of linear members and also between transverse and rotation motions in stiffness matrixes of non-linear members. In chapter 7.1 non-linear partial differential equations were derived for forced vibration of the Timoshenko damaged beam. As a consequence of damage, the existence of longitudinal vibration of a doubly clamped beam was detected with their component mode shapes having a graphic representation (in case of a doubly clamped beam with no damage, there are no longitudinal motions). It has been concluded that the existence of longitudinal vibration may be used to detect and localize damage more easily than changes in component mode shapes (rotational vibration of cross-sections are difficult to use for experimental purposes). Greatest longitudinal motions of the beam do not depend on the system vibration mode and occur in places of boundary damage areas. Depending on the damage depth and location, mode shapes of transverse and rotational displacement of beams were determined. It has been concluded that the deviation in mode shape in relation with a non-damaged beam, rises with the increase of damage depth and vibration mode. It can be noted in the tables representing the natural frequencies that they have lower values for damaged beams. Numerical experiment included experimentally treated instance of a damaged beam showing an excellent correspondence with obtained results. In chapter 7.2 using the Newmark method the solutions to the set of non-linear partial differential equations were obtained which describe the displacement of the system in the time domain. It has been concluded that amplitudes of the damaged beam increase with the increase of damage depth. This occurrence is greater in the region of damage. In addition to amplitude alteration resulting from changed geometry, vibration asymmetry occurs, which is particularly prominent in higher modes of forced vibration. In higher modes of forced action, beams move in a vertical plane towards the side of damage orientation. By analyzing the system in a frequency domain, the bifurcation points and amplitude-frequency characteristics were obtained for the first and third harmonics. Based on the results shown, it can be concluded that in case of damaged beams internal resonance occurs in places depending on damage location. General conclusion may be reached that due to the interaction of frequencies between higher modes, it is necessary to perform the amplitude-frequency beam analysis for each case of damage (the problem may be solved only numerically – Continuation method was used and yielded no analytical solution).

Formulated mathematical models in present research can be used for forming new models which would take into account the geometric type of non-linearity and the change in the stiffness of elastic inter-layers with the component motions

under damping. The present research forms a complete whole for comprehensive further analysis of non-linear vibration of damaged dynamic systems giving the possibility of determining conditions for the behavior of such a system as non-damaged by including the elastic foundation with variable stiffness, the study of which could have wide application in technical practice. Determined conditions for the behavior of thicker beams as the dynamic absorber can be very useful in the construction of bridges exposed to aero-elastic vibration. The present research may serve as the basis for further analysis of non-linear free and forced vibrations of elastic bodies in the mechanics of a continuum (forming of a mathematical model which takes into account the coupling of longitudinal, transverse, torsion and rotary vibration of cross-sections of elastically connected beams and beams with three-dimensional damage). This would enable detailed understanding of three-dimensional behavior of oscillatory continuous dynamic systems which could play a part in constructing active two-layered bridges of greater thickness with the new generation suspension systems. Evolution in the technology of bridge construction and monitoring extends to this day, but the boundaries could be further expanded though new research and development. The possibility of building various dynamic continuous systems made of composite plates and shells in cosmic, aeronautical and military industry, robust bridge systems of various types with an even greater span and other types of non-linear problems in the mechanics of the continuum can be achieved through further scientific research, new theories in the field of vibration and material resistance, the development of new software, numerical methods and the verification of obtained results in experimental laboratory conditions.

Based on the foregoing, further scientific research by this author shall focus on the development of new theories in non-linear mechanics of deformable bodies, development of new numerical methods enabling their solution and the development of software for determining stress-deformation state of mechanical systems with damage, the field in which the first step towards a new approach of finite element method has already been made.

Literature

[1] Seelig, J.M., Hoppmann, W.H.: Impact on an elastically connected double-beam system. J. Appl. Mech. 31, 621–626 (1964)

[2] Oniszczuk, Z.: Free transverse vibrations of elastically connected simply supported double-beam complex system. J. Sound and Vib. 232, 387–403 (2000)

[3] Oniszczuk, Z.: Forced transverse vibrations of an elastically connected complex simply supported double-beam system. J. Sound and Vib. 264, 273–286 (2003)

[4] Zhang, Y.Q., Lu, Y., Wang, S.L., Liu, X.: Vibration and buckling of a double-beam system under compressive axial loading. J. Sound and Vib. 318, 341–352 (2008)

[5] Zhang, Y.Q., Lu, Y., Ma, G.W.: Effect of compressive axial load on forced transverse vibrations of a double-beam system. Int. J. of Mech. Sci. 50, 299–305 (2008)

[6] Vu, H.V., Ordonez, A.M., Karnopp, B.H.: Vibration of a double-beam system. J. Sound and Vib. 229, 807–822 (2000)

[7] Li, J., Hua, H.: Spectral finite element analysis of elastically connected double-beam systems. Fin. Elem. Analysis Des. 15, 1155–1168 (2007)

[8] Li, J., Chen, Y., Hua, H.: Exact dynamic stiffness matrix of a Timoshenko three-beam system. Int. J. Mech. Sci. 50, 1023–1034 (2008)

[9] Kelly, S.G., Srinivas, S.: Free vibrations of elastically connected stretched beams. J. Sound and Vib. 326, 883–893 (2009)

[10] Ariaei, A., Ziaei-Rad, S., Ghayour, M.: Transverse vibration of a multiple-Timoshenko beam system with intermediate elastic connections due to a moving load. Arch. Appl. Mech. 81, 263–281 (2011)

[11] Mao, Q.: Free vibration analysis of elastically connected multiple-beams by using the Adomian modified decomposition method. J. Sound and Vib. 331, 2532–2542 (2012)

[12] Stojanović, V., Kozić, P., Pavlović, R., Janevski, G.: Effect of rotary inertia and shear on vibration and buckling of a double beam system under compressive axial loading. Arch. Appl. Mech. 81, 1993–2005 (2011)

[13] Stojanović, V., Kozić, P.: Forced transverse vibration of Rayleigh and Timoshenko double-beam system with effect of compressive axial load. Int. J. Mech. Sci. 60, 59–71 (2013)

[14] Stojanović, V., Kozić, P., Janevski, G.: Buckling instabilities of elastically connected Timoshenko beams on an elastic layer subjected to axial forces. J. Mech. Materials Struct. 7, 363–374 (2012)

[15] Stojanović, V., Kozić, P., Janevski, G.: Exactclosed-form solutions for the natural frequencies and stability of elastically connected multiple beam system using Timoshenko and high-order shear deformation theory. J. Sound and Vib. 332, 563–576 (2013)

[16] Christides, S., Barr, A.D.S.: One dimensional theory of cracked Bernoulli-Euler beams. Int. J. Mech. Sci. 26, 639–648 (1984)

[17] Sinha, J.K., Friswell, M.I.: Edwards S Simplified models for the location of cracks in beam structures using measured vibration data. J. Sound and Vib. 251, 13–38 (2002)

[18] Pandey, A.K., Biswas, M., Samman, M.M.: Damage detection from change in curvature mode shapes. J. Sound and Vib. 145, 321–332 (1991)
[19] Panteliou, S.D., Chondros, T.G., Argyrakis, V.C., Dimarogonas, A.D.: Damping factors as an indicator of crack severity. J. Sound and Vib. 241, 235–245 (2001)
[20] Bikri, E.I., Benamar, R., Bennouna, M.M.: Geometrically non-linear free vibrations of clamped–clamped beams with an edge crack. Comput. Struct. 84, 485–502 (2006)
[21] Andreaus, U., Casini, P., Vestroni, F.: Non-linear dynamics of a cracked cantilever beam under harmonic excitation. Int. JNon-Linear Mech. 42, 566–575 (2007)
[22] Stojanović, V., Ribeiro, P., Stoykov, S.: Non-linear vibration of Timoshenko damaged beams by a new p-version finite element method. Comput. Struct. 120, 107–119 (2013)
[23] Stojanović, V., Ribeiro, P.: Modes of vibration of damaged beams by a new p-version finite element. Paper presented at the 23rd International Congress of Theoretical and Applied Mechanics, Beijing, China, August 19-24 (2013)
[24] Kaneko, T.: On Timoshenko's correction for shear in vibrating beams. J Physics D 8, 1927–1936 (1975)
[25] Kelly, S.G.: Mechanical Vibrations: Theory and Applications. Cengage, Stamford (2012)
[26] De Rosa, M.: A Free vibrations of Timoshenko-beams on two-parameter elastic foundation. Comput. Struct. 57, 151–156 (1995)
[27] Timoshenko, P.S., Gere, M.J.: Theory of Elastic Stability. McGraw-Hill, New York (1964)
[28] Rašković, D.: Theory of Oscillations. Naučnaknjiga, Belgrade (1965)
[29] Reddy, J.N.: Energy and Variational Methods in Applied Mechanics. John Wiley, New York (1984)
[30] Reddy, J.N.: Mechanics of Laminated Composite Plates: Theory and Analysis. CRC Press, Boca Raton (1997)
[31] Wang, C.M., Reddy, J.N., Lee, K.H.: Shear deformable beams and plates. Elsevier, Oxford (2000)
[32] Petyt, M.: Introduction to Finite Element Vibration Analysis. Cambridge University Press, Cambridge (1990)
[33] Ribeiro, P.: A p-version, first order shear deformation, finite element for geometrically non-linear vibration of curved beams. Int. J. Numer. Methods Eng. 61, 2696–2715 (2004)
[34] Szabó, B.A., Sahrmann, G.J.: Hierarchic plate and shell models based on p-extension. Int. J. Numer. Methods Eng. 26, 1855–1881 (1988)
[35] Han, W., Petyt, M., Hsiao, K.M.: An investigation into geometrically nonlinear analysis of rectangular laminated plates using the hierarchical finite element method. Fin Elem Analysis Design 18, 273–288 (1994)
[36] Meirovitch, L., Baruh, H.: On the inclusion principle for the hierarchical finite element method. Int. J. Numer. Methods Eng. 19, 281–291 (1983)
[37] Meirovitch, L.: Elements of Vibration Analysis. McGraw-Hill, New York (1986)
[38] Zhu, D.C.: Development of hierarchical finite element methods at BIAA. In: Conference on Computational Mechanics. Springer, Tokyo (May 1986)
[39] Houmat, A.: Hierarchical finite element analysis of the vibration of membranes. J. Sound and Vib. 201, 465–472 (1997)
[40] Houmat, A.: An alternative hierarchical finite element formulation applied to plate vibrations. J. Sound and Vib. 206, 201–215 (1997)

[41] Bardell, N.S.: Free vibration analysis of a flat plate using the hierarchical finite element method. J. Sound and Vib. 151, 263–289 (1991)
[42] Han, W., Petyt, M.: Linear vibration analysis of laminated rectangular plates using the hierarchical finite element method - I: Free vibration analysis. Comput. Struct. 61, 705–712 (1996)
[43] Han, W., Petyt, M.: Linear vibration analysis of laminated rectangular plates using the hierarchical finite element method - II: Forced vibration analysis. Comput. Struct. 61, 713–724 (1996)
[44] Ribeiro, P.: Hierarchical finite element analyses of geometrically non-linear vibration of beams and plane frames. J. Sound and Vib. 246, 225–244 (2001)
[45] Ribeiro, P.: Non-linear forced vibrations of thin/thick beams and plates by the finite element and shooting methods. Comput. Struct. 82, 1413–1423 (2004)
[46] Wolfe, H.: An experimental investigation of nonlinear behaviour of beams and plates excited to high levels of dynamic response. PhD thesis, University of Southampton (1995)
[47] ANSYS Workbench User's Guide (2009)
[48] Ribeiro, P.: A p-version, first order shear deformation, finite element for geometrically non-linear vibration of curved beams. Int. J. Numerical Methods in Eng. 61, 2696–2715 (2004)
[49] Lewandowski, R.: Non-linear free vibration of beams by the finite element and continuation methods. J. of Sound Vib. 170, 539–593 (1994)
[50] Stojanović, V., Ribeiro, P., Stoykov, S.: A new p-version finite element method for nonlinear vibrations of damaged Timoshenko beams. In: Paper presented at the 6th European Congress on Computational Methods in Applied Sciences and Engineering, September 10-14, University of Vienna, Austria (2012)
[51] Timoshenko, P.S.: Strength of Materials, Advanced theory and problems-part I, New York (1930)
[52] Timoshenko, P.S.: Strength of Materials, Advanced theory and problems-part II, New York (1942)
[53] Kozić, P., Janevski, G., Pavlović, R.: Moment Lyapunov exponents and stochastic stability of a double-beam system under compressive axial loading. Int. J. Sol. Struct. 47, 1435–1442 (2010)
[54] Stojanović, V., Petković, M.: Moment Lyapunov exponents and stochastic stability of a three-dimensional system on elastic foundation using a perturbation approach. J. Appl. Mech. 80, 051009 (2013)

Appendix 2.2.1 (http://www.2shared.com/file/tcb0znSv/prilog_221.html)
Appendix 2.3.1 (http://www.2shared.com/file/QtPhChr2/prilog_231.html)
Appendix 2.3.2 (http://www.2shared.com/file/wGTiFubh/prilog_232.html)
Appendix 2.4.1 (http://www.2shared.com/document/uV4OsB5Z/prilog_241.html)
Appendix 2.2.2 (http://www.2shared.com/file/4_8DxOgf/prilog_222.html)
Appendix 3.2.1 (http://www.2shared.com/file/FY-dZiam/prilog_321.html)
Appendix 3.3.1 (http://www.2shared.com/file/SnRW6x79/prilog_331.html)
Appendix 3.3.1 (http://www.2shared.com/file/SnRW6x79/prilog_331.html)
Appendix 6.1.1 (http://www.2shared.com/file/ZTF0-q8o/Prilog_611.html)
Appendix 6.1.2 (http://www.2shared.com/file/NcyTdJkW/Prilog_612.html)